

Preliminary Hydrodynamic Modeling of the Steep Rock Pit Lakes, Atikokan, Ontario

by

Larissa Mikkelsen

**A thesis submitted in partial fulfillment of
the degree in Masters of Sciences
Department of Geology
Lakehead University**

© Copyright by Larissa Mikkelsen (2012)

ABSTRACT

Pit lakes are often a planned part of an open pit mine closure where the excavations are expected to flood and water quality is not an issue. Common environmental issues regarding pit lakes include their rebound rate, hydrodynamic behaviour and water quality. The water quality of pit lakes can be influenced by their hydrodynamics, for example overturn in a holomictic lake can transport dissolved oxygen down to submerged tailing resulting in the production of acid mine waters if sulphide minerals are present, or the unexpected overturn of a meromictic pit lake can bring stagnant, dissolved metal laden waters to surface that may be toxic to aquatic life. Where water quality is of concern and pit lakes outflow into adjacent watersheds their behaviour can determine if noxious material will be brought to the surface and released. At the former Steep Rock Iron Mines property near Atikokan, Ontario, three pit lakes are currently flooding and will eventually join to form a super pit lake before they outflow into the West Arm and subsequently Seine River system. Previous studies on two of the pit lakes, Caland and Hogarth, have shown that the pit lakes are meromictic and holomictic, respectively, and that both have elevated sulphate concentrations. The aim of this research was to: i) evaluate existing rebound models by modeling rebound and assessing which parameters exert the greatest influence on the rebound rate; and, ii) develop hydrodynamic models of Caland and Hogarth pit lakes to assess if their current limnology will change as rebound continues and they outflow into the West Arm.

Rebound models are constructed using two approaches and compared to the Ontario Ministry of Natural Resources Regional Engineering model that accurately predicted water levels to 2011. The first rebound modeling approach uses two curves to model the stage-volume relationships, a hypsometric curve and a surface area versus elevation curve. The second approach fits an exponential curve to measured water elevations and then future water elevations are forecasted by extrapolation. Rebound Model 2B constructed following the first approach

matched measured water elevations best for the two pit lakes and predicts 2010 measured water elevations better than the Regional Engineering model. Model 2B predicts that Caland will flow into Hogarth in 2070 and that the new Steep Rock pit lake will outflow into the West Arm in 2087, 18 years longer than predictions made by the Regional Engineering model. Based on the water balance parameter sensitivity analysis, the difference between this study's predictions and those of the Regional Engineering model is the result of different pit volume calculation methods. In this study's rebound models the stage-volume relationships for Hogarth are more accurate than for Caland, suggesting that in future work, at minimum, linear interpolation should be used to define the volume in Caland pit lake.

This study is the first to model the hydrodynamics of Caland and Hogarth pit lakes. The Dynamic Reservoir Simulation Model (DYRESM) was used to: i) assess if it can accurately model the current pit lake conditions; and, ii) model the future conditions in Caland and Hogarth for when the pit lakes join and when they outflow to the West Arm. The model salinities are discussed to assess the future toxicity of the pit lakes. DYRESM simulations of current conditions accurately portray the observed limnological characteristics of Caland and Hogarth pit lakes, including: i) that Caland is meromictic and has a lower salinity relative to Hogarth; and, ii) that Hogarth develops a temporary meromix. Simulations of when the two pits join indicate that the freshwater lens in Caland will be maintained, but is thinner, and that Hogarth develops a meromix, which is maintained throughout the simulations. Simulations of when the pit lakes outflow into the West Arm indicate that Caland will maintain its upper freshwater lens and that a fresh water lens is only briefly present in Hogarth. In most cases, variations of the simulations for current and future pit lake conditions, including additional inflows, alteration of the inflow salinities, and the use of a slower rebound rate to define the DYRESM water balance, only produced minor changes in the simulation.

A linear trend between sulphate concentrations and salinity exists for water samples from Caland and Hogarth. Based on this trend, the DYRESM salinity profiles suggest that the waters that outflow from Caland into Hogarth will have sulphate concentrations ranging from 0 mg/L to 100 mg/L and that waters that outflow from Hogarth will have sulphate concentrations ranging from 1700 mg/L to 1900 mg/L. In general, the sulphate concentrations in Caland are below maximum acceptable limit of all water quality standards while those in Hogarth exceed all water quality standards. These results suggest that the waters that outflow from the pit lakes will be toxic.

DYRESM can be used to simulate the future hydrodynamics of Caland and Hogarth pit lakes, however, future studies and field investigations should address some of the areas of uncertainty in the DYRESM simulations for Caland and Hogarth pit lakes, including constraining seep and groundwater volumes and chemistry, on site meteorological monitoring and measurement of the light extinction coefficient.

ACKNOWLEDGEMENTS

A sincere thanks is due to Dr. Andrew Conly for assistance, instruction and constructive criticism. Rob Purdon and Brian Jackson for their help and insight into the study site, Lindsay Moore for assistance in the field, Dr. Mary Louise Hill for her support and encouragement. A special thanks to my husband, family and friends for your support, encouragement and days spent watching Leif.

TABLE OF CONTENTS

Title page	i
Abstract	ii
Acknowledgements	v
Table of Contents	vi
List of Figures	viii
List of Tables	xii
List of Appendices	xiii
Chapter 1: Introduction	1
1.1 General Introduction Regarding the Hydrodynamics of Pit Lakes.....	1
1.2 Scope of Study	7
Chapter 2: Background Information	10
2.1 Location	10
2.2 Geologic Setting.....	10
2.3 Hydrologic Setting	18
2.4 Previous Research.....	22
2.4.1 <i>Previous Rebound Models</i>	26
Chapter 3: Rebound and Water Balance Models	29
3.1 General Introduction and Scope of Work	29
3.2 Conceptual Model.....	30
3.3 Stage – Volume Relationships.....	32
3.4 Water Balance.....	36
3.5 Determination of Meteorological Parameters.....	38
3.5.1 <i>Precipitation</i>	38
3.5.2 <i>Evaporation</i>	43
3.6 Rebound Models and Calibration	46
3.6.1 <i>Models</i>	46
3.6.2 <i>Calibration</i>	47
3.7 Sensitivity Analysis	48
3.8 Results.....	49
3.8.1 <i>Summary of This Study’s Predictions</i>	49
3.8.2 <i>Comparison of This Study’s Predictions to Measured Water Elevations</i>	52
3.8.3 <i>Comparison of This Study’s and the Regional Engineering Model’s Predictions</i>	53
3.8.4 <i>Sensitivity Analysis Results</i>	55
3.9 Discussion.....	60
3.9.1 <i>Study Results</i>	60
3.9.2 <i>Sensitivity Analysis</i>	66
3.9.3 <i>Model Limitations</i>	69

3.10	Conclusions.....	71
Chapter 4:	Hydrodynamic Modeling.....	72
4.1	Description of the Limnological Program DYRESM	73
4.2	Description of the Limnological Program DYRESM	74
4.3	Description of DYRESM Input Files and Their Creation	74
4.3.1	<i>Configuration</i>	75
4.3.2	<i>Physical Data and Lake Morphometry</i>	76
4.3.3	<i>Initial Profile</i>	77
4.3.4	<i>Meteorological Data</i>	77
4.3.5	<i>Stream Inflow</i>	79
4.3.6	<i>Withdrawals</i>	80
4.3.7	<i>Parameters</i>	81
4.4	Simulated Scenarios.....	81
4.4.1	<i>Scenario 1 - Current Conditions</i>	81
4.4.2	<i>Scenario 2: Future Conditions When Pit Lakes Join</i>	84
4.4.3	<i>Scenario 3: Future Conditions When Pit Lake Outflow to the West Arm</i>	85
4.5	Results.....	86
4.5.1	<i>Scenario 1</i>	86
4.5.2	<i>Scenario 2</i>	95
4.5.3	<i>Scenario 3</i>	98
4.6	Discussion.....	105
4.6.1	<i>Study results</i>	105
4.6.2	<i>Implications for the Future Toxicity of Caland and Hogarth</i>	111
4.6.3	<i>Limitations of the study and future work</i>	117
4.7	Conclusions.....	123
Chapter 5:	General Conclusions.....	126
References		129
Appendices		136

LIST OF FIGURES

Figure 1.1: Map showing the four open pits on the former Steep Rock Iron Mines property. (Base map from Google Earth August 24, 2005).....	4
Figure 1.2: Map showing original Steep Rock Lake shoreline, current pit lake shorelines, surrounding lakes and key water control structures. Based on GIS data available from the Ministry of Natural Resources.	5
Figure 1.3: Map showing water flow paths before and after the Seine River and Western Diversions. Based on GIS data available from the Ministry of Natural Resources.....	6
Figure 2.1: Location of study site (Stott et al., 2007). The former Steep Rock Iron Mines site is located on the southern border of the Wabigoon Terrane adjacent to the Quetico Subprovince	11
Figure 2.2: Geological cross-section of Errington pit from Kusky and Hudleston (1999). The geology of Hogarth and Caland pits is similar to that of Errington pit except that there is a greater proportion of the Pyritic Member in Hogarth pit.....	12
Figure 2.3: A schematic east-west cross-section of Caland (East Arm) and Hogarth Pit (Middle Arm) Lakes (from Sowa et al., 2001). Diagram shows approximate 2011 pit lake water elevations, original lake level and water elevations in the Seine River, West Arm, Fairweather Lake (Southeast Arm) and the Rawn.....	22
Figure 2.4: Comparison of previous predictions made for rebound Caland pit lake to measured water elevations.	27
Figure 2.5: Comparison of previous predictions made for rebound in Hogarth pit lake to measured water elevations.	28
Figure 3.1: The hypsometric curve for Caland pit. The hypsometric curve is shown by the black line and the points are the determined accumulated volume with elevation.	34
Figure 3.2: The hypsometric curve for Hogarth pit. The hypsometric curve is shown by the black line and the points are the determined accumulated volume with elevation.	34
Figure 3.3: The elevation – surface area curve for Caland pit. The elevation – surface area curve is shown by the black line and the points correspond to the measured surface area at each ontour interval of the pit.	35
Figure 3.4: The elevation – surface area curve for Hogarth pit. The elevation – surface area curve is shown by the black line and the points correspond to the measured surface area at each contour interval of the pit.....	35
Figure 3.5: Google image of weather station locations used in this study and that of Heineselmen (1996). Weather stations marked by yellow flags are stations with 25 km of Atikokan; blue	

flags are stations within 200 km to West of Atikokan; green are stations used by Heineselmen (1996); and, the orange flag is the Thunder Bay weather station.	40
Figure 3.6: Comparison of monthly precipitation distributions of the index stations to the Atikokan weather station used in the normal inverse ratio method of estimating precipitation.	41
Figure 3.7 Comparison of estimate annual precipitation to measured annual precipitation from 1978 to 2003 at the Atikokan weather station.	43
Figure 3.8: Graph showing measured and estimated monthly evaporation rates.	46
Figure 3.9: Graph showing the results of the rebound models for Caland and measured water levels from 1979 to 2011.	50
Figure 3.10: Graph showing the results of the rebound models for Hogarth and measured water levels from 1979 to 2011.	50
Figure: 3.11: Comparison of measured water elevations to this study's rebound model predictions for Caland and to those of the Regional Engineering model.	54
Figure: 3.12: Comparison of measured water elevations to this study's rebound model predictions for Hogarth and to those of the Regional Engineering model.	55
Figure 3.13: Graph of the sensitivity analysis for precipitation. The predictions shown start in 2006, when the average precipitation rate replaces measured values in the water balance calculations, and end when the predicted water level for each model is equal to or greater than 394 m.....	57
Figure 3.14: Graph of the sensitivity analysis for runoff. The predictions shown start in 2004, when the calibration period ends in the water balance calculations, and end when the predicted water level for each model is equal to or greater than 394 m.	58
Figure 3.15: Graph of the sensitivity analysis for evaporation. The predictions shown start in 2004, when the calibration period ends in the water balance calculations, and end when the predicted water level for each model is equal to or greater than 394 m.	59
Figure 3.16: Graph of the sensitivity analysis for the net groundwater influx. The predictions shown start in 2004, when the calibration period ends in the water balance calculations, and end when the predicted water level for each model is equal to or greater than 394 m.....	59
Figure 3.17: Images showing the irregularities in the shape of Caland and Hogarth pit lakes. (A) Contours of Caland and Hogarth pit lakes at a 10 m interval from 190 masl to 390 masl. (B) Aerial photograph of Caland pit lake taken in 1982, showing the irregular shape of the lake.	62
Figure 4.1: Temperature (°C), salinity (psu) and density (kg/m ³) profiles for scenario 1 simulations 1C1b and 1Cv2 for Caland pit lake. Aside from the salinity at the bottom of the pit increasing earlier in 1Cv2 then 1C1b there are no significant differences in profiles	89

Figure 4.2: Temperature ($^{\circ}\text{C}$), salinity (psu) and density (kg/m^3) profiles for scenario 1 simulations 1C1c and 1C1d for Caland pit lake. The profile for simulation 1C1e is identical to 1C1d and is not shown. Relative to 1C1b, 1C1c and 1C1d do not have a plume in the layer with the highest salinity and the salinity at the bottom of the pit does not change with time 90

Figure 4.3: Temperature ($^{\circ}\text{C}$), salinity (psu) and density (kg/m^3) profiles for scenario 1 simulations 1H1b and 1H3 for Hogarth pit lake. The salinity profile for 1H1b shows a plume and that of 1H3 does not. 92

Figure 4.4: Temperature ($^{\circ}\text{C}$), salinity (psu) and density (kg/m^3) profiles for scenario 1 simulations 1H_MSGW and 1H_HSGW for Hogarth pit lake. Relative to 1H1b the density at the bottom of the pit is greater in simulations 1H_MSGW and 1H_HSGW. Simulation 1H_MSGW shows a plume in the salinity profile and 1H_HSGW does not 93

Figure 4.5: Temperature ($^{\circ}\text{C}$), salinity (psu) and density (kg/m^3) profiles for scenario 1 simulations 2C2 and 2C2 for Caland pit lake. Relative to simulation 1C1b, the salinity in the pit lake is lower in simulations 2C1 and 2C2 and the low salinity surface layers are thinner 96

Figure 4.6: Temperature ($^{\circ}\text{C}$), salinity (psu) and density (kg/m^3) profiles for scenario 2 simulations 2Cv2 and 2Cv3 for Caland pit lake. There are no significant differences between profiles for simulations 2Cv2 and 2Cv3 compared to 2C1 except for a slightly thicker fresh water lens in the salinity profile for 2Cv3 97

Figure 4.7: Temperature ($^{\circ}\text{C}$), salinity (psu) and density (kg/m^3) profiles for scenario 2 simulations 2H1 and 2H1b for Hogarth pit lake. Relative to simulation 1H1b the salinity profiles show a permanent fresh water layer at the surface. Simulation 2H1 has a plume in the salinity profile and simulation 2H1b does not 100

Figure 4.8: Temperature ($^{\circ}\text{C}$), salinity (psu) and density (kg/m^3) profiles for scenario 2 simulations 2H2 and 2H3 for Hogarth pit lake. Relative to simulation 2H1, there are no significant differences in profiles..... 101

Figure 4.9: Temperature ($^{\circ}\text{C}$), salinity (psu) and density (kg/m^3) profiles for scenario 2 simulations 2Hv2 and 2Hv3 for Hogarth pit lake. Relative to simulation 2H1, there are no significant differences in profiles..... 102

Figure 4.10: Temperature ($^{\circ}\text{C}$), salinity (psu) and density (kg/m^3) profiles for scenario 3 simulations 3C_1out and 3Cv3_1out for Caland. Relative to simulation 2C1, the salinity in the pit lake is lower and the fresh water layers are thinner in simulations 3C_1out and 3Cv3_1out..... 103

Figure 4.11: Temperature ($^{\circ}\text{C}$), salinity (psu) and density (kg/m^3) profiles for scenario 3 simulations 3Hv2 and 3Hv3 for Hogarth. Relative to simulation 2H1, the permanent fresh water layers at the surface of the pit lake no longer exist in simulations 3Hv2 and 3Hv3. 104

Figure 4.12: Plot of salinity versus sulphate for all water samples collected from Caland and Hogarth pits and seeps between 1998 and 2009. Caland pit lake samples are represented by squares, black for seeps and grey for lake samples. Hogarth pit lake samples are represent by triangle, black for seeps and grey for lake samples. The black line shows the linear relationship between sulphate and salinity and has a correlation coefficient of 0.9304. 113

Figure 4.13: Comparison of measured salinity for Caland (left) and DYRESM predicted salinity for Caland (right). Note that the measured salinity predictions do not extend to the bottom of the pit lake but the DYRESM predicted values do. Measured values are similar above 100 m depth compared to layer 40 in the DYRESM predicted values. At about layer 35 DYRESM predicts a salinity decrease from the spring to fall. Measured values are derived conductivity measurements from Godwin 2010 115

Figure 4.14: Comparison of measured salinity in Hogarth (left) and DYRESM predicted salinity for Hogarth (right). Measured values indicate a much lower salinity at the surface and bottom of the pit lake in comparison the DYRESM predicted values. DYRESM predicts higher surface salinities in the fall compared to the spring and summer profiles which are similar. Measured values were derived from conductivity measurements from Godwin (2010) 116

LIST OF TABLES

Table 1.1: Timeline of mine opening and closures on the Steep Rock Iron Range.....	4
Table 2.1: Summary of previous rebound model predictions.....	27
Table 3.1: List of weather stations used in the estimation of missing precipitation values from the National Climate Data and Information Archive.....	40
Table 3.2: Rebound model predictions for when Caland and Hogarth join and outflow into the West Arm.....	49
Table 3.3: The net groundwater influx values calculated during each of the models respective calibration period.	49
Table 4.1: Summary of DYRESM simulations for Caland pit lake.	82
Table 4.2: Summary of DYRESM simulations for Hogarth pit lake.....	82

LIST OF APPENDICES

Appendix I: Pit Lake Volume Calculations.....	136
Appendix II: Estimating Precipitation Rates Using the Inverse Ratio Method.....	139
Appendix III: Estimating Evaporation Using the Penman and Thornwaite Equation.....	141
Appendix IV: Water Balance and Rebound Model Results.....	143
Appendix V: Sensitivity Analysis Results.....	162
Appendix VI: Rebound Model – Pit Geometry Modeled Using Linear Interpolation.....	165
Appendix VII: Example DYRESM Input Files.....	175
Appendix VIII: Glossary of Terms.....	196

Chapter 1: Introduction

1.1 General Introduction Regarding the Hydrodynamics of Pit Lakes

Natural water systems can be drastically altered by mining activities. The environmental impacts of mining activities on natural water systems can be categorized accordingly: i) the physical impacts on natural water systems produced by mineral extraction; ii) the inflow of water into active workings; iii) dewatering methods and their design; iv) impacts of dewatering in terms of quantity and quality; v) hydrologic behaviour of rock piles, backfill, and tailings impoundments; vi) physical and chemical changes associated with mine abandonment and the rebound process; and, vii) the long-term hydrologic behaviour of abandoned mine site including, but not limited to, longevity of pollution, contamination migration, discharge from flooded mines and physical and chemical dynamics of pit lakes (Younger et al., 2002). Where mine workings extend below the water table, dewatering is required during operation to keep excavations, underground workings or open pits, dry. Upon cessation of dewatering rebound occurs where ground and surface waters gradually flood mine voids (Younger et al., 2002). Rebound in open pit mining operations results in the formation of a pit lake.

Common environmental issues with respect to pit lakes include the long-term hydrologic behaviour, the rebound rate and water quality. The long-term hydrologic behaviour of pit lakes depends on whether or not the bottom of an open pit extends below the water table. In general a pit lake acts as a regional groundwater sink. Where the floor of open pit mine excavation is below the water table, the pit will gradually flood until the pit lake surface elevation equals that of the groundwater table (Younger et al., 2002). In such cases, pit lakes are often a planned part of the mine after use if no water quality issues are expected. The length of time it will take for an open pit to completely flood, also known as the rebound rate, depends on the volume of the void to be filled and the water balance. Most pit lakes only lose water via evaporation and lateral

groundwater flow, but some pit lakes have surface outlets. Two issues often arise with respect to pit lake water quality. First, water released from the pit lake into downstream watersheds may have chemical constituents exceeding water quality guidelines. Secondly, the disposal of waste rock and tailings in the pit lake may result in the migration of potentially toxic material up to the lake surface (Hamblin et al., 1999).

Unlike natural lakes, the depth to width ratio of most pit lakes is high, which has important implications for lake dynamics. The high depth to width ratio of pit lakes promotes three-layer density stratification where the bottom layer (monimolimnion) is not involved in seasonal overturn resulting in meromictic stratification (Younger et al., 2002). Where meromictic conditions exist the monimolimnion remains stagnant. The unexpected overturn of a meromictic lake can result in acute environmental impacts (Castendyk and Webster-Brown, 2007). The upper layers (mixolimnion and chemolimnion) of a lake can become oxygen depleted due to mixing with the stagnant bottom waters (monimolimnion) and any dissolved or suspended constituents. Where sulphide minerals exist in wall rocks or stored tailings, redox conditions can influence the production of acid mine waters (Castendyk and Webster-Brown, 2007). Typically, waters with low pH and high concentrations of ecotoxic metals occur for a brief time during pit filling and a short period thereafter (Shevenell, 2000a). A pit lake is likely to remain acidic when the terminal water elevation is in contact with sulphur rich rock (Bowell et al., 1998). In contrast, a pit lake water column may turn over completely with seasonal overturn resulting in holomictic stratification (Younger et al., 2002). Where holomictic conditions exist, seasonal overturn can transport dissolved oxygen to submerged mine tailings and can promote oxidation of sulphide-bearing material is present (Younger et al., 2002). For these reasons it is important to understand the likely dynamics of a pit lake before developing a long-term management strategy. However, before the affect of a pit lake on regional hydrology or water quality can be assessed, a knowledge of the fluxes and volumes of water entering and exiting the pit lake is required.

In theory predicting the formation of pit lakes is straightforward and can be addressed by assuming that groundwater inflow will decrease steadily as the pit fills. At the start of rebound, immediately after cessation of dewatering, the groundwater inflow rate will equal the final dewatering rate and once rebound is complete the groundwater inflow will equal the sum of evaporative losses plus any groundwater outflow (Younger et al, 2002). In practice the prediction of pit lake formation is complicated by local site conditions that influence the components of the total water balance (Younger et al, 2002). Unfortunately, there has not been a significant amount of work done to address the prediction of pit lake rebound rates. However, models have been made that reproduce observed pit filling rates and may be applicable to the prediction of future pit filling rates (e.g., Capper, 1978; MNR, 1986; Shevenell, 2000a).

The former Steep Rock Iron Mines property located approximately 5 km north of Atikokan, Ontario, provides an excellent opportunity to study the formation of pit lakes. A series of mines operated on the property from 1944 to 1979 (Fig. 1.1 and Table 1.1). Open pit mining proved to be more economic than underground mining due to the complex nature of the local geology and heavy groundwater inflow (Taylor, 1978). The Steep Rock Iron Range ore bodies were located beneath the former Steep Rock Lake. The development of open pit mines on the Steep Rock Iron Range required what was the first ever water diversion in Canadian mining history and altered approximately 259 km² of the Seine River watershed in order to isolate and drain portions of Steep Rock Lake (Taylor, 1978; Fig. 1.2). The Seine River and Western Diversions, along with other water control systems, served to isolate Steep Rock Lake from the Seine River system (Fig. 1.3). The open pit mines were mined to their economic depth of approximately 400 m. Upon the cessation of mining activities in 1979, the open pits have been gradually flooding from runoff, precipitation and groundwater inflows. Between 1979 and 2004 there were four pit lakes (Hogarth, South Roberts, Errington and Caland; Figure 1.1).

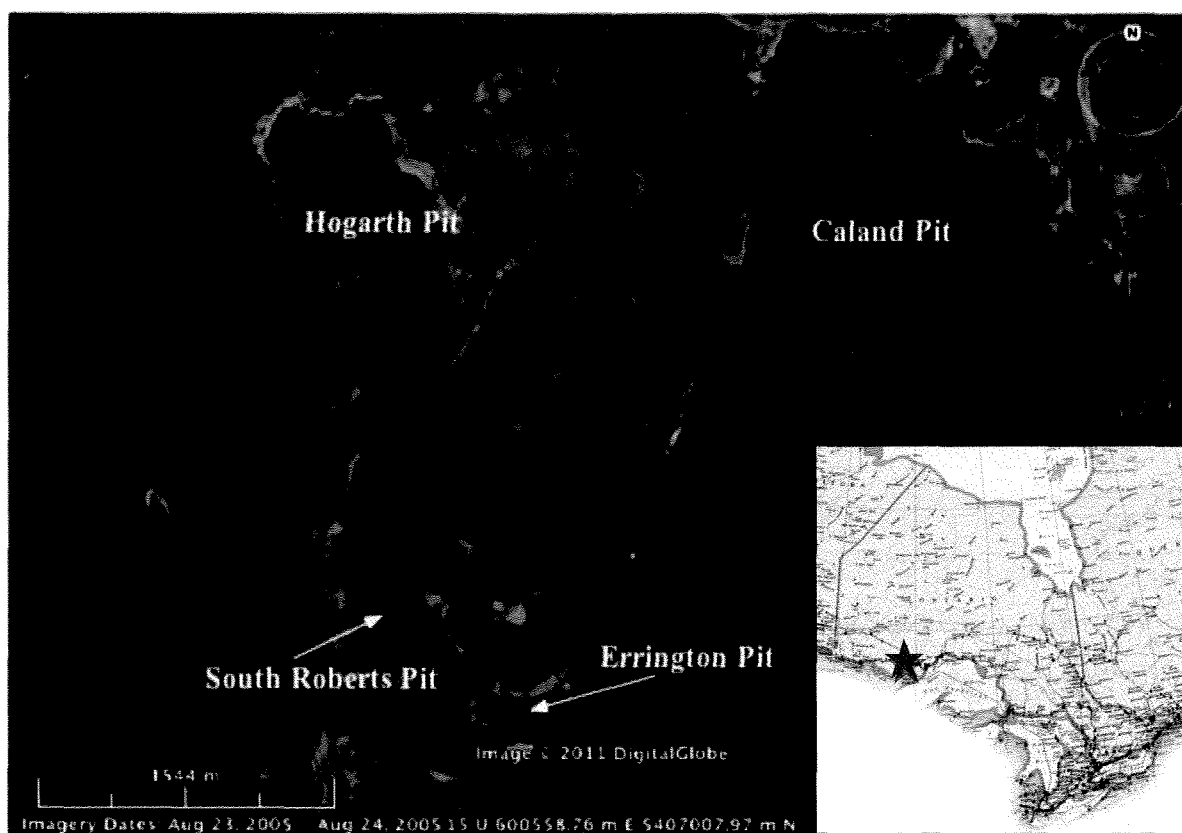


Figure 1.1: Map showing the four open pits on the former Steep Rock Iron Mines property. (Base map from Google Earth, August 24, 2005).

Table 1.1: Timeline of mine opening and closures on the Steep Rock Iron Range

Year(s)	Mine Openings and Closures
1939 – 1940	<ul style="list-style-type: none"> Attempted underground mining of Steep Rock Iron Range fails due to high water inflow
1944	<ul style="list-style-type: none"> Errington Open Pit opens
1953	<ul style="list-style-type: none"> Hogarth Open Pit opens Cessation of mining at economic limit of Errington Open Pit
1956	<ul style="list-style-type: none"> Errington Underground opens
1958	<ul style="list-style-type: none"> Hogarth Underground shaft is sunk and pre-production work complete but project is abandoned
1960	<ul style="list-style-type: none"> Caland Open Pit opens
1961	<ul style="list-style-type: none"> Cessation of mining at economic limit of Hogarth Open Pit
1964	<ul style="list-style-type: none"> Roberts Open Pit opens Errington Underground closed due to high costs associated with complex geology, support required limited drift size, and grade control issues
1971	<ul style="list-style-type: none"> Errington Underground reopened
1972	<ul style="list-style-type: none"> Cessation of mining at economic limit of Roberts Pit Errington Underground closed for same reasons as before
1974	<ul style="list-style-type: none"> Hogarth Open Pit expanded and brought back into production
1978	<ul style="list-style-type: none"> Cessation of mining at economic limit of Hogarth Open Pit Environmental Plan is completed by Steep Rock Iron Mines
1979	<ul style="list-style-type: none"> Cessation of mining at economic limit of Caland Open Pit
1985	<ul style="list-style-type: none"> Steep Rock Iron Mines applies to surrender mining claims
1986	<ul style="list-style-type: none"> Steep Rock Iron Mines application for surrender of mining claims is accepted
Information taken from Steep Rock Men and the Mines by Taylor (1978) and from Report on the Surrender of Mining Claims By Steep Rock Resources Inc., Steep Rock Lake Atikokan District by the Ministry of Natural Resources (1986).	

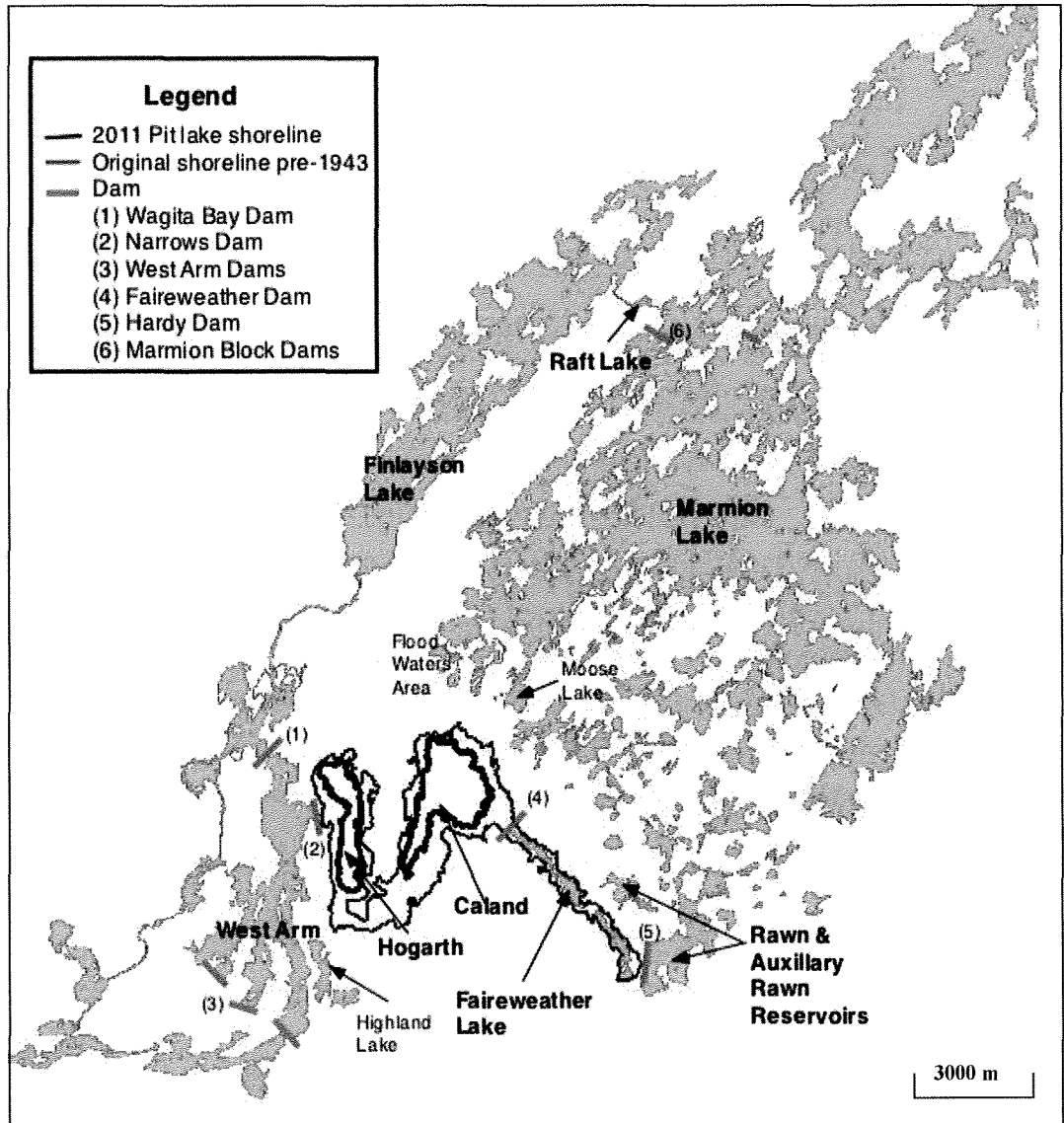


Figure 1.2: Map showing original Steep Rock Lake shoreline, current pit lake shorelines, surrounding lakes and key water control structures. Based on GIS data available from the Ministry of Natural Resources.

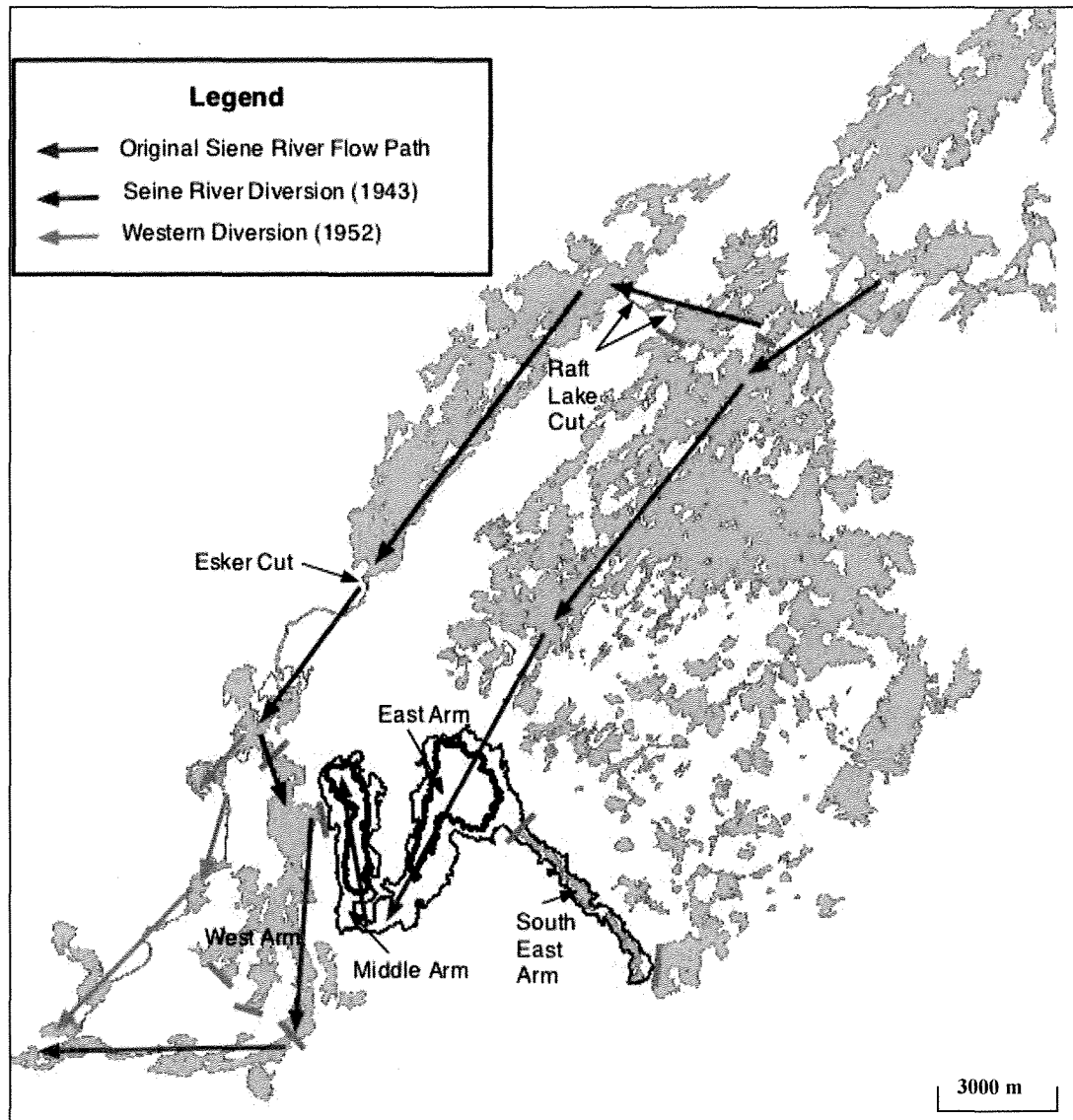


Figure 1.3: Map showing water flow paths before and after the Seine River and Western Diversions. Based on GIS data available from the Ministry of Natural Resources.

Mine closure studies for Steep Rock Iron Mines Ltd. determined that all acid mine drainage that occurs on the property would flow into the pits and be neutralized by carbonate wall-rock and not require treatment (Capper, 1978). Without any intervention the Caland and Hogarth pit lakes are expected to gradually flood until they eventually join, forming one large lake, before

decanting into the West Arm Retention Basin and entering the Seine River System. During the surrender of mining claims, the Ministry of Natural Resources produced a rebound model for Caland and Hogarth. The projected water levels up to the year 2011 have proven to be accurate with respect to observed water levels (MNR, 1986). A later rebound model by Vancook (2002) provided water level predictions further into the future but this model has recently been called into question by Jackson (2007) because of its assumption that the pit lake water elevation will increase linearly with time.

McNaughton (2001), Gould (2008) and Godwin (2010) studied the limnology of Caland and Hogarth pit lakes. Although in close proximity the two pit lakes have been observed to behave differently, Caland pit lake is meromictic and Hogarth pit lake appears to be temporarily meromictic. The differences in stratification have been attributed to the differences in the amount of fresh water input and the greater amount of pyritic material present in the ore zones mined in Hogarth pit (McNaughton, 2001; Godwin, 2010). Over time the rebound process will change the dynamics of the lakes, specifically the inflows and outflows, as Caland and Hogarth gradually flood the lake basin of the former Steep Rock Lake. However, to date no studies have been done to model the hydrodynamics of the Caland and Hogarth pit lakes.

1.2 Scope of Study

The aim of this research was: i) evaluate existing rebound models through remodeling rebound and assess which parameters exhibit the greatest control on rebound rates; and ii) develop hydrodynamic models of Caland and Hogarth pit lakes in order to assess if their current limnology will change as rebound continues and they outflow into the West Arm. Analytical rebound and water balance models are created for Caland and Hogarth pit lakes in order to extend water elevation predictions into the future. A number of different rebound models are made using different prediction methods and calibration methods. The model that best matches

measured water levels was used to conduct a sensitivity analysis designed to investigate the influence of individual parameters on the rebound model results. The selected model was also used to define simulation inputs in the hydrodynamic model including: the volume of inflows and withdrawals, and the initial water surface heights in the pit lakes.

Previous rebound models for Caland and Hogarth include: Capper (1978), MNR (1986), Vancook (2005) and Jackson (2007). Of the four studies, that of the MNR (1986) has proven to be reliable, however, it only made water level prediction until 2015. Currently the Caland and Hogarth pit lakes are filling independently of each other (Godwin, 2010). Since the reliable water level predictions are only available until 2015, well before the pit lakes join, the rebound model in this study will extend water level predictions into the future in order to determine Hogarth's water level when Caland reaches 385 m, and the water balance will be used to define volumes of water entering the pit lakes in the hydrodynamic models.

This study is the first to attempt to conduct hydrodynamic modeling of Caland and Hogarth pit lakes. An understanding of the future hydrodynamics of Caland and Hogarth pit lakes is important because of the implications that lake dynamics can have on outflow water quality when the joined Caland-Hogarth pit lake eventually spills into West Arm. The hydrodynamic model Dynamic Reservoir Simulation Model (DYRESM) by Imberger and Patterson (1981) and by the Centre for Water Research at the University of Western Australia (www.cwr.uwa.edu.au) was used to establish hydrodynamic models of Caland and Hogarth pit lakes in order to assess if the salinity, density and temperature profiles of the pit lakes change at key times during the rebound process. Of specific interest was whether or not DYRESM can accurately simulate current conditions in the Caland and Hogarth pit lakes and if the stratification of the two lakes will change when the two pit lakes join and outflow.

Rebound models and hydrodynamic models of pit lakes should be an essential component of the pit lake management strategy especially where future water quality is of concern. At Steep Rock, the quality of the waters that will outflow from the pit lakes is of concern since both pit lakes contain high concentrations of sulphate. The current the sulphate concentrations in Caland range between 200 mg/L and 500 mg/L and Hogarth between 1200 mg/L and 1900 mg/L (McNaughton, 2001; Gould, 2008; Godwin, 2010; Shankie, 2011). The Canadian Drinking Water Guidelines recommend that sulphate concentrations in drinking water should not exceed 500 mg/l while the Environmental Protection Agency (EPA) Secondary Maximum Contaminant Level (SMCL) is at or below 250 mg/L (EPA, 2003; Health Canada, 2010). Rebound and hydrodynamics models should be a component of the pit lake management strategy and of environmental assessments regarding the future use of the Steep Rock property because the pit lakes will outflow into the Seine River which connects to a number of popular fishing lakes and because the Ontario Government has accepted proposals for the future use of the site to process iron ore and dispose of other mine tailings which will influence water chemistry on the property ([http://www.bendinglakeiron.com/MEDIA%20-%20Rehabilitating%20 The%20 Steep%20Rock%20Mine%20Site.pdf](http://www.bendinglakeiron.com/MEDIA%20-%20Rehabilitating%20The%20Steep%20Rock%20Mine%20Site.pdf), Accessed: December 6, 2010). Furthermore, this study's rebound model water level predictions may help validate the use of analytical methods to estimate pit lake rebound rates by comparing predicted water levels to future measured levels, and to validate the use of DYRESM to model the pit lake hydrodynamics.

Chapter 2: Background Information

2.1 Location

Steep Rock Resource Inc. and Caland Ore mining claims encompassed an area of 52 km² including the entire area of Steep Rock Lake (MNR, 1986). Steep Rock Lake was located about 5 km north of Atikokan, Ontario (48°48'N, 91°39'W) and is about 208 km west of Thunder Bay, Ontario.

2.2 Geologic Setting

The Archean iron ore body mined by Steep Rock Iron Mines Ltd. and Caland Ore Ltd. is located on the southern border of the Wabigoon subprovince and adjacent to the Quetico subprovince of the Superior Province (Fig. 2.1). The Wabigoon subprovince is a volcano-plutonic subprovince consisting of greenstone belts that are bordered and intruded by felsic plutonic rocks (Card and Ciesielski, 1986). The Quetico subprovince consists primarily of metasedimentary rocks. The Quetico and Seine River Faults mark the border between the Wabigoon and Quetico subprovinces (Card and Ciesielski, 1986). The east-trending Wabigoon-Quetico boundary separates metavolcanic rocks to the north from the metasedimentary rocks to the south and has been attributed to subduction-related accretion of the Quetico sedimentary prism against the Wabigoon volcanic arc about 2695 Ma (Stone et al., 1992). A number of other faults including the Atikokan Fault, Samuels Fault and Bartley Fault run through the Steep Rock area (Stone et al., 1992). The Steep Rock Lake area shows indications of multiple periods of metamorphism, metasomatism and deformation. The main periods of metamorphism correlate with the Kenoran, Hudsonian, and Grenville orogenies. The main types of metasomatism that occurred in the area include carbonatization, quartz veins, silicification, iron-sulphur metasomatism, spilitization, and hydration (Shklanka, 1972).

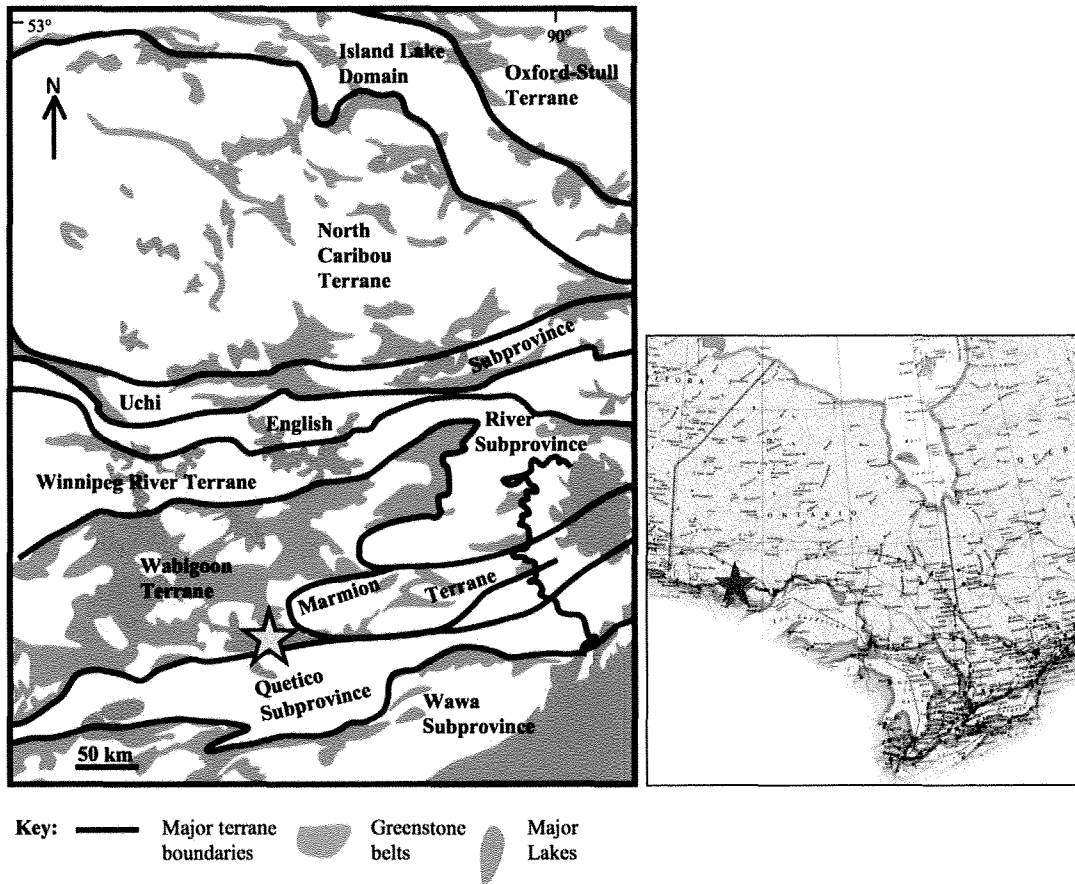


Figure 2.1: Geologic location of study site (Stott et al., 2007). The former Steep Rock Iron Mines site is located on the southern border of the Wabigoon Terrane adjacent to the Quetico Subprovince.

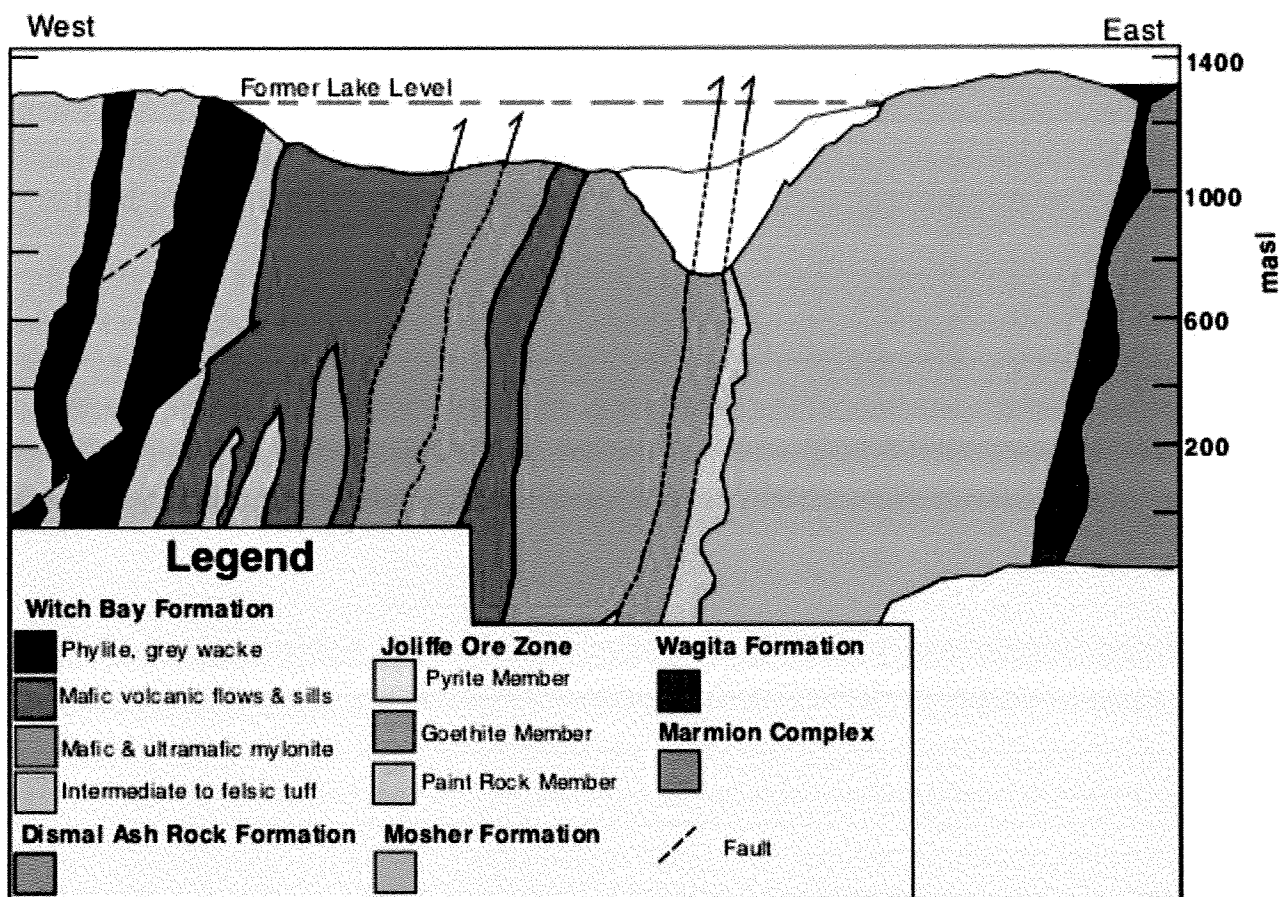


Figure 2.2: Geological cross-section of Errington pit (from Kusky and Hudleston 1999). The geology of Hogarth and Caland pits is similar to that of Errington pit except that there is a greater proportion of the Pyritic Member in Hogarth pit.

Study site geology consists of the Marmion Gneiss complex and the Steep Rock greenstone belt. The Marmion Gneiss Complex is a composite unit that includes mafic tonalitic gneiss, a leucocratic tonalite containing amphibolized remnants of mafic volcanics, several units of felsic and intermediate tuffaceous rock that are all intruded by granodiorite and gabbro dikes (Stone et al., 1992). The Steep Rock Group overlies the Marmion Gneiss Complex and consists of the Wagita Formation, Mosher Carbonate Formation, Jolliffe Ore Zone, Dismal Ash Rock, Witch Bay Formation (Fig. 2.2; Jolliffe, 1955; Shklanka, 1972; Stone et al., 1992; Kusky and Hudleston, 1999). The Wagita Formation overlies the Marmion Gneiss Complex and is a discontinuous conglomerate, sandstone sequence consisting of poorly sorted angular fragments of granite and mafic dike material passing upwards into a conglomerate with well-rounded clasts of the same rock types (Jolliffe, 1955). The Wagita Formation is up to 150 m thick and is interpreted as alluvial fan deposits on fault scarps or low-lying areas on the Marmion Complex (Shklanka, 1972). The contact between the Marmion Complex and the Wagita Formation has been interpreted to be conformable marking a change from volcanism to sedimentary deposition (Kusky and Hudleston, 1999). Shklanka (1972) proposed the Steep Rock Group to be fault bounded. However, other authors have interpreted the contact to be an unconformity between the Marmion Complex and the Wagita Formation (Jolliffe, 1966; Wilks and Nesbitt, 1988; Stone et al., 1992).

The Wagita Formation is overlain by the Mosher Carbonate Formation, a sequence up to 500 m thick that represents a shallow ocean environment. The Mosher Carbonate Formation ranges from well banded, to massive, to brecciated, and shows marked changes in chemical composition. The carbonate is made up of calcite, ankerite, and dolomite with minor amounts of cherty layers. Stromatolites are common through the formation (Wilks and Nisbet, 1988). Small-scale stromatolites exist throughout the formation and are best formed near the bottom of the Mosher Carbonate Formation. The most common small-scale morphology is *Stratifera*-like

stromatolites with laminae from 0.5 mm to 4 cm thick and that can be traced up the formation into *Irregularia* –like stromatolites. The *Irregularia* –like stromatolites are pseudo-columnar and laterally linked with wavy-laminae 0.5 cm to 3.5 cm and are 2 cm to 10 cm high and 5 cm to 15 cm in basal diameter. The upper 50 m of the formation is dominated by large-scale stromatolites that form continuous horizons. The large-scale stromatolites are domed structures ~ 3 m in diameter to more tabular bodies up to 5 m or more long (Wilks and Nisbet, 1988). Brecciated units have been associated to fault zones (Shklanka, 1972; Stone et al., 1992, Kusky and Hudleston, 1999).

The Jolliffe Ore zone overlies the Mosher Carbonate Formation and is a 100 m to 400 m thick iron formation that consists of three members, the lower Magniferous Paint, the Middle Goethite, and the upper Pyrite members. The lower Magniferous Paint member is 100 m to 300 m thick and is enriched in manganese and contains large blocks of weathered carbonate (Stone et al., 1992). The Magniferous Paint member has a sharp but irregular contact with the Mosher Carbonate Formation believed to represent a paleosoil on karst topography remaining from the subareal exposure of the Mosher Carbonate Formation (Shklanka, 1972; Kusky and Hudleston, 1999; Stone et al., 2000). The middle Goethite member overlies the lower Magniferous Paint member and is distinguished by an increase in the iron/manganese ratio (Stone et al., 1992). The middle Goethite member is 50 m to 100 m thick and occurs as brecciated masses and as well-banded iron formation. The middle Goethite member is an iron formation made up of more than 90% goethite and hematite with remaining portion of the rock made up of quartz and kaolin in a lighter coloured matrix of gibbsite and kaolinite (Shklanka, 1972). Near the top of the middle Goethite member there is an irregular material called “buckshot” ore that is made up of pisolites and fragments of hematite in a lighter coloured matrix of gibbsite and kaolinite (Shklanka, 1972). Sporadically overlying the Goethite Member is the conformable upper Pyritic member. The majority of the pyrite is contained in well-bedded iron formation that resembles the well-banded

iron formation of the middle Geothite member except for the increased pyrite content (Shklanka, 1972).

Stratigraphically overlying the Jolliffe Ore zone is the Dismal Ashrock Formation. The contact between these two formations is marked by a brittle fault (Stone et al., 1992). The Dismal Ashrock Formation is 50 m to 400 m thick and consists of ductily deformed komatiitic pyroclastic rocks, including tuff, lapilli tuff, and lapilli-stone, collectively called ashrock, and a lesser component of pillowed lava flows (Stone et al., 1992). Lapilli tuffs are the dominant rock type and are made up of poorly sorted fragments with respect to size and are rounded to subrounded. The texture of these rocks is similar to modern day tuff cones suggesting a similar style of volcanism may have occurred as the hot komatiitic magma came into contact with the low-lying Mosher Carbonate and Jolliffe Ore zone Formations (Stone et al., 1992). The contact between the Dismal Ashrock and the Witch Bay volcanic rocks is a regional scale shear zone (Kusky and Hudleston, 1999). Shklanka (1972) identified the Atikokan Fault between the Dismal Ashrock and Witch Bay Formation.

The Witch Bay Formation is made up of mafic with minor felsic metavolcanic rocks and rare metasedimentary rocks. The Witch Bay Formation is at least 1 km thick and extends up to 5 km thick and represents subaqueous volcanism (Stone et al., 2000).

Kusky and Hudleston (1999) interpreted the Mosher Carbonate to be a shallow water carbonate platform that formed along the margin of the Marmion Complex at approximately 3.0 Ga. At the time, the Marmion Complex was part of a larger regional belt of arc type plutons and volcanic rocks in the Central Wabigoon subprovince and is thought to be similar to La Grand River and Sachigo subprovinces. It is proposed that these different terrains may have been continuous until dextral strike-slip faulting occurred through the Superior Province from 2.9 to 2.7 Ga, and that the Steep Rock greenstone belt is part of a shallow-water subsiding arc terrain that was ripped apart (Kusky and Hudleston, 1999). Mafic metavolcanic rocks may have

overlain the ashrock within a poorly constrained time interval, up to 300 million years in length, the contact of which is locally folded and faulted (Stone et al., 1992). Alternatively, the mafic metavolcanic rocks of the Witch Bay Formation could be allochthonous and are different in age with respect to the ashrock and shifted into position by the Atikokan Fault implying that all contacts between the ashrock and metavolcanic rocks are faulted (Stone et al., 1992). The stratigraphic relationship between the Dismal Ashrock Formation and metavolcanic rocks is unclear due to their tectonized and poorly exposed nature of their contacts and depends on the interpretation of the contact between these two formations, the Dismal Ashrock Formation and Witch Bay Formation (Stone et al., 1992).

The Pleistocene surface deposits in the Steep Rock area consist of glacial moraine, glaciolacustrine and rare aeolian deposits on a Precambrian peneplane (Stone, 1992). Ground moraine till is typically 1 m, but is thicker in topographic depressions. The till is unsorted, poorly stratified and composed of pebbles and cobbles in a variable sand, silt and clay matrix. There are two recessional moraines, the Steep Rock and Eagle-Finlayson that cross the Steep Rock area. Both trend east-south-east and are parallel to each other (Shklanka, 1972). The portion of the Steep Rock moraine that crosses the study site is an irregular, interrupted belt of elongate hills, hummocks and gravel flats. Glacier movement over the study scored out the Joliffe Ore zone and deposited iron bearing gravel located immediately south of the East Arm of Steep Rock Lake (Shklanka, 1972; Taylor, 1976, Stone et al., 2002). The Eagle-Finlayson moraine is an elongate, rounded hill consisting of sand and gravel with scattered boulders. The moraine crosses at the southern end of Finlayson Lake. A portion of this moraine was removed during the diversion of the Seine River (Taylor, 1976). Highway 622 runs along the top of the Eagle-Finlayson moraine (Stone et al., 1992).

Varved clays overlie the glacial till in the Atikokan and Seine River systems. These clays received special attention on the Steep Rock Iron Mines site because they were exposed after

Steep Rock Lake was drained and removed during dredging. The lake bed sediments were found to consist of a few feet of glacial till overlain by varved clay over 100 feet thick, followed by a thin layer of sand, and a black gelatinous ooze (Stone et al., 1992). These glacial features have been attributed to three phases of ice retreat of the Patricia ice mass during the late Wisconsin glaciation (Shklanka, 1972). First the ice sheet retreated to the Steep Rock moraine, then advanced again before retreating to the Eagle-Finlayson moraine. Glacial Lake Agassiz bordered the ice sheet to the south and west of the two terminal moraines during its retreat resulting in the varved silts and clays (Shklanka, 1972; Stone et al., 1992). Recent peat deposits overlay the Pleistocene deposits in low-lying areas and lake basins.

The mineralogy of lower Magniferous Paint Member consists of quartz, chert, goethite, hematite, pyrolusite, illite, kaolinite, cryptomelane, manganite, gibbsite, muscovite, apatite and carbon (Stone et al., 1992). In terms of geochemistry, manganese, alumina and iron abundances increase towards the base (Stone et al., 1992).

The middle Goethite Member is considered a variation of the underlying Magniferous Paint Member, and shows marked increases in the iron/manganese ratio and is composed dominantly of goethite, hematite, kaolinite and quartz (Stone et al., 1992).

The upper Pyrite Member consists of pyrite grains and aggregates, up to several centimeters in diameter, that are interbedded with cherty and aluminous sediments with small amounts of goethite, hematite and carbonaceous material (Stone et al., 1992). The Pyrite member is composed dominantly of pyrite with goethite, hematite, chert, quartz, calcite, limonite and with minor kaolinite and elemental carbon (Shklanka, 1972). The upper Pyrite Member, and its generated mine waste, is the acid generating unit at Steep Rock (Conly and MacDonald, 2004; MacDonald, 2005); Cockerton, 2007; and, Conly et al., 2008ab).

The acid neutralizing unit is the Mosher Carbonate Formations that is composed of calcite, ankerite, dolomite and minor amounts of quartz, pyrite and kerogen (Stone et al., 1992). All

other units, the Marmion Complex, Witch Bay Formation, Wagita Formation and Dismal Ashrock typically contain low abundances of pyrite and, although undetermined, the acid generating capacity is believed to be low.

2.3 Hydrologic Setting

Prior to 1943, most of the study site was beneath Steep Rock Lake, a widening of the Seine River System (Fig. 1.2; Steep Rock Iron Mines, 1943; Taylor, 1976; Surrender 1986). Steep Rock Lake was 14 miles long and took on the shape of a roughly drawn “M”. From east to west the arms of Steep Rock Lake are referred to as Southeast Arm, East Arm, Middle Arm, and West Arm (Fig. 1.3). The headwaters of the Seine originate in a swampy region near Raith, Ontario an unorganized settlement approximately 93 km northwest of Thunder Bay, Ontario on Highway 17. From Raith the water flows through Lac Des Mille Lacs and then through a winding river into Lake Marmion. At the north end of the Southeast Arm, the outlet of Marmion Lake plunged about 30 m into Steep Rock Lake. The Seine River then traveled south down the East Arm, north up the Middle Arm, and then turned south, exiting at the southern end of the West Arm. From there the Seine river continues through Perche Lake, Banning Lake, Chub Lake, Calm Lake, and over Sturgeon Falls before it enters into Rainy Lake at Seine Bay, marking the end of the river system (MNR, 1986).

The first water control developments on the Seine River occurred in 1929 and included the construction of three power generating stations by the Ontario-Minnesota Pulp and Paper Company Limited to power a paper mill in Fort Frances (MNR, 1986). The power generating stations are called Moose Lake (between Marmion Lake and Steep Rock Lake), Calm Lake, and Sturgeon Falls. Lac Des Mille Lacs serves as a reservoir to even flows in the Seine River to ensure steady flow for the hydroelectric dams through the use of a forth dam. The Moose Lake hydroelectric dam was closed to accommodate the Seine River Diversion in 1943, the first water

diversion in Canadian mining history (Taylor, 1978). After failure of underground mining techniques in 1940, a plan was created to divert the Seine River and drain Steep Rock Lake to allow the use of open pit mining methods to mine the iron ore from beneath the Middle and East Arms of Steep Rock Lake. The plan was to isolate Steep Rock Lake by diverting the flow from Marmion Lake through Raft Lake, into Finlayson Lake, and then connect to the West Arm of Steep Rock Lake. The major problem to be overcome during the diversion was the elevation differences between the lakes because Raft Lake and Finlayson Lake water levels were higher than the water elevations of Marmion Lake. At the time the water level in Raft Lake was about 10 m (35 ft) higher than Marmion Lake and the water level in Finlayson Lake close to 0.5 m (2 ft) higher than Raft Lake. The diversion occurred in stages beginning with the Esker Cut at the southern end of Finlayson Lake.

The first stage of the Seine River Diversion involved lowering the water level in Finlayson Lake. A swampy valley sloped down from Finlayson Lake to Wagita Bay in the West Arm of Steep Rock Lake. A channel was dug down the valley, trees were cleared, and a concrete dam was built at Wagita Bay to control the flow of water into the West Arm. The Eagle-Finlayson moraine blocked water from flowing from Finlayson Lake toward the West Arm. To avoid uncontrolled flooding a tunnel was dug in bedrock beneath the esker and up into the bottom of the lake. Once the lake level dropped ~12 m a channel named the Esker Cut at the south end of Finlayson Lake was widened. This segment of the diversion was completed in July 1943. The next stage of the diversion plan was to lower the water level by ~18 m in Raft Lake using pumps so that two ~30 m wide channels could be dug to the east and west of Raft Lake into Marmion Lake and Finlayson respectively. The Raft Lake Cut was completed in December 1943 (Fig. 1.3). Raft Lake Dam was built to control the flow from Marmion Lake to Finlayson Lake. Another dam was constructed across 'The Narrows' between the Middle and West Arm of Steep Rock Lake. Following the completion of the Seine River Diversion work began to drain

the Middle and East Arms of Steep Rock Lake and then to dredge the overburden overlying the ore body (Taylor, 1976; MNR 1985).

The overburden consisting of a thick layer of clay with sand gravel and occasional boulders had a tendency to liquefy. A series of suction dredges were used to pump the overburden through a tunnel from the Middle Arm into the West Arm. The silty-clay overburden deposited in the West Arm washed down the Seine River from Steep Rock Lake to Rainy Lake in 1951 turning the clear waters a muddy grey colour. Complaints of pollution came and as a result a second diversion, called the Western Diversion, was constructed to eliminate the pollution problem (MNR, 1986; Fig. 1.3). The Western Diversion was small relative to the Seine River diversion and served to isolate the West Arm of Steep Rock Lake from the Seine River turning the West Arm into a retention basin for the dredged overburden. The Western Diversion involved increasing the height of Wagita Bay dam and construction of Reed Lake dam and three earth dams at the southern end of West Arm. A channel constructed above Wagita Bay dam diverts water through a series of lakes west of the West Arm reconnecting the Seine River and effectively isolating the West Arm of Steep Rock Lake (Taylor, 1976; MNR, 1986). The Western Diversion was complete in 1952 and successfully eliminated the pollution problem in the Seine River and Rainy Lake.

Caland Ore Limited also undertook its own water diversions, lake draining, and dredging. To minimize the cost of continuous pumping a number of dams, channels and tunnels were constructed to divert water around the East and South East Arms of Steep Rock Lake (Fig. 1.2). Hardy Dam was constructed across Hancock Creek blocking its flow in the South East Arm creating the Rawn Reservoir (MNR, 1986). Water was released from the Rawn Reservoir to Margret Lake flows to the Atikokan River watershed through two tunnels. The flow from three other streams obstructed by the construction of Highway 622 is diverted into the Rawn Reservoir creating the Auxillary Rawn Reservoir via a series of channels and tunnels. Water flowing from

the Southeast Arm into the East Arm is blocked by Fairweather dam where it is pumped up into the Marmion watershed against 47 m of head. The overburden dredged from East Arm was pumped into the southern end of Marmion Lake. A series of dams joining islands just south of Raft Lake outlet were constructed turning the southern end of Marmion Lake into a sediment retention basin (MNR, 1986).

Over 259 km² of the Seine River watershed were affected by the water control structures and retention basins put in place to develop the mines on the Steep Rock Iron Range, permanently changing the watershed. The Seine River Act of 1952 made the changes to the West Arm of Steep Rock Lake irreversible in order to avoid a similar pollution problem to that which occurred in 1951. The conversion of the West Arm increased its water level by 7 m (24 ft) from its original level of 384 m and reduced its depth to about 3 m. Mining activities left large open excavations. The former Steep Rock Lake basin was originally 21 m to 91 m deep and is now up to 335 m below the original lakebed. Since mine closure in 1979 the four open pit mines have been flooding (Fig. 1.1). In 2004, Hogarth and South Roberts pit lakes merged together forming one large pit lake known as Hogarth. Caland and Hogarth pit lakes have been filling independently of each other with all runoff with each of their drainage basins' entering the pits while losses are attributed to infiltration, evaporation and evapotranspiration (MNR, 1986). In 2011 the water level in Caland and Hogarth Pit Lakes was 318.9 m and 313.7 m, respectively. The pit lakes lie in the Seine River watershed, which marks the lowest elevation in the region, 385 m. The only outlet from the pit lakes is through the West Arm's southern outlet because the land surrounding the pit lakes is higher (Figure 2.3).

The regional groundwater flow rate includes groundwater flow seeping through surficial soils and fissures in the surrounding rock. Drainage into Hogarth Pit originates from the West Arm and Highland Lake areas. Drainage into Caland Pit is from the Floodwater Area and

Fairweather Dam and drainage into Fairweather Lake from the based of Hardy Dam, part of the Auxiliary Rawn Reservoir system (Fig. 1.2; Capper, 1978).

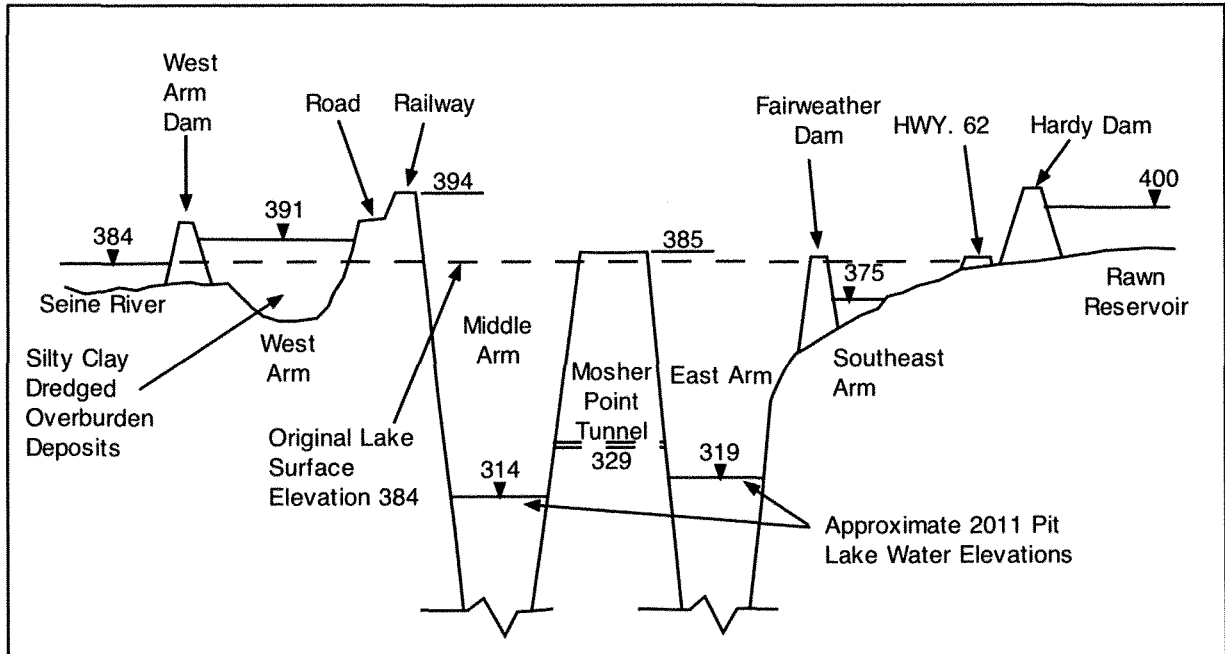


Figure 2.3: A schematic east-west cross-section of Caland (East Arm) and Hogarth Pit (Middle Arm) Lakes (from Sowa et al., 2001). Diagram shows approximate 2011 pit lake water elevations, original lake level and water elevations in the Seine River, West Arm, Fairweather Lake (Southeast Arm) and the Rawn Reservoir.

2.4 Previous Research

Prior to mine closure Steep Rock Resources Ltd. completed an environmental plan (Capper, 1978). The purpose of this plan was to minimize leaching, prevent harmful substances from entering natural watercourses and increase aesthetics of the property. The plan proposed methods for treatment of tailings basins, pyritic stockpiles, water drainage and water quality (Capper, 1978). Tailings ponds and surrounding areas were treated with various amounts of limestone and fertilizer and then seeded with grasses and legumes. Spillways were built in tailings dams in case drainage culverts became plugged. A combined total of 232,000 tonnes of pyritic crude waste is located on the property (Capper, 1978). The majority of the acidic mine waters detected was expected to drain into Hogarth Pit and be neutralized. Some stockpiles were

covered with carbonate and low sulphur waste and other stockpiles in the open pits were submerged as the water levels in the pits increased (Capper, 1978). The environmental plan noted that major influences on water quality were the waste rock piles, pyritic crude ore, and dolomite. Theoretical calculations and experiments led to the conclusion that there was enough carbonate in the wall-rock of the pits to neutralize all the acid that could potentially be generated by the pyrite on the property and thus no treatment would be required (Steep Rock Resources Ltd., 1978). The study also included a rebound model for the water level in the pit lakes.

In 1985, Steep Rock Iron Mines approached the Ministry of Natural Resources (MNR) for a surrender of mining claims covering 52 km² (20 miles²) including all of the former Steep Rock Lake lakebed (MNR, 1986). The main concerns of the MNR included: the changes in water flow and lake elevations, mine waste deposits, structures that could not be removed and two sites contaminated with PCBs. Prior to acceptance of the surrender of mining claims, a two year long study was conducted and focused on the condition of water control structures and the future cost to maintain them. The study concluded that the West Arm water level would remain at or near its current level because the changes made to the West Arm are irreversible under the Seine River Diversion Act of 1952. Thus future management of water levels on the property only includes the Middle, East, and South East Arms. The three main approaches that exist for future management are: 1) protect all developments on lakebed from flooding by keeping the East Arm water level below an elevation of 357 m and the Middle Arm water level to rise to 384 m; 2) let the water level rise to 385 m and gravity flow occur through the West Arm and relocate all developments as the water reaches them; or, 3) select an appropriate water level the Middle and East Arms between the range of 357 m to 388 m based on least cost analysis (MNR, 1986). Two alterations to the current water management system are being considered but only on a conceptual level (R. Purdon, per. comm., September 19, 2011). The first change is to add a culvert or construct an overflow saddle weir at Fairweather dam in order to stabilize water levels

and to eliminate the need for pumping water from Faireweather Lake into Marmion Lake. The second change is to lower the level of the emergency spillway of Hardy dam in order to relieve pressure on the structure during high water levels. Both of these alterations would result in increased volumes of water flowing into Caland pit lake. The surrender report study also included a rebound model for the water level in the pit lakes that has proven to be accurate and will be referred to as the Regional Engineering model in the remainder of this paper. The MNR accepted the surrender of mining claims with the exception of two PCB contaminated sites. Since the surrender, the MNR have had assessments and maintenance works on the various dams associated with the water control structures of Steep Rock Iron Mines.

The water contamination in Hogarth and Caland pit lakes was not a known issue until 1998 when a study was conducted to investigate the impact of a fish farm on pit lake limnology (McNaughton, 2001). Since Caland and Hogarth pit lakes are in close proximity, mined the same ore bodies, and because Caland hosted a fish farm and Hogarth did not, the pit lakes provided an opportunity to look influence of a fish farm on pit lake limnology. In the study, McNaughton (2001) had intended for Hogarth pit lake to be a control lake because no fish farm was present there. However, the study found that Hogarth was acutely toxic while Caland was not. Moreover, the stratification of the two pit lakes was different, Hogarth was a holomictic lake and Caland was a meromictic lake (McNaughton, 2001). The difference in chemistry and stratification was attributed to the greater fresh water input into Caland and the higher pyrite content in the Hogarth pit. Note that the fish farm in Caland pit lake was not part of the closure plan and ceased operation in 2010. The anoxic nature of the lower part of the Caland water column has generally been attributed, although not fully substantiated (Conly et al., 2008), to fish farm activities. Owing to the effect the fish farm had on Caland water quality, resuming such activity is consider by many, including the author, to be highly unlikely. A number of other biology and geology students at Lakehead University have completed research projects

investigating toxicity, fill rates, flooding, and remediation methods at the former Steep Rock Iron Mines site as well as a water quality monitoring program.

Aside from McNaughton (2001) other Lakehead University biology research projects include Vancook (2002), Gould (2008), and Godwin (2010). Vancook (2002) and Lee et al. (2008) conducted a study to predict the future water chemistry of the pits, to model the pit filling rates, and conducted preliminary work on the use of wetlands for the remediation of contaminated water. The accuracy of the pit filling model had recently been questioned, and will be reevaluated in this study. Gould (2008) identified and evaluated the toxicant in the pit lakes. The toxicant was identified to be elevated sulphate concentrations and it was found that the water in Hogarth pit lake has changed from acutely toxic to chronically toxic. Godwin (2010) and Godwin et al. (2010) looked at the productivity of the contaminated waters in Hogarth and did a toxicity assessment. The study examined the effects of different water mixing scenarios between Hogarth and Caland pit lakes on toxicity in an effort to predict future water chemistry changes.

Lakehead University geology, water resource science, and environmental earth science research projects include: MacDonald and Conly (2004), MacDonald (2005), Cockerton (2007), Perusse (2009), Shankie (2011), Timmis (2011), Greiner (in progress) and this study. Conly and MacDonald (2004), MacDonald (2005) and Conly et al. (2008a) conducted a stable isotope study and determined that the source of the elevated sulphate levels in the pits was the pyritic material found in the ore body and submerged waste. Column leaching experiments confirmed that pyritic waste rock was responsible for acid generation and sulphate production (Cockerton, 2007; Conly et al., 2008b). The column leaching experiments confirmed that the carbonate present on the property is capable of neutralizing acid production (Cockerton, 2007). A study by Perusse (2008) was done on groundwater quality downstream from iron oxide and iron sulphide waste tailings ponds and waste dumps in order to investigate if there were differences in groundwater chemistry. The study found high sulphate groundwater down gradient of the sulphide waste

tailings ponds and waste rock dumps (Perusse, 2008). A study completed by Conly et al., (2010) and Shankie (2011) assessed the potential use of permeable reactive barriers for the remediation of high sulphate concentrations in Hogarth pit lake. The tailings and waste rock materials on the Steep Rock site is under study by Timmis (2011) and Greiner (in progress). Timmis (2011) looked at the contamination of small catchment basins and the contamination from surrounding waste rock piles. Greiner (in progress) is conducting kinetic humidity cell tests.

2.4.1 Previous Rebound Models

Four rebound models for the Caland and Hogarth have previously been created, including: Steep Rock Resources for their Environmental Plan (Capper, 1978); the Regional Engineering model by the MNR for the Surrender of Mining Claims Report (1986); Vancook (2002); and Jackson (2007). The Steep Rock Resource Environmental Plan model predicts a rebound rate about 10 years faster than the MNR Regional Engineering Model (MNR, 1986). Based on extrapolation of rebound graphs given in the Surrender Report (1986), the water level in the East Arm will reach 385 masl in 2057 and will reach 394 masl in elevation in 2068 (Table 2.1). The water elevation of the West Arm (391 masl) is used in the Vancook (2002) and Jackson (2007) models as the final water elevation reached in their models. This is below the elevation of the expected outlet to the West Arm but is above the elevation where Caland and Hogarth are expected to join. According to Vancook (2002) Caland and Hogarth will reach an elevation of 390 masl in 2030 (Table 2.1). However, the accuracy of Vancook's (2002) model is questionable because it predicts a significantly quicker rebound rate than the Regional Engineering model (Figs. 2.4 and 2.5). The model made by Jackson (2007) predicts the pit lakes will reach an elevation of 390 masl in 2082 (Table 2.1). The Regional Engineering model has proven to be reasonably accurate with respect to measured water elevations for both pit lakes and is generally within 1 to 2 m of measured water elevations between 1979 and 2011 (Figs. 2.4 and 2.5). Since the predictions of

the Regional have proven most accurate it will be the only model used for comparison with study’s rebound model predictions. Although the Regional Engineering model is reasonably accurate, documentation describing the methods used to construct the model is poor. Furthermore, this study’s models will contain more measured meteorological data to better constraining parameters such as precipitation volumes.

Table 2.1: Summary of previous rebound model predictions.

Model	Pits Join		Pits Outflow	
	Predicted Year	Years from closure	Predicted Year	Years from closure
Previous Works				
Capper (1978)*	2044	65	2049	70
Regional Model (1986)*	2057	78	2069	90
Vancook (2002)	2027	49	2030	51
Jackson (2007)	2059	80	2059	80

* Values extrapolated from graph provided in reports.

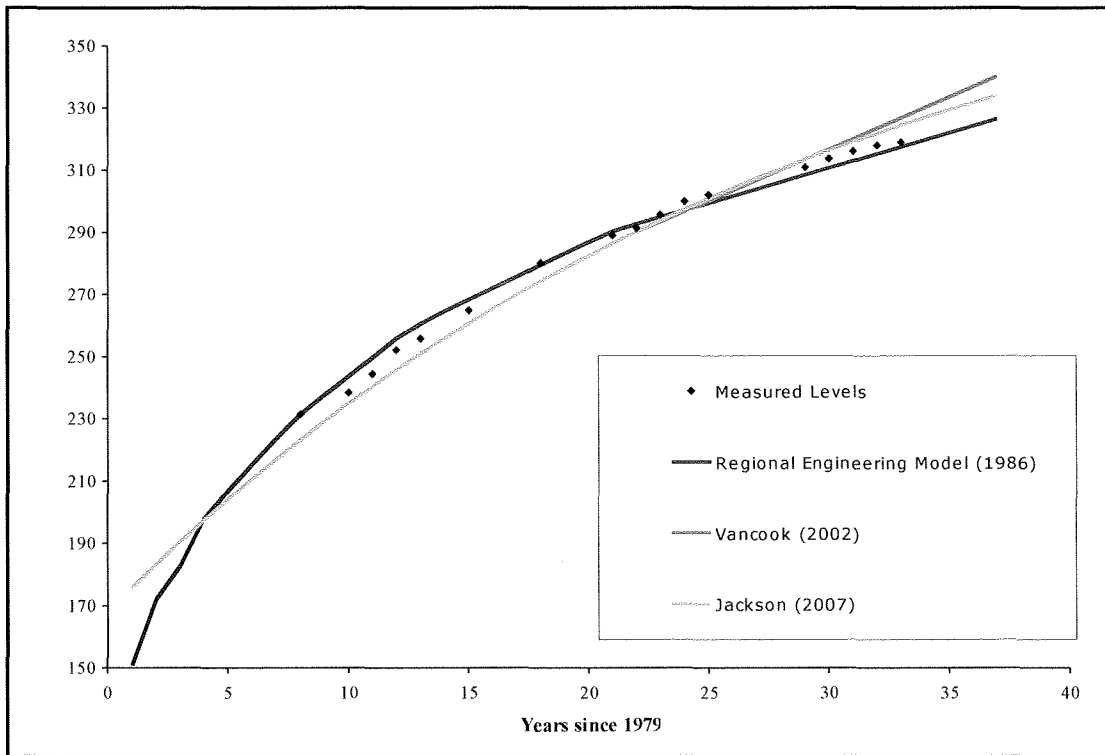


Figure 2.4: Comparison of previous predictions made for rebound Caland pit lake to measured water elevations.

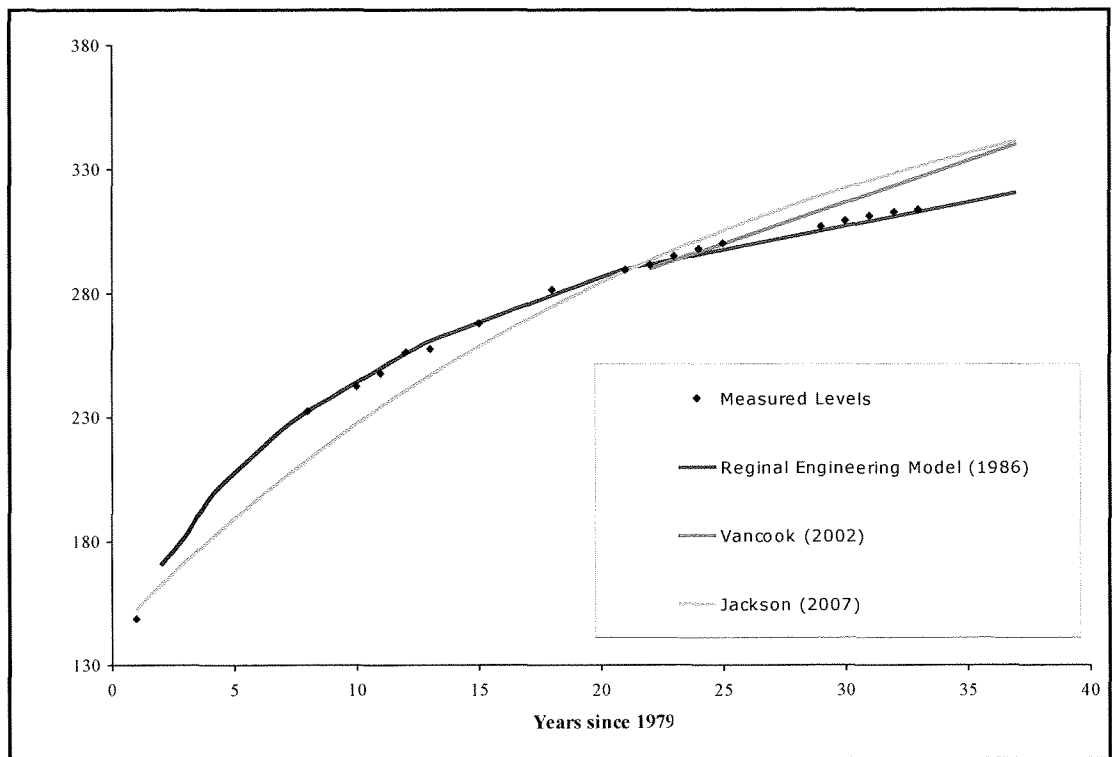


Figure 2.5: Comparison of previous predictions made for rebound in Hogarth pit lake to measured water elevations.

Chapter 3: Rebound and Water Balance Models

3.1 General Introduction and Scope of Work

When undertaking a hydrologic study it is important to understand the principle of conservation of mass or ‘mass continuity’. This is considered by some to be the core paradigm in hydrology, as a failure to consider mass continuity can lead to major calamities (Surrano, 1997; Younger et al, 2002). A basic application of mass continuity in hydrology is the water balance that can simply be expressed as:

$$\text{“water entering”} - \text{“water exiting”} = \text{“change in stored volume”} \quad (\text{Eqn. 3.1})$$

Water level changes are easily related to the changes in storage: the volume of the void taken up by water as it rises to a new level equals the amount of water added to the system (Younger et al., 2002). Therefore, by modeling the relationships between stage, volume and surface area of an open pit mine void and calculating a water balance, it is possible to predict the rebound rate and future water levels. Before predictions can be made with any model the project objectives and a conceptual model of the system in question must be clearly defined. Construction of a conceptual model usually includes definition of limits, assumptions and parameters and is followed by calibration (Bear, 1979; Younger et al., 2002). It is important to understand the limitations and assumptions in the model as they introduce uncertainty (Bear, 1979).

The aim of this chapter is to develop a rebound model for Caland and Hogarth pit lakes and compare results to measured water elevations and to previous predictions. Three different approaches are used to predict rebound in this study. The first two models use a void filling

approach, where void volumes with elevation are represented by a “hypsothetic curve”, which is a cumulative frequency curve of mine void volume against height. These models assume that the water level in the pit lakes will follow the shape of the hypsothetic curve. The water balance of each pit lake is computed following the equation from Shevenell (2000a) for the Gretchell pit lakes in Nevada. The difference between hypsothetic models is the calibration (see sections 3.6.1 & 3.6.2). The first calibration method is based on adjusting the rate of groundwater inflow until predicted water levels match measured water levels during the calibration period. The second calibration method determines the groundwater term by difference between years with measured water elevations. The final modeling method consists of fitting an exponential curve to measured water elevations and forecasting future water levels.

This study’s models will provide annual water level predictions up to an elevation of 394 m, the elevation of the outlet to the West Arm, which is higher than the final water elevations assumed in previous models. In addition a sensitivity analysis is completed to investigate the individual influence of each parameter on the model results.

3.2 Conceptual Model

Caland and Hogarth pit lakes can be conceptualized as two misshapen bowls open to the atmosphere. The pits receive water from precipitation landing on the pit lake surface, runoff from pit walls and from lateral groundwater flow. The pit lakes lose water via evaporation at the pit lake surface and eventually from outlets. The conceptual model for this study assumes that Caland and Hogarth will be allowed to flood unabated and as the pit lakes flood they will join forming one lake large pit lake. After the pit lakes join, they will continue to flood until they reach the elevation of an outlet into the West Arm.

The land area that contributes runoff to the pit lakes is a key control in the calculation of the water inputs. As rebound progresses and with alteration to water control structures the

watershed area contributing runoff to the pit lakes changes. These changes occur at key elevations during the rebound process. Caland and Hogarth pit lakes are located in the East and Middle Arms, respectively (Figs. 1.2 and 1.3). Fairweather Lake comprises the Southeast Arm and is separated from the East Arm by Fairweather Dam. The East and Southeast Arms were originally one large catchment with an area of approximately 64.7 km^2 . The Auxillary Rawn Reservoir System was created to divert runoff from approximately 40.1 km^2 of the catchment out of the Seine River watershed and into the Atikokan River system (Fig. 1.2). Alteration of the Auxillary Rawn Reservoir system can change the watershed area draining into the Southeast Arm and subsequently the East Arm. This study does not take into account any changes to the Auxillary Rawn Reservoir System. The total catchment areas that contributing water to the Middle, East and Southeast Arms, are $\sim 7.4 \text{ km}^2$, $\sim 16.8 \text{ km}^2$ and $\sim 7.8 \text{ km}^2$, respectively (MNR, 1986).

Currently, a pumping station at the base of Fairweather Dam controls the water level in Fairweather Lake; however, it is assumed that pumping will cease in 2014 and that an overflow saddle weir will be constructed to allow water to flow from the Southeast Arm into East Arm (R. Purdon, per. comm., Sept. 19, 2011). The water level of Fairweather Lake after the dam breach is assumed to remain at its current level (375 masl) until the water level in Caland reaches the same elevation. In the water balance calculations, the Southeast Arm catchment area is added to the East Arm catchment area for the determination of the Caland watershed area contributing runoff starting in 2014. The model assumes that Caland and Hogarth pit lakes will join before water from the pits outflow into the West Arm. Contours based on 1982 aerial photographs were visually examined using ArcGIS 9 to determine the elevation at which Caland and Hogarth join. It is determined that water from Caland will flow into Hogarth when the water level in Caland reaches an elevation of 385 masl. In the water balance calculations, once the water level in

Caland reaches 385 masl, the East and Southeast catchment areas are added to the Middle Arm catchment area in the calculation of runoff for Hogarth. At this point in the water balance calculations and water level predictions terminate for the individual pit lakes and the all the lakes are considered as one in the remainder of the water balance calculations for Hogarth pit lake's rebound models. Because both pits are currently flooding independently of each other and the water level in Caland is rising at a slightly faster rate, Caland will flow into Hogarth following the original flow of the former Steep Rock Lake (Figs. 1.2 and 1.3). After the two pit lakes join, they are predicted to outflow into the West Arm at the Narrows Dam (Fig. 1.2). The crest of the Narrows Dam has an elevation of 396 to 397 masl but the model assumes a water control channel 2 m lower will be constructed (R. Purdon, per. comm. Jan. 12, 2011). The termination of the rebound model is when the predicted water level in for the new Steep Rock Pit Lake reaches 394 masl.

3.3 Stage – Volume Relationships

The stage-volume relationships, which define the volume of the pits to be flooded, are key parameters in the rebound model. The volumes of Hogarth, Caland and Fairweather Lake are calculated using contour intervals and the surface area computed for each contour interval up to an elevation of 400 masl. For the pit elevations below 200 masl, measurements are taken directly from the pit limits based on 30 m contour interval provided in the Steep Rock Environmental Plan (Capper, 1978). Data for elevations from 200 to 400 masl are taken from 10 m contours based on 1982 aerial photography. Using ArcGIS 9, contours were traced to create polygons then the surface area of each polygon was measured. Islands were traced and their areas subtracted from the appropriate contour surface areas. The surface areas for Fairweather Lake were added to those of Caland at the appropriate elevations and the areas of all three lakes are summed at an elevation of 390 masl. The volumes of each pit lake are summed in ascending order with

elevation to determine the cumulative volume of the lakes with elevation. The volume between each contour interval is calculated using the equation:

$$\text{Volume (m}^3\text{)} = (h/3) \cdot (a_1 + a_2 + \sqrt{a_1 \cdot a_2}) \quad (\text{Eqn. 3.2})$$

Where:

- h = contour interval (m)
- a₁ = area of lower contour (m²)
- a₂ = area of upper contour (m²)

The elevation, surface area and accumulated volume data are used to create hypsometric curves and elevation – surface area curves for Caland and Hogarth pit lakes. The pit lake volume calculations are provided in Appendix I. Exponential trendlines are fitted to scatter plots of cumulative volume and elevation data to create hypsometric curves, and to surface area and elevation data (Figs. 3.1 and 3.2). The equations for these relationships are used in the water balance calculations to determine the water surface elevation and pit surface area for each timestep (Figs. 3.1, 3.2, 3.3 and 3.4). The hypsometric curves are used in the water balance calculations to determine the initial volume of water in the pits given known water elevations and water elevations given the accumulated volume calculated for that year. The determined elevation is then used in the elevation – surface area equation to determine the surface area of the pit for that year.

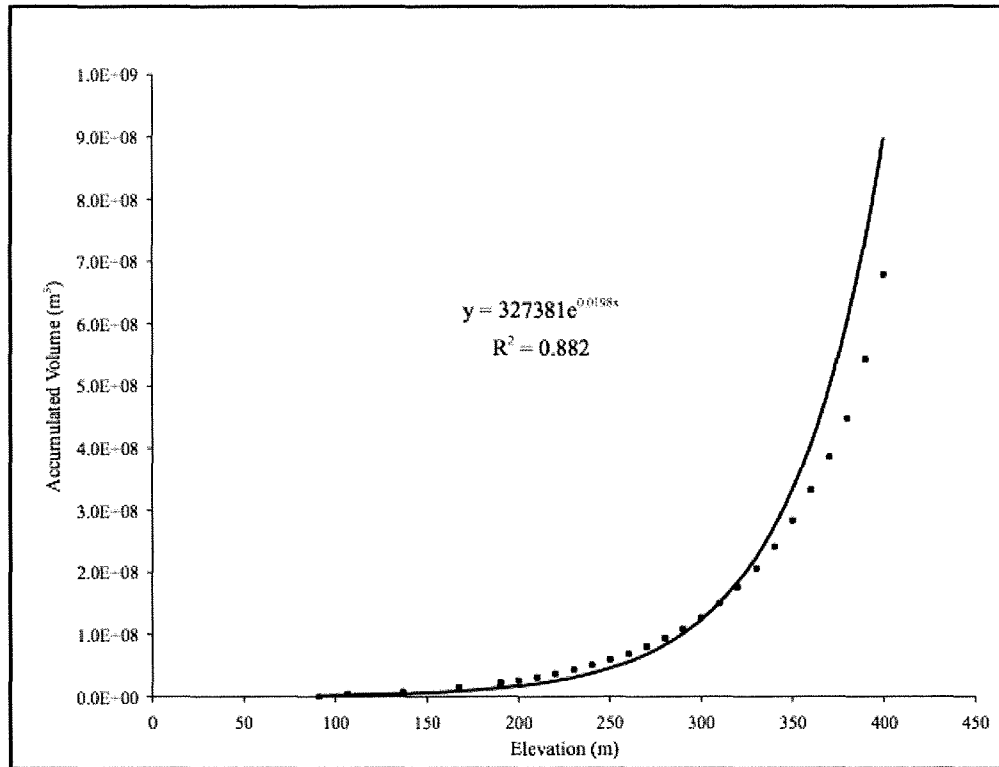


Figure 3.1: The hypsometric curve for Caland pit. The hypsometric curve is shown by the black line and the points are the determined accumulated volume with elevation.

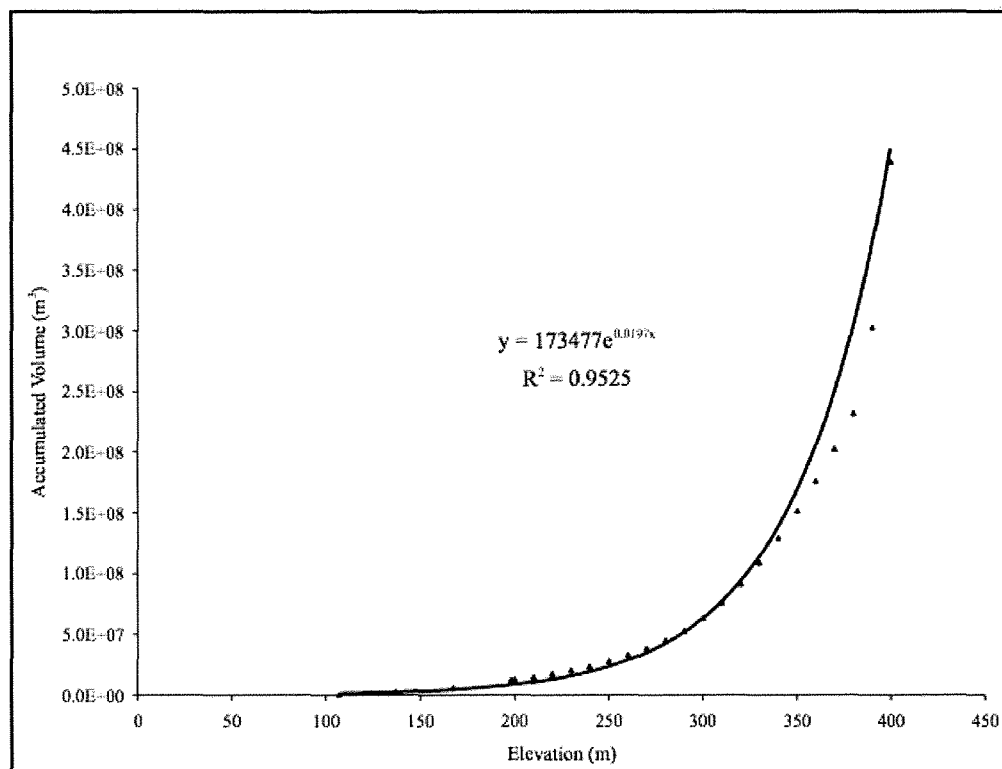


Figure 3.2: The hypsometric curve for Hogarth pit. The hypsometric is shown by the black line and the points are the determined accumulated volume with elevation.

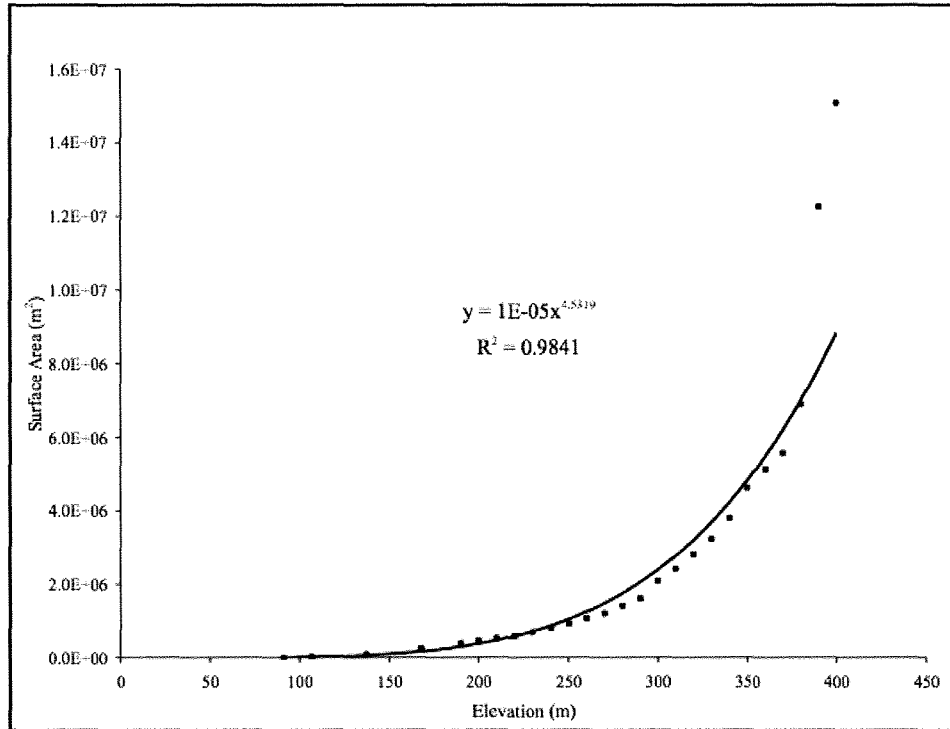


Figure 3.3: The elevation – surface area curve for Caland pit. The elevation-surface area curve is shown by the black line and the points correspond to the measured surface area at each contour interval of the pit.

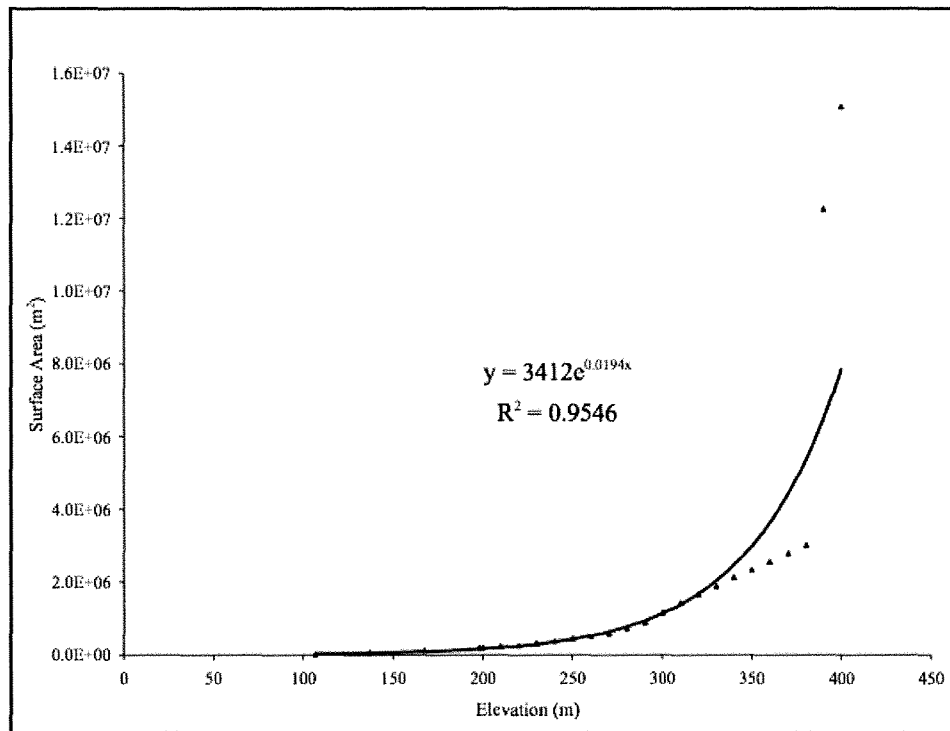


Figure 3.4: The elevation – surface area curve for Hogarth pit. The elevation-surface area curve is shown by the black line and the points correspond to the measured surface area at each contour interval of the pit.

3.4 Water Balance

The water balance of Caland and Hogarth pit lakes was determined following the example of Shevenell (2000a). The Caland and Hogarth water balance are calculated separately until the pits join when the water level reaches 385 m in elevation, as described in the conceptual model (section 3.2). The pit lake water balances are represented by the equation:

$$P + R - E + (GW_i - GW_o) = \Delta S \quad (\text{Eqn. 3.3})$$

Where:

- P = precipitation (m³/year)
- R = runoff (m³/year)
- E = evaporation (m³/year)
- (GW_i - GW_o) = net groundwater flux (m³/year)
- ΔS = change in storage (m³/year)

The change in storage (ΔS) was calculated annually, from 1980 until the pit lake water level reaches 394 masl. The change in storage was summed to the accumulated volume in the previous year in order to determine that years accumulated volume. The initial pit volume was determined using the known elevation in 1979 and 1986 in Hogarth and Caland, respectively, and the stage-volume relationships.

Precipitation (P) is the amount of precipitation that lands directly on the pit lake surface each year and was calculated using the equation (Surrano, 1997):

$$P = p/1000 * SA_P \quad (\text{Eqn. 3.4})$$

Where:

- p = annual precipitation rate (mm/year)
- SA_P = area of the pit lake surface (m²)

The annual precipitation rate (p) was calculated from historical weather records from the National Climate Data and Information Archive (see section 3.5.1). The surface area of the pit

lake (SA_p) varies through time and was determined from the accumulated volume from the previous timestep and the stage-volume relationships described in section 3.3.

Runoff (R) is the amount of precipitation landing within the watershed that drains into the pits and is not lost to evaporation, infiltration or soil absorption. R was calculated using the equation based on the equation used in the Regional Engineering model (MNR, 1986):

$$R = p/1000 * SA_w * RF \quad (\text{Eqn. 3.5})$$

Where:

SA_w = watershed surface area

RF = retention factor

The watershed surface area (SA_w) varies through time and was calculated by taking the total watershed areas contributing water to each pit and subtracting surface area of the pit lakes calculated in the previous timestep. The total watershed areas draining into Caland and Hogarth Pit Lakes changes as described in the conceptual model.

The retention factor (RF) is the percentage of precipitation landing within the watershed area that enters the pit lakes as runoff. A 40% retention factor was used, which is the same as in previous water balance calculations (MNR, 1986). The methods used to determine the retention factor was not described in the Surrender Report (MNR, 1986).

Evaporation (E) is the amount of water evaporating from the pit lake surfaces each year and was calculated accordingly:

$$E = e/1000 * SA_p \quad (\text{Eqn. 3.6})$$

Where:

e = annual evaporation rate (mm/year)

SA_p = pit lake surface area

The annual evaporation rate (e) was determined using historical weather data from National Climate Data and Information Archive, and is estimated following the method described in section 3.5.2.

In order to simplify the model, groundwater inflow (GW_i) and groundwater outflow, (GW_o) were considered as a combined term, the net groundwater flux ($GW_i - GW_o$) following the example of Shevenell (2000a). The net groundwater flux does not consider where or how the water is entering or exiting the pit lakes. Therefore, the model does not require constraints on hydraulic properties or gradients for which there is limited information for the study area. The net groundwater flux term is used to calibrate the model as described in section 3.6.2.

3.5 Determination of Meteorological Parameters

The required meteorological parameters for the water balance calculations are precipitation and evaporation. Meteorological data was acquired from the National Climate Data and Information Archive (www.climate.weatheroffice.gc.ca). Measured values without missing or estimated data are used in water balance calculations whenever possible. The proceeding sections (3.5.1 and 3.5.2) described how annual precipitation and evaporation rates were determined for use in the water balance calculations.

3.5.1 Precipitation

Precipitation data was acquired from National Climate Data and Information Archive for weather stations within 25 km of Atikokan. Four weather stations met the search criteria, but only two had monthly precipitation data during the period of between 1979 and 2009. For each year the monthly precipitation totals were summed to determine the total annual precipitation. Measured precipitation data (without missing or estimated values) exists for 1979 to 1987 and 1995 to 2005 from Atikokan and Atikokan-Marmion weather stations, respectively.

For the period from 1988 to 1994, the missing precipitation data is estimated. Two estimation methods for precipitation were considered: the weighted average method and the normal inverse ratio method (Surrano, 1997). The weighted average method, developed by the

U.S. Weather Service, requires data from four index stations located as close as possible to the station with missing data. One of the index stations must be located in one of the four quadrants delimited by a north-south and east-west axis drawn through the station in question. This method cannot be used in mountainous regions (Surrano, 1997). In the normal inverse ratio method, the missing precipitation value is estimated based on at least three index stations that are as evenly spaced from the station with missing data as possible. Annual precipitation values are typically used in the calculation but monthly values can be used as well.

Potential index weather stations within 200 km of Atikokan and with monthly precipitation data for the period from 1979 to 2006 are listed in Table 3.1 and their locations are shown Figure 3.5. After examining the weather station locations it was concluded that there was insufficient data for the weighted average method because the requirement of having a weather station in each of the four quadrants was not met. A cluster of relatively equally spaced weather stations exists to the west of Atikokan. Consequently, the normal inverse ratio method is well suited to the available data because the weather stations are evenly spaced around Atikokan, and located to the west eliminating the influence of Lake Superior. Precipitation across the region is influenced to varying degrees by Lake Superior. Winds off Lake Superior can increase atmospheric moisture, an affect that decreases with distance (Heinselman, 1996). This affect on precipitation can be seen by looking at the precipitation rates and the distance of index weather stations from Atikokan, the further the index weather station is to the west the lower its annual precipitation rate (Table 3.1). To further evaluate whether the precipitation values from the index stations are representative of Atikokan, the average monthly distribution values from 1971 to 2000 Canadian Climate Normals were plotted for comparison (Fig. 3.6).

Table 3.1: List of weather stations used in the estimation of missing precipitation values from the National Climate Data and Information Archive.

Station Identifier	Climate ID	Approx. Distance from Atikokan (km)	Latitude °N	Longitude °W	Elevation (m)	Annual Precipitation (mm/year)
Atikokan Marmion	6020384	-	48°48.000'	91°34.800'	442	-
Atikokan	6020379	-	48°45.000'	91°37.200'	395	739.7
Fort Francis A	6022476	133	48°39.000'	93°25.800'	342	720.7
Fort Francis	6022475	134	48°37.200'	93°25.200'	343	709.5
Dryden A	6032117	144	48°46.800'	92°49.800'	372	701.5
Dryden	6032119	145	48°49.800'	92°45.000'	413	705.5
Mine Centre	6025203	74	48°46.200'	92°37.200'	343	728.6
Rawson Lake	6036904	183	48°39.000'	93°43.200'	358	688.4
Stratton Romyn	6028182	188	48°42.000'	94°10.200'	366	711.1



Figure 3.5: Google image of weather station locations used in this study and that of Heineselmen (1996). Weather stations marked by yellow flags are stations with 25 km of Atikokan; blue flags are stations within 200 km to West of Atikokan; green are stations used by Heineselmen (1996); and, the orange flag is the Thunder Bay weather station.

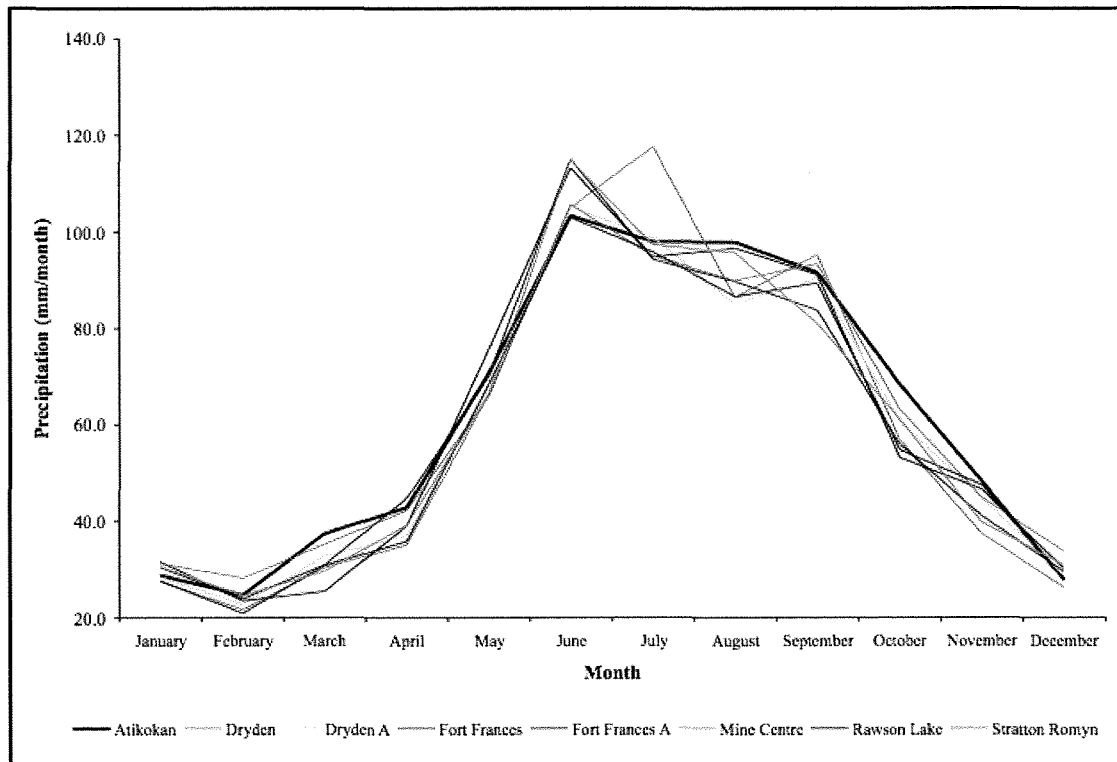


Figure 3.6: Comparison of average monthly precipitation distributions of the index stations to the Atikokan weather station used in the normal inverse ratio method of estimating precipitation.

All weather stations except those in Dryden have a similar monthly precipitation distribution; however, Dryden stations are used in the estimation of precipitation in order to meet the minimum required number of index stations for each year precipitation is estimated. The monthly precipitation rates in Dryden are close to those in Atikokan but Dryden has a higher maximum monthly precipitation rate (117.5 mm/month) and it occurs in July instead of June like Atikokan (103.3 mm/month; Fig. 3.6).

Precipitation data from the index weather stations was processed in the same manner as the Atikokan data described above to determine annual precipitation totals for each station. The normal inverse ratio is expressed accordingly (Surrano, 1997):

$$\frac{P_1}{P_1} = \frac{1}{(N-1)} \left(\frac{P_1}{P_1} + \frac{P_2}{P_2} + \frac{P_3}{P_3} + \frac{P_4}{P_4} + \dots + \frac{P_N}{P_N} \right) \quad (\text{Eqn. 3.7})$$

Where:

P_1 = missing measured precipitation value at station of interest

$P_2 \dots P_n$ = measured precipitation value at index stations for the concurrent period

$P_{1(\text{bar})}$ = mean annual precipitation value at station of interest

$P_2 \dots P_{n(\text{bar})}$ = mean annual precipitation value at index station

N = total number of weather stations (Surrano, 1997).

The total number of weather stations varies depending on the number of index stations with measured data for that particular year. The mean annual precipitation values are equal to the total precipitation from the 1971 – 2000 Canadian Climate Normals for each station. The calculation of the missing precipitation data using the normal inverse ratio method is given in Appendix II.

Predicted precipitation values were compared to measured values (Fig. 3.7). The estimated precipitation values followed a similar pattern to measured values. The percent difference between measured and estimated values is less than or equal to 13% except in 2003 where there is a 25% difference. The large variation in 2003 is likely because the index weather stations on average had annual precipitation values significantly less than those measured in Atikokan. All variations in the estimated precipitation values likely result from the index stations having on average higher or lower measured annual precipitation relative to Atikokan. The variance in measured precipitation may be due to the fact that the Atikokan weather stations are located at a higher elevation than the index stations (Table 3.1). The error in precipitation measurements from a rain gauge that is properly sited, maintained and calibrated is +/- 10% and the difference between estimated precipitations rates and measured rates in this study is typically less than or equal to 13%, the error in the estimated precipitation values is considered acceptable for use in the water balance model (Levin and Cotton, 2009). From the year 2003 and to model termination, an annual precipitation value of 739.6 mm/year (based on the 1971-2000 Canadian Climate Normals) is used in the water balance calculations. The year 2003 is the last year with

measured precipitation data. The use of predicted precipitation values may increase the accuracy of the models compared to a constant rate because the predicted values would show precipitation variability over time.

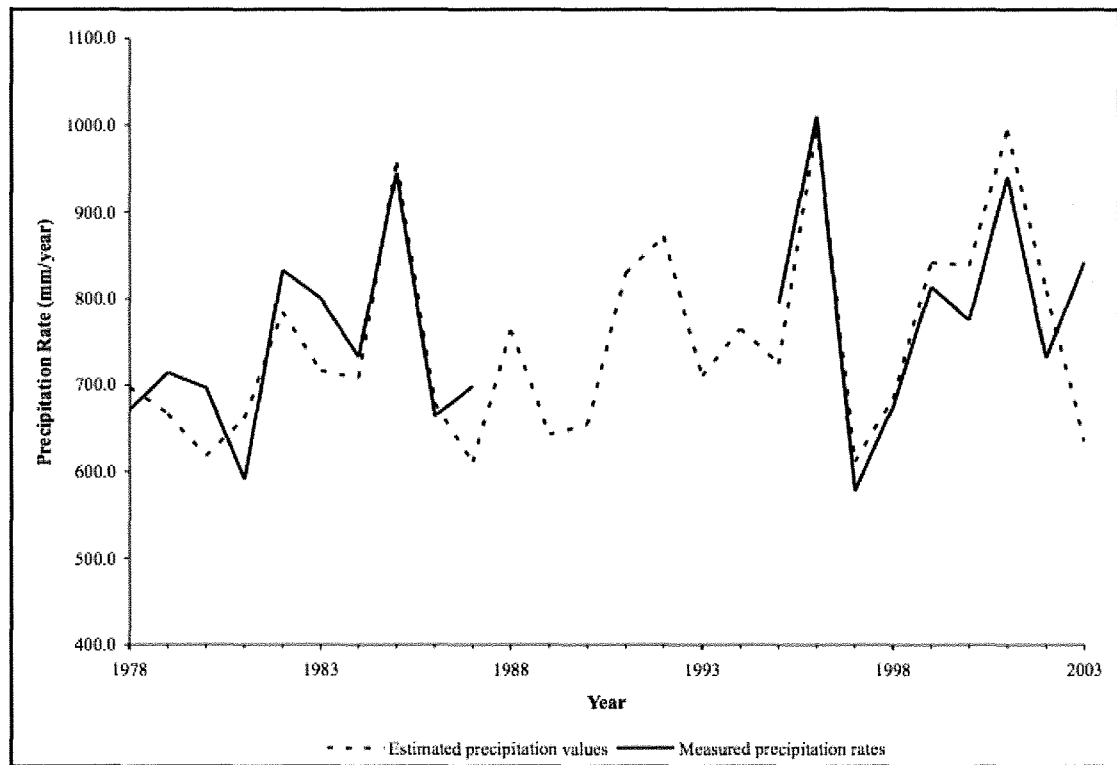


Figure 3.7 Comparison of estimate annual precipitation to measured annual precipitation from 1978 to 2003 at the Atikokan weather station.

3.5.2 Evaporation

One weather station, Atikokan, has pan evaporation measurements for 1966 to 1988.

Evaporation was measured each year for a period of six months, May to October. Annual totals are based on cumulative daily values. Measured evaporation data was used in the water balance calculation from 1979 to 1988. The average evaporation value for that period is 511.4 mm/year, which is higher than that for the period 1966 to 1988 (461.3 mm/year). An attempt was made to predict evaporation rates for the remaining years during the calibration period. Two methods, the

Penmen Equation and the Thornwaite Equation, were used (Penman, 1948; Thornwaite, 1948; Surrano, 1997; Cornwell and Harvey 2007). The Penman method estimates evaporation using the following equations (Eqns. 3.8 – 3.10):

$$PET = (aE_n + E_a)/(a-1) \quad (\text{Eqn. 3.8})$$

Where:

PET = potential evapotranspiration (mm/day)

a = function of air temperature (Ponce, 1989)

E_n = net radiation in evaporation units (mm/day)

E_a = mass-transfer in evaporation rate units (mm/day)

$$E_n = (C_1 Q_n)/pL \quad (\text{Eqn. 3.9})$$

Where:

C₁ = unit conversion constant (1000 mm/m)

Q_n = net radiation (cal/m²•day)

p = density of water (1000 kg/m³)

L = latent heat of evaporation (cal/kg)

$$E_a = ((100-r)/100)(c_2+c_3W)e_s \quad (\text{Eqn. 3.10})$$

Where:

r = relative humidity (%)

c₂ = 0.1733 mm/day•mmHg

c₃ = 0.0512 mm•hour/day•km•mmHg

W = wind speed (km/hour)

E_s = saturated vapour at surface air temperature (mmHg)

The Thornwaite method estimates evaporation (E_p) using the equations (Eqn. 3.11 – 3.13):

$$E_p = \begin{cases} 0.444h((10T_a)/I)^m, & 0 \leq T_a \leq 26.5^\circ\text{C} \\ -13.862 + 1.0747T_a - 0.01442T_a^2, & T_a \geq 26.5^\circ\text{C} \\ 0, & T_a < 0^\circ\text{C} \end{cases} \quad (\text{Eqn. 3.11})$$

Where:

T_a = air temperature

h = hours of sunlight per day

$$I = \text{sum of } (T_M/5)^{1.514} \quad (\text{Eqn. 3.12})$$

Where:

$I > 0$

T_M = average monthly temperature

$$m = (6.75 \cdot 10^{-7})I^3 - (7.71 \cdot 10^{-5})I^2 + (1.79 \cdot 10^{-2})I + 0.492 \quad (\text{Eqn. 3.13})$$

The Penman method generally overestimates evaporation rates whereas the Thornwaite method tends to underestimate rates (Serrano, 1997). Evaporation estimates were calculated as daily average values using the Penman and Thornwaite equations. The solar radiation data was measured at a weather station in Moosonee, Ontario, which is the nearest weather station to Atikokan that measures global solar radiation. The Penman estimates are close to measured values, overestimating them in the spring and underestimating them in the fall. The Thornwaite equation significantly underestimates the evaporation rates, even when corrected for latitude using correction constants given in Surrano (1997; Fig. 3.8). The calculation of missing evaporation data using the Penman and Thorwaite equations is provided in Appendix III.

Although, the Penman evaporation estimates are close to average monthly values, the annual total evaporation predicted 548 mm/year, is higher than the average measured evaporation rates for the period from 1979 to 1988 (511.4 mm/year) and from 1966 to 1988 (461 mm/year). Because the estimated evaporation rates over- and underestimate measured values and could not be calculated for each year during the remainder of the calibration period because of data limitation, the average annual measured evaporation rate of 511.4 mm/year is used in the calculations from 1989 and on. Like precipitation, the use of estimated evaporations rates, if data is available, would likely increase the accuracy of the models compared to constant rates because the estimate evaporation rates would show annual variability.

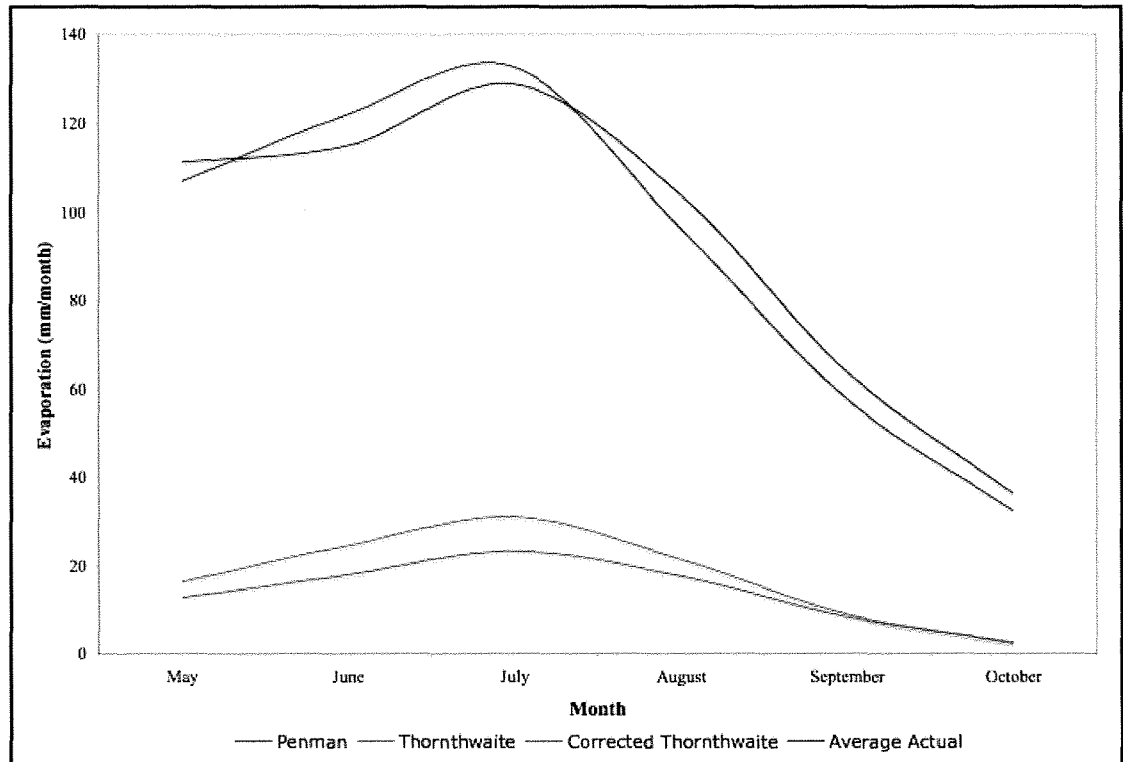


Figure 3.8: Graph showing measured and estimated monthly evaporation rates.

3.6 Rebound Models and Calibration

3.6.1 Models

Rebound in the Steep Rock pit lakes is predicted in two ways. First, a void filling approach is used where the stage-volume relationship are described in section 3.3. Two variations of each of the rebound prediction methods, Models 1A & B and Models 2A & B, are made based on different calibration methods described in section 3.6.2. Secondly, rebound is predicted by simply extrapolating an exponential curve fitted to measured water elevations. In this method an exponential trend line is based on measured water level taken between 1979 – 2009 for Caland and Hogarth and the curve was forecasted into the future until predicted water

levels reach 394 masl. Exponential curves were calculated for Caland and Hogarth in Model 3A and 3B, respectively, and these models are not calibrated.

3.6.2 Calibration

The groundwater water flux term is used to calibrate the rebound models 1A, 1B, 2A and 2B. In the first calibration method (Model 1), the average net groundwater flux term is found by adjusting the net groundwater flux term by trial and error each year so that predicted water levels match measured levels during the calibration period. For the second calibration method (Model 2), the net groundwater flux term is determined by difference for years with measured water levels, precipitation and evaporation data.

Model 1A and 1B are constructed using the first calibration method. The difference between Model 1A and 1B is the length of the calibration period. In model 1A, the calibration periods for Caland and Hogarth are from 1986 to 2009 and 1979 to 2009, respectively. In model 1B, the calibration periods for Caland and Hogarth are from 1986 to 2003 and 1979 to 2003, respectively. The difference between Model 1A and Model 1B is that Model 1A includes a period of time, from 2006 – 2009, where a constant precipitation rate is used instead of measured or predicted precipitation due to data limitations whereas Model 1B calibration period only includes years with measured and estimate annual precipitation values. During the calibration period measured water levels were not available for 1979 – 1985, 1987, 1992, 1994, 1995, 1997, 1998, 2005 and 2006 with the exception of a measured level in 1979 for Hogarth only. The annual net groundwater flux rate is only changed on or immediately after years with measured water levels and remains constant for years between measured water levels. Once predicted water levels matched measured water levels for the calibration period, the net groundwater influx values for the calibration period are averaged to determine the average annual net groundwater influx rate for each pit. The average annual net groundwater flux is then used in the water

balance calculations for each pit lake starting in 2010 to predict future water levels and to back cast water levels in Caland to the year 1979.

The second calibration method is used for Models 2A and 2B. In these models the net groundwater flux term is determined by difference using the equation from Shevenell (2000a):

$$(GW_i - GW_o) = (V_2 - V_1) - P - R + E \quad (\text{Eqn. 3.14})$$

Where:

V_1 = volume of pit lake at time, t_1

V_2 = volume of pit lake at time, t_2

V_2 and V_1 are calculated using the stage-volume relationships and water balance calculations for years with known water elevations. Then net groundwater flux is computed by difference between the timesteps with measured elevations. The net groundwater influx was calculated for both pit lakes for 1988 to 1991, 1993, 1996 and 1999 to 2003, with one additional timestep, 1986 for Hogarth only. The average annual net groundwater flux value is computed by averaging the net groundwater flux values determined by difference in the calibration period. The difference between Model 2A and 2B is that the computed average annual net groundwater flux values for Model 2B only includes net groundwater flux values calculated where back-to-back annual measured water levels exist, whereas Model 2A includes net groundwater influx values averaged between years without back-back measured water elevations. After the calibration period, the groundwater influx value is held constant and equals the average net groundwater flux calculated by calibration method.

3.7 Sensitivity Analysis

The model that best matches measured water elevations between 1979 and 2011 and the predictions of any previous rebound model that has proven accurate, will undergo a sensitivity

analysis designed to investigate how sensitive model results are to variations in individual parameter values. The selected rebound model was run a number of times with an individual parameter varied by a certain percentage each time, in order to see the parameters influence on rebound rate predictions. The water balance parameters that are varied are precipitation, runoff, evaporation and the net groundwater influx. The model selected and the manner in which each parameter is varied is described in section 3.8.5 and subsections within.

3.8 Results

3.8.1 Summary of this study's predictions

Results of the rebound models are summarized in Table 3.2 and Figures 3.9 and 3.10. The calculated average annual groundwater influx rates determined during the calibration period are given in Table 3.3. Complete water balance calculations and water level predictions for rebound Models 1A, 1B, 2A, 2B, 3A and 3C are provided in Appendix IV.

Table 3.2: Rebound model predictions for when Caland and Hogarth join and outflow into the West Arm.

Model	Pits Join		Pits Outflow	
	Predicted Year	Years from closure	Predicted Year	Years from closure
This Study				
1A	2075	96	2093	114
1B	2077	98	2095	116
2A	2064	85	2078	99
2B	2070	91	2087	108
3A	2067	88	2080	101
3B	2123	144	2152	173

Table 3.3: The net groundwater influx values calculated during each of the models respective calibration period.

Calculated Annual Net Groundwater Influx (m ³ /year)		
Model	Hogarth	Caland
1A	322319	80300
1B	322295	620500
2A	1031614	2106246
2B	625289	1401100

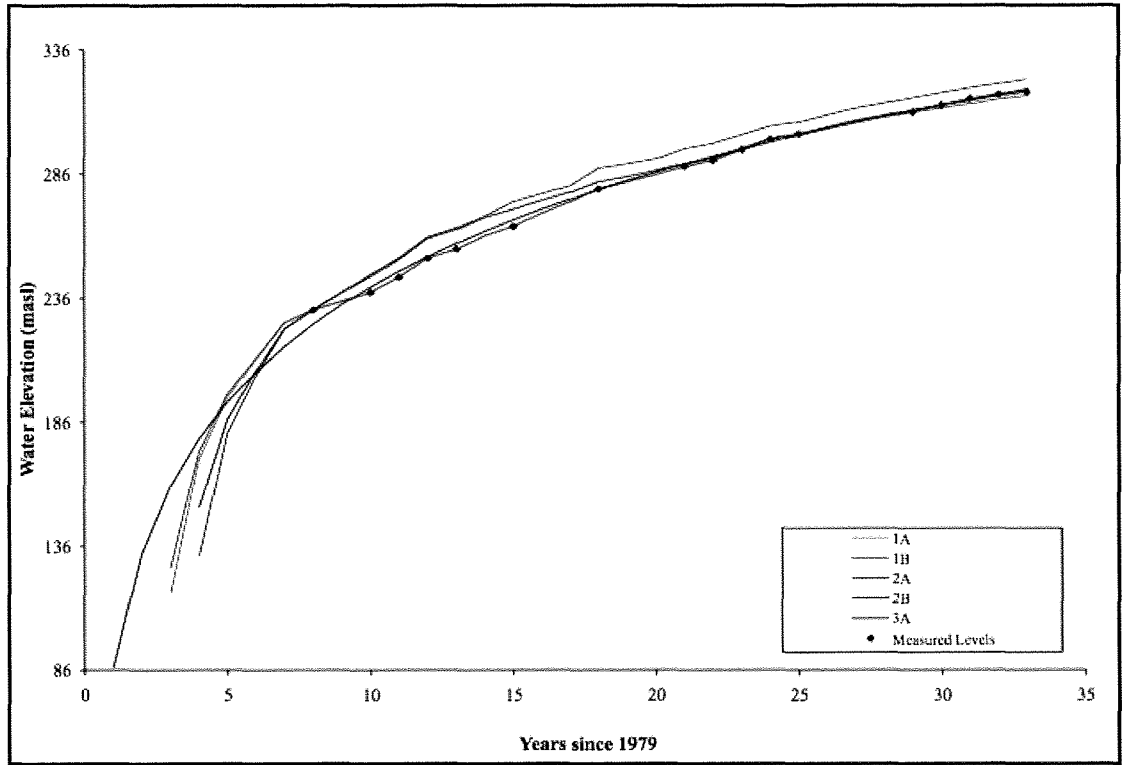


Figure 3.9: Graph showing the results of the rebound models for Caland and measured water levels from 1979 to 2011.

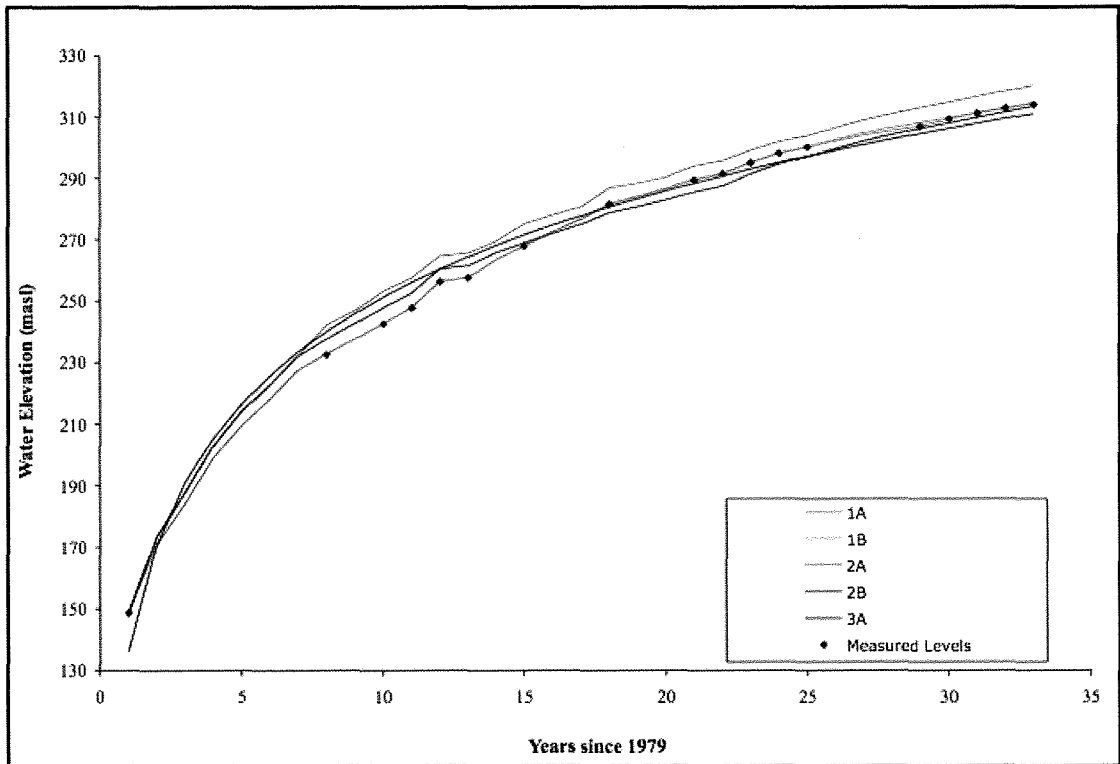


Figure 3.10: Graph showing the results of the rebound models for Hogarth and measured water levels from 1979 to 2011.

Predictions For When the Caland Pit Lake Surface Reaches 385 masl: Model 1A and 1B predict that it will take between 96 and 98 years, respectively, from mine closure for Caland to reach the joining elevation of 385 masl. This is 5 and 7 years longer than Model 2B predictions and 11 to 13 years longer than Model 2A (Table 3.2). Model 3A estimates it will take 88 years from mine closure for the water level in Caland to reach 385 masl which is intermediate to Models 2A and 2B.

Predictions for When the New Steep Rock Pit Lake Surface Reaches 385 and 394 masl: All models (1A, 1B, 2A, 2B, 3A and 3B) predict it will take Hogarth water levels longer to rebound to an elevation of 385 masl than Caland. This is in agreement with the fact that water levels in Caland are currently rising quicker than Hogarth and with the original flow path through the former Steep Rock Lake.

Models 1A and 1B predict it will take 114 to 116 years from mine closure, respectively, for the pit lake water elevation to reach 394 masl (Table 3.2). Models 2A and 2B predict it will take 99 and 108 years from mine closure, respectively. Model 3A predicts that water levels will reach an elevation of 394 masl in 101 years from mine closure. Model 3B predicts the longest rebound rate, with the water level reaching 394 masl in elevation in 173 years from mine closure. The prediction by Model 3A is only 2 years longer than Model 2A and 7 years shorter than Model 2B.

Models 3A and 3B inherently assume that factors controlling the decline in the rate of rebound remains constant through time, which is not the case. The factors controlling the rebound rate change when Caland water surface reaches 385 masl in elevations and water begins to flow into Hogarth. Caland's water level will no longer rise until the water level in Hogarth reaches 385 masl in elevation and Hogarth will receive a constant source of water from outside

its watershed changing its water balance. These changes in the factors controlling the rebound rate are accounted for in Model 1A, 1B, 2A and 2B.

3.8.2 Comparison of This Study's Predictions to Measured Water Elevations

Caland Models: All models except 3A begin with the same initial water elevation of 231.3 masl in 1986 (Fig. 3.9). Models 1A and 1B follow a similar trend between 1986 and 2003 as they are forced to match measured water levels during that period of time. In 2003, the calibration period for Model 1B terminates, but continues to 2009 in Model 1A. Model 1A water level predictions are within 1m of measured water elevations for 2010 and 2011. Model 1B water level predictions become progressively lower than measured water levels from 2007 to 2011. Model 2A predictions are higher than all measured water levels except for the initial water level of 231.3 masl in 1986. Model 2B initially predicts higher water levels but begins to match measured water levels in 1999, after which its predictions are within 1 m of measured water elevations. Model 3A water level predictions are all lower than measured water elevations, but the predicted levels for 2011 are within 1 m of the measured level. The lowest depth of Caland pit lakes' water level is back cast by Model 3A with an elevation of approximately 86 masl. The lowest water elevations in Models 1A and 1B are 117 masl and 127 masl, respectively, and lower elevations than Models 2A and 2B at 132 masl and 152 masl, respectively.

Hogarth Models: All models except 3B begin with the same initial water elevation of 148.7 masl in 1979 (Fig. 3.10). Model 1A and 1B follow a similar trend between 1986 and 2003 as they are forced to match measured water levels during that period of time. The calibration period for Model 1B ends in 2003 and that for Model 1A continues until 2009. Models 1A and 1B both predict water levels within 1 m of measured elevations from the end of their respective calibration periods to 2011. In general the predictions by Model 2A are 5 m to 10 m higher than measured water levels from 1979 to 2011. Model 2B predictions for water levels are higher by

up to 4 m from 1986 to 1991 and in 1993 the predicted water level is within 1 m of the measured elevation for that year. From 1996 to 2003, Model 2B water level predictions are lower than measured elevations by up to 4 m and from 2007 to 2011 predictions are within 1 m of measured levels. Model 3B has a lower initial water elevation in 1979 at 136 masl. Model 3B predictions for 1996, 1999 and 2000 are within 1 m of measured water elevations however; in general, predictions made by Model 3B overestimate measured water levels prior to 1996 and underestimate water levels after 2000 by about 4 m.

3.8.3 Comparison of This Study's and the Regional Engineering Model's Predictions

Caland Models: The results of all the rebound models for Caland pit lake are compared to the Regional Engineering model in Figure 3.11. The lowest water elevation predicted by the Regional Engineering model (1986), 151 masl, is similar to that of Model 2B, 152 masl, except that the Regional Engineering model's the water elevation occurs in 1979 as opposed to 1982 for Model 2B. The lowest water elevations, back cast in all other models, are below the estimate in the Regional Engineering model. Model 2A water level predictions from 1986 to 2011 are higher than those of the Regional Engineering model. Model 1B matches the overall trend of the Regional Engineering model relatively well but predicts a lower water level, 323.9 masl in 2015 compared to the Regional Engineering model's prediction of 326.4 masl. In general, Models 1A and 2B predictions best match the overall trend of the Regional Engineering model from 1986 to 2015. Model 1A is forced to match all the measured water elevations except for 2010 and 2011. Model 1A 2010 prediction, 317.3 masl, is closer to the measured elevation, 317.9 masl, than the predicted water level by the Regional Engineering model, 315.1 masl. Model 2B predictions from 1986 to 1994 are greater than those by the Regional Engineering model by 2 m or more and from 1995 to 2015 the difference is less than 2 m. In 1999, 2000 and 2010, the predicted water

levels by Model 2B are closer to measured elevations than the Regional Engineering model predictions.

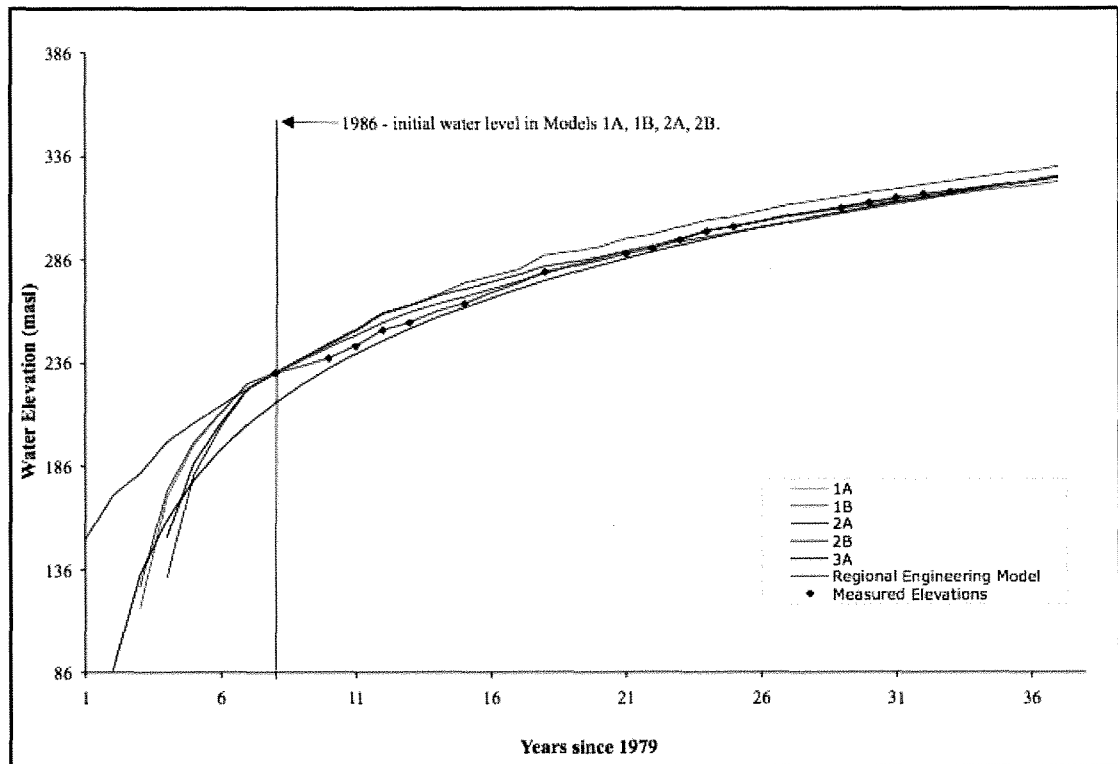


Figure: 3.11: Comparison of measured water elevations to this study's rebound model predictions for Caland and to those of the Regional Engineering model.

Hogarth Models: The results of all the rebound models for Hogarth pit lake are compared to the Regional Engineering model in Figure 3.12. The Regional Engineering model predictions for Hogarth begin in 1980, a year after those in this study. This study's models all have a minimum water elevation below that predicted by the Regional Engineering model (1986). Model 1A and 1B are forced to match all the measured water elevations except for 2010 and 2011. The predicted 2010 water level of models 1A and 1B 2010 (312.7 masl) is closer to the measured elevation (312.8 masl) than that predicted by the Regional Engineering model (310.9 masl). Model 2A predictions are higher than the Regional Engineering model predictions from 1980 to 2015 with the length of time predicted for the pit lakes to completely fill by Model 2A

being approximately 9 years longer. Water levels estimates of Model 2B are within 6.5 m of the Regional Engineering model estimated water levels. In all years except 2010, the water level predictions made by the Regional model are closer to the measured than Model 2B. In 2010, the water level prediction by Model 2B (311.5 masl) is closer to the measured elevation (312.8 masl) than the Regional Engineering model (310.9 masl).

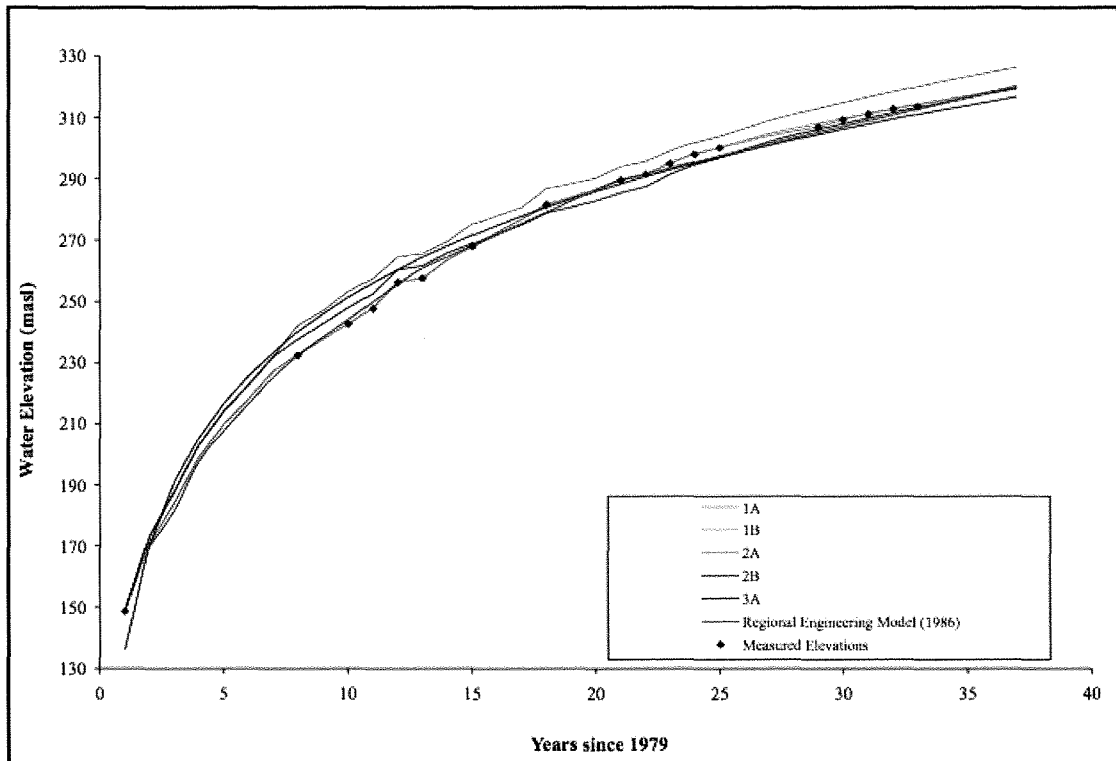


Figure: 3.12: Comparison of measured water elevations to this study's rebound model predictions for Hogarth and to those of the Regional Engineering model.

3.8.4 Sensitivity Analysis Results

Based on the comparative analysis (Section 3.8.2), Models 1A, 2B and 3A best match measured for Caland pit lake and Models 1A, 1B and 2B best match measured and predicted water levels for Hogarth pit lake. Of these models, Models 1A and 2B predictions provide predictions close to measured water elevations for both Caland and Hogarth pit lakes. Since Model 1A is forced to match measured water levels until 2009 only the 2010 and 2011 measures

levels can be compared with model predictions. The 2010 and 2011 water level predictions in Models 1A and 2B are within 1 m of measured levels for both pit lakes. Variances in Model 2B water level predictions from the measured water levels are likely the result of the limited number of years with measured water levels, precipitation and evaporation rates during calibration. From 2011 to 2017 the difference between Model 1A and 2B predictions progressively decreases to 10 cm in 2016 and 2017. After 2017 Model 2B water level predictions become higher than those by Model 1A. There is a 5 year difference between the predicted time until the pits join by Model 1A and 2B and a 6 year difference between the predicting total filling time (Table 3.2). Therefore the Model 1A and 2B predictions are reasonable close to each other. Since 2B matches the 2011 measured water elevations for Caland better than Model 1A and both models predict water elevations within 1 m for Hogarth, Model 2B was selected for the sensitivity analysis. Caland received more runoff resulting in Caland having greater control on the rebound rate than Hogarth. Waters that outflow from Caland into Hogarth significantly increases the rate of water level rise in Hogarth. Thus, the accuracy of the Caland predictions took precedent over those for Hogarth in the selection of the best-calibrated model for the pit lakes. Water balance and water level predictions each of the models run in the sensitivity analysis are provided in Appendix V.

Precipitation: A total of eight rebound models were run where the average annual precipitation rate used in Model 2B (739.6 mm/year) was varied by a certain percentage (5-40%; Fig. 3.13). The maximum (1010 mm/year) and minimum (578 mm/year) measured precipitation rates for 1979 to 2006 are within the variance in precipitations rates for the sensitivity analysis. A decrease in precipitation rate by 20% is approximately equal to the minimum measured precipitation rate and a 40% increase in precipitation is approximately equal to the maximum precipitation rate. A decrease in the precipitation rate creates a greater difference in rebound rate

than an increase (Fig. 3.13). A 5% variance in precipitation rate results in a 4-year difference in rebound rate and a 10% variance results in a 9-year difference in rebound rate.

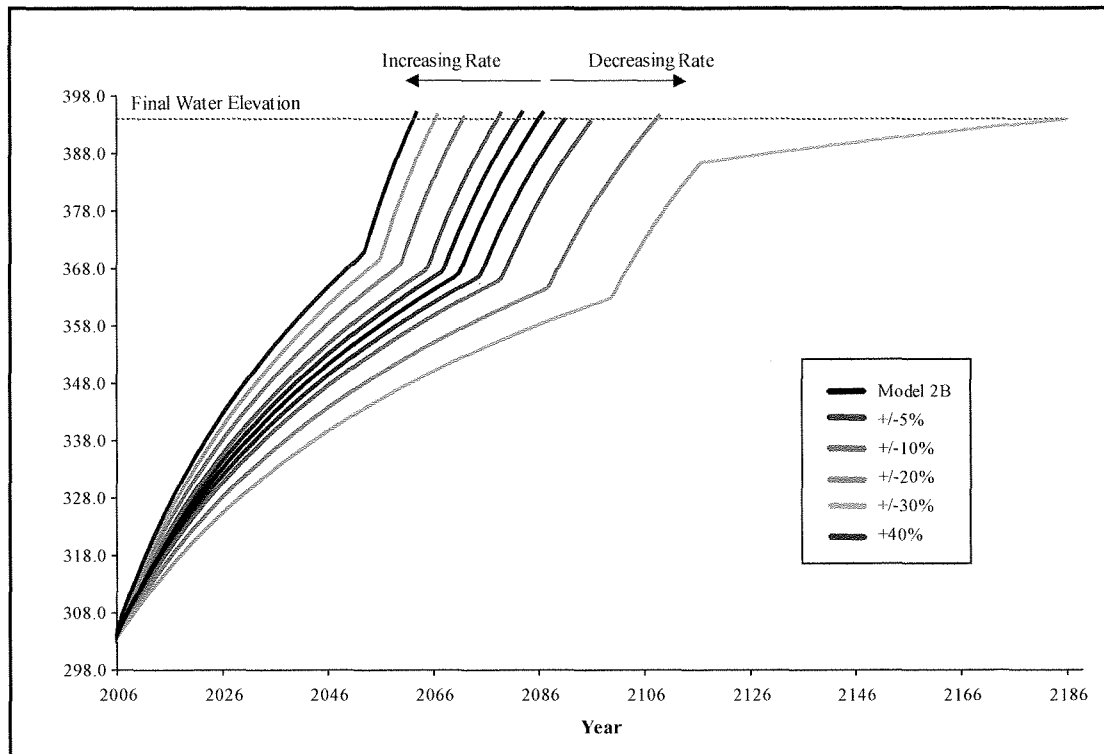


Figure 3.13: Graph of the sensitivity analysis for precipitation. The predictions shown start in 2006, when the average precipitation rate replaces measured values in the water balance calculations, and end when the predicted water level for each model is equal to or greater than 394 m.

Runoff: A total of six models were run that vary the retention factor in the runoff volume calculation from that used in Model 2B and are shown in Figure 3.14. The initial retention factor (40%) value is varied by 5%, 10% and 20%. A 5% variance in the retention factor resulted in a 7-year difference in rebound rate.

Evaporation: A total of ten models were run that each vary the average annual evaporation rate used in Model 2B and are shown on Figure 3.15. The initial evaporation rate (511.4 mm/year) was varied by 5%, 10%, 20%, 30% and 40%. The range of evaporation rates used in the sensitivity analysis extends beyond the maximum (595.9 mm/year) and minimum

(317.6 mm/year) measured evaporation rates from 1966 to 1988. A 20% change in the evaporation rate is required before a significant change (>5 years) occurs in the rebound rate. A 40% change in the evaporation rate is required to change the rebound rate by more than 10 years.

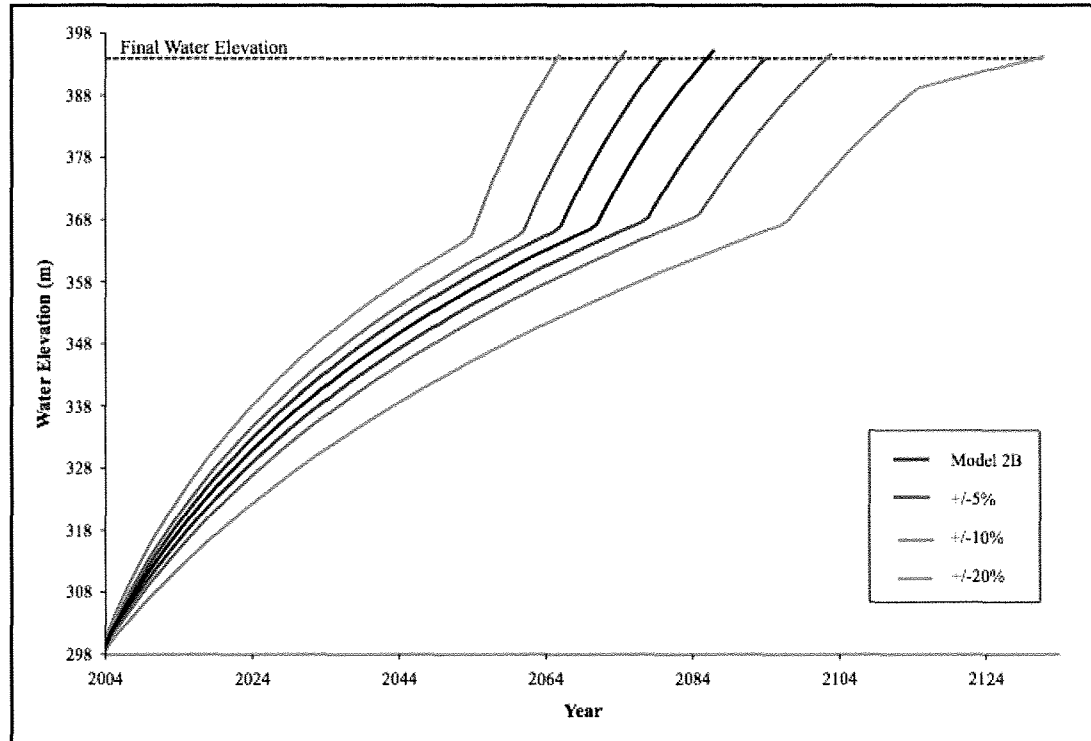


Figure 3.14: Graph of the sensitivity analysis for runoff. The predictions shown start in 2004, when the calibration period ends in the water balance calculations, and end when the predicted water level for each model is equal to or greater than 394 m.

Net Groundwater Influx: A total of twelve rebound models were run that each vary the average groundwater influx value for Caland and Hogarth, 1,401,100 m³/year and 625,289 m³/year, respectively, by 5 to 70% are shown on Figure 3.16. A 30% increase or decrease in the groundwater rate is required to change the rebound rate by 5 years, and a change of 70% results in a difference of 10 years.

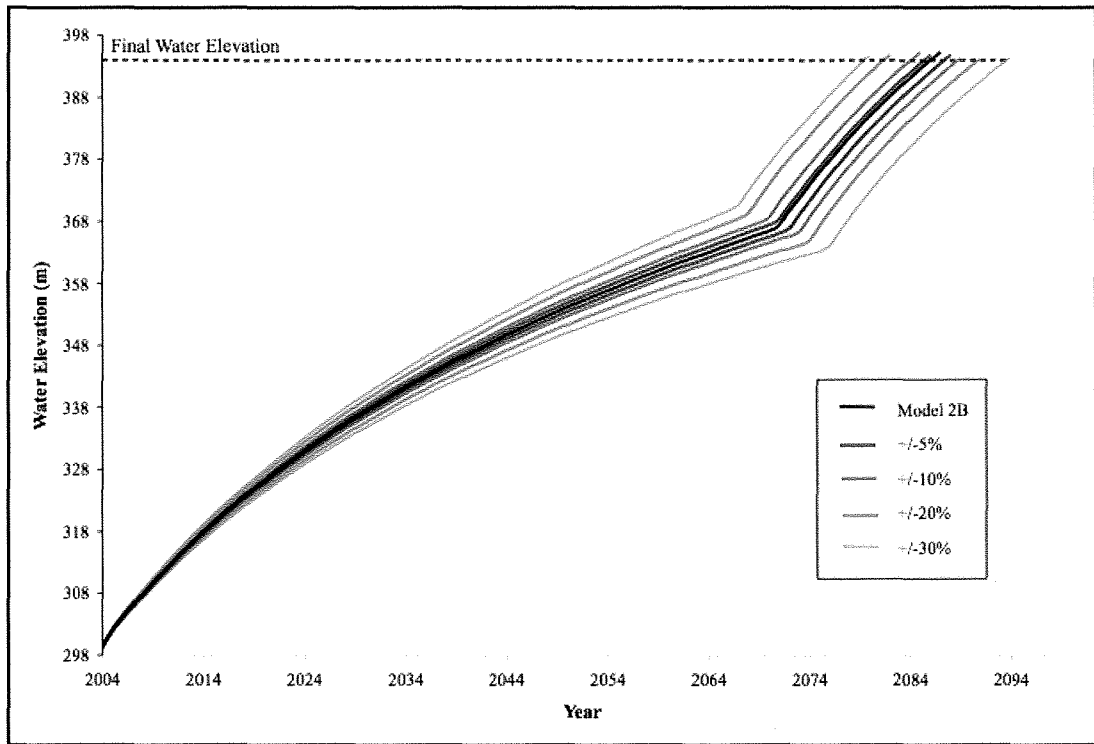


Figure 3.15: Graph of the sensitivity analysis for evaporation. The predictions shown start in 2004, when the calibration period ends in the water balance calculations, and end when the predicted water level for each model is equal to or greater than 394 m.

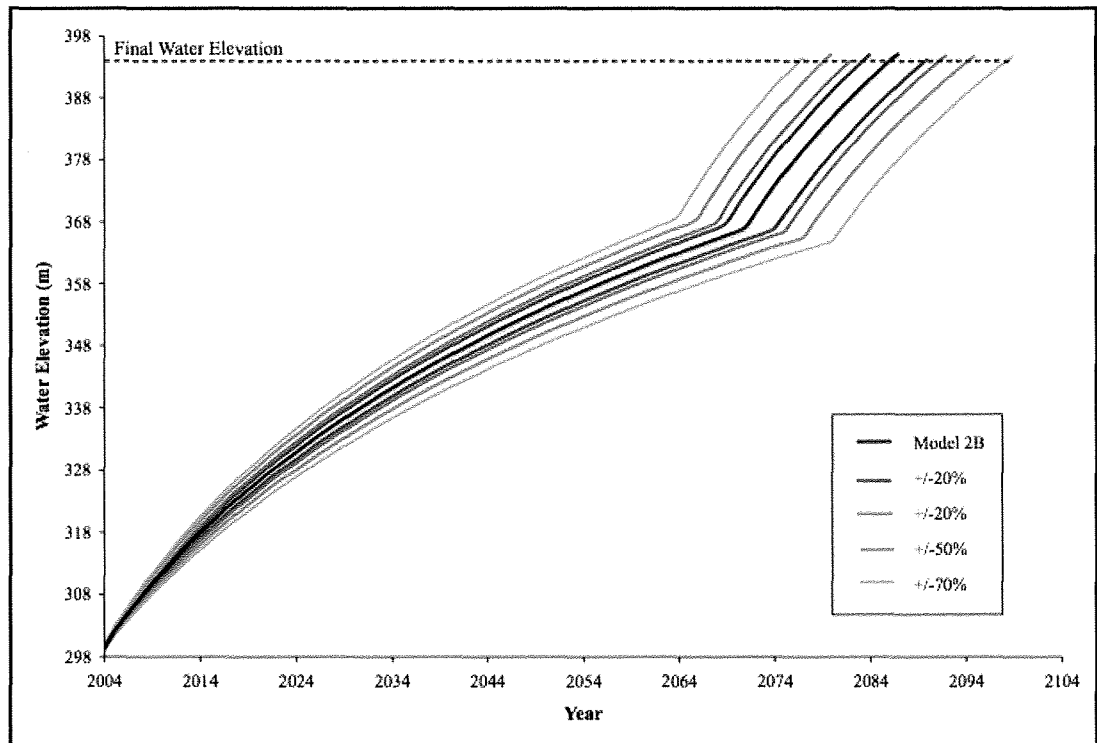


Figure 3.16: Graph of the sensitivity analysis for the net groundwater influx. The predictions shown start in 2004, when the calibration period ends in the water balance calculations, and end when the predicted water level for each model is equal to or greater than 394 m.

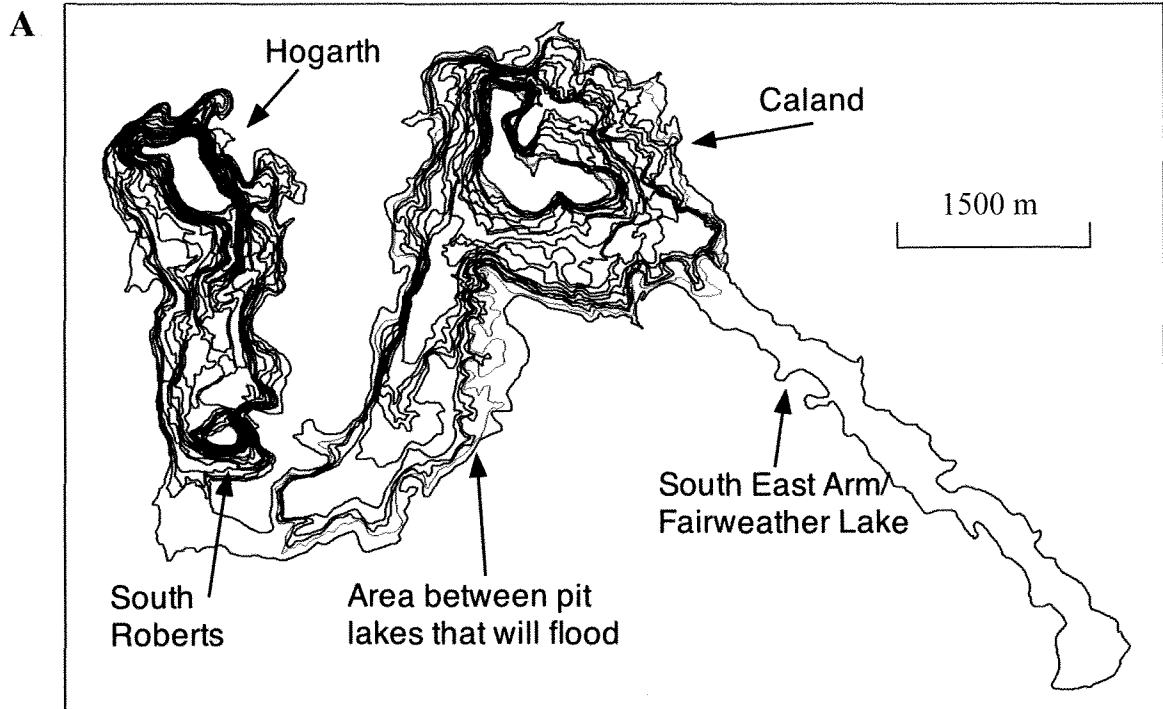
3.9 Discussion

3.9.1 Study Results

A number of rebound models have been made for Caland and Hogarth pit lakes (Capper, 1978; MNR, 1986; Vancook, 2002; Jackson, 2007; this study). The methods and data used to predict rebound in Caland and Hogarth pit lakes vary. The Steep Rock Resources model used the ultimate pit limits at ~30 m (100 ft) intervals to define the accumulated volume capacity of the Middle and East Arms (Hogarth and Caland Pit Lakes; Capper, 1978). The Regional Engineering model (1986) refers to the Steep Rock Resources model for information on stored water volumes below 200 masl. Above 200 masl the volume calculation was based on a 30 m contour intervals with linear interpolation between the contours at a 1 m interval in the form of a look up table (MNR, 1986). The Regional Engineering model (1986) predicts a slightly slower rebound rate than that of Capper (1978), but in general predicted water elevations have been within 1 to 2 m of measured elevations (Figs. 2.3 and 2.4) Rebound models by Vancook (2002) and Jackson (2007) do not accurately predict water levels (Figs. 2.3 and 2.4).

The differences in the water level predictions between the Regional Engineering Model (1986), Vancook (2002), and Jackson (2007) reflects differences in the modeling methods. Unlike the Regional Model, a water balance was not calculated as part of the determination of the rebound rates calculated by Vancook (2002) and Jackson (2007). Vancook (2002) assumes a linear rate of increase in water elevation overtime based on measured elevation changes that were relatively constant between 1982 and 2004. This model is flawed because volume calculations show an increase in volume with elevation. Thus if inflowing water volumes remain relatively constant a decrease in the rate of elevation increase is expected. Prior to 1993, when the open pits were much narrower with steeper pit walls (below 270 masl) a near linear increase in water elevations occurred. Above 270 masl a decrease in slope occurs as the pit walls widen

and begin to follow the contours of the former lakebed until the former Steep Rock Lake shoreline is reached. Figure 3.17 shows the irregularities in the pit lakes, especially in Caland. The volume of Caland pit lake significantly changes again at ~ 300 masl when the pit lake surface begins to move to the southwest following the original flow path in the former Steep Rock Lake (Figs. 1.3 and 3.17). The quicker rate of rebound predicted by Vancook (2002) results from the assumption that the water elevation increases linearly based on water levels below 300 m. Where head-independent flows predominate or where water availability depends on a remote source for instance where a surface water course cascades into an open pit, rebound is likely to approximately be linear (Younger et al, 2000). Thus the linear model of Vancook (2002) inherently assumes that head-independent flows predominate. However, head-dependent inflows are significant in the study area. The study area is known to have high groundwater inflows since groundwater inflow hindered underground mining and was a major factor leading to the Seine River Diversion (Capper, 1978). Jackson's (2007) rebound model did not use stage-volume relationships for the entire pit volume. The volume of the pit lake is only calculated from 210 m contour and above for each pit lake. The annual inflow rate is calculated by dividing the volume between two elevations by the number of years required to fill that volume for three different periods of time where measured elevations were close to contour elevations. The average annual volume of water entering the pit lakes is then assumed to be constant. The approach to predict rebound used in Models 3A and is similar to that used by Vancook (2002) in that an equation was fitted to measured water levels. However, instead of a linear equation like Vancook (2002), Models 3A and 3B fit an exponential curve to water level data. Fitting an exponential curve to measured water elevations by simple regression is a method of predicting rebound where head-dependent flows are significant and is more likely to be successful in large systems (Younger et al., 2002).



B

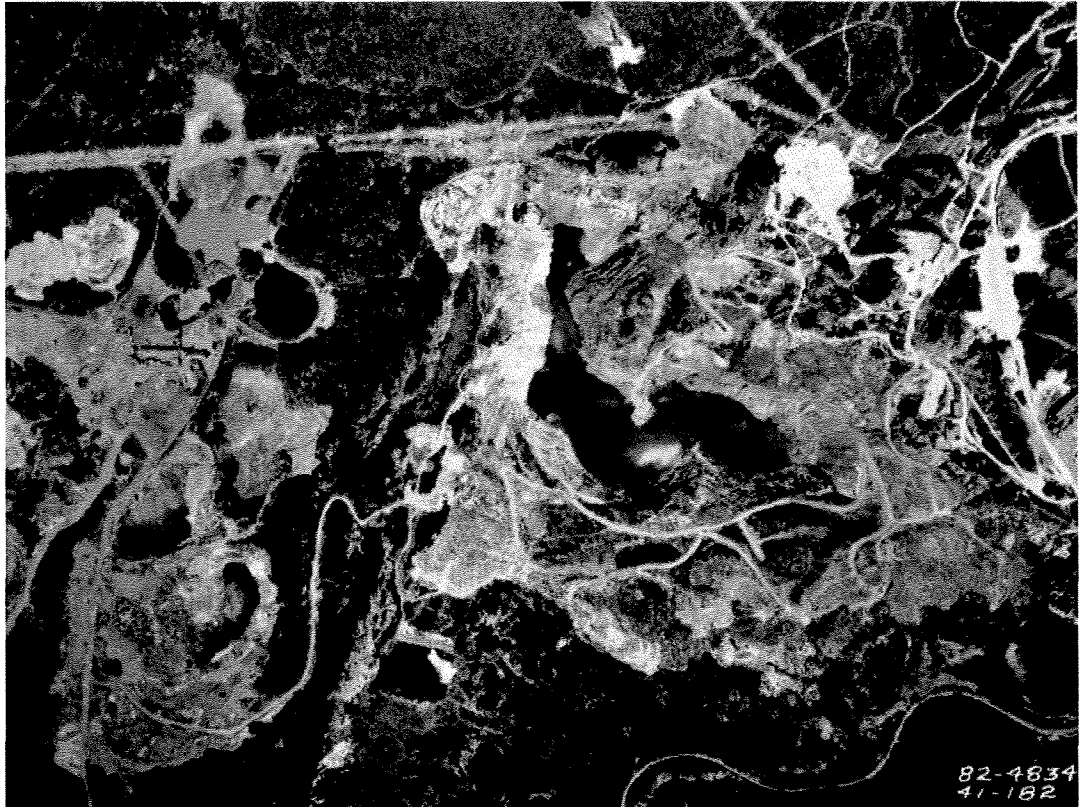


Figure 3.17: Images showing the irregularities in the shape of Caland and Hogarth pit lakes. (A) Contours of Caland and Hogarth pit lakes at a 10 m interval from 190 masl to 390 masl. (B) Aerial photograph of Caland pit lake taken in 1982, showing the irregular shape of the lake.

As previously stated, head-dependent inflows are significant for Hogarth and Caland. Head-dependent inflows represent water flowing from adjoining aquifers, where the rate of inflow depends on the degree to which the hydraulic head of the aquifer exceeds the head elevation plus atmospheric pressure in the mine void (Younger et al., 2002). The difference in head decreases with time, leading to a slow reduction in inflow rate and a deceleration of water level rise. Such a pattern is seen in the water level predictions made by the rebound models by Capper (1978), MNR (1986), and Jackson (2007) as well as this study. Where head-independent flows predominate or where water availability depends on a remote source, for instance where a surface watercourse cascades into an open pit, rebound is likely to be approximately linear (Younger et al., 2002). Although Caland does receive more surface water runoff than Hogarth, head-dependent inflows are still a significant factor. Generally, rebound curves for most systems fall between an exponential and linear curve and can show stepwise jumps where mine void volume changes (Younger et al., 2002). In addition, the use of simple regression to predict pit lake rebound rates inherently assumes that the factors controlling the rebound rate remain constant, which is not the case in Caland and Hogarth (see section 3.8.1).

The water balance equation used in Models 1A, 1B, 2A and 2B is from Shevenell (2000a). This study follows the general approach used by Shevenell (2000a), for Gretchell Mine pit lakes, Nevada, however, the determination of some parameters in the water balance and the method used to calculate pit volumes differ slightly (e.g., the equation for an ellipse is used to represent the surface areas, the volume is calculated in successive layers downward at a 15 mm height increment, and the length and width of the ellipse is determined assuming a slope of 40°). Also, there are major differences between the study area under consideration here and that of Shevenell (2000a). First, the Gretchell pit lakes only lose water via evaporation and lateral groundwater flow and the pit lakes are considered full when the change in storage equals zero.

Caland and Hogarth are expected to outflow into the West Arm and, therefore, the model ends when the water levels reach the outlet elevation. Secondly, Gretchell pit lakes have previously filled and been drained, and have a record of data on water elevation through time from when the pit lakes previously flooded. Water levels in the Gretchell pit lakes were observed to follow a hyperbolic function and this curve is compared to other analytical models prepared for Gretchell pit lakes that use different approaches to model groundwater inflows. It was found that model results were not unique and measured water levels can be predicted relatively well using a number of groundwater inflow and outflow assumptions (Shevenell, 2000a). From 1979 to 2011, many of this study's models reasonably predicted water levels that were close to measured water levels. The differences between water level predictions in Models 1A, 1B, 2A and 2B only reflect differences in the calibration method, as all other parameters are the same.

In Models 1A, 1B, 2A and 2C the groundwater water flux term is used to calibrate the rebound models. Model 1A and 1B are calibrated by adjusting the net groundwater flux term by trial and error but the lengths of the calibration periods are different (see section 3.4.4). Models 2A and 2B are calibrated by determining the net groundwater flux term difference using the equation from Shevenell (2000a) over calibration periods of different lengths (see section 3.4.4). The different calibration methods resulted in different net groundwater flux values used in the water budget calculations (Table 3.3). The groundwater influx values calculated in Model 1A and 1B are significantly lower than those calculated in Models 2A and 2B. The differences in predicted rebound rates correlate to the differences in the groundwater influx rates (Tables 3.2 and 3.3).

Similar to the Regional Engineering model, Models 1A, 1B, 2A and 3B calculate a water budget, but differ in the method of defining the stage-volume relationships. This study's rebound models uses a hypsographic curve and a surface area – elevation curve to model the stage –

volume relationships. The stage-volume relationships in the Regional Engineering model are listed in a look up table containing elevation, surface area and volume data. The table was created by using linear interpolation at a 1 m interval between each of the contours of the pit lakes (MNR, 1986). Results of the sensitivity analysis suggest the differences in predicted rebound rates are the result of the different methods used to define the stage-volume relationships and that linear interpolation is more accurate, particularly for Caland (see section 3.9.2).

The hypsometric curves and elevation-surface area curves for Caland initially under estimate measured levels then overestimate levels after ~ 330 masl (Figs. 3.1 and 3.3). On the other hand, Hogarth curves initially are close to measured levels until ~330 masl, after which the curve overestimate values (Figs.3.2 and 3.4). Thus water elevations during particular time periods are over and underestimated. To assess if this is a problem inherent to hypsometric curves and elevation-surface area curves, a rebound model with pit geometry modeled using the linear interpolation method at a 1 m interval was derived. This rebound models used the same water balance parameter values as the other models and an assumed groundwater influx rate of 100 gpm(US). The assumed groundwater influx is close to that estimated by the Steep Rock Environmental Plan and the Regional Engineering Model for Caland of 95 gpm and 90 gpm (Capper 1978; MNR 1986). The revised rebound model predicted similar rebound rate to Models 2A and 2B with the pit lake joining in 2057 and the combined lake outflowing in 2077 (see Appendix VI). The difference between the predicted joining dates of Models 2A and 2B and the rebound model that used linear interpolation to model pit geometry suggests that the later predicts incremental water elevations more accurately because the over/under estimation is resolved but both methods produced similar rebound rates for when the pit lake overflow into the West Arm. Based on these results, hypsometric curves should not be used where the slopes of the

pit walls varies over time, as see in Caland and Hogarth (Fig. 3.17) because the curves will over- and underestimate water elevations at different points in time.

3.9.2 Sensitivity Analysis

All the rebound models in this study predict a longer rebound rate than the Regional Engineering model's prediction of 90 years from mine closure. Models 1A and 2B predictions match 2011 measured values better than the Regional Engineering model. The predictions by Model 2A are the closest at 99 years from mine closure, which has the highest groundwater influx rate of this study's models. In addition to the differences in the stage-volume relationships as discussed previously, some parameters used in the water balances of this study differ from Regional Engineering model. The retention factors used in both models are the same (40%); however, the sensitivity analysis suggests that even small changes in the value can result in significant changes to the rebound rate. For example, a 5% increase or decrease in the retention factor would change the rebound rate by 7 years (Fig. 3.14). No effort has been made to estimate the retention factor of the land since the surrender report by the MNR (1986) and the growth of vegetation on the property since mine closure likely has changed the amount of surface runoff.

The precipitation rate used in the Regional Engineering model is 728.9 mm/year (28.7 in), slightly lower than that in this study, 739.6 mm/year. The difference between the two precipitation rates is approximately 1.4%. However, the sensitivity analysis indicates that this difference in precipitation rate would probably account for only a 1-year variance in the rebound rate (Fig. 3.13). The precipitation rate used in this study is likely a better estimate since it is based on the 1971 to 2000 Climate Normals. Also, this study uses measured precipitation values for a longer period of time. The evaporation rate used in the Regional Engineering model is 457.2 mm/year, close to the average evaporation rate of 461 mm/year calculated for 1966 to 1988 and lower than the average evaporation rate of 511.4 mm/year for 1979 to 1988 used in this

study. The difference between the evaporation rate used in this study and that of the Regional Engineering model is approximately 11%. Based on the sensitivity analysis, this difference would result in about a 2-year increase in the rebound rate (Fig. 3.15). Furthermore, the difference between the determined Penman potential evapotranspiration rate, 548 mm/year, and the average evaporation rate used in this study, 511.4 mm/year, is 7% and would result in about 1- or 2-years decrease in the rebound rate based on sensitivity analysis results. Thus the use of the Penman equation to estimate evaporation for years with missing data would likely have little influence on the predicted rate of rebound.

The amount of seepage that was determined to enter the pit lakes in the Regional Engineering model, approximately 129,210 m³/year into the East Arm and 179,215 m³/year into the Middle Arm, which are 91% and 71 %, respectively, lower than the net groundwater flux values determined in Model 2B (Table 3.2). Based on the sensitivity analysis, these differences in groundwater flow rates would result in a rebound rate approximately a 9 to 16 year longer and close to the 18 year difference between the Regional Engineering model rebound and Model 2B (Fig. 3.16). However, the seepage rates in the Regional Engineering model are much lower than those in this study and one would expect that the Regional Engineering model's rebound rate predictions to be slower longer than those in this study. But in fact the model's predicted rebound rate is shorter than those predicted by the models in this study.

The results of the sensitivity analysis suggest that the differences in the precipitation and evaporation rates used in this study and the Regional Engineering model are not significant enough to account for the 18-year difference in predicted rebound rates. The results of the sensitivity analysis contradict what one would expect based on the differences in the net groundwater flux and seepage values determined in this study and the Regional Engineering model. Because the determination of the net groundwater influx in this study is based on the

stage-volume relationships, this contradiction suggests that the different approach used to define the pit geometry between the this study and the Regional Engineering model accounts for the difference in the predicted rebound. In addition, the R^2 value for the Caland hypsometric curve is 0.88 much lower than that of Hogarth at 0.95. Examination of the Caland hypsometric curve indicates that the volume of Caland pit lake is overestimated by the hypsographic curve.

Therefore, since the Regional Engineering models' Caland pit volume, determined using linear interpolation, is likely more accurate than that determined in this study, the longer rebound rates predicted in this study are probably the results of a difference in calculated pit volumes. A simple model of the pit lake stage volume relationships was used in this study in order to assess if simple models could provide accurate volume calculations. Based on these results, simple methods of modeling pit lake stage-volume relationships should not be used, particularly for Caland pit.

An attempt has been made to estimate errors associated to rebound model predictions based on the sensitivity analysis results. Estimating the error associated to the rebound models is difficult because of the number of assumptions required to construct the models, the use of estimated data and because model parameters vary overtime. To determine an at best error in the estimated rebound rates, an average of the number of years difference in the rebound rate resulting from a 5% change in parameter values. The upper limit of error or worst case scenario for an the amount of error in the rebound rates was determined by averaging the number of years difference in rebound rates resulting from a the lowest percent change in parameters values that created significant differences in rebound rates (> 5 year difference). Significant changes occurred in the rebound rate when precipitation values change by 10%, evaporation by 30%, runoff by 10% and groundwater by 70%. Based on the sensitivity analysis results, at best the models likely have an error of about +/- 3 years and, at worst an error of about +/- 10 years.

3.9.3 Model Limitations

There are a number of data limitations with respect to rebound and water balance models in this study. In the water balance model the meteorological data available was limited. Evaporation data was not available for Atikokan after 1988. Annual precipitation values had to be estimated for a period of time during the calibration period, 1988 to 1994, because of availability and quality. The difference between the calculated average evaporation rate and Penman estimates (7%) results in a two year or less increase in rebound rate. The use of Penman estimates in future studies may improve the accuracy of the calculated net groundwater influx in Model 2A and 2B by providing evaporation rates that vary each year reflecting meteorological conditions, as opposed to an average rate. However, the solar radiation data required for the Penman calculation was taken from a weather station located more than 800 km away from Atikokan and therefore the Penman estimates are not based on study site conditions. The difference between measured and predicted precipitation rates is typically 13% and, based on the sensitivity analysis would result in an approximately 9-year difference in rebound rates. However, the use of the estimated precipitation values may have improved the calibration by providing precipitation rates that vary from year to year based on meteorological conditions, as opposed to an average rate.

The use of measured precipitation and evaporation data is important in the calibration of rebound models, especially in Model 2A and 2B that are calibrated by calculating the net groundwater influx by difference, because known evaporation and precipitation estimates increase the accuracy of the net groundwater flux calculation. The calculation of the groundwater influx in rebound models Model 1A, 1B, 2A and 2B is also limited by sporadic measurements of the pit lake surface elevation over the calibration period. Furthermore the number of sequential

years with measured elevations and measured annual precipitation and evaporation values are few.

The percentage of precipitation entering the pit lakes as runoff was assumed to be the same as in the Regional Engineering model however this value may no longer be representative of the amount of water entering into the pits now. Since mine closure the amount of vegetation on the property has increased which has likely changed the amount of runoff from the Caland and Hogarth watersheds.

The initial volume of the pit lakes at the start of the rebound model was determined using the measured pit lake water elevations and the stage-volume relationships. The water elevation of Caland at the time of mine closure in 1979 is unknown.

Large open pit lakes of complex geometry are difficult to simulate (Sinton, et al., 2002). In this study the stage-volume relationships are two exponential curves, a hypsometric curve and an elevation versus surface area curve. The R^2 values for the hypsometric and elevation versus surface area curves, respectively, for Caland are 0.882 and 0.9841 and for Hogarth 0.9525 and 0.9546. The R^2 value for the Hogarth hypsometric curve (0.9525) is higher than that for Caland (0.882) indicating the hypsometric curves provide a better representation of the pit volume with elevation for Hogarth than for Caland. Examination of the hypsometric curve indicates that the curve overestimates the volume of Caland (Fig. 3.1). Thus the models will inherently predict a longer rebound rate because more water is required to fill the pit. The R^2 values and the sensitivity analysis results suggest that the use of linear interpolation to define pit volumes, as in the Regional Engineering model (1986), is more accurate than the hypsometric curves used in this study, especially for Caland. The pit lake volume estimates affect the calculated net groundwater influx in Models 1A, 1B, 2A and 2B and result in an overestimate of the groundwater influx rates.

3.10 Conclusions

The rebound model 2B is the best overall rebound model for Caland and Hogarth pit lakes based on comparisons to measured water levels and the Regional Engineering model predictions that have proven to be reasonably accurate. Model 2B predicts that Caland will flow into Hogarth in 2070 and that the new Steep Rock Pit Lake will outflow into the West Arm in 2087, 13 and 18 years, respectively, longer than the Regional Models predictions. Based on the sensitivity analysis results, the difference between the Model 2B predictions and the Regional Engineering model predictions can be attributed to the manner in which the pit volumes are calculated because the differences between the water balance parameter values used in the models cannot account for the 18-year difference in the prediction rebound rate.

In this study, the relationships between the accumulated volume, surface area and elevation, are modeled by fitting exponential curves to measured data as described in section 3.3. The Regional Engineering model defines the pit volumes using linear interpolation at a 1 m scale between contour elevations. The stage-volume relationships for Hogarth pit lake appear to be more accurate than for Caland, suggesting that at minimum linear interpolation should be used to define the volume in Caland pit lake. In general, hypsometric curves should not be used where the slopes of the pit walls varies over time, as see in Caland and Hogarth (Fig. 3.17) because the curves will over- and underestimate water elevations at different points in time. However, the overall rebound rates, when the pit lakes reach their outlet, predicted using the hypsometric curves and linear interpolation produce similar results.

Chapter 4: Hydrodynamic Modeling

The nature of mixing that occurs between the upper and lower layers of a lake and the cycling of nutrients as well as other chemical species is controlled by the physical limnology of the pit lake (Castendyk & Eary, 2009). Thus, knowledge of the likely long-term hydrologic behaviour of pit lakes is important when developing a management or remediation strategy for pit lakes. The hydrologic behaviour of pit lakes influences water quality and whether or not stored toxic material migrates to the surface and is released. The high depth to surface area ratio of pit lakes compared to natural lakes promotes density stratification, where the dense bottom layer is not involved in seasonal overturn. This is called meromictic stratification. In a meromictic lake, the bottom layer, the monimolimnion, remains stagnant and where sulphide-bearing minerals exist, reducing conditions can prevent the production of acidic waters (Castendyk and Webster-Brown, 2007). An unexpected turnover event in a meromictic lake can bring stagnant bottom waters to the surface, which may result in adverse environmental impacts (Castendyk and Webster-Brown, 2007). Alternatively, the entire water column of a pit lake can be involved in seasonal overturn resulting in holomictic stratification. In these lakes, overturn can bring oxygen in contact with stored tailings allowing oxidation of sulphide minerals (if present) in the tailings (Younger et al., 2000).

For these reasons, an effort should be made to model future pit lake conditions where water quality may be an issue in order to avoid any short- or long-term adverse environmental impacts. The Dynamic Reservoir Simulation Model (DYRESM) from the Centre for Water Research at the University of Western Australia (www.cwr.uwa.edu.au) has successfully reproduced observed conditions in a number of pit lakes including: Brenda Lake in British Columbia (Hamblin et al., 1999); the Island Copper Lake in British Columbia (Fisher, 2002);

Dexter lake in Nevada (Balistrerier al., 2006); and, a coal mine lake in Western Australia (Ivey et al., 2006).

The objective of this chapter is to use DYRESM to conducted preliminary simulations of the future limnology of Caland and Hogarth pit lakes in order to investigate if changes in the hydrology of the pit lakes during rebound will affect the stratification of the pit lakes. Each pit lake is modeled individually, using a number of different scenarios. The modeling scenarios are designed to simulate current conditions and predict future conditions at key points during the rebound process (i.e., when Caland and Hogarth pit lakes join, and when the joined pit lake over flows into the West Arm of Steep Rock Lake).

This study is the first to attempt to model the hydrodynamics of Caland and Hogarth pit lakes. The modeling effort will serve to assess whether there is sufficient data available for the pit lakes to accurately model the behaviour of the pit lakes hydrodynamics. DYRESM was also be used to model the future toxicity of the pit lakes based on predicted salinity values.

4.1 Conceptual Model

Three periods, or scenarios, during the process of water level rebound are investigated in this study: i) current conditions; ii) when Caland begins to flow into Hogarth; and, iii) when Caland and Hogarth pit lakes are combined and outflow into the West Arm of Steep Rock Lake. All simulations for Caland are run of 160 days and for Hogarth 158 days. The Hogarth simulations are run for a shorter period of time because surface water temperatures dropped below zero and terminated the simulation when the simulation period was 160 days long. The first scenario models the initial water levels are equal to 2008 (313.0 masl) and 2007 (306.9 masl) water levels for Caland and Hogarth, respectively. The 2007 and 2008 water levels correspond to the years the *in situ* measurements used for constructing the initial profiles were taken. In the second scenario, the water level in Caland is assumed to be 385 masl and the water

level is Hogarth is assumed to be 366.5 masl as predicted by Model 2B when Caland's water level reaches 385 masl. In the third scenario, the water level in both pit lakes is assumed to be 394 masl. The three scenarios are described in greater detail in section 4.4.

4.2 Description of the Limnological Program DYRESM

The DYRESM-CAEDYM (Dynamic Reservoir Simulation Model – Computation Aquatic Ecosystem Dynamic Model) package release 4.0.0 beta-2 by Imberger and Patterson (1981) and the Centre for Water Research at the University of Western Australia (www.cwr.uwa.edu.au) is used in this study. DYRESM is a one-dimensional hydrodynamic model for predicting the vertical distribution of temperature, salinity and density in lakes and reservoirs that satisfy the one-dimensional assumption (Imerito, 2007a). The one-dimensional assumption assumes that vertical variation is greater than horizontal variation. This gives rise to a layered structure whereby a lake is modeled as a series of horizontal layers. The one-dimensional assumption is valid when forces destabilizing the water column do not act over a long period of time (Imerito, 2007). The restriction to vertical variation in the water column is least problematic in pit lakes because of their high depth to width ratio (Hamblin et al., 1999). The hydrodynamic component of the model is process based, not empirical, and is unique in that it does not require calibration (Imerito, 2007; CWR, 2002). The data requirements for the model are basin geometry, hydrology and surface meteorology (Imerito, 2007). The model is initialized with field observations and is run over a simulation period. The layer structure of DYRESM assumes there is no lateral variation in the layers. The layers differ in thickness, and vary in thickness to accommodate volumes changes in response to inflows and outflows.

4.3 Description of DYRESM Input Files and Their Creation

The DYRESM computer model parameterizes the main physical processes leading to temporal changes in the salinity, density and temperature distributions in lakes and reservoirs

(CWR, 2002). The DYRESM computer program requires a number of input text files and data preparation programs. First, all data relating to meteorological, morphometry, inflows and outflows covering all possible days of the simulation are written into a netCDF file called the Reference file (Ref file). The Ref file and remaining input text files are translated into another netCDF file called the Simulation file (Sim file). The Sim file is compiled using the graphical user interface. Then the Sim file is visualized with Modeller v2b2 by the Centre for Water Research and the University of Western Australia.

The following provides a brief description of each input file and a general description of how parameters within each file were determined where applicable. See the DYRESM User Manual (CWR, 2002) for a more detailed description of the parameters in the DYRESM input files. Example input files can be found in Appendix VI.

4.3.1 Configuration

The DYRESM configuration file (*.cfg) contains configuration information for a particular simulation. The configuration data for Caland and Hogarth remains the same for all simulations. All simulations begin on May 25 and run for 160 days in Caland and 158 days in Hogarth. Hogarth simulations prematurely terminate when surface temperatures were below zero, thus the simulation period was shortened. The configuration file requires a value for the light extinction coefficient (m^{-1}), a measure of the ability of a water sample to exponentially attenuate light shining on its surface. The light extinction coefficient has not been measured for either Caland or Hogarth. The light extinction coefficient was estimated by comparing the average secchi depths for Caland (3.9 m) and Hogarth (3.3 m; from Gould 2008), to other lakes with measured secchi depths and light extinction coefficient available on Water on the Web (http://www.waterontheweb.org/under/lakeecology/04_light.html; Accessed: July 21, 2011). The light extinction coefficient value of 0.82 m^{-1} is similar to values seen in two mesotrophic lakes

with similar secchi disk depths, Grindstone Lake, Pine Country Minnesota and Ice Lake, Itasca Country, Minnesota that have light extinction coefficients of 0.82 and 0.83 and secchi depths of 3 to 6 m and 2 to 5 m, respectively.

4.3.2 Physical Data and Lake Morphometry

The physical data and lake morphometry file (*.stg) contains information describing the characteristics of the water body. Most information included in this file remains the same for all simulations with the exception of data regarding inflows. For surface inflows the streambed half angle was calculated based on field measurements of cross-sections taken of surface seeps running into Hogarth pit lake. All surface inflows are assumed to equal the average streambed half angle that was calculated to be 74.7° . Streambed slope is taken from dip measurements and is also arbitrarily defined to represent streams that inflow at angles steeper than those measured where cross-sections could be completed. The streambed drag coefficient is assumed to be 0.015 (CWR, 2002). For groundwater inflows or inflows below the lake surface, the elevation of the inflow into the pit lake was arbitrarily set at 1 m from the bottom of the pit lake and is varied to see if the groundwater entrance height influenced on the simulation results.

For each pit lake, the crest of the lake above mean sea level is assumed to equal the water elevation in the West Arm, 390 masl. The Crest Elevation or elevation of the height of the Narrows Dam, the elevation of the outflow point to the West Arm is 394 masl (R. Purdon, pers. comm., Jan 2011). Caland is assumed to have one outlet at 385 masl, corresponding to when Caland flows into Hogarth. Hogarth only has one outlet to the West Arm at 394 masl. The physical data and lake morphometry file also includes a matrix of height-area data that describes the hypsographic curves of the water body. For each pit this data was taken from the pit geometry described in section 3.2. The lowest elevation for each pit defines the respective zero height elevation.

4.3.3 Initial Profile

The initial profile file (*.pro) contains the initial vertical profile of water temperature and salinity. The variables are measured values and not derived by DYRESM. The height of each layer is relative to the zero height elevation. The vertical profile of temperature and conductivity values for Caland and Hogarth were taken from Hydrolab Surveyor data collected in spring of 2007 and 2008, respectively (Gould, 2008; Godwin, 2010). Salinity values for the initial profile were then calculated using the *in situ* conductivity measurements and the Practical Salinity Scale 1978 and its extension to lower salinities (UNESCO, 1978; Eaton et al., 2005). In order to simulate future conditions, the height of the measurements in the water column are adjusted so that the initial water elevation in the profiles matched the initial water elevations assumed in each scenario (see section 4.1). The depths of the initial profile measurements below the initial surface water level were assumed to be at the same relative to the lake surface but their elevations increased to higher levels in the water column given the initial water levels for scenarios 2 and 3 (see section 4.1). The Hogarth and Caland pit lake profiles have not changed since 2004 and, therefore it is assumed that the profiles will continue to remain the same in the future (Vancook, 2005; Gould, 2008; Godwin 2010; Conly and Lee, Unpublished Data).

4.3.4 Meteorological Data

The meteorological data file (*.met) contains surface meteorological data that covers the span of the simulation period on a daily or sub-daily interval. Data required in this file includes: input timestep, type of long-wave radiation data, sensor type and a table with each column representing a parameter and each row a specific timestep. A daily time step is used, as sub-daily data for all required parameters is not available for the study site. Cloud cover, instead of measured values, is selected as the type of long wave radiation because long wave radiation is not measured at weather stations near the study site. A fixed height sensor is selected for the type

of sensor because the meteorological data is taken from fixed weather stations as opposed to a floating sensor that would be located on the lake surface. Each time step includes an ordinal date, shortwave radiation, cloud cover, air temperature, vapour pressure and wind speed values averaged over the timestep. Data is from the National Climate Data and Information Archive for the period from 1985 to 1987, as this period had datasets for all required parameters. The data covered in the meteorological file is not from the same period as the initial profile data because solar radiation and evaporation data was not available in 2007 and 2008. Hourly wind speed and relative humidity and daily mean temperature and total precipitation data was available online from the National Climate Data and Information Archive for the weather station Atikokan (climate ID 6020379). Mean daily temperature values were added directly to the meteorological file from the National Climate Data and Information Archive files available online. The hourly data for relative humidity and wind speed was averaged on a daily basis. The temperature and relative humidity values were used as a basis to calculate vapour pressure following the equation provided in the DYRESM User Manual (CWR, 2002). The global solar radiation and cloud cover data was acquired from National Climate Data and Information Archive. Short wave radiation was determined by summing global solar radiation data for the day. The nearest weather station to Atikokan, Ontario with short wave radiation data is Moosonee, Ontario (climate ID 6075425, approximately 840 km north east of Atikokan). Cloud cover data is available for three stations, Thunder Bay, Kenora and Sioux Lookout weather stations, all of which are within 250 km of Atikokan. Climate normal data for cloud cover for each location was compared and monthly cloud cover distributions in Atikokan were found to be similar to Thunder Bay (climate ID 6048261).

4.3.5 Stream Inflow

The stream inflow file (*.inf) contains the following data for each inflow for each day of the simulation: daily average volume of water entering the pits, temperature and salinity. Streams into Caland and Hogarth are not gauged and there is considerable overland flow into the pits. Therefore, inflows are calculated using the water balance Model 2b results and the following equation provided in the DYRESM user manual (CWR, 2002):

$$\text{Inflow} = \Delta\text{storage} + \text{outflow} + \text{evaporation} - \text{rainfall} \quad (\text{Eqn. 4.1})$$

Where:

$$\Delta\text{storage} = \text{storage}_{\text{final}} - \text{storage}_{\text{initial}}$$

Outflow, evaporation and rainfall are all non-negative quantities

Inflows into the pits include groundwater and surface inflows. The annual groundwater volume for both Caland and Hogarth is taken from Model 2b of the water balance and is divided by 365 days to find a daily average volume of groundwater inflow for the year of interest. The temperature of the groundwater inflow was estimated to be 3°C based on a map of average shallow groundwater temperatures in the United State (http://www.epa.gov/athens/learn2model/part-two/onsite/ex/jne_henrys_map.html; Accessed July 25, 2011 at 3:30 pm EST). Shallow groundwater is defined as groundwater that can be reached through dug wells in areas where recent precipitation is trapped underground. Compared to measured water column temperature, the groundwater temperature is 1 to 2°C cooler than the water temperatures at the bottom of the pit lake. The salinity of the groundwater is assumed to remain constant and was calculated from the conductivity measurement of a water sample taken by Godwin (2010) in a well at the airport in Atikokan. The groundwater salinity is 0.43 psu.

An annual inflow value for both Caland and Hogarth is calculated for a year of interest. The volume of inflowing water distributed over the simulation period is a percentage based on the monthly distribution of precipitation for Atikokan based on the Canadian Climate Normals

for 1971 to 2000 from the National Climate Data and Information Archives. It was assumed that overland inflows do not flow during the winter (November to March) and that the accumulated volume during the winter period will enter the pit as spring runoff (April – June). The volume of water accumulated during the winter period was summed together and divided by three and then added to the inflow totals for April, May and June. The daily average inflow volumes are calculated for April to October by dividing the total for each month by the number of days in that month. The salinity of the input waters is calculated from laboratory conductivity measurements taken from 2008 samples of surface streams (Gould, 2008, Godwin 2010) flowing into the pits using the Practical Salinity Scale 1978 and its extension to lower salinities (UNESCO, 1978; Eaton et al., 2005). Caland pit lake has two inflow types: i) low salinity inflow of fresh waters, and ii) high salinity inflow of water that is reacting with tailings/waste rock associated catchment. There is only one inflow source to Hogarth pit that flows for most of the year from spring to fall. There are a number of other seeps that enter Hogarth pit; however, flow only occurs after rain events. In some simulations additional inflows were added to simulate the addition of inflow from Fairweather into Caland and from the Rawn Reservoir into the South East Arm and will be described in sections 4.3.1, 4.3.2 and 4.3.3.

4.3.6 Withdrawals

The withdrawals file (*.wdr) contains daily withdrawal volume (m^3) for the duration of the simulation period. The file consists of daily outflow volumes from the lake for individual outlets. The number of withdrawals must equal the number of outlets indicated in the physical data and morphometry file. Depending on the simulation, the pits were modeled with and without outflows as described in sections 4.3.1, 4.3.2 and 4.3.3. For Caland, the withdrawal volume was assumed to equal the change in storage volume of the pit when it reaches an elevation of 385 masl in the water balance Model 2b. For Hogarth, the withdrawal volume was

assumed to equal the change in storage volume of the pit lakes after they reach an elevation of 394 masl in water balance Model 2b.

4.3.7 Parameters

The parameter file (*.par) included, but was not limited to, time of day for output, buoyant plume entrainment coefficient, emissivity of a water surface, mean albedo of water and critical wind speed. A complete list of parameters and an example of a parameter file are provided in Appendix VI. With the exception of the time of day, the values for the other parameters in this file correspond to values recommended by the Centre for Water Research (CWR, 2002). The time of day for output is adjusted to 1 pm because *in situ* measurements of the water column have historically been done beginning at 1 pm or later in the afternoon.

4.4 Simulated Scenarios

A number of different simulations are created to investigate three specific points of interest during the rebound process in Caland and Hogarth pit lakes. The first scenario was designed to assess if DYRESM can model current conditions in Caland and Hogarth pit lakes. The second scenario consists of a series of simulations that were designed to predict the future limnology of the pit lakes when Caland outflows into Hogarth. The third scenario involves simulations to predict the future limnology of the pit lakes when the rebound processes is complete and the joined pit lakes outflow into the West Arm. Each pit lake is modeled separately in DYRESM. Tables 4.1 and 4.2 provide summaries of each simulation for Caland and Hogarth, respectively.

4.4.1 Scenario 1 - Current Conditions

In this scenario water surface elevations are below the outlet elevation at 385 masl; and Caland and Hogarth only lose water via evaporation and receive water from precipitation and inflows. The calculation of the amount of water entering the pit from groundwater and inflows is

described in section 4.2.5. In Caland, the volume of inflowing water is divided between a higher salinity (0.51 psu) inflow and a lower salinity (0.18 psu) inflow based on two samples from streams known as Caland Seep 5 and Seep 1, respectively (Godwin, 2010). Hogarth has one inflow (Hogarth Seep 2a), which has a relatively high salinity of 1.35 psu.

Table 4.1: Summary of DYRESM simulations for Caland pit lake.

Caland Simulations	Scenario	Inflows	Outlets	Groundwater Entrance Height	Comments
1C1b 1C1c 1C1d 1C1e	1	low salinity seep (0.18 psu); high salinity seep (0.51 psu); groundwater (0.43 psu)	none	100 m 10 m 140 m 200 m	Assess the affect of groundwater entrance height on Caland limnology.
1Cv2	1	low salinity seep (0.18 psu); high salinity seep (0.51 psu); groundwater (0.43 psu); Fairweather Lake (0.18 psu)	none	100 m	Assess the affect of inflow from Fairweather Lake on the limnology of Caland.
2C1	2	low salinity seep (0.18 psu); high salinity seep (0.51 psu); groundwater (0.43 psu)	at 385 masl	100 m	Assess the affect of groundwater entrance height on Caland limnology.
2C2	2	low salinity seep (0.18 psu); high salinity seep (0.51 psu); groundwater (0.43 psu)	at 385 masl	10 m	
2Cv2	2	low salinity seep (0.18 psu); high salinity seep (0.51 psu); groundwater (0.43 psu); Fairweather Lake (0.18 psu)	at 385 masl	100 m	Assess the affect of inflow from Fairweather Lake on the limnology of Caland.
2Cv3	2	low salinity seep (0.18 psu); high salinity seep (0.51 psu); groundwater (0.43 psu); Fairweather Lake (0.18 psu)	at 385 masl	100 m	A slower rebound rate is used in the water volume calculations.
3C_1out	3	low salinity seep (0.18 psu); high salinity seep (0.51 psu); groundwater (0.43 psu); Fairweather Lake (0.18 psu)	at 385 masl	100 m	Predicts the future limnology of Caland.
3Cv3_1out	3	low salinity seep (0.18 psu); high salinity seep (0.51 psu); groundwater (0.43 psu); Fairweather Lake (0.18 psu); inflow from Rawn Reservoir (0.18 psu)	at 385 masl	100 m	Assess the affect of increased inflow volumes into the Southeast Arm from the Rawn Reservoir on the future Caland limnology.

Table 4.2: Summary of DYRESM simulations for Hogarth pit lake.

Hogarth Simulations	Scenario	Inflows	Outlets	Groundwater Entrance Height	Comments
1H1b 1H2 1H3	1	seep (0.4 psu); groundwater (0.43 psu)	none	100 m 10 m 180 m	Assess the affect of groundwater entrance height on Hogarth limnology.
1H_HSGW	1	seep (0.4 psu); groundwater (2.4 psu)	none	100 m	Assess the affect of groundwater salinity on Hogarth limnology.
1H_MSGW		seep (0.4 psu); groundwater (1.3 psu)			
2H1	2	seep (0.4 psu); groundwater (0.43 psu); Caland inflow (0.35 psu)	none	100 m	Assess the affect of groundwater entrance height on Hogarth limnology. Note that the Caland inflow salinity varies overtime.
2H1b	2	seep (0.4 psu); groundwater (0.43 psu); Caland inflow (0.35 psu)	none	180 m	
2H2	2	seep (0.4 psu); groundwater (0.43 psu); Caland inflow (0.37 psu)	none	100 m	Assess the affect of Caland inflow salinity on Hogarth limnology.
2H3	2	seep (0.4 psu); groundwater (0.43 psu); Caland inflow (0.41 psu)	none	100 m	
2Hv2	2	seep (0.4 psu); groundwater (0.43 psu); Caland inflow	none	100 m	Assess the affect of the Caland on Hogarth limnology when inflow from Fairweather Lake is added to Caland. Note that the Caland inflow salinity varies overtime.
2Hv3	2	seep (0.4 psu); groundwater (0.43 psu); Caland inflow	none	100 m	A slower rebound rate is used in the water volume calculations. Note that the Caland inflow salinity varies overtime.
3Hv2	3	seep (0.4 psu); groundwater (0.43 psu); Caland inflow	at 394 masl	100 m	Predicts the future limnology of Hogarth. Note that the Caland inflow salinity varies overtime.
3Hv3	3	seep (0.4 psu); groundwater (0.43 psu); Caland inflow	at 394 masl	100 m	Assess the affect of increased inflow volumes into the Southeast Arm from the Rawn Reservoir on the future Hogarth limnology. Note that the Caland inflow salinity varies overtime.

Groundwater entering both pits is assumed to have the same salinity and temperature with the exception of two Hogarth simulations described below. Since water only exits via evaporation, no withdrawals are taken from either pit lake in this scenario. The simulations for Caland are initialized with spring 2008 *in situ* conductivity measurements assuming a water surface elevation of 313.9 masl measured for that year. The simulations for Hogarth were initialized with spring 2007 *in situ* conductivity measurements and an initial water surface elevation of 306.9 m. The actual entrance elevation of groundwater entry is unknown so a number of different simulations were run with groundwater entering at different heights to see if there was any effect on the limnology. Caland simulations 1C1b, 1C1c, 1C1d, 1C1e vary the groundwater entrance height from 100 m, 10 m 140 m and 200 m, respectively. An additional model for Caland, 1Cv2 adds an inflow into Caland from Fairweather Lake to see if the limnology of Caland would be impacted by increased freshwater inflow into the pit lake. In this simulation, the temperature of the inflow over the course of the simulation was the average of 1 m, 2 m and 5 m water temperatures from simulation 1C1b. Therefore, the temperature of the water inflowing into Caland from Fairweather was higher than that of the seeps, which have temperatures equal to the air temperatures during the simulation. The salinity of the Fairweather Lake inflow is the same as the fresh water or low salinity seep into Caland, Seep 1. For Hogarth simulations 1H1b, 1H2 and 1H3 the groundwater entrance height was varied from 100 m, 10 m, and 180 m, respectively. In addition, two variations of simulation 1H1b (1H_HSGW and 1H_MSGW) were conducted with groundwater salinity values of 2.4 psu and 1.3 psu, respectively, which are higher than that used in 1H1b (0.4 psu). These simulations were performed to examine if the salinity of groundwater has any influence on the limnology and stratification of Hogarth pit lake.

4.4.2 Scenario 2: Future Conditions When Pit Lakes Join

In this scenario, the water surface elevation in Caland has passed 385 masl in elevation and begins to flow into Hogarth. Consequently, Caland now loses water from an outlet as well as evaporation and Hogarth gets a new inflow source from Caland. With respect to the initial profile, it was assumed that the pit lake limnology has remained constant and the simulations for both pits are initialized with the same temperature and salinity profiles as in Scenario 1. However, the depths of the measurements in the initial profile are adjusted to correspond to the new water surface elevations of 385 masl and 366.5 masl for Caland and Hogarth, respectively, based on rebound Model 2B. For Caland a withdrawal is added at the 385 m outlet. The determination of the volume of the withdrawal is described in section 4.2.6. Simulations for Caland, 2C1 and 2C2, assess the effect of groundwater entrance height has on limnology. Simulation 2Cv2 considered the influence of inflow from Fairweather Lake on Caland pit lake limnology. Simulation 2Cv3 used water elevations and volumes calculated for rebound model 1B, which has a slower rate of rebound than model 2B, in order to see the effects on the limnology of the pit lake. This simulation also included inflow from Fairweather Lake.

For Hogarth simulations, an inflow was added to account for water flow from Caland into Hogarth upon joining of the pit lakes. The water elevation in Hogarth is below the 385 masl outlet from Caland. For simulations 2H1 and 2H1b, temperature and salinity values of the inflow from Caland into Hogarth were an average of simulation 2C1 results at 2 m, 5 m, 10 m, 15 m and 20 m. The difference between 2H1 and 2H1b was the groundwater entrance heights of 100 m and 180 m, respectively. To simulate the potential affect of water outflow from deeper in the Caland water column, where salinity values were higher, variations of Model 2H1 were made; Models 2H2 and 2H3 used temperature and salinity values averaged from 40 to 60 m and 100 to 140 m, respectively. As with Caland two alternate versions of this scenario were run for Hogarth (2Hv2 and 2Hv3). In 2Hv2 the temperature and salinity values of the Caland inflow are taken

from simulation 2Cv2 and were the average of results for 2 m, 5 m, 10 m, 15 m and 20 m. This simulation was to assess if the addition of inflow from Fairweather Lake into Caland changes the resultant limnology of Hogarth when the pits join. For simulation 2Hv3, rebound Model 1b was used to determine water elevations and inflow volumes, and includes inflow from Fairweather Lake into Caland to assess if the slower rebound rate influences pit lake limnology.

4.4.3 Scenario 3: Future Conditions When Pit Lake Outflow to the West Arm

In this scenario, the two pit lakes have already joined and their water surface elevation has passed the elevation of the outlet to the West Arm (394 masl). With respect to the initial profile, both pits were initialized with the same temperature and salinity profiles as in Scenarios 1 and 2. However, the depths of the measurements in the initial profile were adjusted to correspond to the new water surface elevation of 394 masl. In this scenario Caland has one withdrawal from an outlet with an elevation of 385 masl and Hogarth now has one outlet at 394 masl. In the meteorological file, the height of the weather station above the lake bottom has been increased by 2 m in these simulations. This was done so that the water level in Caland pit lake does not rise above the weather station height which results in the termination of the simulation. The change in the height of the weather stations was made instead of changing the physical morphometry of the lake. Only one simulation was conducted for each pit with and without an additional inflow into Caland. The simulations with an additional inflow simulated if water level was lowered behind Hardy Dam resulting in greater inflow into South East Arm and, subsequently, Caland and Hogarth pit lakes. Simulations 3C_1out and 3Hv2 were without the additional inflow and 3Cv3_1out and 3Hv3 were with the additional inflow. Similar to previous simulations, including 2Hv2, the temperature and salinity values of the inflow from Caland simulations 3Hv2 and 3Hv3 were taken from results of simulations 3C_1out and 3Cv3_1out,

respectively. All scenario 3 simulations included an inflow from Fairweather Lake because at this point in the rebound process the three lakes are joined.

4.5 Results

Temperature, salinity and density profiles for each simulation are illustrated in Figures 4.1 to 4.9. The illustrations output by Modeller v2b2 indicates a layer's height in the water column relative to the zero-height elevation (equals the bottom of the pit). In order to facilitate the interpretation and description of results, a depth scale was added to each illustration and all discussions of the position of layers within the water column was with respect to the depth scale. The depth scale indicates the depth of layer in the water column relative to surface. All of the illustrations also include temperature ($^{\circ}\text{C}$), salinity (psu) and density (kg/m^3) scales. The temperature scale used in the illustrations is the same for both Hogarth and Caland results. In order to maintain detail in the salinity and density profile illustrations for Caland and Hogarth pit lakes, different scales are used for each pit. For each pit all simulations use the same scales with the following exceptions: 1H_HSGW and 1H_MSGW density scales are increased. The year 1991 appears on each diagram because the meteorologic data file requires the data to be after 1990. Thus, the dates in the meteorologic data file were arbitrarily set to the year 1991 although data is from 1986 for both pits.

4.5.1 Scenario 1

Caland: The temperature, salinity and density profiles of Caland simulations 1C1b, 1C1c, 1C1d, and 1C1e are largely similar. A steep thermal gradient exists 10 m below the surface in all temperature profiles indicating the presence of a thermocline (Figs 4.1 and 4.2). The 10 m epilimnion¹ remains warmer throughout the simulation, and thermally stratifies in the summer

¹ A glossary of terms can be found in appendix VII.

and mixes in the fall. Below the thermocline is a layer of cold water ($\sim 4^{\circ}\text{C}$) approximately 15 m thick that exists throughout the simulation. The water column gradually warms from the cold layer down to a depth of 50 m, at which point the water column's temperature ($\sim 5.9^{\circ}\text{C}$) is relatively uniform down to the bottom. The difference between the temperature profiles of Caland simulations is that simulation 1C1b and 1C1d have plumes at depths of 90 m and 60 m, respectively, and all other simulations do not (Figs. 4.1 and 4.2). This suggests that the groundwater entrance heights influence plume formation.

The salinity of the epilimnion (0.3 to 0.4 psu) was slightly lower than the cold layer below the thermocline (0.5 psu). The salinity increases to 0.7 psu from the bottom of the cold layer to a depth of 50 m. From 50 m to 150 m the salinity of water column varies between 0.7 psu and 0.8 psu. The highest salinity water, 0.8 psu occurs as a layer between 90 m and 110 m. From a depth of 150 m to the bottom of the water column the salinity is 0.6 psu. The salinity change in the water column from 150 m to bottom in simulation 1C1b and 1Cv2 is not significant (<0.01 psu). Changes in salinity for 1C1b and 1Cv2 correspond to loss of thermal stratification, which occurs slightly earlier in 1Cv2.

The density profiles vary in accordance to the temperature profile in the epilimnion. The density of the water column below the thermocline attains a maximum density of 1001 kg/m^3 that was maintained to the bottom. In simulation 1C1b, the highest density layer begins at a depth of 110 m and in the other simulations the layer begins at 120 m. The top of the highest density layer corresponds to the bottom of the high salinity layer (90 to 110 m) indicating the presence of a chemocline at a depth of 110 m.

The temperature, salinity and density gradients indicate that Caland is meromictic with a mixolimnion from the surface to 35 m in the water column, a chemolimnion from 35 to 110 m, and a monimolimnion from 110 m to the bottom. The upper 30 m of the water column thermally stratifies with an epilimnion from the surface to 10 m, a metalimnion from 10 to 15 m and a

hypolimnion from 15 to 35 m. Meromictic stratification in Caland has been previously observed (McNaughton, 2001; Vancook, 2005; Gould, 2008; Godwin, 2010). The mixolimnion predicted by DYRESM (35 m) is thicker than the measured thickness of the mixolimnion (20 m) reported by Godwin (2010). The addition of inflow to Caland from Fairweather Lake did not change the range in values or patterns for the temperature, salinity, and density profiles with the exception of slightly increasing the thickness of the mixolimnion (Fig. 4.1). The salinity profiles for Caland show a salinity inversion in the middle of the lake that may be an artifact of the initial profile used in this study. This artifact is likely a result of the in situ conductivity measurements used to calculate salinity, which increased down to the middle of the water column and then undergo a slight decrease to the bottom of the pit lake.

Hogarth: The temperature, salinity and density profiles for Hogarth simulations 1H1b and 1H3 are very similar (Fig. 4.3). The profiles show that below a depth of 55 m to the bottom of the pit lake the temperature of the water column ($\sim 4.6^{\circ}\text{C}$) is uniform. From the start of the simulation until mid-August there is a layer 1 - 3 m that was generally 10°C warmer than the water below. Below the warm layer to a depth of 20 m the water column thermally stratifies. As the water column begins to cool in mid-August thermal stratification is lost, including the warm layer.

The thin warm water layer at the surface of Hogarth also has the lowest salinity (0.9 psu) Immediately below this layer to a depth of 20 m is the highest salinity layer (2.2 psu). The bottom of the high salinity layer (20 m) corresponds to the maximum depth that thermal stratification extends to, and suggests the existence of a thermocline. When thermal stratification is lost in August, the top 20 m of the water column mix and the thin 1 to 3 m layer of warm, low salinity water disappears. During this period the water column gradually increases in salinity from the surface to a depth of about 20 m, which is in contrast to the sharp gradients at the beginning of the simulation.

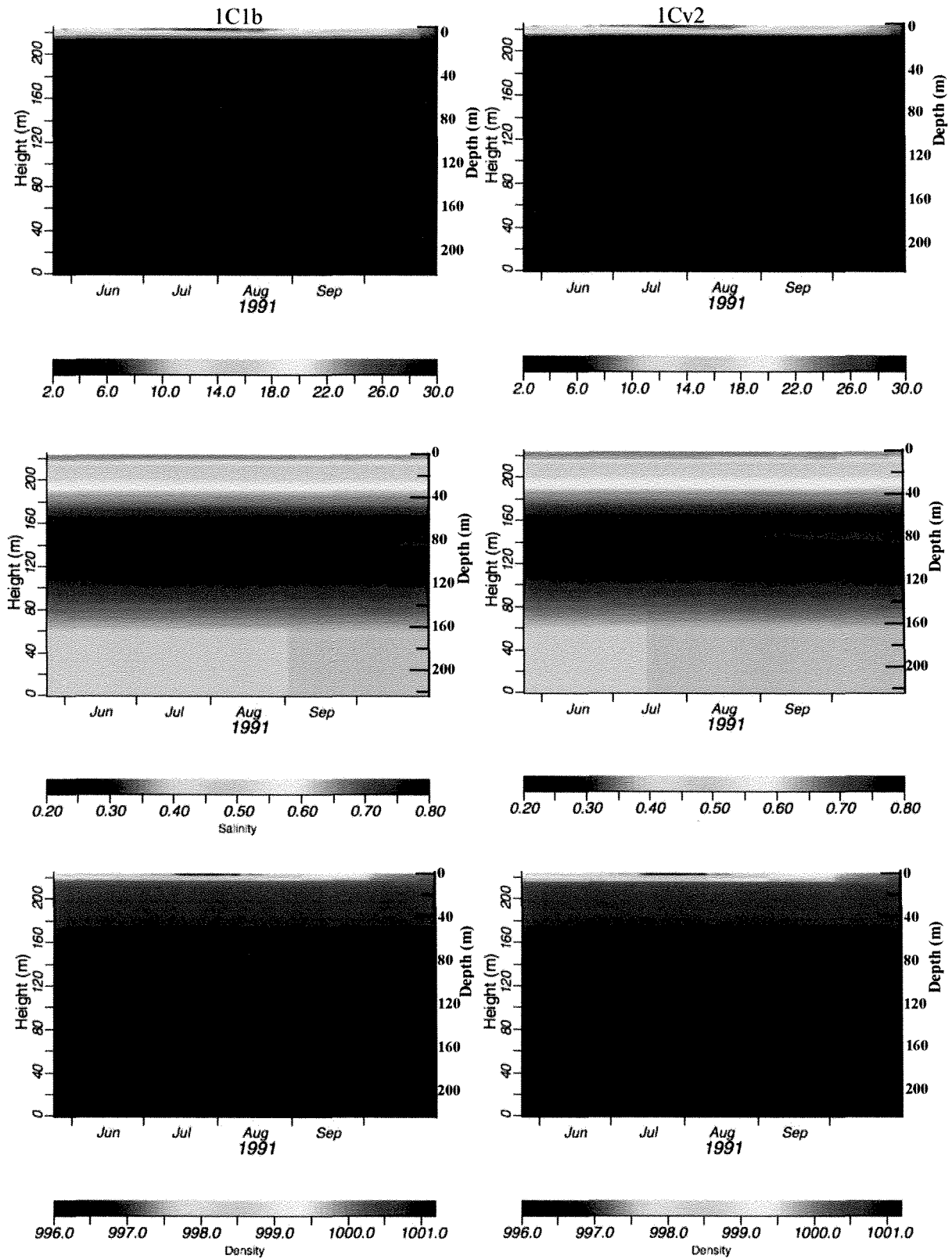


Figure 4.1: Temperature (°C), salinity (psu) and density (kg/m³) profiles for scenario 1 simulations 1C1b and 1Cv2 for Caland pit lake. Aside from the salinity at bottom of the pit increasing earlier in 1Cv2 than 1C1b there are no significant differences in profiles.

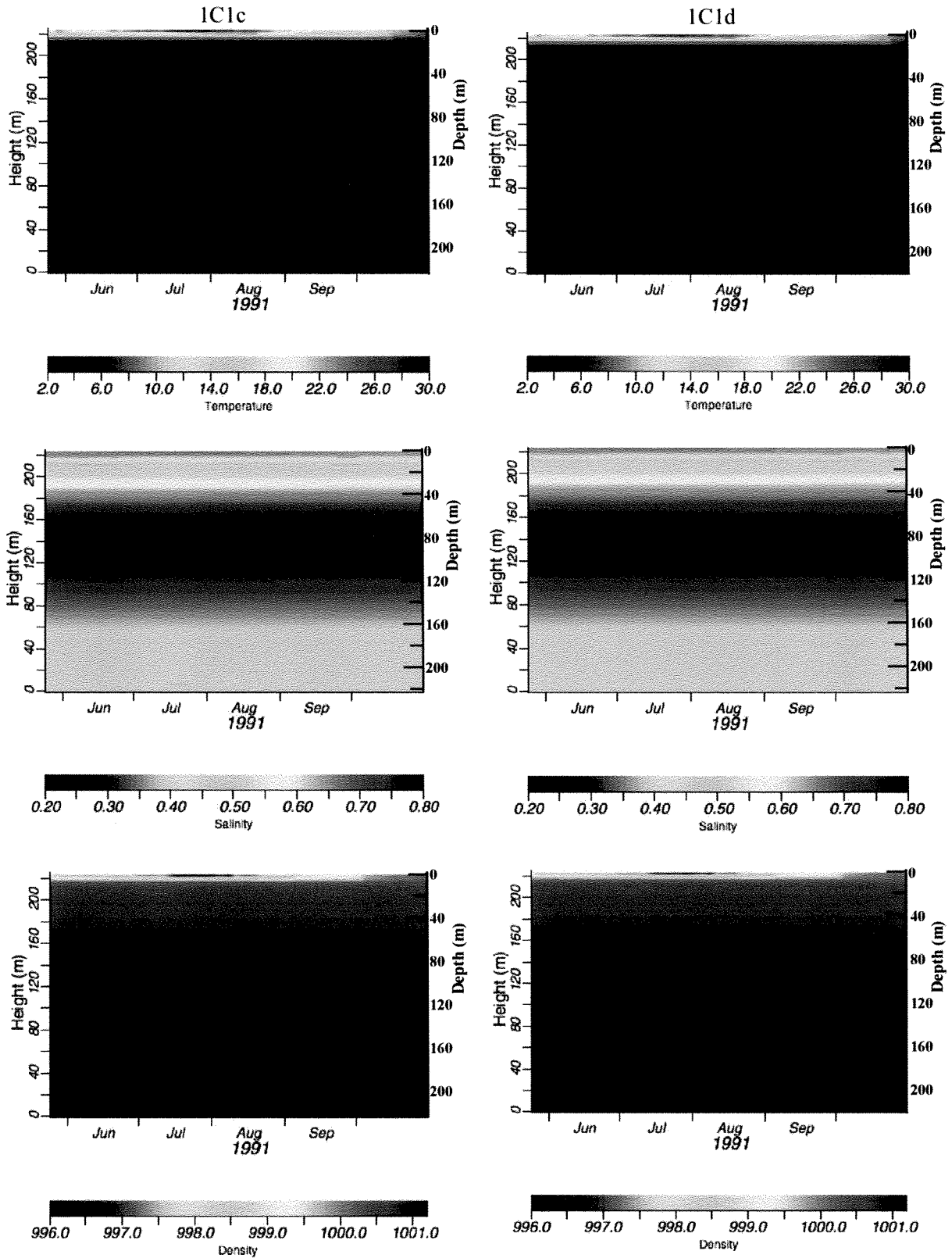


Figure 4.2: Temperature ($^{\circ}\text{C}$), salinity (psu) and density (kg/m^3) profiles for scenario 1 simulations 1C1c and 1C1d for Caland pit lake. The profile for simulation 1C1e is identical to 1C1d and is not shown. Relative to 1C1b, 1C1c and 1C1d do not have a plume in the layer with the highest salinity and the salinity at the bottom of the pit does not change with time.

Below a depth of 20 m the water column consists of two layers: i) a higher salinity layer (2.1 psu) from 20 to 110 m; and ii) a lower salinity layer (1.9 psu) that extends from 110 m to the bottom. In simulation 1H1b, a plume is present in the low salinity layer but is absent in simulation 1H3, indicating the influence of the groundwater entrance height on plume formation.

The density of the upper 20 m of the water column varies in accordance with temperature. Below a depth of 20 m, density gradually increases, reaching a maximum (1002.1 kg/m^3) at a depth of 80 m, which is maintained to the bottom of the pit lake. Simulation 1H2, with the groundwater entrance height at 10 m, would terminate prematurely due to an error regarding buoyant inflow during initialization.

Simulation 1H_MSGW is largely similar to 1H1b (Figs. 4.3 and 4.4). The maximum depth that thermal stratification extends to is 20 m. In the salinity profile, the 1 to 3 m thick low salinity layer (0.9 psu) at the surface overlies a layer with highest salinity (2.2 psu), which extends to a depth of 20 m. Below a depth of 20 m the water column consists of two layers: i) a higher salinity layer (2.1 psu) from 20 to 110 m; and ii) a lower salinity layer (1.9 psu) that extends from 110 m to the bottom of the lake. Relative to simulation 1H1b, the salinity in the bottom low salinity layer in 1H_MSGW is 0.02 psu higher. A plume is present in the high salinity layer of 1H_MSGW at depth of 60 m. The density gradually increases below a depth 20 m, reaching a maximum (1002.2 kg/m^3) at a depth of 80 m, which is maintained to the bottom of the pit lake.

There are a number of differences between the salinity and density profiles of simulation 1H_HSGW in comparison to 1H_MSGW (Fig. 4.4). Below 20 m in simulation 1H_HSGW, the water column can still be divided into two layers but they occur at different depths: the high salinity (2.1 psu) layer extends from 20 m to 80 m; and, the low salinity (1.9 psu) layer from 80 m to the bottom. Also, no plume is present in the high salinity layer.

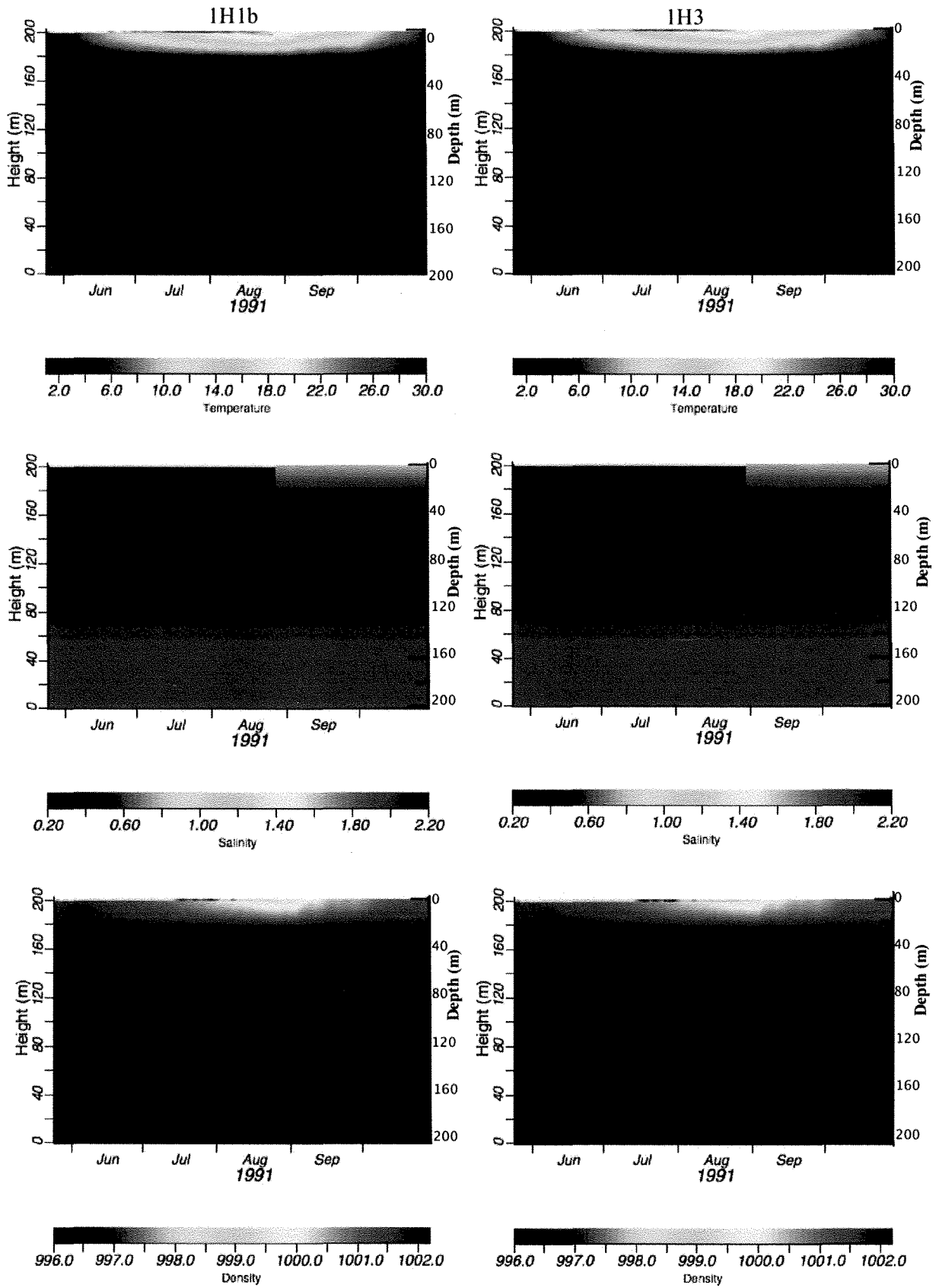


Figure 4.3: Temperature (°C), salinity (psu) and density (kg/m³) profiles for scenario 1 simulations 1H1b and 1H3 for Hogarth pit lake. The salinity profile for 1H1b shows a plume and that of 1H3 does not.

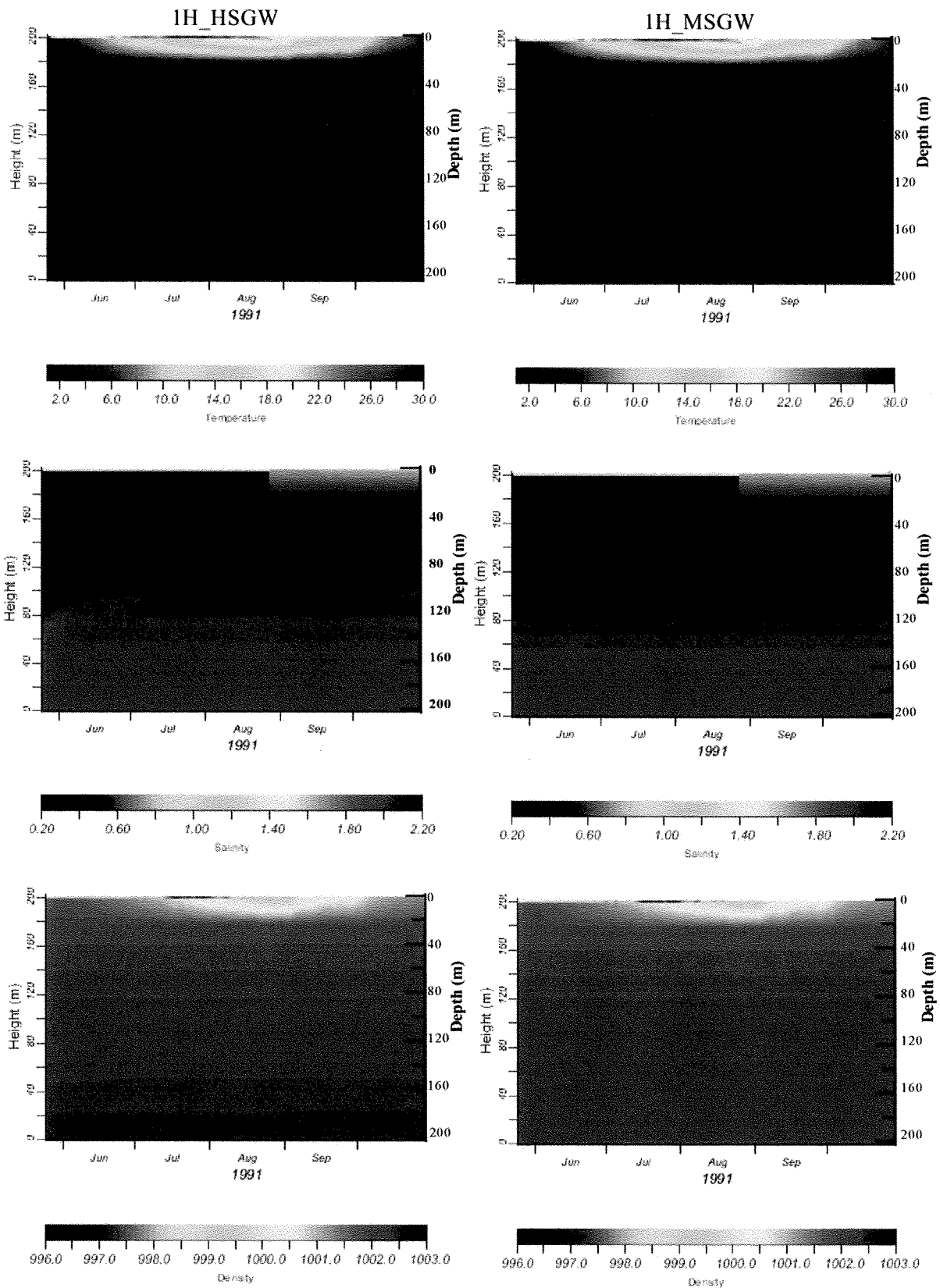


Figure 4.4: Temperature (°C), salinity (psu) and density (kg/m³) profiles for scenario 1 simulations 1H_MSGW and 1H_HSGW for Hogarth pit lake. Relative to 1H1b the density at the bottom of the pit is greater in simulations 1H_MSGW and 1H_HSGW. Simulation 1H_MSGW shows a plume in the salinity profile and 1H_HSGW does not.

From the surface to 20 m depth the density profile varies according to temperature. Below 20 m the density gradually increases reaching a maximum (1002.4 kg/m^3) at 180 m, which is maintained to the bottom. This layer occurs lower in the water column and is denser than 1H1b and 1H_HSGW. The presence of this layer suggests that the colder and higher salinity (2.2 psu) groundwater plunges to the bottom of the pit.

Based on simulation 1H1b, Hogarth can be classified as meromictic because of the presence of a thermocline at a depth of 20 m and the steep salinity gradient between the 1 to 3 m low salinity lens (0.5 psu) and the high salinity water (2.2 psu) below it. The steep chemical gradient dissipates when thermal stratification is lost in August; however, the salinity of the water column from the surface to 20 m remains lower than the water below (Fig. 4.3). The loss of the steep chemical gradient suggests that the meromictic conditions are temporary. This supports the observations by McNaughton (2001), Gould (2008) and Godwin (2010), that a thin fresh water lens exists, at least temporarily, at the surface of Hogarth pit lake. The thin 1 to 3 m fresh water lens predicted by DYRESM is similar to the thin 1 to 2 m fresh water lens reported by McNaughton (2001), Gould (2008) and Godwin (2010). A distinct chemocline is not present throughout the scenario 1 simulations for Hogarth as it is in Caland, where density and salinity changes occur at the same depth (110 m) (Fig. 4.1 & 4.3). In Hogarth the top of highest density layer does not correspond to the bottom of the highest salinity layer.

Based on simulations 1H1b and Hogarth's classification as meromictic, the mixolimnion extends from the surface to 20 m, the chemolimnion from 20 m to 80 m, and the monimolimnion from 80 m to the bottom. Here the contact between the chemolimnion and monimolimnion is defined to be the depth at which the maximum density is reached (Fig. 4.3).

4.5.2 Scenario 2

Caland: In general, Caland temperature, salinity and density profiles do not change in scenario 2 relative to simulations 1C1b with the following exceptions: i) the mixolimnion is thinner (20 m thick); ii) the chemocline is located higher in the water column (at a depth of 120 m); iii) the monimolimnion is thicker and has a lower salinity (0.5 psu) (Fig. 4.5).

Relative to simulation 2C1, increasing the groundwater entrance height in simulation 2C2 slightly increased the thickness (<5 m) of the epilimnion in the temperature, salinity and density profiles (Fig. 4.5). This may be because less groundwater is lost to entrainment when the groundwater entrance height is higher in the water column since the groundwater travels up the water column a shorter distance. Relative to 2C1, the increased freshwater inflow into Caland from the addition of inflow from Fairweather Lake (simulation 2Cv2) produced a slightly thicker freshwater lens at the top of the water column (Fig. 4.6). The use of a longer rebound rate in simulation 2Cv3 did not significantly change the temperature, salinity and density profiles in Caland compared to 2Cv2 (Fig. 4.6).

Hogarth: Relative to simulation 1H1b, Hogarth scenario 2 simulations (2H1, 2H1b, 2H2, 2H2, 2Hv2 and 2Hv3) are significantly different (Figs. 4.3, 4.7, 4.8 and 4.9). The main differences are that the surface low salinity layer (0.9 psu) that was 1 to 3 m deep in simulation 1H1b is a permanent feature of simulation 2H1 and is 10 m deep. Also, thermal stratification in Hogarth does not penetrate as deeply into the water column in simulation 2H1 compared to 1H1b. The density profile varies according to temperature from the surface to a depth of 10 m. Below 10 m, the water column density increases to a maximum of 1002.1 kg/m^3 at a depth of 80 m, the same as in simulation 1H1b. Based on these differences Hogarth can be considered a permanent meromix; however, the mixolimnion occurs from the surface to a depth of 10 m in scenario 2 simulations and is thinner than that in simulation 1H1b (20 m). The chemolimnion in simulation 2H1 occurs from 10 m to 80 m and the monimolimnion from 80 m to the bottom.

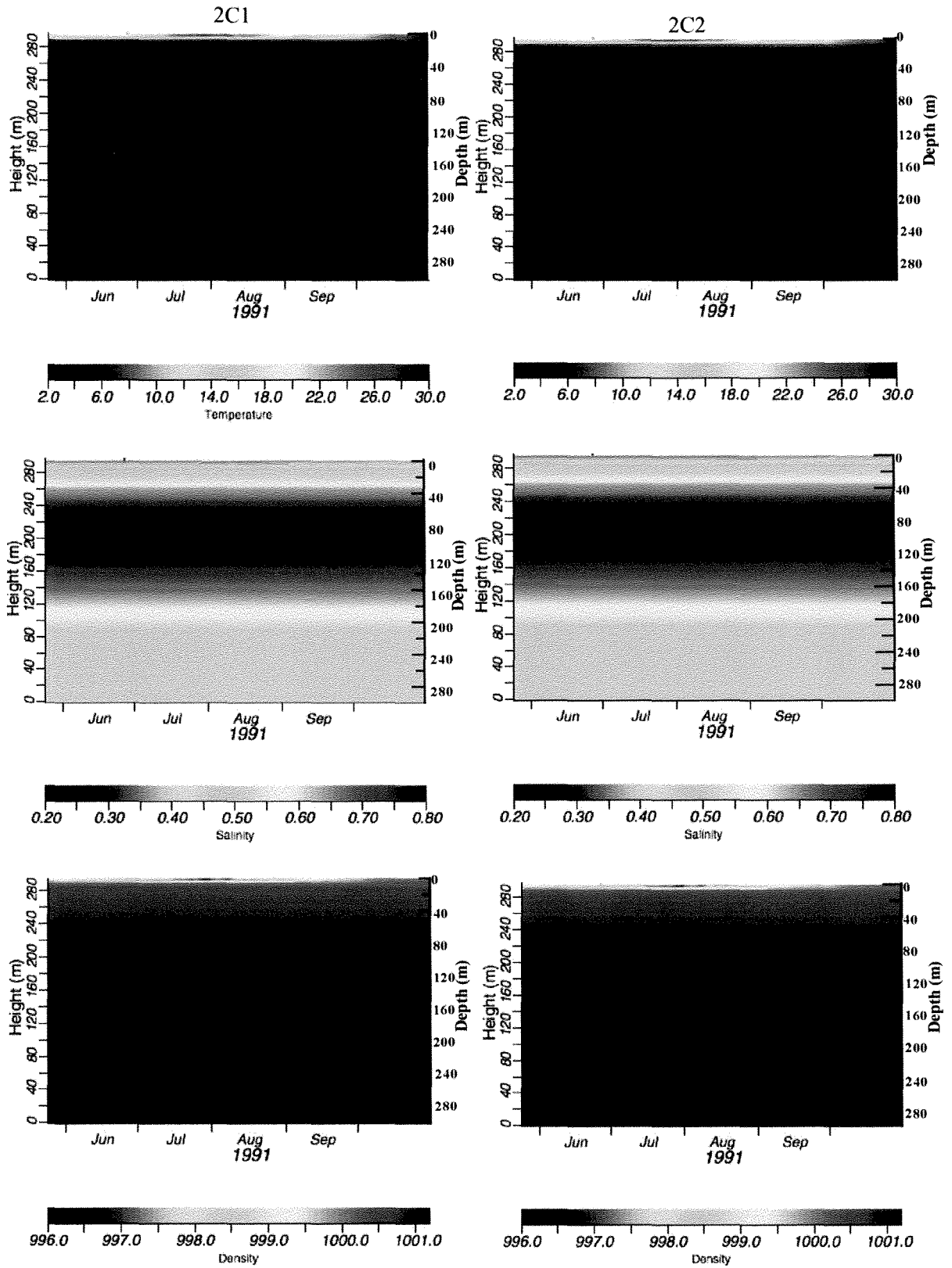


Figure 4.5: Temperature (°C), salinity (psu) and density (kg/m³) profiles for scenario 1 simulations 2C1 and 2C2 for Caland pit lake. Relative to simulation 1C1b, the salinity in the pit lake is lower in simulations 2C1 and 2C2 and the low salinity surface layers are thinner.

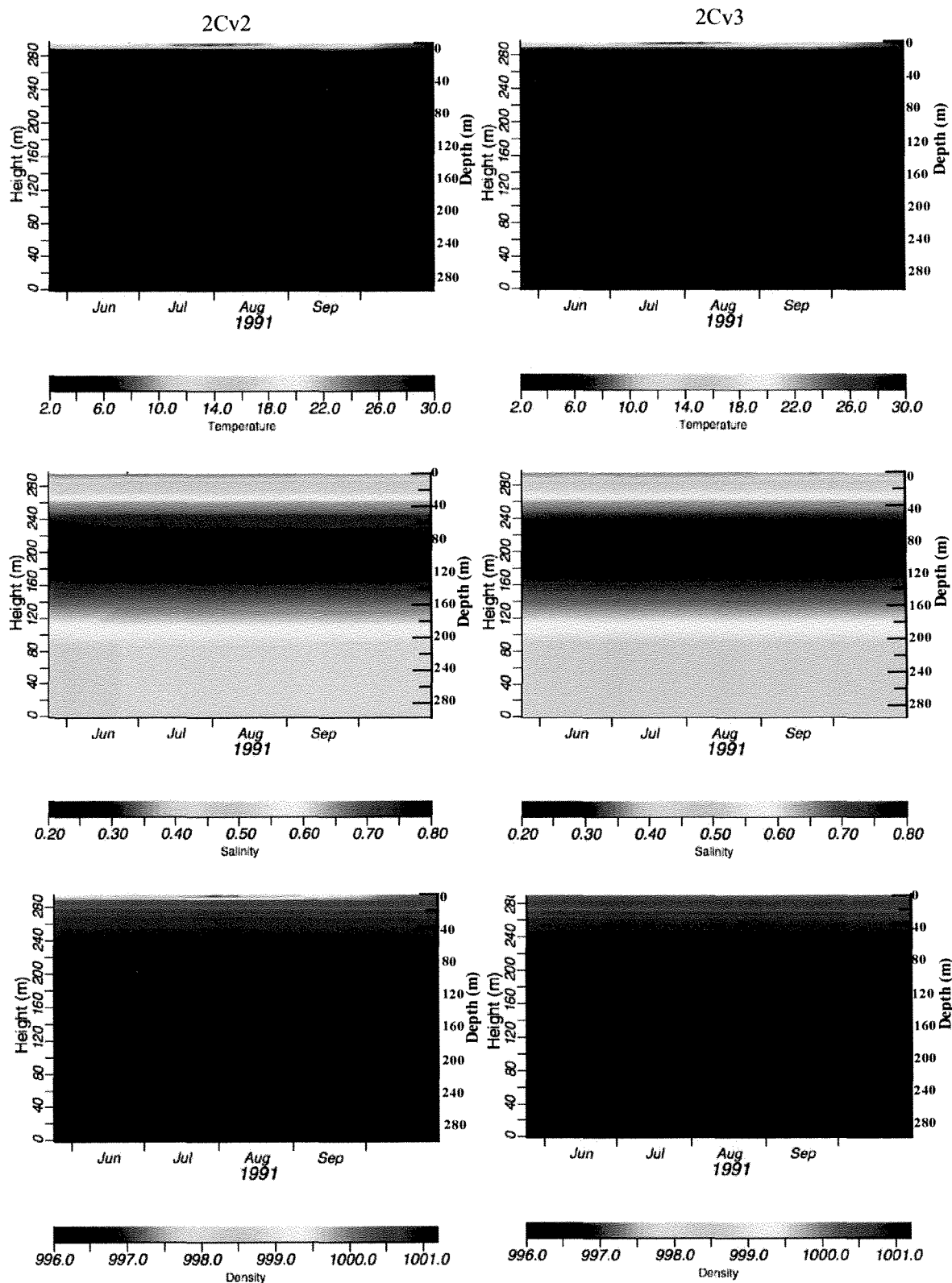


Figure 4.6: Temperature ($^{\circ}\text{C}$), salinity (psu) and density (kg/m^3) profiles for scenario 2 simulations 2Cv2 and 2Cv3 for Caland pit lake. There are no significant differences between profiles for simulations 2Cv2 and 2Cv3 compared to 2C1 except for a slightly thicker fresh water lens in the salinity profile for 2Cv3.

Altering the groundwater entrance height from 100 m in simulation 2H1 to 180 m in 2H1b changed the position and thickness of a plume in the chemolimnion from between 20 and 80 m in 2H1 and between 30 and 35 in 2H1b (Fig. 4.7). Again, simulations 2H1 and 2H1b indicated that plume formation is affected by the groundwater entrance height. Altering the chemistry of the inflow from Caland pit to higher salinity values in simulations 2H2 and 2H3 representing water from lower levels in Caland does not change the temperature, salinity and density profiles in comparison to 2H1 (Figs. 4.7 and 4.8). Similarly, the change in Caland inflow chemistry as a result the additional fresh water inflow into Caland from Fairweather Lake (simulation 2Hv2) does not change the temperature, salinity and density profiles in comparison to 2H1 (Figs. 4.7 and 4.9). This is likely because the salinity of Caland, including its highest salinity layer (0.8 psu), is significantly lower than the salinity of Hogarth (1.9 to 2.2 psu), with the exception of the low salinity surface layer (0.9 psu) from 0 to 10 m. The use of a slower rebound rate in simulation 2Hv3 did not produce any significant changes to the profiles relative to simulation 2H1 (Figs. 4.7 and 4.9).

4.5.3 Scenario 3

Caland: Temperature, salinity and density profiles in simulation 3C_1out and 3Cv3_1out for Caland are not significantly different than simulation 2C1 except for: i) the maximum temperature of the surface waters and the length of time it is maintained progressively decreases from simulations 2C1 to 3C_1out to 3Cv3_1out; and, ii) the density profile parallels the temperature profile with the density in the surface layer progressively decreasing from simulations 2C1 to 3C_1out to 3Cv3_1out (Figs. 4.5 and 4.10). The top of the dense bottom layer still correlates to the depth of the chemocline. The addition of an inflow into Caland from the Auxillary Rawn Reservoir did not significantly change profiles between simulations 3Cv3_1out and 3C_1out, with and without the additional inflow, respectively (Fig. 4.10).

Hogarth: In this scenario the temperature, salinity and density profiles in simulations, 3Hv2 and 3Hv3 significantly change relative to 2H1 (Figs. 4.7 and 4.11). For these simulations the warm temperature layer near the surface extends to greater depths (~20 m as opposed to ~ 10 m in simulation 2H1). Thermal stratification in upper 20 m of the water column in simulations 3Hv2 and 3Hv3 varies more over the course of the simulations compared to 2H1 and 1H1b. In simulations 2H1 and 1H1b an elevated surface water temperatures (~26°C) exists from July to August while in simulations 3Hv2 and 3Hv3 high surface temperature only exists for brief periods in July (Figs. 4.3, 4.7 and 4.11). There is no significant difference between the temperature profiles for simulations 3Hv2 and 3Hv3 (Fig. 4.11). The salinity profiles are significantly different in 3Hv2 and 3Hv3 relative to 2H1 and 1H1b (Figs. 4.3, 4.7 & 4.11). A low salinity layer exists at the surface at the start of the simulation, but is lost for the remainder of the simulation. The withdrawal from Hogarth at the outlet to the West Arm likely accounts for the loss of the low salinity layer at the surface of Hogarth in scenario 3 simulations compared to scenarios 1 and 2 simulations, which do not have a withdrawal. For the majority of the simulations the lowest salinity waters are at the bottom of the pit lake. The highest salinity waters are between 10 to 110 m and is split by a low salinity plume, which results in a gradual increase in depth of the lower contact of the high salinity layer overtime. There are no significant differences in salinity profiles between simulations 3Hv2 and 3Hv3. The density profiles for simulations 3Hv2 and 3Hv3 closely follow the temperature profiles at the surface (<10 m) and the top of the highest density layer is at the same depth as the bottom of the highest salinity layer. Other than the variations due to temperature, there are no other significant differences in the density profiles for simulations 3Hv2 and 3Hv3 in comparison to 2H1.

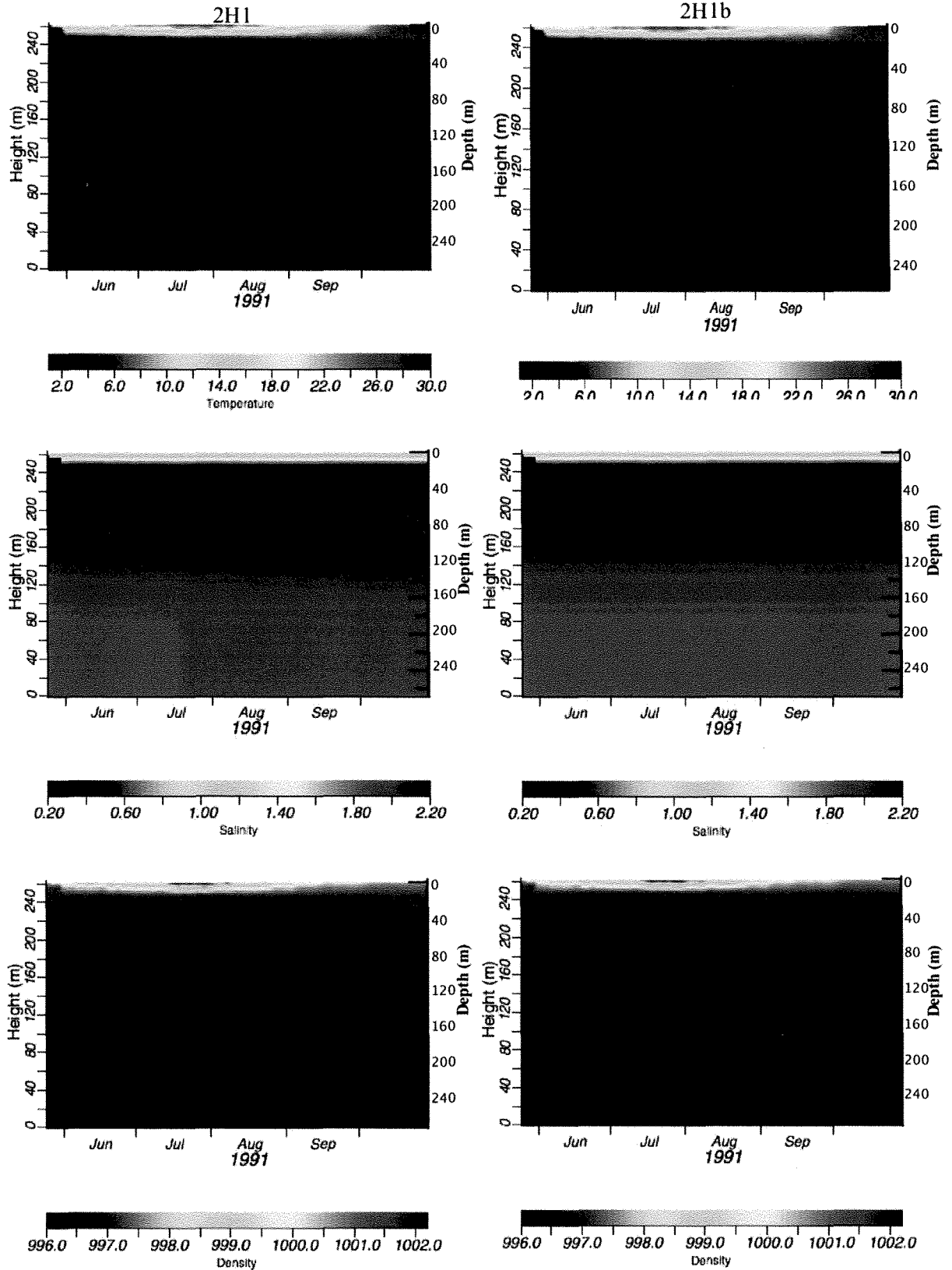


Figure 4.7: Temperature ($^{\circ}\text{C}$), salinity (psu) and density (kg/m^3) profiles for scenario 2 simulations 2H1 and 2H1b for Hogarth pit lake. Relative to simulation 1H1b the salinity profiles show a permanent fresh water layer at the surface. Simulation 2H1 has a plume in the salinity profile and simulation 2H1b does not.

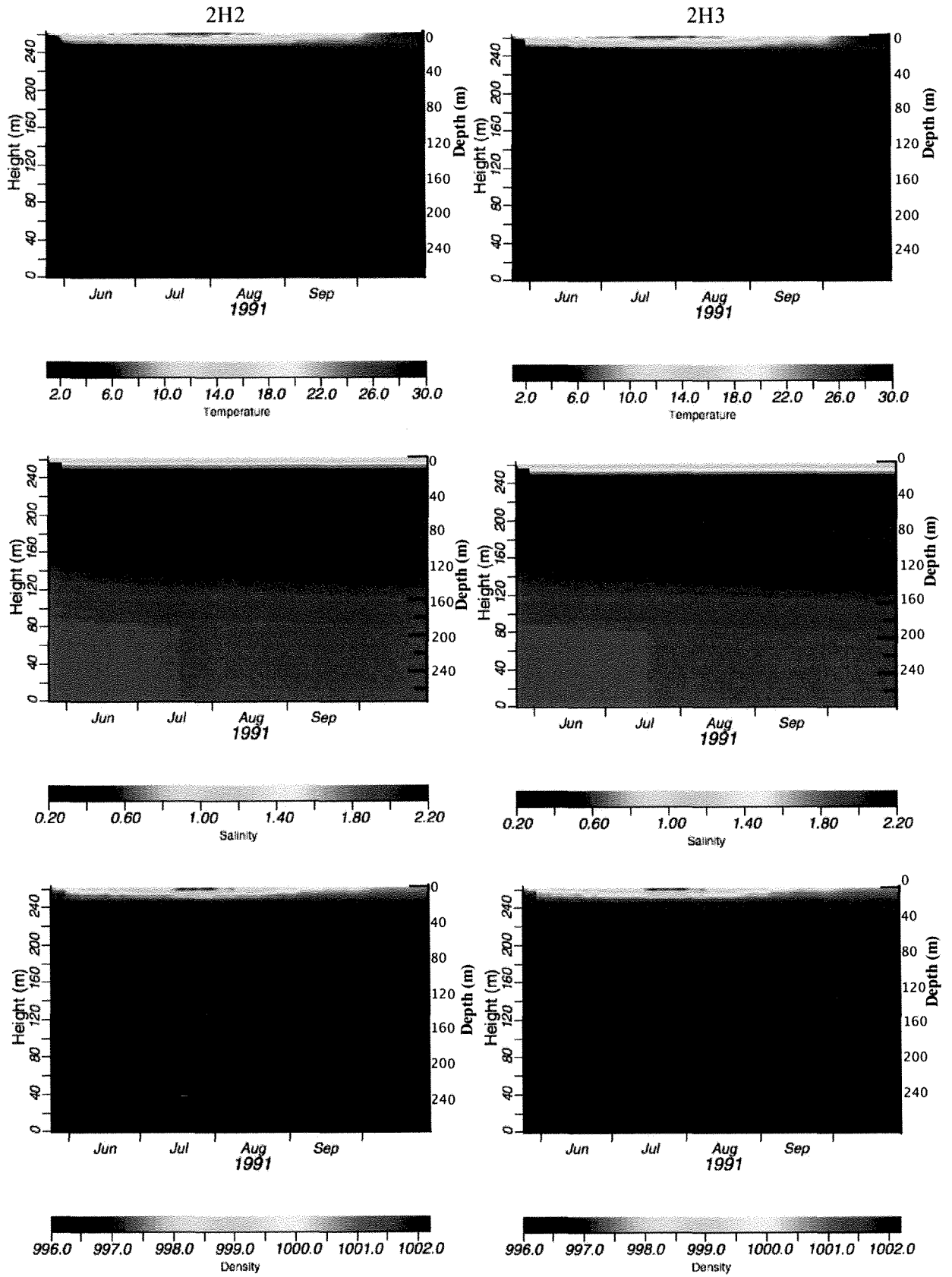


Figure 4.8: Temperature (°C), salinity (psu) and density (kg/m³) profiles for scenario 2 simulations 2H2 and 2H3 for Hogarth pit lake. Relative to simulation 2H1, there are no significant differences in profiles.

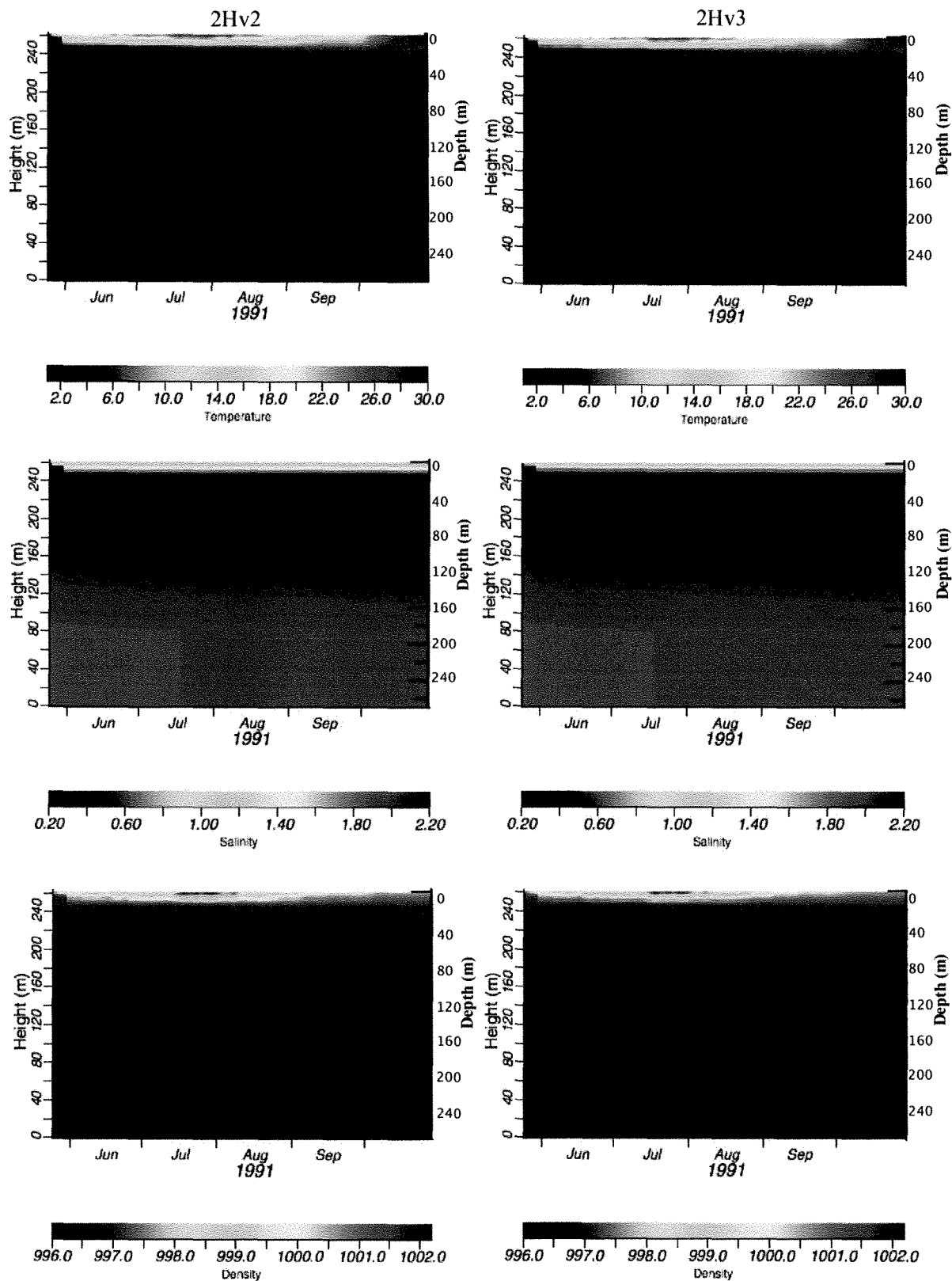


Figure 4.9: Temperature (°C), salinity (psu) and density (kg/m³) profiles for scenario 2 simulations 2Hv2 and 2Hv3 for Hogarth pit lake. Relative to simulation 2H1, there are no significant differences in profiles.

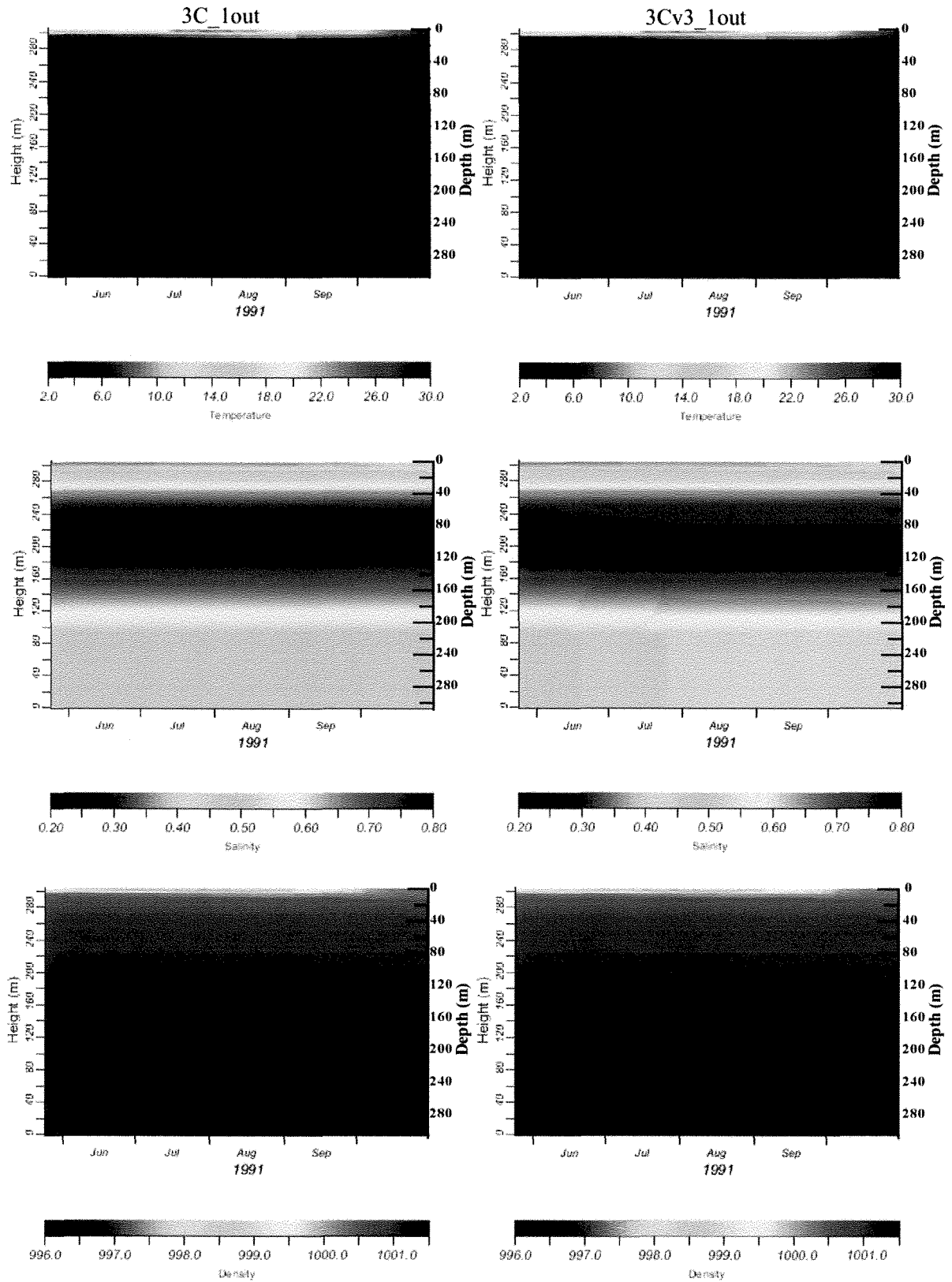


Figure 4.10: Temperature ($^{\circ}\text{C}$), salinity (psu) and density (kg/m^3) profiles for scenario 3 simulations 3C_1out and 3Cv3_1out for Caland. Relative to simulation 2C1, the salinity in the pit lake is lower and the fresh water layers are thinner in simulations 3C_1out and 3Cv3_1out.

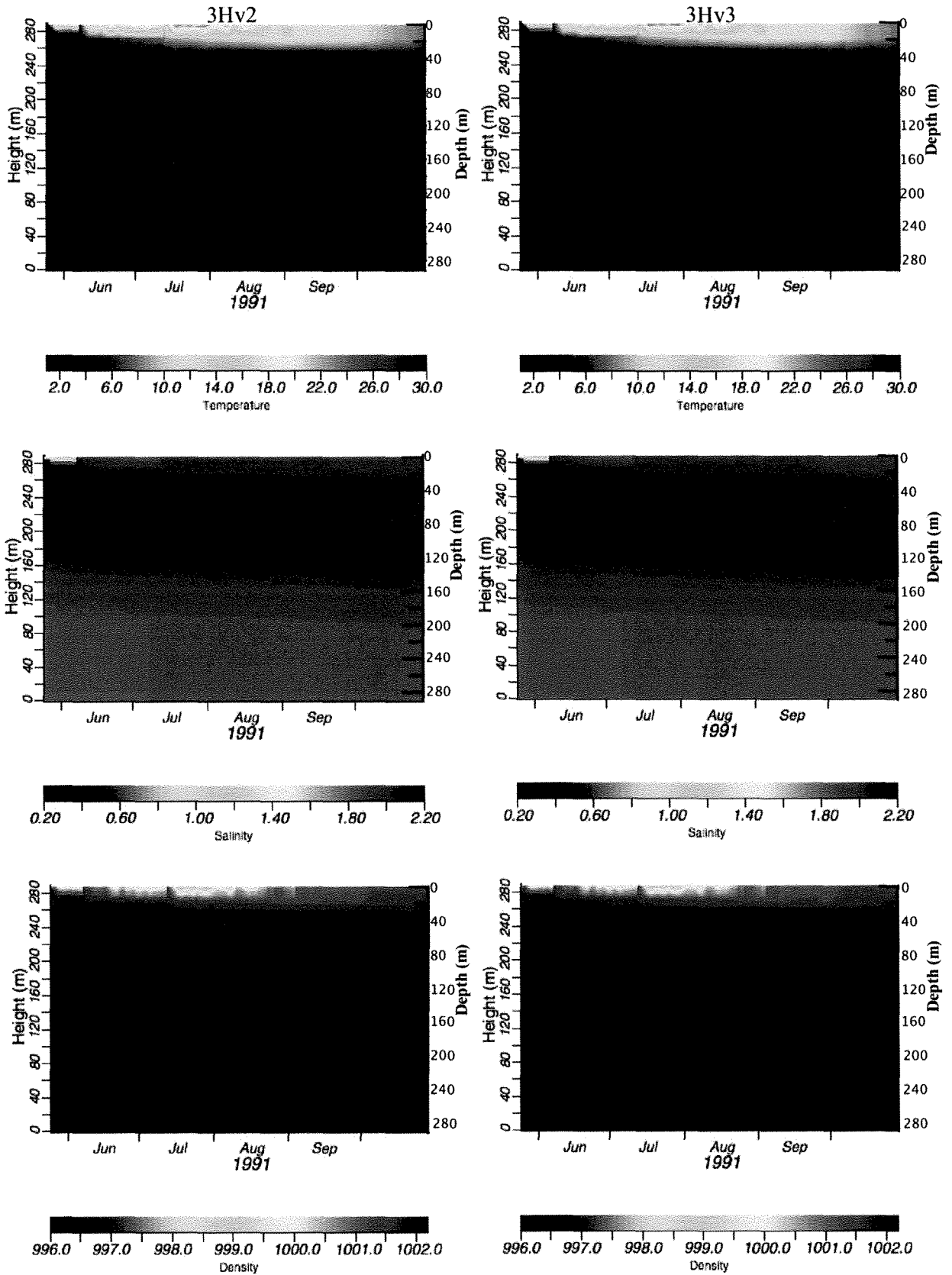


Figure 4.11: Temperature (°C), salinity (psu) and density (kg/m³) profiles for scenario 3 simulations 3Hv2 and 3Hv3 for Hogarth. Relative to simulation 2H1, the permanent fresh water layers at the surface of the pit lake no longer exist in simulations 3Hv2 and 3Hv3.

4.6 Discussion

4.6.1 Study results

Caland has previously been described as a meromictic lake because it has a well-defined chemocline and as a hard water alkaline lake with high sulphate concentrations in the chemolimnion and monimolimnion relative to the fresh water lens (mixolimnion) that forms the upper 20 m of the water column (McNaughton, 2001; Vancook, 2005; Gould, 2008; Godwin, 2010). Hogarth was previously described as holomictic not meromictic because most parameters appeared homogenous with depth; however, Hogarth did show an evident meromix during a period of increased rainfall in 1999 (McNaughton, 2001). Later studies also observed the development of a 1 to 2 m fresh water or low salinity lens (freshwater; 10 to 20 mg/L SO_4^{2-}) at the surface of Hogarth in the summer (Gould, 2008; Godwin, 2010). Hogarth water quality has gradually changed from acutely toxic to chronically toxic but still has a higher salinity than Caland (McNaughton, 2001; Gould, 2008). The difference in the limnology of the two lakes has been attributed to a greater amount of freshwater inflows into Caland and higher amounts of sulphide minerals present in the strata mined in Hogarth pit (McNaughton, 2001, Conly et al., 2005, 2007; MacDonald, 2005; Cockerton, 2007; Godwin, 2010).

Overall the DYRESM scenario 1 simulations appear to accurately portray the present day characteristics and the major differences between Caland and Hogarth pit lakes (Figs. 4.1 and 4.3). The presence and positions of distinct gradients in the temperature, salinity and density for scenario 1 simulations of Caland suggest that Caland pit lake is meromictic (Figs. 4.1 and 4.2). The simulated mixolimnion in Caland (simulation 1C1b) is slightly thicker than the measured fresh water lens reported in previous studies (McNaughton, 2001; Gould, 2008; Godwin, 2010). Relative to Hogarth, the Caland water column is simulated to have a lower salinity and is in agreement with observed conditions (Figs. 4.1 and 4.3). Scenario 1 salinity and density profiles for Hogarth indicate the presence of a temporary thin fresh water lens at the surface or a

meromix (Fig. 4.3 and 4.4). This layer exists from May to mid-August in the Hogarth simulations and then mixes with the underlying high-salinity layer in late August. The timing and depth of the mixing from the surface in the salinity profile corresponds to the loss of thermal stratification.

For scenarios 1 and 2, a number of simulations were done for both pit lakes that only varied the entrance height of groundwater inflows into the water column as the actual height of the groundwater inflow is unknown. The termination of simulation 1H2 is due to an error involving a buoyant inflow and suggests that the groundwater inflow into Hogarth must originate at or above 100 m in height from the bottom of the pit, because simulations 1H1b and 1H3, with groundwater entrance heights of 100 m and 180 m, respectively, did not terminate prematurely.

The groundwater entrance height also influences the formation of plumes in a number of simulations. Although DYRSEM uses a 1-dimensional assumption, vertical movement of low density plumes have been successfully modeled in Island Copper pit lake and Brenda pit lake (Hamblin et al., 1999; Fisher & Lawrence, 2000). Plumes are formed in Caland scenario 1 simulations 1C1b (100 m) and 1C1d (140 m) suggesting that entrance groundwater height at or above 100 m results in their formation. Changes in salinity of the bottom layer for 1C1b and 1Cv2, which correspond to loss of thermal stratification suggest that mixing is occurring in the bottom layers and may be result of inflows plunging to the bottom. Also, 1C1b and 1Cv2 both have the same ground water entrance height suggesting that the groundwater entrance height influences mixing in the bottom of Caland pit since the other simulations do not show this change. No plumes were formed in scenario 2 simulations for Caland suggesting that mixing resulting due to outflow from Caland into Hogarth increases mixing in the water column and inhibits plume formation. For the Hogarth simulations, plumes are formed in scenario 1 simulations 1H1b (100 m), 1H_MSGW (100 m), and 1H_HSGW (100 m) and in all scenario 2 simulations. The plumes in simulations 2H1, 2H2, 2H3, 2Hv2, 2Hv3 are similar in terms of

thickness and height in the salinity profile, but that of simulation of 2H1b is thinner and located higher in the water column (Figs. 4.6 and 4.7). The groundwater entrance height of all the simulations except 2H1b is the same, suggesting that the differences between the plumes is influenced more by the groundwater entrance height than the salinity of the inflows.

Based on results for all three scenarios, the limnology of Caland will vary much less over time compared to Hogarth as rebound progresses. In Caland the temperature, salinity and density gradients maintain the same relative positions in the water column, but are shifted to higher levels in the water column relative to the bottom and the mixolimnion in Caland becomes progressively thinner overtime (Figs. 4.1, 4.5 and 4.10). The shift of the gradients to shallower depth reflects the increase in the water elevation from scenario 1 through 3. The thinning of the layers can be explained by the increase in surface area with elevation that occurs in each pit that coincides with an increase in pit volume with elevation. Relative to scenario 1, the salinity in the layers above and below the chemocline is higher than in scenarios 2 and 3. This may be the result of mixing caused by the withdrawal at 385 masl in scenarios 2 and 3. Thus suggesting the overall salinity of Caland pit lake appears to undergo a minor decrease as rebound progresses to completion. Also in Caland, the maximum temperature of the mixolimnion and length of time the temperature is maintained decreases, due to the increases in outflow volume between the three scenarios. The density profile in the surface layers of the mixolimnion (depths <10 m), follow the changes in the temperature profile.

In Hogarth, the salinity and temperature profiles vary more among the scenarios than the density profiles. In scenario 1 Hogarth has a temporary fresh water lens that mixes with the underlying high salinity water as the water column begins to cool in the last two months of the simulation (Fig. 4.3). In scenario 2, with the addition of relatively low salinity water from Caland the fresh water lens is thicker and becomes a permanent feature of the simulation (Fig. 4.7). Finally, in scenario 3, the fresh water lens only exists briefly in the spring (Fig. 4.11). In all three

scenarios, the density profile at the surface follows the temperature profile and in some simulations the salinity profile, where salinity influences the temperature profile. For example: the depth of thermal stratification in Hogarth seems to follow the salinity profiles, in scenario 2, when a significant fresh water lens exists, the depth of thermal stratification is limited to its depth. But in scenarios 1 and 3 when the salinity stratification is not present, thermal stratification extends deeper into the water column from the surface (Figs. 4.3, 4.7 and 4.11); in addition the density profile for model 1H1b and 1H13 only shows a 1 to 3 m fresh water lens from the beginning of the simulation until mid-July, after which the density beneath this layer decreases and follows the pattern of the temperature profile (Fig. 4.3). However, the temperature profile shows that the water below the fresh water surface lens begins to warm in mid-June, which suggests that the salinity is the more important control on density at the start of the simulation (Figs. 4.7).

In general, the addition of inflow from Fairweather Lake into Caland pit lake, simulating if Fairweather Dam were to be breached, does not have a significant impact on the temperature, salinity and density profiles. The addition of inflow from Fairweather in scenario 2 only slightly increased the thickness of Caland's surface fresh water lens (Fig. 4.6). In scenario 2 for Hogarth, the salinity of the inflow from Caland was changed reflecting the different temperature and salinity profiles that occur before and after the addition of Fairweather inflow, and no significant change was seen in the resultant limnology (Fig. 4.8). Apart from the addition of Fairweather inflow to Caland, simulations were conducted that varied the Caland inflow salinity. The change in Caland inflow salinity did not significantly change the salinity (<0.01 psu) of the water column or to the limnology of Hogarth, probably because the Caland water column overall is lower in salinity than Hogarth (Fig. 4.8).

Scenario 3 simulations are designed to simulate what happens when Caland and Hogarth have joined forming one super pit lake with subsequent outflow into the West Arm of the former

Steep Rock Lake. Results of Caland scenario 3 simulations suggest that when the water elevation in Caland reaches 394 masl fresh water will outflow from the pit lake. This is probably because the fresh water lens in Caland has sufficient volume to replenish the water lost due to withdrawal (Fig. 4.10). The thickness of the freshwater lens exceeds the height difference between the outlet elevation (385 masl) and the final surface water elevation of 394 masl. In scenario 3, the fresh water lens that appears throughout scenario 2 simulations for Hogarth is not maintained (Fig. 4.11). The salinity profile suggests that when the super pit lake outflows, any freshwater at the surface of the Hogarth water column will outflow in addition to high salinity waters (1.9 to 2 psu). However, this simulation is only run over a 158 day long period and assumes the conditions represented by the initial profile in scenario 1 represent those in scenario 3, but shifted to up in the water column (which may not be the case). In scenario 2 simulations for Hogarth, a fresh water lens is maintained due to inflow from Caland. The thickness of this fresh water layer may increase overtime from when the pit lakes join to when the joined pit lakes outflow. If the fresh water layer in Hogarth increases in thickness Hogarth may develop a similar profile to that of Caland and have fresh water lens that is thick enough to maintain a constant freshwater outflow. However, further modeling is required to examine the influence of the initial profile on simulation results. A simple manner in which the influence of the initial profile could be examined is by using results of scenario 2 to construct the initial profile for scenario 3. Alternatively, a series of simulations could be run for the period between when the pits join and when they outflow. The results of each simulation could be input into the initial profile of the next simulation in order to if Hogarth's fresh water lens becomes thicker overtime with continued inflow from Caland.

A number of simulations in this study looked at the affects of the groundwater entrance height and groundwater and inflow chemistry. Overtime the groundwater entrance height will change as will the volume of water entering the pits (Castendyk and Eary, 1999). In this study

the change in groundwater volume over time is taken into account in the water balance models calculated for the pit lakes that are used as the basis of the inflow volumes in DYRESM. Castendyk & Webster-Brown (2007) demonstrated that knowledge of the density of major water inputs is important because small changes in chemistry can mean the difference between meromictic and holomictic conditions. When two different sources of water have significant differences in chemistry, a meromictic pit lake is likely to be produced (Bohreret et al., 1998; Fisher & Lawrence, 2000; Castendyk and Webster-Brown, 2007). Based on the prediction of meromictic conditions in Caland, the lake-filling conditions will be analogous to Martha Lake (New Zealand), Lake Goitsche (Germany), and Summer Camp pit lake (Nevada; Castendyk and Webster-Brown, 2007; Parshley and Bowell, 2003; Bohreret et al., 1998) All these pit lakes have major inflows with differences in water chemistry and temperature; specifically low salinity surface water and high salinity groundwater. Caland pit lake receives water from groundwater (0.43 psu), mine-impacted surface runoff (0.5 psu), and surface runoff (0.18 psu). The conditions in Hogarth are opposite of the pit lakes above. In contrast Hogarth pit is being filled by groundwater that has a lower salinity than the overland runoff. However, the true nature of the groundwater flowing into Caland and Hogarth pit lakes is unknown because the groundwater sample used to define the groundwater inflow salinity was taken from a shallow well located in glacial till, and not bedrock, the likely source of groundwater. In scenario 1, the major inflows into Hogarth are groundwater with a salinity of 0.43 psu and mine-impacted overland runoff with a salinity of 1.3 psu. Simulations varying the salinity of the groundwater, 1H_MSGW (1.3 psu) and 1H_HSGW (2.4 psu), increased the salinity and density in the monimolimnion of Hogarth pit lake (Fig. 4.4).

In general, pit lakes flooded by surface and groundwater sources, such as Caland and Hogarth, are more sensitive to changes in input water chemistry (Fisher & Lawrence 2000). The influence inflow salinity changes on the stratification of pit lakes are best observed in the

Hogarth simulations in this study. In scenario 2, an additional low salinity inflow originating from Caland is added to Hogarth. Three simulations were run, 2H1, 2H2 and 2H3 that varied the salinity of the inflow from 0.35 psu to 0.37 psu to 0.42 psu, respectively, representing water flowing from different depths in Caland (Figs. 4.7 and 4.8). Varying the salinity value of the water flowing into Hogarth from Caland did not significantly influence results, probably because all three salinity values tested are significantly lower than the other sources of water for Hogarth. However, the addition of the low salinity inflow into Hogarth produces a thicker (5 m versus 1 to 3 m) low salinity surface layer (Figs. 4.3 and 4.7).

4.6.2 Implications for the Future Toxicity of Caland and Hogarth

In order to assess the future toxicity of the pit lakes, in particular waters outflowing to the West Arm, the relationship between sulphate concentration and salinity was used based on all the pit lake water sampling data from 1998 to 2009 (Fig. 4.12). Four outlying points were excluded. As expected, there was a strong linear correlation ($r^2=0.93$) between salinity and dissolved sulphate (excluding the 4 outlying data points). Because of this relationship the salinity values in the DYRESM simulations can be used as proxies for future sulphate concentrations in the pit lakes, where:

$$[\text{SO}_4^{2-}] = 1185.4 \cdot [\text{salinity}] - 372.87 \quad (\text{Eqn. 4.2})$$

Where:

$[\text{SO}_4^{2-}]$ = sulphate concentration (mg/L)
 $[\text{salinity}]$ = salinity (psu)

As the primary contaminate in Caland and Hogarth is dissolved sulphate (McNaughton, 2001; Gould, 2008; and Godwin, 2010) the future toxicity is assessed relative to various water quality guidelines. Caland and Hogarth pit waters are characterized as Ca-Mg-SO₄²⁻ (Shankie, 2011).

The Canadian Drinking Water Guidelines recommend that sulphate concentrations in drinking water should not exceed 500 mg/l (Health Canada, 2010). This guideline is an aesthetic objective because sulphate concentrations can affect the taste of drinking water and concentrations above this limit increase the number of complaints about gastrointestinal problems in some individuals (WHO, 2004; Health Canada, 2010). The EPA Secondary Maximum Contaminant Level (SMCL) is at or below 250 mg/L (EPA, 2003). The SMCL is based on taste and is not a Federally enforceable regulation but a guideline for U.S. The EPA's health based recommendation for sulphate concentrations is 500 mg/L due to the laxative effects of sulphate at concentrations above this recommended limit (EPA, 2003).

The current the sulphate concentrations in Caland range between 200 mg/L and 500 mg/L with seeps into Caland having concentrations ranging from 5 to 4000 mg/L (McNaughton, 2001; Gould, 2008; Godwin, 2010; Shankie, 2011). The current sulphate concentrations in Hogarth range between 1200 mg/L and 1900 mg/L with seeps into Hogarth having concentrations from 1700 to 5000 mg/L (McNaughton, 2001; Gould, 2008; Godwin, 2010; Shankie, 2011). The sulphate concentrations in Caland are below the drinking water guideline of 500 mg/L but are above the EPA SMCL. However, Caland pit lake has historically supported a commercial fish farm and no toxicity has been attributed to Caland waters (McNaughton, 2001; Gould, 2008; and Godwin, 2010). The sulphate concentrations in Hogarth pit lake exceed all the guidelines for sulphate concentrations in drinking water and freshwater aquatic environments. The source of the high sulphate concentrations in Caland and Hogarth pit lakes is the Pyritic member of the Joliffe Ore zone and the difference in sulphate concentrations between the two lakes is attributed to the greater proportion of the Pyritic member in Hogarth pit (Fig. 2.2; Conly and MacDonald (2004); MacDonald (2005); Cockerton, 2007; and, Conly et al., 2008ab).

Measured salinity values in Caland and Hogarth pit lake water columns vary in a similar manner to observed variations in the pit lakes (McNaughton, 2001; Gould, 2008; Godwin, 2008).

Measured salinity values are compared to DYRESM predictions in order to assess the accuracy of the DYRESM predictions (Figs. 4.13 and 4.14). Note that: i) measured salinity values for Caland and Hogarth do not extend to the bottom; ii) the DYRESM salinity results are for the layers DYRESM divides the water column into; and, iii) the measured salinity values used in the initial profile are compared to DYRESM predictions from 7 days into the simulation. The DYRESM profile for layers 1 to 40 closely match measured values from the surface down to a depth of 100 m (Fig. 4.13). Also, the DYRESM predictions from layer 40 to the bottom (layer 100) and the measured salinity values below 100 m both profiles indicate a decrease in salinity, but the rate of decrease in measured salinity is greater. DYRESM salinity results for Hogarth closely match measured values except for at the surface and bottom where measured salinity values are lower than predicted (Fig. 4.14).

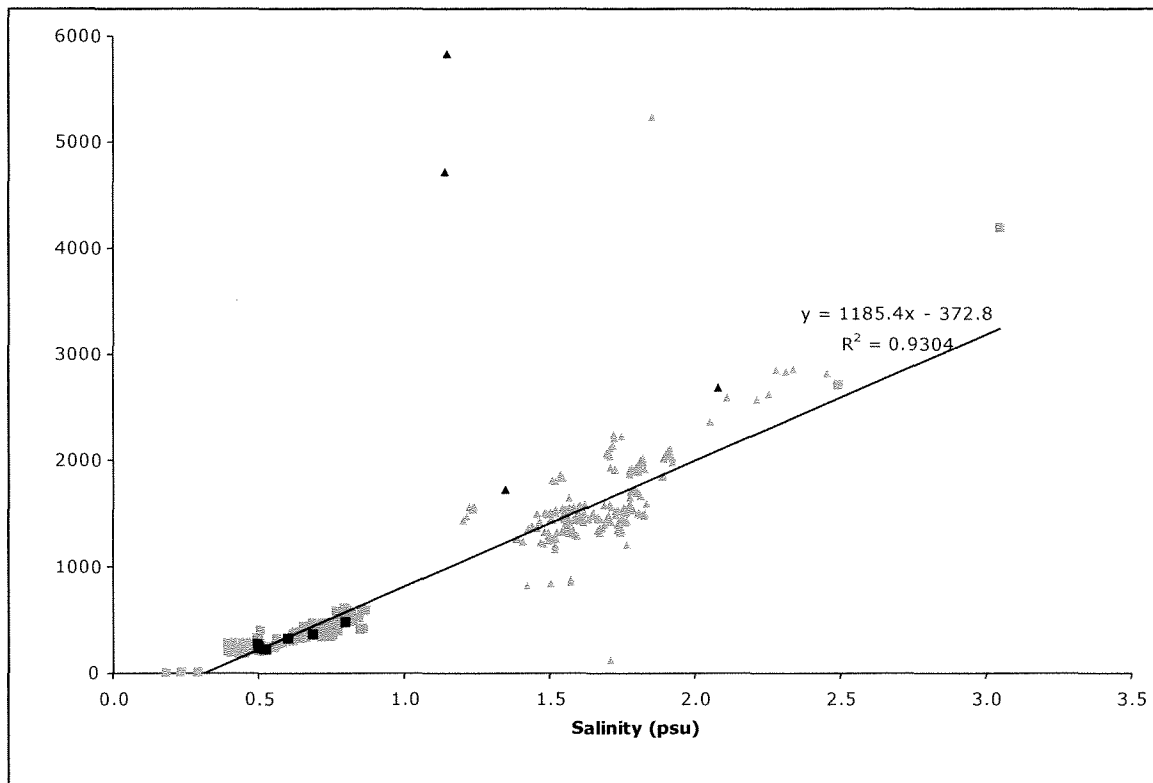


Figure 4.12: Plot of salinity versus sulphate for all water samples collected from Caland and Hogarth pits and seeps between 1998 and 2009. Caland pit lake samples are represented by squares, black for seeps and grey for lake samples. Hogarth pit lake samples are represent by triangles, black for seeps and grey for lake samples. The black line shows the linear relationship between sulphate and salinity and has a correlation coefficient of 0.9304.

The salinity profiles for Caland scenario 1 simulations indicate the sulphate concentrations in epilimnion (0 to 10 m depth) are < 100 mg/L (Fig. 4.1 & 4.12). From 10 m to 30 m in the water column (metalimnion and hypolimnion) the sulphate concentration is ~220 mg/L. The highest salinity layer (0.8 psu) in Caland has a sulphate concentration of ~ 570 mg/L and the bottom layer, below a depth of 155 m is ~350 mg/L. Scenario 2 and 3 simulations indicated similar sulphate concentrations except that the bottom layer has a lower sulphate concentration, ~ 220 mg/L (Figs. 4.5, 4.10 and 4.12). The Caland salinity profiles indicate that the surface fresh water lens will maintain sulphate concentrations below all the water quality standards. Below the freshwater lens the sulphate concentrations are higher, however, only the highest salinity layer exceeds the drinking water quality guidelines for sulphate. Layers above and below the highest salinity layer are close to or exceed the EPA SMCL. The sulphate concentrations indicated by the linear relationship between salinity and sulphate and the DYRESM salinity profiles for all three simulations are in agreement with observed concentrations in Caland (McNaughton, 2001, Gould, 2008; Godwin, 2010; and Shankie, 2011). Results suggest that the sulphate concentrations in the bottom of the Caland pit lake will decrease slightly overtime: however, the sulphate concentrations in the remaining portions of the water column do not appear to change across the three simulations.

The salinity of the entire Hogarth pit lake water column, including the low salinity layers at the surface, exceeds drinking water quality standards for sulphate (Figs. 4.3, 4.7, 4.11 and 4.12). The salinity profiles from all three scenarios indicate that the low salinity layers at the surface have sulphate concentrations from 570 mg/L to 1300 mg/L. The sulphate concentrations of the remaining portion of the water column range from 1500 mg/L to 2200 mg/L. Based on the scenario 3 simulations waters with sulphate concentrations between 1700 and 1900 mg/L will outflow from Hogarth, well above all water quality guidelines for sulphate.

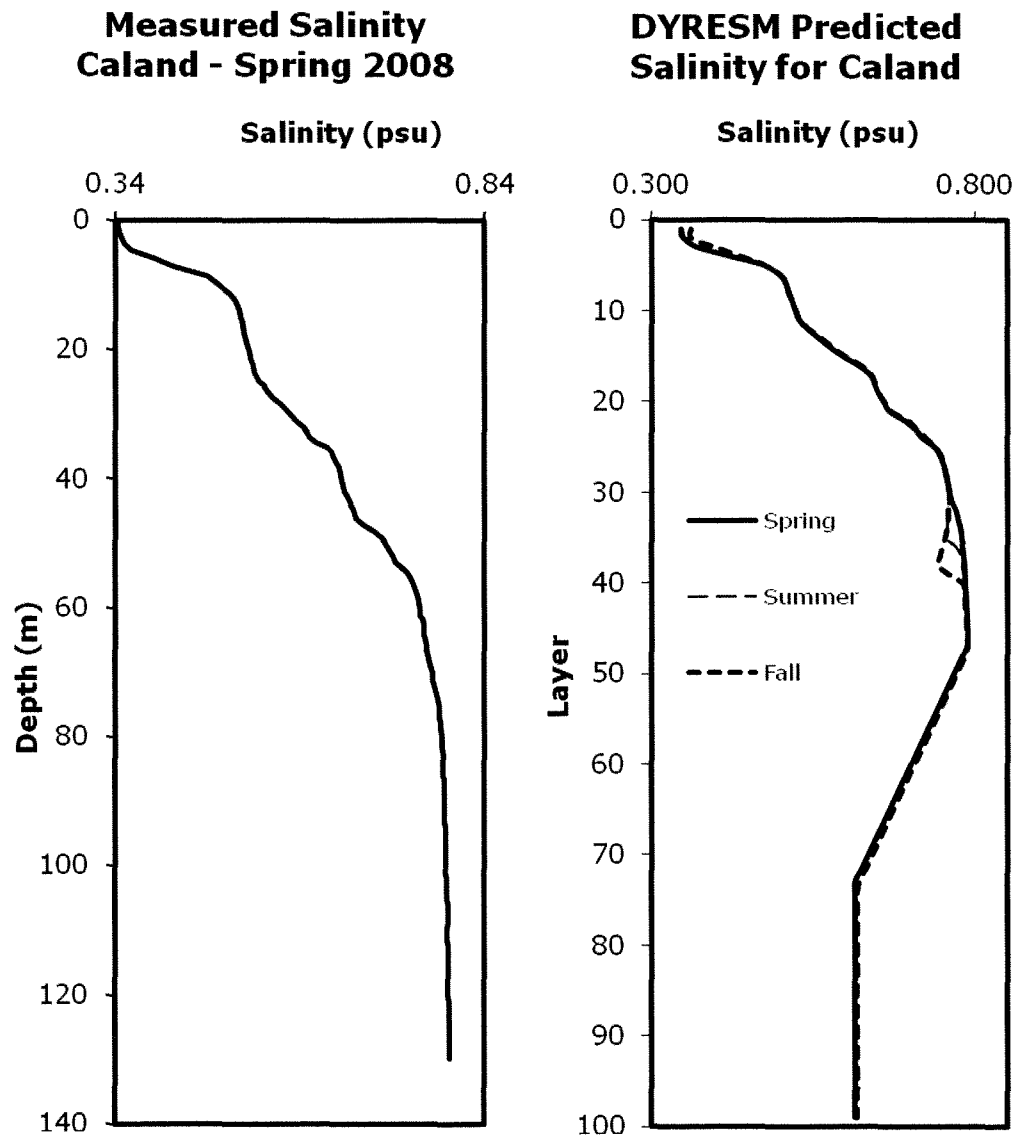


Figure 4.13: Comparison of measured salinity for Caland (left) and DYRESM predicted salinity for Caland in the spring, summer and fall (right). Note that the measured salinity predictions do not extend to the bottom of the pit lake but the DYRESM predicted values do. Measured values are similar above 100 m depth compared to layer 40 in the DYRESM predicted values. At about layer 35 DYRESM predicts a salinity decrease from the spring to fall. Measured values are derived conductivity measurements from Godwin 2010.

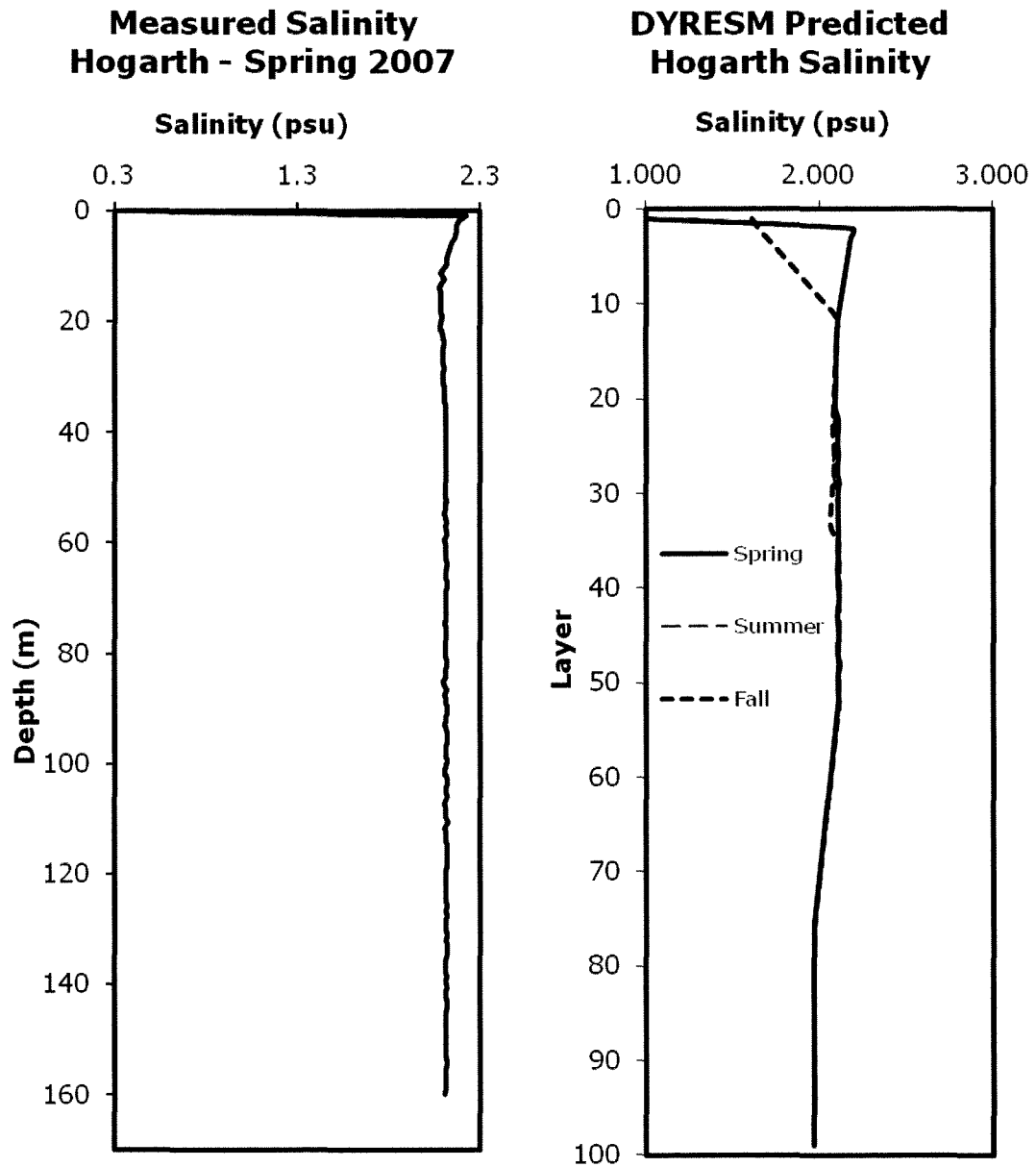


Figure 4.14: Comparison of measured salinity in Hogarth (left) and DYRESM predicted salinity for Hogarth in the spring, summer, and fall (right). Measured values indicate a lower salinity at the surface of the pit lake in comparison to the DYRESM predicted values. DYRESM predicts higher surface salinities in the fall compared to the spring and summer profiles which are similar. Measured values were derived from conductivity measurements from Godwin (2010).

Based on the DYRESM simulations for both pits it is likely that the waters flowing out of the pit lakes will be toxic. This is in agreement with the conclusions of an empirical geochemical study by Godwin (2010) that chronically toxic effects in the pit lakes are likely and that downstream communities will be negatively impacted. The column experiments conducted by

Godwin (2010) indicate the sulphate concentrations of outflowing waters to the West Arm ranging between 800 and 1400 mg/, which is below the sulphate concentrations predicted by scenario 3 simulations of the Hogarth-Caland combined pit lake (1700 and 1900mg/L). Godwin (2010) predicts that the joined super pit lake will likely overturn in the spring and fall because there is little resistance to mixing resulting from density differences. Results of the scenario 2 and 3 simulations for Caland suggest that Caland will not overturn when the pit lakes join are joined and outflow (Figs. 4.5, 4.6 and 4.10). Scenario 2 simulations for Hogarth indicate that a more pronounced meromix forms when Caland waters begin to flow into Hogarth (Figs. 4.7, 4.8 and 4.9). However, the salinity profiles for scenario 3 simulations indicate that Hogarth's surface layers will mix when the pit lakes outflow into the West Arm (Fig. 4.11). DYRESM results suggest that the current that will run through the two pit lakes will remove the freshwater bringing more saline water the surface of Hogarth.

4.6.3 Limitations of the study and future work

There are a number of assumptions and uncertainties inherent in DYRESM (Castendyk & Eary, 1999). Often weather stations are located away from the site and it must be assumed that conditions at the pit lake surface are equal to those at a nearby weather stations. When this assumption is made, as in this study, the affects of sheltering and shading of the pit walls on wind and solar radiation is not taken into account (Castendyk & Eary, 1999). Also, it must be assumed that past meteorologic conditions accurately reflect future conditions, which may not be the case given temperature increases due to global warming. However, the use of short time scales for simulations would reduce the affect of climate changes on model results (Castendyk & Eary, 1999). Assumptions must be made about the elevation, timing and chemistry of inflows prior to pit filling. Coupling hydrodynamic modeling to geochemical predictions can help improve the accuracy of models, specifically the chemistry of inflows. For example, the use of

batch experiments and column leaching experiments to better constrain the chemistry of drainage produced by difference rock types surrounding the pit lakes and the affect of any remediation strategies used to remediate sources of acid mine drainage waters (e.g., Cockerton, 2007; Shankie, 2011; Greiner, in progress).

The accuracy of any model depends on the validity of model input values. The following outlines the uncertainties and assumptions used in this study. Any uncertainty in the water balance and rebound models outlined in section 3.9.3 will carry over to the DYRESM simulations, because the water balance is used to calculate inflow volumes entering the pit lakes and to determine the water elevation in Hogarth once Caland begins to overflow. However, the DYRESM model of pit lake morphology is based on the raw data used to make the exponential curves in the stage-volume relationships and not from the curves, thus eliminating the curves as a source of error. Any changes to the pit lake depth, volume or surface area would warrant remodeling the hydrodynamics of the pit lakes (Castendyk and Eary, 1999). For example, changes to the water level management strategy for the study area, as described in 2.4, would require derivation of new hydrodynamic models to account for the variation in water flow into Caland. The calculation of a Lake Number is typically used to determine if a lake can be modeled using DYRESM (Imerito, 2007). The Lake Number of Caland and Hogarth has not been calculated instead it was assumed that because the pit lakes have a high surface area to depth ratio Caland and Hogarth satisfy the one-dimensional assumption. The results of scenario 1 simulations suggest the use of DYRESM to simulate conditions in Caland and Hogarth is appropriate since the simulations portray the key characteristics of the Caland and Hogarth pit lake limnology (Figs. 4.1 and 4.3). A limitation involving the version of DYRESM used in this study is the fact that the water surface temperature cannot be below zero or that DYRESM cannot simulate conditions involving ice. This limited the length of the simulation because the

pit lakes freeze over during the winter and water temperatures at the surface are close to zero in the spring and fall. Therefore, simulations could not be run continuously for an entire year.

There are a number of data limitations with regard to other required parameters in the DYRESM input files. All the DYRESM input files, except the withdrawals file and the parameters file, include at least one parameter that had to be estimate because a measured value was not available for Atikokan or the study area. Any uncertainty regarding the withdrawal files stems from the water balance model used to define the volume of water exiting the pit lakes. In the configuration file, the light extinction coefficient of the lakes was estimated based on comparisons to other lakes, where the light extinction coefficient was measured based on secchi disk measurements. The light extinction coefficient can be influenced by the precipitation of iron oxide in the water column (Castendyk and Eary, 1999). This is a potential issue at Steep Rock as iron oxides are transported in surface runoff, particularly after major rain events. Geochemical modeling could be used to indicate the amount of iron oxide likely to be produced and a sensitivity analysis on the light extinction coefficient can be complete to better constrain its influence on simulation results.

In the physical data and lake morphometry file, all streams are assumed to have the same streambed half angle. The slopes in Caland were arbitrarily defined because they were not measured in the field. As discussed earlier, there is no data on the height of the groundwater inflow into the water column so simulations were done that varied the entrance height to look at its influence on limnology. In addition, the initial profiles used to initialize all the simulations are the same but with the height of the *in situ* measurements changed. This may not be an accurate representation of future water column conditions. This may be a significant issue in modeling Hogarth as the limnology varies significantly between the simulations performed in this study. Simulations could be conducted that use a profile based on scenario 2 simulation results to see if the resultant limnology in Hogarth changes. Alternatively, a series of sequential simulations for

years between the time the pits join and outflow could be run using the previous year's results for the present year's initial profile.

Meteorological data used in the DYRSEM simulation was collected from a number of weather stations that are not located on the study site. In the meteorological data file, the global solar radiation data used to determine the short wave radiation is for Moosonee, Ontario, which is located approximately 840 km north east of Atikokan, Ontario. Also, the cloud cover data used to determine the amount of long wave radiation in DYRESM is from Thunder Bay, Ontario, located approximately 208 km east of Atikokan. In addition the weather data was collected in a different year than the *in situ* measurements used in the initial profile. This may affect results because the weather conditions for day one of the simulation may be accurately reflect the conditions during the periods when the initial profile parameter measurements were taken. Having meteorological data that matches the time period of the *in situ* measurement may increase the accuracy of the model, particularly if sub-daily data were to be used. The addition of the long wave and short wave radiation data to weather monitoring in Atikokan would increase the accuracy of future models simulations.

For inflow file, the amount of inflow from sources with different salinities was arbitrarily assumed based on available data and the fact that Caland gets more freshwater inflow than Hogarth. Although there is data on seep chemistry, the volume of water discharged from the seeps and variations in flow rates overtime is poorly constrained. Many of the seeps at the Steep Rock site are intermittent, only flowing after major rain events. Changes in the flow of water into the pit lakes was not investigated in this study but changes in volumes due to major rain events could impact the hydrodynamics. This may be of particular concern in Hogarth whose water column showed the most variation throughout this studies simulations. Another concern regarding surface water on the site is the stockpiles of pyritic material along the former Steep Rock Lake shoreline. As Caland and Hogarth water level approach the original shoreline there

will be an increase in pit water interaction with pyritic waste rock. Geochemical models could be used to better constrain the effect of this material being flooded on water quality, which can then be input into DYRESM to examine the potential effects on limnology.

Previous studies have recommended extensive studies be undertaken to understand the chemical and physical properties of pit lake-filling waters, the timing and locations of inputs and on site meteorological monitoring (Castendyk and Eary, 1999; Castendyk and Webster-Brown, 2007; Hamblin, et al., 2009). Overall, an extensive field-monitoring program designed to fill in the information gaps described above would increase the accuracy of the DYRESM simulations. Some key areas of research that would increase the accuracy of DYRESM models of Caland and Hogarth include:

- A groundwater study to better constrain where the groundwater enters the pit lakes, the approximately flow rate and its chemistry;
- An effort can be made to constrain the volume of inflows entering the pit lakes from surface seeps and the fluctuations in seep chemistry;
- A limnology study to measure the light extinction coefficient in Caland and Hogarth and chemical species that influence turbidity, for example, iron and manganese;
- An onsite weather station would provide more accurate measurements of the meteorological conditions that occur at the study. Accuracy could further be improved by a weather station located on the pit lake surface. Measurement from a weather stations located on the pit lake surface would taken into account sheltering and shading affects on wind speed and solar radiation at the surface of the pit lake;
- Global solar radiation and cloud cover or long-wave radiation could be added to the meteorological data collection for Atikokan; and

- Further DYRESM simulations could be run and compared with years with *in situ* conductivity measurements using the Hydrolab Surveyor 4 (Gould, 2008; Godwin, 2010). These comparisons would help calibrate and validate the model and to predict limnological predictions between sampling events (Castendyk and Eary, 1999).

In addition, the full capabilities of the DYRESM could be used including the use of sub-daily measurements or by coupling DYRESM Computational Aquatic Ecosystem Dynamic Model (CAEDYM). The use of sub-daily measurements may be useful to understand the influence of short-term events that may affect limnology such as extreme rainfall events or the initial effects of an addition of a new inflow source. Coupling DYRESM to CAEDYM would permit the simulation of more parameters (Hipsey et al., 2006a,b). Parameters of interest for Caland and Hogarth pit lakes that can be modeled by CAEDYM include dissolved oxygen, iron and manganese. The amount of dissolved oxygen in Caland is lower than that in Hogarth. This has been attributed to the decomposition of waste produced by the fish farm that used to operate at Caland (McNaughton, 2001; Gould, 2008; Godwin, 2010). CAEDYM could be used to investigate how dissolved oxygen trends in Caland will change overtime after the cessation of fish farming. Understanding the distribution of dissolved oxygen in Caland and Hogarth will help in understanding the redox conditions within the pit lakes and subsequently whether submerged pyritic material or wall-rock in the pit lakes exposed to oxidizing conditions. CAEDYM could also be used to investigate the speciation and concentrations of iron and manganese in the pit lakes. Iron and manganese are present in high concentrations in the ore zone and wall-rock as described in section 2.2. Iron and manganese are typically in particulate, colloidal or organic complexes in neutral or alkaline surface waters (Wetzel, 2000). The presence of particulate material increases the turbidity of the water column and will affect the light extinction coefficient (Castendyk and Eary, 1999). The light extinction coefficient is an

important parameter in the determination of heat fluxes in the DYRESM (Imerito, 2007).

CAEDYM simulations would require a field program that would include measurement of a number of parameters that have not been analyzed in the pit lakes previously (McNaughton, 2001; Imerito, 2007; Gould, 2008; Godwin, 2010). Another future study could also assess if inducing meromictic conditions in Hogarth would be beneficial.

There are a limited number of publications providing predictions of pit lake limnology (Castendyk and Eary, 1999). Any study providing predictions on pit lake limnology and the influence on different parameters on model results will help close the knowledge gap in this area of pit lake research. The hydrodynamics of pit lakes influences the distribution of chemical species in the water column (Wetzel, 2000). Also, small changes to the salinity, density and temperature of inputs can produce significant changes to pit lake stratification (Castendyk and Webster-Brown, 1999; Castendyk and Eary, 1999). Therefore, further hydrodynamics studies should be completed if there are any changes to the volume or chemistry of inflows, the pit morphology, or the current water level management strategy (see section 2.4). Also, this study did not consider the influence of Errington pit lake in its calculation of final pit volumes, nor did it consider current limnological conditions in Errington. The addition of Errington to the hydrodynamic model of Caland and Hogarth would add complexity to the current flow through system conceptualized in this study and may warrant a more detailed two or three-dimensional model of the future Steep Rock super pit lake.

4.7 Conclusions

The Dynamic Reservoir Simulations Model (DYRESM) simulations of current conditions (scenario 1) did accurately portray the key observed characteristics of and the differences between the Caland and Hogarth pit lake limnology. These key characteristics include that Caland is meromictic and has a lower overall salinity relative to Hogarth. Also,

Hogarth simulations showed the development of a temporary meromix, as has been observed previously (McNaughton, 2001; Gould, 2008; and Godwin, 2010. Simulations of when the two pits join (scenario 2), indicate that Caland will maintain its meromictic stratification but that the upper freshwater lens becomes thinner and, that Hogarth will develop a freshwater lens thick enough to remain stable during the loss of thermal stratification in response to seasonal overturn. The salinity differences between the two pit lakes is great enough that water from any depth in Caland will increase the thickness of the upper low salinity layer in Hogarth (Fig. 4.10). Scenario 3 simulations indicate the Caland will still maintain its upper freshwater lens and that the fresh water lens in Hogarth will not be maintained over the course of the simulation. The use of a difference rebound model did not result in any significant changes to the limnology of either pit lake. In Hogarth, the salinity of the inflow from Caland and the salinity of groundwater did not significantly affect the pit lakes stratification. These results suggest that the fresh water lens in Caland is currently thick enough and that the pit lake receives enough fresh water inflow that the outflow from Caland will probably be low in salinity. Outflow from Hogarth will include any fresh water inflow it receives and will likely be mixed with some high salinity water. Further modeling is required better constrain the future salinity of the outflow water from Caland and Hogarth pit lakes.

In general variations of the simulated scenarios did not significantly change the overall limnology of either pit lake. The entrance height of the submerged groundwater inflow influenced the development of plumes in both pit lakes. The addition of inflow from Fairweather Lake into Caland only slightly increased the thickness of the freshwater lens in Caland in scenario 1 and lowered the changes the depth of the high salinity layers in scenario 2.

There is a linear relationship between sulphate concentrations and salinity values for water samples from the Caland and Hogarth pit lake water and seep samples. This trend allowed the DYRESM salinity profile results to be used as proxies for sulphate concentrations. Based on

the DYRESM scenario 3 results and the linear relationship between salinity and sulphate concentrations, it appears that water exiting Caland will have sulphate concentrations up to 100 mg/L. On the other hand, water entering the West Arm from the combined Hogarth-Caland pit lake will have sulphate concentrations ranging from 1700 mg/L to 1900 mg/L. In general, the sulphate concentrations in Caland are below water quality standards, while future Hogarth waters exceed all water quality standards.

Based on the results of these preliminary DYRESM simulations it is possible to conclude that DYRESM can be used to simulate the future hydrodynamics of Caland and Hogarth pit lakes. Future efforts should address some of the areas of uncertainty. Any study that aims to decrease the uncertainty surrounding one or more parameters or assumptions described in section 4.5.3 will increase the accuracy of the DYRESM simulations. Studies that better constrain the light extinction coefficient, groundwater volumes and chemistry, on site meteorologic data and surface seep volumes and chemistry should be the primary focus if an extensive field monitoring program is to be undertaken.

Chapter 5: General Conclusions

Rebound model 2B provides the best estimate for rebound at Caland and Hogarth pit lakes, and yields results that are comparable to measured water levels and the Regional Engineering model (MNR, 1986). Model 2B predicts that Caland will flow into Hogarth in 2070 and that the new Steep Rock Pit Lake will outflow into the West Arm in 2087. Differences in water balance parameters (i.e., precipitation, evaporation, groundwater inflow and runoff) cannot account for the 18-year difference in the predicted rebound rate between Model 2B and the Regional Engineering model. The difference between Model 2B predictions and the Regional Engineering model predictions can be attributed to the manner in which the pit volumes are calculated.

In this study, the relationships among accumulated volume, surface area and elevation, are modeled by fitting exponential curves to measured data as described in section 3.3. The Regional Engineering model defines the pit volumes using linear interpolation at a 1 m scale between contour elevations. In this study, the stage-volume relationships for Hogarth pit lake are more accurate than for Caland. This is likely because the shape of Caland pit lake is more irregular than that of Hogarth. Hogarth is a long, narrow lake of relatively consistent width. In contrast, Caland pit lake has a complex shape, that includes islands and has pit walls that are more varied in slope. The surface area calculations for Caland include the portion of the land that will be flooded in between Caland and Hogarth pits once the water level in Caland reaches 385 m. This along with changes in slope likely account for the variation seen between actual pit volumes and the hypsographic curve used in this study. These results suggest that in future work, at minimum, linear interpolation should be used to define the volume in Caland pit lake due to its complex shape.

The Dynamic Reservoir Simulations Model (DYRESM) simulations for current conditions (scenario 1) did accurately portray the key observed characteristics of and the differences in

limnology between the Caland and Hogarth pit lakes. These characteristics include that Caland is meromictic and has a lower overall salinity relative to Hogarth, and that Hogarth begins to show the development of a meromix. Simulations of when the two pits join (scenario 2) indicate that Caland will maintain its stratification but that the upper freshwater lens becomes thinner and, that Hogarth will develop a freshwater lens thick enough to remain stable during the loss of thermal stratification. Simulation of when the pit lakes outflow into the West Arm (Scenario 3) indicate that Caland will maintain its upper freshwater lens but that a fresh water lens in Hogarth is briefly present at the start of the simulations. These results suggest that the fresh water lens in Caland is currently thick enough and that the pit lake receives enough fresh water inflow that the outflow from Caland will probably be low in salinity. On the other hand, outflow from Hogarth-Caland combined pit lake will probably have a high salinity. In general variations of the simulated scenarios, including altering the groundwater entrance height, inflow chemistry and the use of a longer rebound rate in the water balance calculations, did not significantly change the overall limnology of either pit lake.

The correlation between sulphate concentration and salinity for Caland and Hogarth waters enables the use of the DYRESM salinity profile results as proxies for sulphate concentrations. Consequently, water leaving Caland will have sulphate concentrations of <100 mg/L, and water leaving Hogarth-Caland combined pit lake will have sulphate concentrations ranging from 1700 mg/L to 1900 mg/L. In general, the sulphate concentrations in Caland are below the Canadian Water Quality Guidelines (500 mg/L) and EPA SMCL (250 mg/L) water but exceed the British Columbia Ambient Water Quality Guidelines (50 mg/L and 100 mg/L) while those in Hogarth waters will exceed all the water quality standards. Consequently, the outflow from the combined Hogarth-Caland pit lake will be toxic.

Based on the results of this study, DYRESM can be used to simulate the future hydrodynamics of Caland and Hogarth pit lakes. However, future research should include a field

monitoring program to address some of the areas of uncertainty including, the chemistry and entry height of groundwater in each pit, measurement of the light extinction coefficient, on site meteorologic data including measurements for solar radiation and surface seep volumes and chemistry. Furthermore, future hydrodynamic studies should include more comparisons to observed conditions in order to better calibrate and validate the models. Any of the aforementioned studies to decrease uncertainty in the DYRESM simulations will not only create more accurate models of Caland and Hogarth but will also help validate the use DYRESM in the prediction of limnology conditions in pit lakes.

References

- Balistrieri, L.S., Temple, R.N., Stillings, L., Shevenell, L.A., 2006. Predicting spatial and temporal variations in temperature, salinity, and conservative elements during stratification and overturn in Dexter pit lake, Tuscarora, Nevada, USA. Interactive Pit Lakes 2004 Conference. United States Environmental Protection Agency, Washington, D.C. EPA/625/C-06/002, 1184 – 1203 p.
- Bear, J. 1979. *Hydraulics of Groundwater*. New York: Dover Publications Inc. 436 – 462 p.
- Bohreret, B., Heidenreich, H., Schimmele, M., and Schultze, M. 1998. *International Journal of Salt Lake Research* v. 7, 235-260.
- Bowell, R.J., Barta, J., Mansanares, W. and Parshley, J. 1998. Geological controls on pit lake chemistry: Implications for the assessment of water quality in inactive open pits. In: *Proceedings of the International Mine Water Association Symposium on “Mine Water and Environmental Impacts”*, Johannesburg, South Africa, 7-13th September 2008. (Volume II) v. 2, 375-386.
- Capper, P.S. 1978. *Environmental Plan for Steep Rock Iron Mines Limited*. Atikokan, Ont. 113 p.
- Card, K.D. and Ciesielski, A. 1986. DNAG 1: Subdivisions of the Superior Province of the Canadian Shield; *Geoscience Canada* v. 13, 5 – 13.
- Castendyk, D.N. and Eary, L.D. (Eds) 2009. *Mine pit lakes: characteristics, predictive modeling, and sustainability* vol. 3. Society for Mining, Metallurgy, and Exploration, Inc. Littleton, Colorado, USA. 33-44, 61-75, 91-98, 101-114 p.
- Castendyk, D.N. and Webster-Brown, J.G. 2007. Sensitivity analysis in pit lake prediction, Martha Mine, New Zealand 1: Relationship between turnover and input water density. *Chemical Geology*, v. 244, 42-55.
- Center for Water Research (CWR). 2002. *Dynamic reservoir simulation model DYRESM: user manual*. Report WP 1573 JA. Centre for Water Research, Univeristy of Western Australia, Perth, Australia 38 p.
- Cockerton, S., 2007. *An experimental water-rock interaction study into the origins of the chemical characteristics, of the Hogarth and Caland pit lakes, Steep Rock Lake, Atikokan*. Unpublished H.SBc. thesis, Lakehead University, Thunder Bay, ON, Canada 48 p.
- Conly, A., and MacDonald, J. 2005. Origin of high-sulphate waters of Hogarth Pit Lakes, Steep Rock Iron Mine, Atikokan, Ontario. 51st Annual Institute on Lake Superior Geology Proceedings and Abstracts. p. 12 – 13.

- Conly, A., Cockerton, S., and Lee, P. 2007. An experimental water-rock interaction study into the origin of high-sulphate waters associated with the Steep Rock Iron Mines, Atikokan, Ontario. 53d Annual Institute on Lake Superior Geology Proceedings and Abstracts. 22 – 23 p.
- Conly, A. G., Lee, P. F., Godwin, A., Cockerton, S. 2008. Experimental Constraints for the Source of Sulfate Toxicity and Predictive Water Quality for the Hogarth and Caland Pit Lakes, Steep Rock Iron Mine, Northwestern Ontario, Canada. – In: Rapantova, N. & Hrkal, Z.: Mine Water and the Environment. – Paper #139; Ostrava (VSB – Technical University of Ostrava). (http://www.imwa.info/docs/imwa_2008/IMWA2008_139_Conly.pdf Accessed December 8, 2011)
- Conly, A. G., Lee, P. F., Goold, A., Godwin, A. 2008. Geochemistry and Stable Isotope Composition of Hogarth and Caland Pit Lakes, Steep Rock Iron Mine, Northwestern Ontario, Canada. – In: Rapantova, N. & Hrkal, Z.: Mine Water and the Environment. – Paper #133; Ostrava (VSB – Technical University of Ostrava). (http://www.imwa.info/docs/imwa_2008/IMWA2008_133_Conly.pdf Accessed December 8, 2011)
- Conly, Andrew George; Shankie, Simon; Lee, Peter 2010. Treatment of sulphate toxic waters using permeable reactive barriers: batch and flow-through reactor experiments. – In: Wolkersdorfer, Ch. & Freund, A.: Mine Water & Innovative Thinking. Sydney, Nova Scotia (CBU Press). 221 – 225 p.
- Cornwell, A.R., and Harvey, L.D. 2007. Soil moisture: a residual problem underlying AGCMs. *Climatic Change*, v. 84, 313-336.
- Eary, L.E. 1999. Geochemical and equilibrium trends in mine pit lakes. *Applied Geochemistry* v. 14, 963-987.
- Fisher, T.S.R., 2002. Limnology of the meromictic Island Copper Mine Pit Lake, PhD thesis, University of British Columbia, Canada, 228 p.
- Eaton, A.D., Clesceri, L.S., Rice, E.W., and Greenberg, A.E. (Eds) 2005. Standard methods for the examination of water and waste water 21st Edition. American Public Health Association. 1368 p..
- Environment and Land HQ Division, 2000. Water quality: ambient water quality guidelines for sulphate, overview report. Prepared pursuant to Section 2(e) of the Environmental Management Act. 1981. (<http://www.env.gov.bc.ca/wat/wq/BCguidelines/sulphate/sulphate.html#summary>; accessed December 8, 2011)
- EPA, 2003. Drinking Water Advisory: Consumer Acceptability Advice and Health Effects Analysis on Sulfate. U.S. Environmental Protection Agency Office of Water (4304T) Health and Ecological Criteria Division, Washington, D.C. EPA 822-R-03-007, 29 p.
- Fisher, T.S.R., and Lawrence, G.A. 2000. Observations at the upper halocline of the Island Copper pit lake. In: Lawrence, G.A., Pieters, R., Yonemitsu, N. (Eds) Proceedings of the 5th International Symposium on Stratified Flows, Vancouver, British Columbia, Canada 413 – 418 p.

- Godwin, A. 2010. Geochemical and toxicological investigations of the Hogarth and Caland pit lakes, Steep Rock iron mine site. Unpublished MSc. thesis, Lakehead University, Thunder Bay, ON, Canada 122 p.
- Godwin, Amy Lynn, Lee, Peter Ferguson, Conly, Andrew George, Goold, Andrea R. (2010): Predicting toxicity of future combined pit lakes at the former Steeprock Iron Mine near Atikokan, Ontario. – In: Wolkersdorfer, Ch. & Freund, A.: Mine Water & Innovative Thinking. – p. 343 – 347; Sydney, Nova Scotia (CBU Press). 343 – 347 p.
- Gould, A.R. 2008. Water quality and toxicity investigations of two pit lakes at the former Steep Rock iron mines, near Atikokan, Ontario. Unpublished MSc thesis, Lakehead University, Thunder Bay, ON, Canada, 122 p.
- Hamblin, P.F., Stevens, C.L., Lawrence, G.A., 1999. Simulation of vertical transport in mining pit lake. *Journal of Hydraulic Engineering* v. 125, 1029-1038.
- Heinselman, M. 1996. *The Boundary Waters Wilderness Ecosystem*. Minneapolis: University of Minnesota Press. 334 p.
- Health Canada, 2010. Guidelines for canadian drinking water quality: summary table. Federal-Provincial-Territorial Committee on Drinking Water, 15 p.
- Hipsey, M.R., Romero, J.R., Antenucci, J.P., and Hamilton, D. 2006a. *Computation Aquatic Ecosystem Models: CAEDYM v2, v2.3 Science Manual*. Contract Research Group, Centre for Water Research, University of Western Australia. 90 p.
- Hipsey, M.R., Romero, J.R., Antenucci, J.P., and Hamilton, D. 2006b. *Computation Aquatic Ecosystem Models: CAEDYM v2, v2.3 User Manual*. Centre for Water Research, University of Western Australia. WP 1387.1 MH. 58 p.
- Imberger, J. and Patterson, J.C. 1981. A Dynamic Reservoir Simulation Model – DYRESM: 5. In: *Proceedings of the Symposium on predictive ability of transport models for inland and coastal waters*. Academic Press Inc. 310 – 361 p.
- Imerito, A.J. 2001. *The CWR dynamic reservoir simulation model DYRESM: Science manual: Report WP 1573 JA*. Centre for Water Research, Univeristy of Western Australia, Perth, Australia 38 p.
- Ivey, G.N., Oldham, C.E., Huber, A., Wake, G., 2006. Hydrodynamic processes in a Western Australian coal mine pit lake. *Interactive Pit Lakes 2004 Conference*. United States Environmental Protection Agency, Washington, D.C., EPA/625/c-06/002.
- Jackson, B. 2007. *Area, Volumes and Water Fill Calculations for Steep Rock Mine Area*. Unpublished manuscript. Ministry of Natural Resources.
- Jolliffe, A.W. 1955. Geology and Iron Ores of Steep Rock Lake. *Economic Geology*. v. 50, 373-398 p.

- Kusky, T.M., and Hudleston, P.J. 1999. Growth and demise of an Archean carbonate platform, Steep Rock Lake, Ontario, Canada. *Canadian Journal of Earth Science*. v. 36, 565-584.
- Lee, P. F.; Cook, M. V.; Conly, A. G. (2008): Predicting Discharge Water Quality from Steeprock Pit Lakes in Atikokan, Ontario, Canada. – In: Rapantova, N. & Hrkal, Z.: *Mine Water and the Environment*. – Paper #137; Ostrava (VSB – Technical University of Ostrava). (http://www.imwa.info/docs/imwa_2008/IMWA2008_137_Lee.pdf, accessed December 9, 2011).
- MacDonald, J.C. 2005. An Integrated Mineralogy, Geochemistry, and Stable Isotope Geochemistry Investigation into Potential Sulphate Sources of the Hogarth Pit Lake, Steep Rock Iron Mine, Atikokan. HB.Sc. Thesis, Lakehead University Department of Geology, Thunder Bay, ON., 73 p.
- McNaughton, K.A. 2001. The limnology of two proximate pit lakes after twenty years of flooding. Unpublished MSc. thesis, Lakehead University, Thunder Bay, ON, Canada, p. 85.
- MNR (Ministry of Natural Resources). 1986. Report on the Surrender of Mining Claims By Steep Rock Resources Inc., Steep Rock Lake Atikokan District., Ontario. 146 p.
- Parshley, J.V., and Bowell, R.J., 2003. The limnology of Summer Camp Pit Lake: a case study. *Mine Water and the Environment* v. 22, 170-186.
- Penman, H.L. 1948. Natural evaporation from open water, bare soil and grass. *Proceedings of the Royal Society of London*. A193, 120-145.
- Perusse, C.B., 2009. Hydrogeological and geochemical assessment of two tailings impounds at the former Steep Rock Iron Mine, Atikokan, Ontario. Unpublished HSc thesis, Lakehead University, Thunder Bay, ON, 39 p.
- Shankie, S.J. 2011. Assessment of Permeable Reactive Barriers for Sulphate Reduction at the Former Steep Rock Iron Mine Site, Atikokan, Ontario. MSc thesis, Lakehead University Department of Geology, Thunder Bay, ON, Canada 151 p.
- Shevenell, L. 2000a. Analytical method for predicting filling rates of mining pit lakes: example from the Gretchell Mine, Nevada. *Mining Engineering*, v. 52, p. 53 – 60.
- Shevenell, L.A. 2000b. Water quality in pit lakes in disseminated gold deposits compared to two natural, terminal lakes in Nevada. *Environmental Geology*, v. 39, 807 – 815.
- Shklanka, R. 1972. Geology of the Steep Rock Lake Area District of Rainy River. Ontario, Department, Mines and Northern Affairs. *Geology*. Report. 93.
- Steep Rock Mines. 1943. The Steep Rock Iron Ore Deposits. A Story of Patient Investigation and Development. *Can. Min. J.* v. 63, 437-444.

- Sowa, V.P., Adamson, R.B., and Chow, A.W. 2001, Water Management of the Steep Rock Iron Mines At Atikokan, Ontario During Construction, Operations, and After Mine Abandonment. – IN: Proceedings of the 25th Annual British Columbia Mine Reclamation Symposium in Campbell River, BC, 2001. The Technical and Research Committee on Reclamation. 104 – 115 p.
- Stinton, P., Moreno, J., Bartlett, D., and Williamson, A. 2002. A method for simulating pit lake development and passive containment resulting from complex geometry pit lakes. Agenda of the Hardrock mining 2002: issues shaping the industry. Westminster, Colorado. 25 p.
- Stone, D., Kamineni, D.C., and Jackson, M.C. 1992. Precambrian geology of the Atikokan area, northwestern Ontario. Geological Survey of Canada. Bulletin 405, 106 p.
- Stone, D., Tomlinson, K., Bernatchez, R., and Fralick, P., 2000. Geology of the Archean Steep Rock Lake – Finlayson Lake Greenstone Belt. Forty-sixth Annual Meeting, Institute on Lake Superior Geology, Thunder Bay, ON. v.46(2), 179-214.
- Stott, G., Corkery, T., Leclair, A., Boily, M., and Percival, J.A., 2007, A revised terrane map for the Superior Province as interpreted from aeromagnetic data: *in* Institute on Lake Superior Geology Proceedings, 53rd Annual Meeting, Lutsen, Minnesota, Abstract, v.53, part 1, p. 74–75.
- Surrano, S.E. 1997. Hydrology for engineers, geologists and environmental professionals: an integrated treatment of surface, subsurface and contaminant hydrology. Hydroscience Inc. Lexington, Ky. 466 p.
- Taylor, B. 1978. Steep Rock The Men and the Mines. Quetico Publishing: Atikokan Ontario.
- Thorntwaite, C.W. 1948. An approach toward a rational classification of climate. Geography. Rev. v. 38, 55-89.
- Timmis, B.B., 2011. An investigation of acid rock drainage interaction with waste rock materials and catchment ponds at Steep Rock Mine Site, Atikokan, ON. Unpublished HBSc thesis, Lakehead University, Thunder Bay, ON, 62 p.
- UNESCO, 1981. Background papers and supporting data on the Practical Salinity Scale 1978. Unesco technical papers in marine science 37. United Nations Educational, Scientific and Cultural Organization, Place de Fontenoy, 75700, Paris.
- Vancook, M. 2005. The limnology and remediation of two proximal pit lakes in northwestern Ontario. Unpublished MSc thesis, Lakehead University, Thunder Bay, ON, Canada, 105 p.
- Wetzel, R.G. 2001. Limnology: Lake and River Ecosystems Third Edition. San Deigo: Elsevier Academic Press. 1006 p.

- Wilks, M.E. and Nisbet, E.G. 1988. Stratigraphy of the Steep Rock Group, northwestern Ontario: a major Archean unconformity and Archean stromatolites. *Canadian Journal of Earth Sciences* V. 25 p. 370-391.
- Younger, P.L., Banwart, S.A. and Hedin, R.S. 2002. Mine Water Hydroogy, Pollution, Remediation (Environmental Pollution Vol. 5 Edited by Alloway, B.J.) The Nethrlands: Kluwer Academic Publishers Dordrecht. 442 p.
- WHO, 2004. Sulfate in drinking-water: backpny of document for development of WHO guidelines for drinking-water quality. World Health Organization
WHO/SDE/WSH/03.04/114

APPENDICES

APPENDIX I
Pit Lake Volume Calculations

Volume Calculations							
Hogarth & South Roberts Pits							
Elevation	Elevation	Surface Area	Surface Area	Elevation	Volume	Volume	Accu. Volume
ft	m	ft ²	m ²	m	ft ³	m ³	m ³
350	107	120,000	11,148	-	12,000,000	339,804	339,804
450	137	700,000	65,030	-	69,600,000	1,970,863	2,310,667
550	168	1,370,000	127,273	-	136,800,000	3,873,766	6,184,433
650	198	2,250,000	209,025	-	224,800,000	6,365,662	12,550,094
656	200	-	203,285	2	-	412,297	12,962,391
689	210	-	227,493	10	-	2,152,755	15,115,147
722	220	-	257,195	10	-	2,421,918	17,537,065
755	230	-	326,279	10	-	2,910,527	20,447,591
787	240	-	383,765	10	-	3,546,335	23,993,926
820	250	-	443,218	10	-	4,131,350	28,125,276
853	260	-	516,338	10	-	4,793,129	32,918,405
886	270	-	594,288	10	-	5,548,561	38,466,966
919	280	-	723,967	10	-	6,580,615	45,047,582
951	290	-	892,445	10	-	8,067,386	53,114,967
984	300	-	1,153,413	10	-	10,201,433	63,316,400
1,017	310	-	1,428,569	10	-	12,885,404	76,201,804
1,050	320	-	1,657,287	10	-	15,415,136	91,616,940
1,083	330	-	1,885,570	10	-	17,702,012	109,318,952
1,115	340	-	2,124,754	10	-	20,039,719	129,358,671
1,148	350	-	2,336,667	10	-	22,298,713	151,657,383
1,181	360	-	2,564,542	10	-	24,497,209	176,154,593
1,214	370	-	2,782,689	10	-	26,728,731	202,883,324
1,247	380	-	3,007,558	10	-	28,943,954	231,827,278
1,280	390	-	12,255,672	10	-	71,114,818	302,942,096
1,312	400	-	15,090,689	10	-	136,486,219	439,428,314

Note: Between 107 m and 198 m in elevation surface area data taken from the Steep Rock Environmental Plan (Capper, 1978) and from 200 m to 400 m in elevation from contour data.

Volume Calculations							
Caland & Fairweather Lake							
Elevation	Elevation	Surface Area	Surface Area	Elevation Increment	Volume	Volume	Accu. Volume
ft	m	ft ²	m ²	m	ft ³	m ³	m ³
300	91	86,000	7,989	-	4,300,000	121,763	121,763
350	107	220,000	20,438	-	22,000,000	622,974	4,421,763
450	137	1,050,000	97,545	-	105,000,000	2,973,285	7,395,048
550	168	2,650,000	246,185	-	265,000,000	7,504,005	14,899,053
623	190	-	403,058	22	-	7,186,844	22,085,898
656	200	-	468,151	10	-	4,351,986	26,437,884
689	210	-	533,470	10	-	5,004,554	31,442,438
722	220	-	595,153	10	-	5,640,306	37,082,744
755	230	-	699,952	10	-	6,468,449	43,551,193
787	240	-	801,325	10	-	7,500,674	51,051,867
820	250	-	926,292	10	-	8,630,539	59,682,406
853	260	-	1,063,724	10	-	9,942,161	69,624,567
886	270	-	1,211,989	10	-	11,370,505	80,995,072
919	280	-	1,418,072	10	-	13,136,825	94,131,897
951	290	-	1,612,916	10	-	15,144,491	109,276,388
984	300	-	2,092,535	10	-	18,475,302	127,751,690
1,017	310	-	2,426,946	10	-	22,576,757	150,328,447
1,050	320	-	2,819,470	10	-	26,207,576	176,536,024
1,083	330	-	3,232,622	10	-	30,236,929	206,772,953
1,115	340	-	3,800,716	10	-	35,128,386	241,901,338
1,148	350	-	4,621,438	10	-	42,043,963	283,945,301
1,181	360	-	5,124,131	10	-	48,706,226	332,651,527
1,214	370	-	5,565,141	10	-	53,431,191	386,082,718
1,247	380	-	6,894,340	10	-	62,178,896	448,261,614
1,280	390	-	12,255,672	10	-	94,473,719	542,735,333
1,312	400	-	15,090,689	10	-	136,486,219	679,221,552

Note: Between 107 m and 198 m in elevation surface area data taken from the Steep Rock Environmental Plan (Capper, 1978) and from 200 m to 400 m in elevation from contour data.

APPENDIX II
Estimating Precipitation Rates Using the Inversion Ration Method

Estimation of Missing Precipitation Data Using the Normal Inverse Ratio Method											
Year	Estimate Precipitation		Atikokan Marmion	Atikokan	Dryden	Dryden A	Fort Frances	Fort Frances A	Mine Centre	Rawson Lake	Stratton Romyn
	$P_i/P_j^{(bar)}$	P_i									
1978	0.943	697.3		671.7	568.9	535.3	767.4	814.2	696.7	632.7	
1979	0.901	666.8		714.4	619.5		682.5		662.4		609
1980	0.835	618.0		696.7	562.9	638.1	582.8	617.5		544.7	
1981	0.895	661.9		591.5		616.3	617.2	646.2		642.8	636.4
1982	1.061	784.6		832.7		766.3	768.2	764.9	681.5	709.4	826
1983	0.968	716.4		799.8	576.6		793.8	743.3		548.9	766
1984	0.958	708.8		732.7		709.6	671.6	684.8		596.8	722.2
1985	1.294	957.0		944.5	871.3	882.9	984.2				
1986	0.917	678.6		664.3	718	683.4	631.6	629.4		642.2	580.4
1987	0.826	611.2		698.8	592.1	566.2	680.2	599.8	616.8	493.5	556.4
1988	1.033	763.9			635.1	659.2	807	759.7	988.3	639.2	648.6
1989	0.870	643.3			549.2	519.8	665.4		703.1	563.1	695
1990	0.885	654.3			682.5	695.8	626.9	618.7	688.6	548.2	532.8
1991	1.122	829.7			838.3	835.3	766.2	762.6	785.4		807
1992	1.178	871.6			908	824.3		800.5	845	835	799.8
1993	0.961	710.7				627.7		703.9	714	628.1	739.8
1994	1.034	764.9			793.7	712.3	638	688.6	733.1	769.2	795.8
1995	0.980	724.8	795		700.9	619.3		721.2	779.3	610.6	743.4
1996	1.352	1000.1	1010.2		892.2	838.2		1071.8	989.4	1002.2	
1997	0.827	611.5	577.8			664.1		499.4	550.6	627.3	
1998	0.926	684.7	675.5			647		716.7	598.4	664	
1999	1.138	841.5	813.4			811.4		722.7	889.1	805.9	
2000	1.133	838.1	775.1			846.1		734.2	723	923.1	787
2001	1.344	994.5	941			901.6		865.5	1070.8	979	
2002	1.095	809.6	731.8			734.8		723.6	931	654.7	847.8
2003	0.858	634.8	842.3			642.5		552.6	622.5	616.7	
2004			868.2					849.9	843.6		
2005			905					949			
Average Annual Precipitation Rates				739.7	705.5	701.5	709.3	720.7	728.6	688.4	711.1
Quality of Weather Station Data				D	A	A	A	A	A	A	C
All values in mm/year except the ratio $P_i/P_j^{(bar)}$											
A no more than 3 consecutive or 5 total missing years between 1971-2000											
B at least 25 years of record between 1971-2000											
C at least 20 years of record between 1971-2000											
D at least 15 years of record between 1971-2000											

APPENDIX III
Estimating Evaporation Rates Using the Penman and Thornwaite Equations

Evaporation Estimate Calculated Using the Penmen Equation							
Calculation of E_n							
	C_1	Q_n (cal/m ² .day)	p (kg/m ³)	L (cal/kg)	E_n (mm/day)		
May	1000	2275173.374	1000	591700	3.845146821		
June	1000	2597307.781	1000	588900	4.410439432		
July	1000	2524152.183	1000	586000	4.307426933		
August	1000	1929306.652	1000	588900	3.276119294		
September	1000	1070132.094	1000	591700	1.80857207		
October	1000	366343.5761	1000	597300	0.613332624		
Calculation of E_a							
	T^*	r (%) [*]	c_2 (mm/day.mmHg)	c_3 (mm.hour/day.km.m mHg)	W (km/hour)	c_e (mmHg) [*]	E_a (mm/day)
May	10.4	46.2	0.1733	0.0512	8.3	9.2	2.961147696
June	14.7	53.8	0.1733	0.0512	8.2	12.78	3.50211209
July	17.7	55.1	0.1733	0.0512	7.1	17.53	4.225294115
August	16.1	57.6	0.1733	0.0512	6.8	12.78	2.825645731
September	10.4	60.8	0.1733	0.0512	7.8	9.2	2.065241024
October	4.5	63.6	0.1733	0.0512	8.5	6.54	1.44857076
Calculation of PET							
	T (°C) [*]	a^1	PET (mm/day)	PET (mm/month)			
May	10.4	1.25	3	107			
June	14.7	1.66	4	122			
July	17.7	2.19	4	133			
August	16.1	1.66	3	96			
September	10.4	1.25	2	58			
October	4.5	0.93	1	32			
* Values taken from the 1971 - 2000 Canadian Climate Normals for the weather station Atikokan.							
1 Values originally from Ponce (1989)							

Evaporation Estimate Calculated Using the Thornwaite Equation						
	T_a^*	I	Total Hours per Sunlight Month [*]	Average Hours of Sunlight per Day	mm/month	mm/month corrected for latitude
May	10.4	3.030734475	248.6	8.019354839	13	16
June	14.7	5.117735756	247.7	8.256666667	18	25
July	17.7	6.779395	279.4	9.012903226	23	31
August	16.1	5.873456948	231.7	7.474193548	18	22
September	10.4	3.030734475	157.9	5.263333333	8	9
October	4.5	0.852556479	109.8	3.541935484	3	2
Sum of $I = 25.10029078$ $m = 0.903394624$						
* Values taken from the 1971 - 2000 Canadian Climate Normals for the weather station Atikokan.						

APPENDIX IV
Water Balance and Rebound Model Results

Hogarth Groundwater Calculations			
	m ³ /year	m ³ /day	gpm
MAX	2263000	6200	947
MIN	-1788500	-4900	-749
AVERAGE	322319	883	135

Model 1A - Hogarth Pit Lake/Middle Arm											
Year	Annual Precipitation	Runoff Pit	Runoff Land	Pit Evaporation	Gwi - Gwo	Change in Storage	Accu. Volume	Measured Water Elevation	Water Elevation	Pit Lake Surface Area	Watershed Area
	mm/year	m ³ /year	m	m	m ²	m ²					
1979	714	43631	2084474	29138	511000	2609967	3249081	148.7	148.7	61074	7294492
1980	697	42550	2032829	33157	-246375	1795847	5044928		171.1	94261	7261305
1981	592	55756	1718025	48563	-246375	1478842	6523770		184.1	121416	7234150
1982	833	101103	2409551	58268	-246375	2206011	8729781		198.9	161754	7193812
1983	800	129371	2301444	93672	-246375	2090768	10820549		209.8	199839	7155727
1984	733	146422	2097200	82973	-246375	1914274	12734824		218.1	234611	7120955
1985	945	221590	2690297	97997	-246375	2567515	15302338		227.4	281124	7074442
1986	664	186751	1879821	151891	-246375	1668305	16970644	232.6	232.6	311282	7044284
1987	699	217524	1969018	171330	-273750	1741463	18712106		237.6	342714	7012852
1988	764	261793	2142797	204223	-273750	1926617	20638723	242.6	242.6	377437	6978129
1989	643	242797	1795553	193021	401500	2246829	22885553	247.8	247.8	417868	6937698
1990	654	273431	1815863	213698	2263000	4138596	27024149	256.3	256.3	492188	6863378
1991	830	408375	2277859	251705	-1789500	646030	27670178	257.5	257.5	503772	6851794
1992	872	439111	2388934	257629	839500	3409916	31080094		263.4	564854	6790712
1993	711	401462	1930560	288866	839500	2882655	33962749	267.9	267.9	616411	6739155
1994	765	471462	2061780	315232	985500	3203510	37166259		272.4	673628	6681938
1995	795	535534	2124856	344493	985500	3301397	40467656		276.8	732515	6623051
1996	1010	739986	2676243	374608	985500	4027121	44494777	281.6	281.6	804248	6551318
1997	578	464694	1514141	411292	547500	2115043	46609820		283.9	841882	6513684
1998	676	568691	1759997	430538	547500	2445650	49055470		286.5	885366	6470200
1999	813	720157	2105144	452776	547500	2920025	51975495	289.5	289.5	937242	6418324
2000	775	726456	1989937	479306	-219000	2018088	53993583	291.4	291.4	973068	6382498
2003	842	932550	2105217	566195	219000	2690572	64246690	300.2	300.2	1154787	6200779
2004	868	1002586	2153406	590558	-109500	2455935	66702625		302.1	1198246	6157320
2005	905	1084413	2228950	612783	-109500	2591079	69293704		304.1	1244070	6111496
2006	740	920114	1808025	636217	-109500	1982422	71276126		305.5	1279112	6076454
2007	740	946031	1797658	654138	-109500	1980051	73256177	306.9	306.9	1314097	6041469
2008	740	971906	1787308	672029	1460000	3547185	76803363	309.3	309.3	1376737	5978829
2009	740	1018234	1768777	704063	912500	2995448	79798811	311.2	311.2	1429598	5925968
2010	740	1057331	1753138	731096	322319	2401691	82200502	312.8	312.7	1471960	5883606
2011	740	1088661	1740606	752760	322319	2398826	84599328	313.7	314.2	1514252	5841314
2012	740	1119941	1728094	774388	322319	2395965	86995293		315.6	1556475	5799091
2013	740	1151169	1715603	795982	322319	2393109	89388402		317.0	1598631	5756935
2014	740	1182347	1703132	817540	322319	2390258	91778660		318.3	1640719	5714847
2015	740	1213476	1690680	839064	322319	2387411	94166071		319.6	1682740	5672826
2016	740	1244555	1678249	860553	322319	2384569	96550640		320.9	1724695	5630871
2017	740	1275585	1665837	882009	322319	2381731	98932370		322.1	1766585	5588981
2018	740	1306566	1653444	903432	322319	2378897	101311268		323.3	1808409	5547157
2019	740	1337499	1641071	924820	322319	2376068	103687336		324.5	1850169	5505397
2020	740	1368385	1628717	946176	322319	2373244	106060580		325.7	1891864	5463760
2021	740	1399223	1616382	967499	322319	2370423	108431003		326.8	1933496	5422070
2022	740	1430014	1604065	988790	322319	2367608	110798611		327.9	1975064	5380502
2023	740	1460758	1591768	1010048	322319	2364796	113163407		329.0	2016570	5338996
2024	740	1491455	1579489	1031274	322319	2361988	115525395		330.0	2058013	5297553
2025	740	1522106	1567228	1052468	322319	2359185	117884580		331.0	2099394	5256172
2026	740	1552712	1554986	1073630	322319	2356386	120240967		332.0	2140713	5214853
2027	740	1583272	1542762	1094761	322319	2353591	122594558		333.0	2181971	5173595
2028	740	1613786	1530556	1115860	322319	2350801	124945359		334.0	2223168	5132398
2029	740	1644255	1518369	1136928	322319	2348014	127293373		334.9	2264305	5091261
2030	740	1674680	1506199	1157965	322319	2345232	129638604		335.9	2305381	5050185
2031	740	1705060	1494047	1178972	322319	2342453	131981057		336.8	2346397	5009169
2032	740	1735395	1481913	1199947	322319	2339679	134320736		337.7	2387354	4968212
2033	740	1765687	1469796	1220893	322319	2336909	136657645		338.5	2428251	4927315
2034	740	1795934	1457697	1241808	322319	2334142	138991787		339.4	2469089	4886477
2035	740	1826138	1445615	1262692	322319	2331380	141323167		340.2	2509868	4845698
2036	740	1856299	1433551	1283547	322319	2328622	143651789		341.1	2550589	4804977
2037	740	1886416	1421504	1304371	322319	2325867	145977656		341.9	2591252	4764314
2038	740	1916490	1409475	1325166	322319	2323117	148300773		342.7	2631857	4723709
2039	740	1946521	1397462	1345932	322319	2320370	150621144		343.5	2672404	4683162
2040	740	1976510	1385467	1366667	322319	2317628	152938771		344.3	2712894	4642672
2041	740	2006456	1373488	1387374	322319	2314889	155253660		345.0	2753326	4602240
2042	740	2036360	1361527	1408051	322319	2312154	157565815		345.8	2793702	4561864
2043	740	2066222	1349582	1428699	322319	2309423	159875238		346.5	2834021	4521545

2044	740	2096042	1337654	1449318	322319	2306696	162181934	347.2	2874283	4481283
2045	740	2125820	1325743	1469909	322319	2303973	164485906	347.9	2914490	4441076
2046	740	2155557	1313848	1490470	322319	2301253	166787160	348.7	2954640	4400926
2047	740	2185252	1301970	1511003	322319	2298537	169085697	349.3	2994734	4360832
2048	740	2214905	1290108	1531507	322319	2295825	171381522	350.0	3034773	4320793
2049	740	2244518	1278263	1551983	322319	2293117	173674639	350.7	3074756	4280810
2050	740	2274090	1266435	1572430	322319	2290413	175965052	351.4	3114685	4240881
2051	740	2303621	1254622	1592850	322319	2287712	178252764	352.0	3154558	4201008
2052	740	2333111	1242826	1613241	322319	2285015	180537779	352.7	3194376	4161190
2053	740	2362561	1231046	1633604	322319	2282322	182820101	353.3	3234140	4121426
2054	740	2391970	1219283	1653939	322319	2279632	185099732	353.9	3273850	4081716
2055	740	2421339	1207535	1674247	322319	2276946	187376678	354.6	3313505	4042061
2056	740	2450668	1195803	1694526	322319	2274264	189650942	355.2	3353106	4002460
2057	740	2479957	1184088	1714778	322319	2271585	191922527	355.8	3392654	3962912
2058	740	2509207	1172388	1735003	322319	2268910	194191437	356.4	3432147	3923419
2059	740	2538416	1160704	1755200	322319	2266239	196457676	357.0	3471587	3883979
2060	740	2567586	1149036	1775370	322319	2263571	198721247	357.5	3510974	3844592
2061	740	2596716	1137384	1795512	322319	2260907	200982154	358.1	3550308	3805258
2062	740	2625808	1125748	1815627	322319	2258246	203240400	358.7	3589588	3765978
2063	740	2654860	1114127	1835716	322319	2255589	205495990	359.2	3628816	3726750
2064	740	2683872	1102522	1855777	322319	2252936	207748926	359.8	3667991	3687575
2065	740	2712846	1090932	1875811	322319	2250286	209999212	360.3	3707114	3648452
2066	740	2741781	1079358	1895818	322319	2247640	212246852	360.9	3746184	3609382
2067	740	2770678	1067800	1915798	322319	2244997	214491850	361.4	3785202	3570364
2068	740	2799535	1056257	1935752	322319	2242358	216734208	361.9	3824168	3531398
2069	740	2828354	1044729	1955679	322319	2239722	218973930	362.5	3863082	3492484
2070	740	2857135	1033217	1975580	322319	2237090	221211021	363.0	3901944	3453622
2071	740	2885878	1021720	1995454	322319	2234462	223445482	363.5	3940754	3414812
2072	740	2914582	1010238	2015302	322319	2231837	225677319	364.0	3979513	3376053
2073	740	2943248	998771	2035123	322319	2229215	227906534	364.5	4018221	3337345
2074	740	2971876	987320	2054918	322319	2226597	230133130	365.0	4056877	3298689
2075	740	3000467	975884	2074687	322319	2223982	232357112	365.5	4095483	3260083
2076	740	3029019	964463	2094430	1125319	3024371	235381483	366.1	4147973	27812480
2077	740	3067841	8228044	2121273	1125319	10299930	245681413	368.3	4326659	27633794
2078	740	3199997	8175182	2212653	1125319	10287844	255969257	370.4	4505021	27455432
2079	740	3331914	8122415	2303868	1125319	10275779	266245036	372.4	4683066	27277387
2080	740	3463596	8069742	2394920	1125319	10263736	276508773	374.3	4860797	27099656
2081	740	3595046	8017162	2485812	1125319	10251715	286760487	376.2	5038220	26922233
2082	740	3726268	7964673	2576546	1125319	10239714	297000201	377.9	5215339	26745114
2083	740	3857265	7912275	2667124	1125319	10227733	307227935	379.7	5392157	26568296
2084	740	3988040	7859965	2757549	1125319	10215773	317443708	381.3	5568680	26391773
2085	740	4118596	7807742	2847823	1125319	10203833	327647541	382.9	5744910	26215543
2086	740	4248935	7755606	2937947	1125319	10191913	337839455	384.5	5920850	26039603
2087	740	4379061	7703556	3027923	1125319	10180013	348019467	386.0	6096504	25863949
2088	740	4508975	7651591	3117752	1125319	10168131	358187599	387.5	6271876	25688577
2089	740	4638679	7599709	3207437	1125319	10156269	368343868	388.9	6446966	25513487
2090	740	4768176	7547910	3296979	1125319	10144426	378488294	390.2	6621780	25338673
2091	740	4897468	7496193	3386378	1125319	10132602	388620896	391.6	6796318	25164135
2092	740	5026557	7444558	3475637	1125319	10120796	398741692	392.9	6970584	24989869
2093	740	5155444	7393003	3564757	1125319	10109009	408850701	394.2	7144580	24815873

Caland Groundwater Calculations			
	m ³ /year	m ³ /day	gpm
MAX	5475000	15000	2291
MIN	-2482000	-6800	-1039
AVERAGE	803000	2200	336

Model 1A Caland Pit Lake and Fairweather Lake/East and Southeast Arms

Year	Annual Precipitation	Runoff Pit	Runoff Land	Pit Evaporation	Gwi-Gwo	Change in Storage	Accu. Volume	Measured Water Elevation	Water Elevation	Pit Lake Surface Area	Watershed Area
	mm/year	m ³ /year		m	m ²	m ²					
1981	592	14045	3977525	12233	803000	4782337	3330786		117.2	23744	16811179
1982	833	110799	5563057	63855	803000	6413000	9743786		171.4	133060	16701863
1983	800	196160	5307365	142031	803000	6164494	15908279		196.1	245261	16589662
1984	733	254056	4832357	143966	803000	5745447	21653726		211.7	346740	16488183
1985	945	442668	6183167	195768	803000	7233067	28886793		226.3	468680	16366243
1986	664	344226	4335685	279972	-1350500	3049440	31936233	231.3	231.3	518178	16316745
1987	699	362103	4560857	285205	-2482000	2155754	34091987		234.6	552522	16282401
1988	764	422061	4975135	329248	-2482000	2585949	36677936	238.3	238.3	593038	16241885
1989	643	381489	4179225	303280	438000	4695434	41373370	244.4	244.4	664808	16170115
1990	654	435015	4232344	339983	2445500	6772875	48146245	252.1	252.1	764556	16070367
1991	830	634364	5333529	390994	-2007500	3569399	51715644	255.7	255.7	815479	16019444
1992	872	710808	5585310	417036	-91250	5787833	57503477		261.0	895840	15939083
1993	711	636705	4531388	458133	-91250	4618710	62122187	264.9	264.9	958149	15876774
1994	765	732841	4857348	489997	1460000	6560191	68682379		270.0	1044102	15790821
1995	795	830061	5021481	533954	1460000	6777588	75459967		274.8	1130025	15704898
1996	1010	1141551	6346035	577895	1460000	8369692	83829659	280.1	280.1	1232477	15602446
1997	578	712125	3606037	630288	803000	4490874	88320533		282.7	1285920	15549003
1998	676	868639	4201341	657619	803000	5215360	93535893		285.6	1346741	15488182
1999	813	1095439	5039235	688723	803000	6248951	99784844	288.9	288.9	1417962	15416961
2000	775	1099062	4779875	725146	36500	5190291	104975135	291.4	291.4	1475831	15359092
2001	941	1388757	5781162	754740	2518500	8933679	113908814	295.6	295.6	1572893	15262030
2002	732	1151043	4467501	804377	5475000	10289167	124197981	299.9	299.9	1681014	15153909
2005	905	1631367	5441695	921858	803000	6954205	143151544		307.1	1871064	14963859
2006	740	1383839	4426908	956862	803000	5656885	148808428		309.1	1925722	14909201
2007	740	1424264	4410738	984814	803000	5653188	154461616	310.9	310.9	1979473	14855450
2008	740	1464018	4394836	1012303	3358000	8204552	162666168	313.6	313.6	2056012	14778911
2009	740	1520627	4372193	1051445	3431000	8227375	170938543	316.1	316.1	2131517	14703406
2010	740	1576470	4349856	1090058	803000	5639268	176577811	317.9	317.9	2182080	14652843
2011	740	1613866	4334897	1115916	803000	5635848	182213659	318.9	318.9	2231909	14603014
2012	740	1650720	4320156	1141398	803000	5632477	187846136		320.8	2281034	14553889
2013	740	1687053	4305623	1166521	803000	5629154	193475290		322.3	2329480	14505443
2014	740	1722884	4291290	1191296	803000	5625878	199101168		323.8	2377274	14452613
2015	740	1758232	4257817	1215738	803000	5622479	207022479		325.7	2443550	14416337
2016	740	1807250	4249632	1249632	803000	5618828	214939307		327.6	2508653	14396234
2017	740	1855400	4236950	1282925	803000	5615242	222851732		329.5	2572637	14323250
2018	740	1902722	4218021	1315647	803000	5611697	230759828		331.2	2635553	14269334
2019	740	1949255	4199408	1347822	803000	5608141	238663669		332.9	2697449	142190743
2020	740	1995034	4181096	1379476	803000	5604654	246563323		334.6	2758369	141846518
2021	740	2040090	4163074	1410630	803000	5601167	254458857		336.1	2818353	141486534
2022	740	2084454	4145328	1441306	803000	5597680	262350333		337.7	2877439	141127448
2023	740	2128154	4127848	1471522	803000	5594193	270237813		339.2	2935664	140769223
2024	740	2171217	4110623	1501298	803000	5590706	278121355		340.6	2993060	140411827
2025	740	2213667	4093643	1530651	803000	5587219	286010104		342.1	3049658	140065229
2026	740	2255527	4076899	1559595	803000	5583732	293876845		343.4	3105488	14009399
2027	740	2296819	4060382	1588146	803000	5580245	301748899		344.8	3160577	14004310
2028	740	2337563	4043805	1616319	803000	5576758	309617228		346.1	3214951	14009936
2029	740	2377778	4027999	1644126	803000	5573271	317481878		347.3	3268635	140136252
2030	740	2417482	4012117	1671580	803000	5569784	325342898		348.6	3321651	140183236
2031	740	2456693	3996433	1698692	803000	5566297	333200331		349.8	3374022	140230865
2032	740	2495426	3980939	1725475	803000	5562810	341054222		350.9	3425767	140279120
2033	740	2533698	3965631	1751937	803000	5559323	348904613		352.1	3476908	140327979
2034	740	2571521	3950501	1778091	803000	5555836	356751544		353.2	3527462	140377425
2035	740	2608911	3935546	1803944	803000	5552349	364595057		354.3	3577446	140427441
2036	740	2645879	3920758	1829506	803000	5548862	372435188		355.4	3626878	140477809
2037	740	2682439	3906134	1854786	803000	5545375	380271976		356.4	3675774	140529113
2038	740	2718603	3891669	1879791	803000	5541888	388105456		357.5	3724149	140580873
2039	740	2754380	3877358	1904530	803000	5538401	395935664		358.5	3772017	140632870
2040	740	2789784	3863196	1929009	803000	5534914	403762635		359.5	3819392	140685495
2041	740	2824822	3849181	1953237	803000	5531427	411586401		360.4	3866288	140738599
2042	740	2859506	3835307	1977220	803000	5527940	419406995		361.4	3912717	140792170
2043	740	2893845	3821572	2000963	803000	5524453	427224449		362.3	3958691	140846196
2044	740	2927848	3807971	2024474	803000	5520966	435038793		363.2	4004222	140900665
2045	740	2961522	3794501	2047759	803000	5517479	442850057		364.1	4049320	140955567

2046	740	2994877	6081159	2070822	803000	7808214	450658271	365.0	4093998	20510889
2047	740	3027921	6067941	2093671	803000	7805192	458463462	365.9	4138264	20466623
2048	740	3060660	6054846	2116308	803000	7802198	466265660	366.7	4182129	20422758
2049	740	3093103	6041869	2138741	803000	7799231	474064891	367.6	4225603	20379284
2050	740	3125256	6029008	2160973	803000	7796290	481861181	368.4	4268693	20336194
2051	740	3157125	6016260	2183010	803000	7793375	489654556	369.2	4311409	20293478
2052	740	3188718	6003622	2204855	803000	7790486	497445042	370.0	4353760	20251127
2053	740	3220041	5991093	2226513	803000	7787621	505232663	370.8	4395753	20209134
2054	740	3251099	5978670	2247988	803000	7784781	513017444	371.6	4437397	20167490
2055	740	3281899	5966350	2269285	803000	7781964	520799409	372.3	4478698	20126189
2056	740	3312445	5954132	2290406	803000	7779171	528578579	373.1	4519665	20085222
2057	740	3342744	5942012	2311356	803000	7776400	536354979	373.8	4560303	20044584
2058	740	3372800	5929990	2332139	803000	7773651	544128630	374.5	4600621	20004266
2059	740	3402619	5918062	2352757	803000	7770924	551899554	375.3	4640624	19964263
2060	740	3432205	5906228	2373215	803000	7768218	559667772	376.0	4680319	19924568
2061	740	3461564	5894484	2393515	803000	7765533	567433305	376.7	4719711	19885176
2062	740	3490698	5882830	2413660	803000	7762869	575196173	377.3	4758808	19846079
2063	740	3519614	5871264	2433654	803000	7760224	582956397	378.0	4797614	19807273
2064	740	3548315	5859784	2453500	803000	7757599	590713996	378.7	4836135	19768752
2065	740	3576806	5848388	2473200	803000	7754994	598468990	379.3	4874377	19730510
2066	740	3605089	5837074	2492756	803000	7752407	606221397	380.0	4912345	19692542
2067	740	3633170	5825842	2512173	803000	7749839	613971236	380.6	4950043	19654844
2068	740	3661052	5814689	2531452	803000	7747289	621718524	381.3	4987477	19617410
2069	740	3688738	5803615	2550596	803000	7744757	629463281	381.9	5024652	19580235
2070	740	3716232	5792617	2569607	803000	7742242	637205524	382.5	5061571	19543316
2071	740	3743538	5781695	2588487	803000	7739745	644945269	383.1	5098240	19506647
2072	740	3770659	5770846	2607240	803000	7737265	652682533	383.7	5134664	19470223
2073	740	3797597	5760071	2625867	803000	7734801	660417335	384.3	5170845	19434042
2074	740	3824357	5749367	2644370	803000	7732354	668149688	384.9	5206788	19398099
2075	740	3850941	5738733	2662752	803000	7729923	675879611	385.5	5242498	19362389

Hogarth Groundwater Calculations			
	m ³ /year	m ³ /day	gpm
MAX	2263000	6200	947
MIN	-1788500	-4900	-749
AVERAGE	322295	883	135

Model 1B - Hogarth Pit Lake/Middle Arm											
Year	Annual Precipitation	Runoff Pit	Runoff Land	Pit Evaporation	Gwi-Gwo	Change in Storage	Accu. Volume	Measured Water Elevation	Water Elevation	Pit Lake Surface Area	Watershed Area
	m/m/year	m ³ /year	m	m	m ²	m ²					
1979	714	43631	2084474	29138	511000	2609967	3249081	148.7	148.7	61074	7294492
1980	697	42550	2032829	33157	-246375	1795847	5044928		171.1	94261	7261305
1981	592	55756	1718025	48563	-246375	1478842	6523770		184.1	121416	7234150
1982	833	101103	2409551	58268	-246375	2206011	8729781		198.9	161754	7193812
1983	800	129371	2301444	93672	-246375	2090768	10820549		209.8	199839	7155727
1984	733	146422	2097200	82973	-246375	1914274	12734824		218.1	234611	7120955
1985	945	221590	2690297	97997	-246375	2567515	15302338		227.4	281124	7074442
1986	664	186751	1879821	151891	-246375	1668305	16970644	232.6	232.6	311282	7044284
1987	699	217524	1969018	171330	-273750	1741463	18712106		237.6	342714	7012852
1988	764	261793	2142797	204223	-273750	1926617	20638723	242.6	242.6	377437	6978129
1989	643	242797	1795553	193021	401500	2246829	22885553	247.8	247.8	417868	6937698
1990	654	273431	1815863	213698	2263000	4138596	27024149	256.3	256.3	492188	6863378
1991	830	408375	2277859	251705	-1788500	646030	27670178	257.5	257.5	503772	6851794
1992	872	439111	2388934	257629	839500	3409916	31080094		263.4	564854	6790712
1993	711	401462	1930560	288866	839500	2882655	33962749	267.9	267.9	616411	6739155
1994	765	471462	2061780	315232	985500	3203510	37166259		272.4	673628	6681938
1995	795	535534	2124856	344493	985500	3301397	40467656		276.8	732515	6623051
1996	1010	739986	2676243	374608	985500	4027121	44494777	281.6	281.6	804248	6551318
1997	578	464694	1514141	411292	547500	2115043	46609820		283.9	841882	6513684
1998	676	568691	1759997	430538	547500	2445650	49055470		286.5	885366	6470200
1999	813	720157	2105144	452776	547500	2920025	51975495	289.5	289.5	937242	6418324
2000	775	726456	1989937	479306	-219000	2018088	53993583	291.4	291.4	973068	6382498
2003	842	932550	2105217	566195	219000	2690572	64246690	300.2	300.2	1154787	6200779
2004	868	1002586	2153406	590558	322295	2887730	67134420		302.5	1205884	6149682
2005	905	1091325	2226185	616689	322295	3023116	70157536		304.7	1259341	6096225
2006	740	931409	1803507	644027	322295	2413184	72570719		306.4	1301988	6053578
2007	740	962950	1790891	665837	322295	2410299	74981019	306.9	308.1	1344562	6011004
2008	740	994438	1778296	687609	322295	2407419	77388438	309.3	309.7	1387064	5968502
2009	740	1025873	1765722	709345	322295	2404545	79792983	311.2	311.2	1429495	5926071
2010	740	1057255	1753169	731044	322295	2401675	82194657	312.8	312.7	1471857	5883709
2011	740	1088585	1740637	752707	322295	2398809	84593467	313.7	314.2	1514149	5841417
2012	740	1119864	1728125	774336	322295	2395949	86989415		315.6	1556372	5799194
2013	740	1151093	1715634	795929	322295	2393093	89382508		317.0	1598527	5757039
2014	740	1182271	1703162	817487	322295	2390241	91772749		318.3	1640615	5714951
2015	740	1213399	1690711	839010	322295	2387394	94160144		319.6	1682636	5672930
2016	740	1244478	1678280	860500	322295	2384552	96544696		320.9	1724591	5630975
2017	740	1275507	1665868	881956	322295	2381714	98926410		322.1	1766480	5589086
2018	740	1306489	1653475	903378	322295	2378881	101305291		323.3	1808304	5547262
2019	740	1337422	1641102	924767	322295	2376052	103681343		324.5	1850064	5505502
2020	740	1368307	1628748	946122	322295	2373227	106054570		325.7	1891759	5463807
2021	740	1399145	1616413	967445	322295	2370407	108424977		326.8	1933390	5422176
2022	740	1429935	1604097	988736	322295	2367591	110792568		327.9	1974958	5380608
2023	740	1460679	1591799	1009994	322295	2364779	113157348		329.0	2016464	5339102
2024	740	1491376	1579520	1031219	322295	2361972	115519320		330.0	2057906	5297660
2025	740	1522028	1567260	1052413	322295	2359169	117878489		331.0	2099287	5256279
2026	740	1552633	1555018	1073575	322295	2356370	120234859		332.0	2140606	5214960
2027	740	1583192	1542794	1094706	322295	2353575	122588434		333.0	2181864	5173702
2028	740	1613707	1530588	1115805	322295	2350784	124939218		334.0	2223061	5132505
2029	740	1644176	1518400	1136873	322295	2347998	127287216		334.9	2264197	5091369
2030	740	1674600	1506231	1157910	322295	2345215	129632431		335.9	2305273	5050293
2031	740	1704980	1494079	1178917	322295	2342437	131974868		336.8	2346289	5009277
2032	740	1735315	1481945	1199892	322295	2339663	134314531		337.7	2387245	4968321
2033	740	1765606	1469828	1220837	322295	2336892	136651423		338.5	2428142	4927424
2034	740	1795854	1457729	1241752	322295	2334126	138985549		339.4	2468980	4886586
2035	740	1826058	1445648	1262636	322295	2331364	141316913		340.2	2509759	4845807
2036	740	1856218	1433584	1283491	322295	2328606	143645519		341.1	2550480	4805086
2037	740	1886335	1421537	1304315	322295	2325851	145971370		341.9	2591142	4764424
2038	740	1916409	1409507	1325110	322295	2323101	148294471		342.7	2631747	4723819
2039	740	1946440	1397495	1345875	322295	2320354	150614825		343.5	2672294	4683272
2040	740	1976428	1385499	1366611	322295	2317612	152932437		344.2	2712783	4642783
2041	740	2006374	1373521	1387317	322295	2314873	155247310		345.0	2753215	4602351
2042	740	2036278	1361559	1407994	322295	2312138	157559448		345.8	2793591	4561975
2043	740	2066140	1349615	1428642	322295	2309407	159868855		346.5	2833910	4521666

2044	740	2095959	1337687	1449261	322295	2306680	162175535	347.2	2874172	4481394
2045	740	2125737	1325776	1469851	322295	2303957	164479492	347.9	2914378	4441188
2046	740	2155474	1313881	1490413	322295	2301237	166780729	348.6	2954528	4401038
2047	740	2185169	1302003	1510945	322295	2298521	169079250	349.3	2994622	4360944
2048	740	2214822	1290142	1531450	322295	2295809	171375060	350.0	3034660	4320906
2049	740	2244435	1278297	1551925	322295	2293101	173668161	350.7	3074643	4280923
2050	740	2274006	1266468	1572373	322295	2290397	175958558	351.4	3114571	4240995
2051	740	2303537	1254656	1592792	322295	2287696	178246254	352.0	3154444	4201122
2052	740	2333027	1242860	1613183	322295	2284999	180531253	352.7	3194263	4161303
2053	740	2362477	1231080	1633546	322295	2282306	182813559	353.3	3234026	4121540
2054	740	2391886	1219316	1653881	322295	2279616	185093175	353.9	3273735	4081831
2055	740	2421255	1207569	1674188	322295	2276930	187370105	354.6	3313390	4042176
2056	740	2450584	1195837	1694468	322295	2274248	189644353	355.2	3352991	4002575
2057	740	2479872	1184122	1714720	322295	2271569	191915922	355.8	3392539	3963027
2058	740	2509122	1172422	1734944	322295	2268894	194184816	356.4	3432032	3923534
2059	740	2538331	1160738	1755141	322295	2266223	196451039	357.0	3471472	3884094
2060	740	2567501	1149070	1775311	322295	2263555	198714595	357.5	3510858	3844708
2061	740	2596631	1137418	1795453	322295	2260891	200975486	358.1	3550192	3805374
2062	740	2625722	1125782	1815568	322295	2258231	203233717	358.7	3589472	3766094
2063	740	2654774	1114161	1835656	322295	2255574	205489290	359.2	3628700	3726866
2064	740	2683786	1102556	1855717	322295	2252920	207742211	359.8	3667874	3687692
2065	740	2712760	1090967	1875751	322295	2250271	209992481	360.3	3706997	3648569
2066	740	2741695	1079393	1895758	322295	2247624	212240106	360.9	3746067	3609499
2067	740	2770591	1067834	1915738	322295	2244982	214485087	361.4	3785084	3570482
2068	740	2799448	1056291	1935692	322295	2242343	216727430	361.9	3824050	3531516
2069	740	2828267	1044764	1955619	322295	2239707	218967137	362.5	3862964	3492602
2070	740	2857048	1033251	1975520	322295	2237075	221204212	363.0	3901826	3453740
2071	740	2885790	1021755	1995394	322295	2234446	223438658	363.5	3940636	3414930
2072	740	2914494	1010273	2015241	322295	2231821	225670479	364.0	3979395	3376171
2073	740	2943160	998807	2035062	322295	2229199	227899678	364.5	4018102	3337464
2074	740	2971788	987355	2054857	322295	2226581	230126259	365.0	4056758	3298808
2075	740	3000378	975919	2074626	322295	2223967	232350226	365.5	4095363	3260203
2076	740	3028931	964498	2094369	322295	2221355	234571581	366.0	4133917	3221649
2077	740	3057445	953093	2114085	322295	2218747	236790329	366.4	4172421	3183145
2078	740	3085922	941702	2133776	942795	2836643	239626972	367.0	4221639	27738814
2079	740	3122324	8206251	2158946	942795	10112424	249739396	369.1	4397026	27563427
2080	740	3252041	8154364	2248639	942795	10100561	259839956	371.2	4572100	27388353
2081	740	3381525	8102570	2338172	942795	10088719	269928675	373.1	4746865	27213588
2082	740	3510781	8050868	2427547	942795	10076897	280005572	375.0	4921326	27039127
2083	740	3639813	7999255	2516766	942795	10065097	290070669	376.7	5095487	26864966
2084	740	3768622	7947731	2605832	942795	10053317	300123986	378.5	5269353	26691100
2085	740	3897213	7896295	2694747	942795	10041556	310165542	380.1	5442927	26517526
2086	740	4025588	7844945	2783513	942795	10029816	320195358	381.8	5616212	26344241
2087	740	4153750	7793680	2872131	942795	10018095	330213453	383.3	5789212	26171241
2088	740	4281701	7742500	2960603	942795	10006393	340219846	384.8	5961930	25998523
2089	740	4409444	7691403	3048931	942795	9994710	350214556	386.3	6134370	25826083
2090	740	4536980	7640388	3137117	942795	9983047	360197603	387.7	6306533	25653920
2091	740	4664312	7589456	3225161	942795	9971402	370169004	389.1	6478423	25482030
2092	740	4791442	7538604	3313066	942795	9959775	380128779	390.5	6650043	25310410
2093	740	4918372	7487832	3400832	942795	9948167	390076946	391.8	6821394	25139059
2094	740	5045103	7437139	3488461	942795	9936576	400013522	393.1	6992479	24967974
2095	740	5171637	7386526	3575954	942795	9925004	409938526	394.3	7163300	24797153

Caland Groundwater Calculations			
	m ³ /year	m ³ /day	gpm
MAX	5475000	15000	2291
MIN	-2482000	-6800	-1039
AVERAGE	620500	1700	260

Model 1B Caland Pit Lake and Fairweather Lake/East and Southeast Arms

Year	Annual Precipitation	Runoff Pit	Runoff Land	Pit Evaporation	Gwi-Gwo	Change in Storage	Accu. Volume	Measured Water Elevation	Water Elevation	Pit Lake Surface Area	Watershed Area
	m ³ /year	m	m	m ²	m ²						
1981	592	20367	3974996	17739	620500	4598123	4061162		127.2	34432	16800491
1982	833	119131	5559724	68657	620500	6230697	10291859		174.1	143065	16691858
1983	800	201406	5305266	145829	620500	5981343	16273202		197.3	251820	16583103
1984	733	256370	4831431	145277	620500	5563024	21836226		212.1	349897	16485026
1985	945	442668	6183167	195768	620500	7050567	28886793		226.3	468680	16366243
1986	664	344226	4335685	279972	-1350500	3049440	31936233	231.3	231.3	518178	16316745
1987	699	362103	4560857	285205	-2482000	2155754	34091987		234.6	552522	16282401
1988	764	422061	4975135	329248	-2482000	2585949	36677936	238.3	238.3	593038	16241885
1989	643	381489	4179225	303280	438000	4695434	41373370	244.4	244.4	664808	16170115
1990	654	435015	4232344	339983	2445500	6772875	48146245	252.1	252.1	764556	16070367
1991	830	634364	5333529	390994	-2007500	3569399	51715644	255.7	255.7	815479	16019444
1992	872	710808	5855310	417036	-91250	5787833	57503477		261.0	895840	15939083
1993	711	636705	4531388	458133	-91250	4618710	62122187	264.9	264.9	958149	15876774
1994	765	732841	4857348	489997	1600000	5650191	68682379		270.0	1044102	15790821
1995	795	830061	5021481	533954	1460000	6777588	75459967		274.8	1130025	15704898
1996	1010	1141551	6346035	577895	1460000	8369692	83829659	280.1	280.1	1232477	15602446
1997	578	712125	3606037	630288	803000	4490874	88320533		282.7	1285920	15549003
1998	676	868639	4201341	657619	803000	5215360	93535893		285.6	1346741	15488182
1999	813	1095439	5039235	688723	803000	6248951	99784844	288.9	288.9	1417962	15416961
2000	775	1099062	4779875	725146	365000	5190291	104975135	291.4	291.4	1475831	15359092
2001	941	1388757	5781162	754740	2518500	8933679	113908814	295.6	295.6	1572893	15262030
2002	732	1151043	4467501	804377	5475000	10289167	124197981	299.9	299.9	1681014	15153909
2005	905	1629724	5442353	920929	620500	6771647	142786486		307.0	1867506	14967417
2006	740	1381207	4427961	955043	620500	5474626	148261112		308.9	1920472	14914451
2007	740	1420381	4412291	982130	620500	5471043	153732155	310.9	310.7	1972585	14862338
2008	740	1458924	4396874	1008780	620500	5467518	159199672	313.6	312.5	2023881	14811042
2009	740	1496862	4381699	1035013	620500	5464048	164663721	316.1	314.2	2074394	14760529
2010	740	1534222	4366755	1060845	620500	5460632	170124352	317.9	315.8	2124157	14710766
2011	740	1571027	4352033	1086294	620500	5457266	175581618	318.9	317.4	2173200	14661723
2012	740	1607298	4337524	1111374	620500	5453948	181035566		319.0	2221550	14613373
2013	740	1643058	4323220	1136101	620500	5450678	186486244		320.5	2269234	14565689
2014	740	1678325	4309114	1160486	620500	5447453	191933697		321.9	2316276	145288611
2015	740	1713118	6593863	1184544	620500	7742937	199676634		323.9	2382128	144822759
2016	740	1761822	6574381	1218220	620500	7738483	207415117		325.8	2446806	144258081
2017	740	1809657	6555247	1251296	620500	7734108	215149224		327.7	2510364	143945523
2018	740	1856666	6536444	1283800	620500	7729809	222879033		329.5	2572856	14352031
2019	740	1902884	6517956	1315759	620500	7725582	230604615		331.2	2634328	143197059
2020	740	1948349	6499770	1347195	620500	7721424	238326039		332.8	2694825	142810062
2021	740	1993093	6481873	1378133	620500	7717332	246043371		334.5	2754387	142485050
2022	740	2037145	6464252	1408594	620500	7713303	253756674		336.0	2813054	142191833
2023	740	2080535	6446896	1438596	620500	7709335	261466008		337.5	2870860	141934027
2024	740	2123288	6429795	1468158	620500	7705425	269171433		339.0	2927839	141767048
2025	740	2165430	6412938	1497297	620500	7701571	276873004		340.4	2984023	141620864
2026	740	2206983	6396316	1526029	620500	7697770	284570774		341.8	3039440	141565447
2027	740	2247970	6379922	1554370	620500	7694022	292264796		343.1	3094119	141510768
2028	740	2288411	6363746	1582333	620500	7690324	299955120		344.5	3148085	141456802
2029	740	2328324	6347780	1609931	620500	7686673	307641793		345.7	3201363	141403524
2030	740	2367728	6332019	1637177	620500	7683070	315324863		347.0	3253976	141350911
2031	740	2406640	6316454	1664083	620500	7679511	323004374		348.2	3305945	141298942
2032	740	2445077	6301079	1690660	620500	7675996	330680369		349.4	3357292	141247595
2033	740	2483053	6285888	1716919	620500	7672523	338352892		350.5	3408036	141196851
2034	740	2520584	6270876	1742870	620500	7669090	346021982		351.7	3458196	141146691
2035	740	2557682	6256037	1768521	620500	7665697	353687679		352.8	3507789	141097098
2036	740	2594361	6241366	1793883	620500	7662343	361350022		353.9	3556832	141048055
2037	740	2630633	6226857	1818964	620500	7659026	369009048		354.9	3605341	140999546
2038	740	2666510	6212506	1843771	620500	7655745	376664792		356.0	3653331	140951556
2039	740	2702004	6198308	1868314	620500	7652498	384317291		357.0	3700817	140904070
2040	740	2737124	6184260	1892598	620500	7649287	391966577		358.0	3747813	140857074
2041	740	2771882	6170357	1916631	620500	7646108	399612685		358.9	3794331	140810556
2042	740	2806287	6156595	1940421	620500	7642961	407255646		359.9	3840385	140764502
2043	740	2840349	6142970	1963973	620500	7639846	414895492		360.8	3885987	140718900
2044	740	2874076	6129479	1987294	620500	7636762	422532254		361.8	3931148	140673739
2045	740	2907477	6116119	2010389	620500	7633707	430165961		362.7	3975879	140629008

2046	740	2940560	6102886	2033264	620500	7630681	437796642	363.6	4020191	20584696
2047	740	2973333	6089776	2055926	620500	7627684	445424326	364.4	4064094	20540793
2048	740	3005804	6076788	2078378	620500	7624714	453049041	365.3	4107598	20497289
2049	740	3037980	6063918	2100626	620500	7621772	460670813	366.1	4150713	20454174
2050	740	3069867	6051163	2122675	620500	7618856	468289668	367.0	4193447	20411440
2051	740	3101473	6038520	2144529	620500	7615965	475905633	367.8	4235809	20369078
2052	740	3132804	6025988	2166193	620500	7613100	483518733	368.6	4277808	20327079
2053	740	3163867	6013563	2187671	620500	7610259	491128992	369.4	4319451	20285436
2054	740	3194666	6001243	2208967	620500	7607442	498736434	370.1	4360747	20244140
2055	740	3225208	5989026	2230086	620500	7604649	506341083	370.9	4401703	20203184
2056	740	3255499	5976910	2251031	620500	7601879	513942961	371.7	4442326	20162561
2057	740	3285544	5964892	2271805	620500	7599131	521542092	372.4	4482623	20122264
2058	740	3315348	5952971	2292413	620500	7596405	529138497	373.1	4522601	20082286
2059	740	3344916	5941143	2312858	620500	7593701	536732198	373.8	4562267	20042620
2060	740	3374252	5929409	2333143	620500	7591018	544323216	374.6	4601626	20003261
2061	740	3403363	5917765	2353272	620500	7588356	551911572	375.3	4640685	19964202
2062	740	3432251	5906209	2373247	620500	7585714	559497286	375.9	4679450	19925437
2063	740	3460922	5894741	2393071	620500	7583092	567080378	376.6	4717927	19886960
2064	740	3489379	5883358	2412748	620500	7580489	574660867	377.3	4756121	19848766
2065	740	3517627	5872059	2432280	620500	7577906	582238773	378.0	4794037	19810850
2066	740	3545670	5860842	2451670	620500	7575341	589814114	378.6	4831680	19773207
2067	740	3573511	5849705	2470921	620500	7572795	597386909	379.3	4869057	19735830
2068	740	3601154	5838648	2490036	620500	7570267	604957175	379.9	4906171	19698716
2069	740	3628604	5827668	2509016	620500	7567756	612524932	380.5	4943027	19661860
2070	740	3655863	5816765	2527864	620500	7565263	620090195	381.1	4979630	19625257
2071	740	3682934	5805936	2546583	620500	7562788	627652983	381.7	5015984	19588903
2072	740	3709822	5795181	2565174	620500	7560329	635213311	382.4	5052094	19552793
2073	740	3736529	5784498	2583641	620500	7557886	642771198	383.0	5087964	19516923
2074	740	3763058	5773887	2601985	620500	7555460	650326657	383.5	5123598	19481289
2075	740	3789413	5763345	2620208	620500	7553050	657879707	384.1	5159000	19445887
2076	740	3815596	5752871	2638312	620500	7550655	665430362	384.7	5194173	19410714
2077	740	3841611	5742466	2656300	620500	7548276	672978638	385.3	5229123	19375764

Hogarth Groundwater Calculations			
	m ³ /year	m ³ /day	gpm
MAX	-1776710	-4868	-744
MIN	2498496	6845	1046
AVERAGE	1031614	2826	432

Model 2A - Hogarth Pit Lake/Middle Arm

Year	Annual Precipitation	Runoff Pit	Runoff Land	Pit Evaporation	Gwi - Gwo	Change in Storage	Accu. Volume	Measured Water Elevation	Water Elevation	Pit Lake Surface Area	Watershed Area
	m/m/year	m ³ /year	m	m	m ²	m ²					
1979	714	43631	2084474	29138		2098967	3249081	148.7	148.7	61074	7294492
1980	697	42550	2032829	33157		2042222	5291303		173.5	98793	7256773
1981	592	58436	1716953	50898		1724490	7015793		187.8	130429	7225137
1982	833	108608	2406549	62593		2452564	9468357		203.0	175222	7180344
1983	800	140143	2297136	101471		2335807	11804164		214.2	217717	7137849
1984	733	159521	2091961	90396		2161086	13965250		222.8	256917	7098649
1985	945	242658	2681869	107314		2817214	16782464		232.1	307883	7047683
1986	664	204526	1872710	166349	1794078	3704966	20487430	232.6	242.2	374712	6980854
1987	699	261849	1951288	206241		2006896	22494325		247.0	410833	6944733
1988	764	313828	2121983	244815	758038	2949034	25443359	242.6	253.2	463822	6891744
1989	643	298367	1773325	237199	378767	2213260	27656620	247.8	257.4	503529	6852037
1990	654	329483	1793443	257505	2320010	4185430	31842050	256.3	264.6	578488	6777078
1991	830	479980	2249217	295839	-1776710	656648	32498698	257.5	265.6	590235	6765331
1992	872	514475	2358788	301846		2571418	35070115		269.5	636198	6719368
1993	711	452168	1910277	325352	2118779	4155872	39225988	267.9	275.2	710376	6645190
1994	765	543332	2033032	363286		2213078	41439066		278.0	749827	6605739
1995	795	596113	2100625	383462		2313276	43752342		280.7	791031	6564535
1996	1010	799099	2652597	404533	2498496	5545660	49298002	281.6	286.8	889677	6465888
1997	578	514055	1494396	454981		1553471	50851472		288.4	917278	6438288
1998	676	619622	1739625	469096		1890151	52741623		290.2	950845	6404721
1999	813	773417	2083840	486262	1717616	4088611	56830234	289.5	294.0	1023392	6332174
2000	775	793231	1963227	523363	-325867	1907229	58737463	291.4	295.7	1057205	6298361
2003	842	1004141	2076581	609662	172406	2643466	69001057	300.2	303.8	1238896	6116670
2004	868	1075609	2124197	633571	1031614	3597849	72598906		306.4	1302486	6053080
2005	905	1178750	2191215	666091	1031614	3735487	76334393		309.0	1368458	5987108
2006	740	1012111	1771226	699829	1031614	3115122	79449515		311.0	1423436	5932130
2007	740	1052773	1754961	727945	1031614	3111403	82560918	306.9	313.0	1478315	5877251
2008	740	1093362	1738726	756010	1031614	3107691	85668609	309.3	314.8	1533098	5822468
2009	740	1133879	1722519	784026	1031614	3103986	88772595	311.2	316.6	1587785	5767781
2010	740	1174326	1706340	811993	1031614	3100287	91872881	312.8	318.4	1642378	5713188
2011	740	1214703	1690190	839912	1031614	3096594	94969475	313.7	320.1	1696878	5658688
2012	740	1255011	1674066	867783	1031614	3092907	98062382		321.7	1751286	5604280
2013	740	1295251	1657970	895607	1031614	3089227	101151610		323.3	1805603	5549963
2014	740	1335424	1641901	923385	1031614	3085553	104237163		324.8	1859830	5495736
2015	740	1375530	1625859	951117	1031614	3081885	107319048		326.3	1913968	5441598
2016	740	1415571	1609842	978803	1031614	3078223	110397272		327.7	1968019	5387547
2017	740	1455547	1593852	1006445	1031614	3074567	113471839		329.1	2021982	5333584
2018	740	1495458	1577887	1034042	1031614	3070917	116542757		330.5	2075859	5279707
2019	740	1535306	1561948	1061595	1031614	3067273	119610030		331.8	2129651	5225915
2020	740	1575090	1546035	1089104	1031614	3063635	122673664		333.1	2183358	5172208
2021	740	1614811	1530146	1116569	1031614	3060002	125733666		334.3	2236981	5118585
2022	740	1654471	1514282	1143992	1031614	3056375	128790041		335.5	2290520	5065046
2023	740	1694069	1498443	1171372	1031614	3052754	131842795		336.7	2343976	5011590
2024	740	1733605	1482629	1198710	1031614	3049138	134891933		337.9	2397351	4958215
2025	740	1773081	1466838	1226005	1031614	3045527	137937460		339.0	2450644	4904922
2026	740	1812496	1451072	1253259	1031614	3041923	140979383		340.1	2503856	4851710
2027	740	1851852	1435330	1280472	1031614	3038323	144017706		341.2	2556987	4798579
2028	740	1891148	1419612	1307643	1031614	3034730	147052436		342.3	2610039	4745527
2029	740	1930385	1403917	1334774	1031614	3031141	150083577		343.3	2663011	4692555
2030	740	1969563	1388245	1361864	1031614	3027558	153111135		344.3	2715905	4639661

2031	740	2008683	1372597	1388914	1031614	3023980	156135116	345.3	2768720	4586846
2032	740	2047745	1356973	1415923	1031614	3020408	159155524	346.3	2821457	4534109
2033	740	2086749	1341371	1442893	1031614	3016841	162172365	347.2	2874116	4481450
2034	740	2125696	1325792	1469823	1031614	3013279	165185644	348.2	2926699	4428867
2035	740	2164586	1310236	1496714	1031614	3009722	168195366	349.1	2979205	4376361
2036	740	2203420	1294703	1523565	1031614	3006171	171201537	350.0	3031634	4323932
2037	740	2242197	1279192	1550378	1031614	3002625	174204162	350.9	3083988	4271578
2038	740	2280918	1263704	1577152	1031614	2999083	177203245	351.7	3136266	4219300
2039	740	2319583	1248238	1603887	1031614	2995547	180198792	352.6	3188470	4167096
2040	740	2358192	1232794	1630583	1031614	2992016	183190808	353.4	3240598	4114968
2041	740	2396746	1217372	1657242	1031614	2988490	186179298	354.2	3292652	4062914
2042	740	2435246	1201972	1683862	1031614	2984969	189164268	355.0	3344632	4010934
2043	740	2473690	1186595	1710445	1031614	2981453	192145721	355.8	3396539	3959027
2044	740	2512080	1171239	1736990	1031614	2977942	195123663	356.6	3448372	3907194
2045	740	2550416	1155904	1763497	1031614	2974436	198098100	357.4	3500132	3855434
2046	740	2588698	1140592	1789967	1031614	2970935	201069035	358.1	3551819	3803747
2047	740	2626925	1125300	1816400	1031614	2967439	204036474	358.9	3603434	3752132
2048	740	2665100	1110031	1842796	1031614	2963948	207000422	359.6	3654977	3700589
2049	740	2703221	1094782	1869155	1031614	2960462	209960884	360.3	3706447	3649119
2050	740	2741289	1079555	1895477	1031614	2956980	212917864	361.0	3757847	3597719
2051	740	2779303	1064349	1921763	1031614	2953504	215871368	361.7	3809175	3546391
2052	740	2817266	1049164	1948012	1031614	2950032	218821399	362.4	3860432	3495134
2053	740	2855175	1034001	1974225	1031614	2946565	221767964	363.1	3911618	3443948
2054	740	2893033	1018858	2000401	1031614	2943102	224711067	363.8	3962734	3392832
2055	740	2930838	1003735	2026542	1031614	2939645	227650712	364.4	4013779	3341787
2056	740	2968591	988634	2052647	1031614	2936192	230586904	365.1	4064755	3290811
2057	740	3006293	973554	2078716	1031614	2932744	233519648	365.7	4115661	3239905
2058	740	3043943	958494	2104749	1031614	2929301	236448949	366.4	4166497	3189069
2059	740	3081541	943454	2130747	1031614	2925862	239374811	367.0	4217264	3138302
2060	740	3119089	928435	2156709	1031614	2922429	242297240	367.6	4267962	3087604
2061	740	3156585	913437	2182636	1031614	2918999	245216239	368.2	4318591	3036975
2062	740	3194030	898459	2208528	1031614	2915575	248131814	368.8	4369152	2986414
2063	740	3231425	883501	2234384	1031614	2912155	251043969	369.4	4419645	2935921
2064	740	3268769	868563	2260206	1031614	2908740	253952708	370.0	4470069	2885497
2065	740	3306063	853645	2285993	3137859	5011574	258964283	371.0	4556926	27403527
2066	740	3370303	8107059	2330412	3137859	12284809	271249092	373.3	4769731	27190722
2067	740	3527693	8044103	2439240	3137859	12270415	283519507	375.6	4982140	26978313
2068	740	3684791	7981264	2547866	3137859	12256048	295775554	377.7	5194161	26766292
2069	740	3841601	7918540	2656294	3137859	12241707	308017261	379.8	5405800	26554653
2070	740	3998129	7855929	2764526	3137859	12227391	320244652	381.8	5617063	26343390
2071	740	4154380	7793428	2872566	3137859	12213101	332457753	383.7	5827957	26132496
2072	740	4310357	7731038	2980417	3137859	12198837	344656590	385.5	6038487	25921966
2073	740	4466065	7668754	3088082	3137859	12184596	356841186	387.3	6248658	25711795
2074	740	4621508	7606577	3195564	3137859	12170380	369011567	389.0	6458475	25501978
2075	740	4776688	7544505	3302864	3137859	12156188	381167755	390.6	6667942	25292511
2076	740	4931610	7482537	3409985	3137859	12142020	393309775	392.2	6877063	25083390
2077	740	5086276	7420670	3516930	3137859	12127875	405437650	393.7	7085842	24874611
2078	740	5240689	7358905	3623700	3137859	12113753	417551403	395.2	7294283	24666170

Caland Groundwater Calculations			
	m ³ /year	m ³ /day	gpm
MAX	-1182958	-3241	-495
MIN	5552848	15213	2324
AVERAGE	2106246	5771	881

Model 2A Caland Pit Lake and Fairweather Lake/East and Southeast Arms

Year	Annual Precipitation	Runoff Pit	Runoff Land	Pit Evaporation	Gwi-Gwo	Change in Storage	Accu. Volume	Measured Water Elevation	Water Elevation	Pit Lake Surface Area	Watershed Area
	mm/year	m ³ /year		m	m ²	m ²					
1982	833	34108	5593733	19657	2106246	7714429	4480878		132.1	40961	16793962
1983	800	138756	5330326	100467	2106246	7474861	11955739		181.7	173488	16661435
1984	733	220116	4845933	124733	2106246	7047561	19003300		205.1	300417	16534506
1985	945	421629	6191582	186463	2106246	8532994	27536293		223.8	446405	16388518
1986	664	344226	4335685	279972		4399940	31936233	231.3	231.3	518178	16316745
1987	699	362103	4560857	285205		4637754	36573987		238.2	591424	16243499
1988	764	451778	4963248	352429	657618.2736	5720215	42294202	238.3	245.5	678623	16156300
1989	643	436544	4157203	347048	1832437	6079136	48373338	244.4	252.3	767829	16067094
1990	654	502426	4205379	392668	4134976	8450113	56823452	252.1	260.4	886534	15948389
1991	830	735570	5293046	453373	-1182958	4392286	61215738	255.7	264.2	946042	15888881
1992	872	824613	5539789	483806		5880596	67096333		268.8	1023582	15811341
1993	711	727496	4495071	523460	3651379.35	8350487	75446820	264.9	274.8	1129861	15705062
1994	765	864175	4804814	577811		5011178	80537998		278.0	1192641	15642282
1995	795	948150	4974246	609917		5312479	85850477		281.3	1256651	15578272
1996	1010	1269469	6294868	642652	5552847.683	12745533	98325011	280.1	288.1	1401479	15433444
1997	578	809775	3566978	716716		3660036	101985046		290.0	1442631	15392292
1998	676	974497	4158997	737762		4395733	106380779		292.1	1491311	15343612
1999	813	1213032	4992198	762656	3499152.796	8941726	115322506	288.9	296.2	1587973	15246950
2000	775	1230838	4727164	812089	-436292	4709621	120032127	291.4	298.2	1637688	15197235
2001	941	1541065	5720239	837514	2176092	8599882	128632009	295.6	301.7	1726486	15108437
2002	732	1263442	4422542	882925	4244185	9047244	137679253	299.9	305.1	1817321	15017602
2003	842	1530730	5059730	929378	-960738	4700344	142379597	302.0	306.8	1863536	14971387
2006	740	1492810	4383320	1032211	2106246	6950164	165561986		314.4	2082629	14752294
2007	740	1540312	4364319	1065056	2106246	6945820	172507806	310.9	316.5	2145660	14689263
2008	740	1586930	4345672	1097290	2106246	6941557	179449363	313.6	318.5	2207555	14627368
2009	740	1632707	4327361	1128943	2106246	6937370	186386733	316.1	320.4	2268369	14566554
2010	740	1677686	4309369	1160044	2106246	6933257	193319990	317.9	322.3	2328152	14506771
2011	740	1721901	4291683	1190617	2106246	6929213	200249203	318.9	324.1	2386952	14447971
2012	740	1765390	4274288	1220687	2106246	6925236	207174438		325.8	2444811	14390112
2013	740	1808182	4257171	1250276	2106246	6921322	214095760		327.4	2501769	14333154
2014	740	1850308	4240320	1279405	2106246	6917469	221013230		329.0	2557864	142047023
2015	740	1891796	6522391	1308092	2106246	6912341	230225571		331.1	2631334	141973553
2016	740	1946135	6500656	1345664	2106246	9207372	239432943		333.1	2703423	141901464
2017	740	1999451	6479329	1382530	2106246	9202496	248635439		335.0	2774197	141830690
2018	740	2051796	6458391	1418724	2106246	9197709	257833147		336.8	2843721	141761166
2019	740	2103216	6437823	1454279	2106246	9193006	267026153		338.6	2912054	141692833
2020	740	2153755	6417608	1489224	2106246	9188384	276214537		340.3	2979249	141625638
2021	740	2203452	6397729	1523588	2106246	9183839	285398376		341.9	3045356	141559531
2022	740	2252345	6378172	1557395	2106246	9179367	294577744		343.5	3110421	141494466
2023	740	2300467	6358923	1590669	2106246	9174966	303752710		345.1	3174488	141403999
2024	740	2347852	6339969	1623433	2106246	9170633	312923343		346.6	3237598	141367289
2025	740	2394527	6321299	1655708	2106246	9166364	322089707		348.1	3299787	141305100
2026	740	2440523	6302901	1687511	2106246	9162158	331251865		349.5	3361092	141243795
2027	740	2485863	6284764	1718862	2106246	9158011	340409876		350.8	3421544	141183343
2028	740	2530574	6266880	1749778	2106246	9153922	349563798		352.2	3481176	141123711
2029	740	2574678	6249239	1780273	2106246	9149889	358713686		353.5	3540016	141064871
2030	740	2618196	6231831	1810364	2106246	9145909	367859595		354.8	3598093	141006794
2031	740	2661149	6214650	1840065	2106246	9141980	377001575		356.0	3655431	140949456
2032	740	2703557	6197687	1869387	2106246	9138102	386139677		357.2	37112056	140892831
2033	740	2745436	6180935	1898345	2106246	9134272	395273949		358.4	3767990	140836897
2034	740	2786805	6164388	1926950	2106246	9130488	404404437		359.5	3823256	140781631
2035	740	2827680	6148038	1955213	2106246	9126750	413531188		360.7	3877875	140727012
2036	740	2868076	6131879	1983145	2106246	9123056	422654243		361.8	3931866	140673021
2037	740	2908008	6115907	2010756	2106246	9119404	431773647		362.9	3985248	140619639
2038	740	2947489	6100114	2038056	2106246	9115793	440889440		363.9	4038039	140566848
2039	740	2986534	6084496	2065503	2106246	9112222	450001663		364.9	4090256	140514631
2040	740	3025154	6069048	2091757	2106246	9108690	459110353		366.0	4141916	140462971
2041	740	3063361	6053765	2118176	2106246	9105196	468215549		366.9	4193033	140411854
2042	740	3101167	6038643	2144317	2106246	9101739	477317288		367.9	4243623	140361264
2043	740	3138583	6023676	2170189	2106246	9098317	486415604		368.9	4293699	140311188
2044	740	3175620	6008862	2195798	2106246	9094929	495510534		369.8	4343276	140261611
2045	740	3212287	5994195	2221151	2106246	9091576	504602110		370.7	4392366	140212521
2046	740	3248594	5979672	2246256	2106246	9088256	513690366		371.6	4440981	140163906
2047	740	3284550	5965290	2271118	2106246	9084967	522775333		372.5	4489134	140115753
2048	740	3320163	5951044	2295743	2106246	9081710	531857043		373.4	4536835	140068052
2049	740	3355443	5936932	2320138	2106246	9078484	540935527		374.2	4584097	140020790
2050	740	3390398	5922951	2344307	2106246	9075287	550010814		375.1	4630928	139973959
2051	740	3425055	5909096	2368257	2106246	9072119	559082933		375.9	4677340	139927547
2052	740	3459361	5895365	2391992	2106246	9068980	568151913		376.7	4723342	139881545
2053	740	3493384	5881756	2415517	2106246	9065868	577217782		377.5	4768944	139835943
2054	740	3527111	5868265	2438838	2106246	9062784	586280566		378.3	4814153	139790734
2055	740	3560548	5854891	2461958	2106246	9059726	595340292		379.1	4858980	139745907
2056	740	3593702	5841629	2484883	2106246	9056694	604396985		379.8	4903433	139701454
2057	740	3626579	5828478	2507616	2106246	9053687	613450673		380.6	4947519	139657368
2058	740	3659185	5815436	2530161	2106246	9050705	622501378		381.3	4991246	139613641
2059	740	3691525	5802500	2552523	2106246	9047747	631549125		382.1	5034622	139570265
2060	740	3723606	5789667	2574706	2106246	9044813	640593939		382.8	5077654	139527233
2061	740	3755433	5776937	2596712	2106246	9041903	649635841		383.5	5120349	139484538
2062	740	3787010	5764306	2618546	2106246	9039015	658674856		384.2	5162714	139442173
2063	740	3818343	5751772	2640212	2106246	9036149	667711005		384.9	5204755	139400132
2064	740	3849437	5739335	2661712	2106246	9033306	676744311		385.6	5246479	139358408

Hogarth Groundwater Calculations			
Function	m3/year	m3/day	gpm
MAX	2263000	6200	947
MIN	-1788500	-4900	-749
AVERAGE	322295	883	135

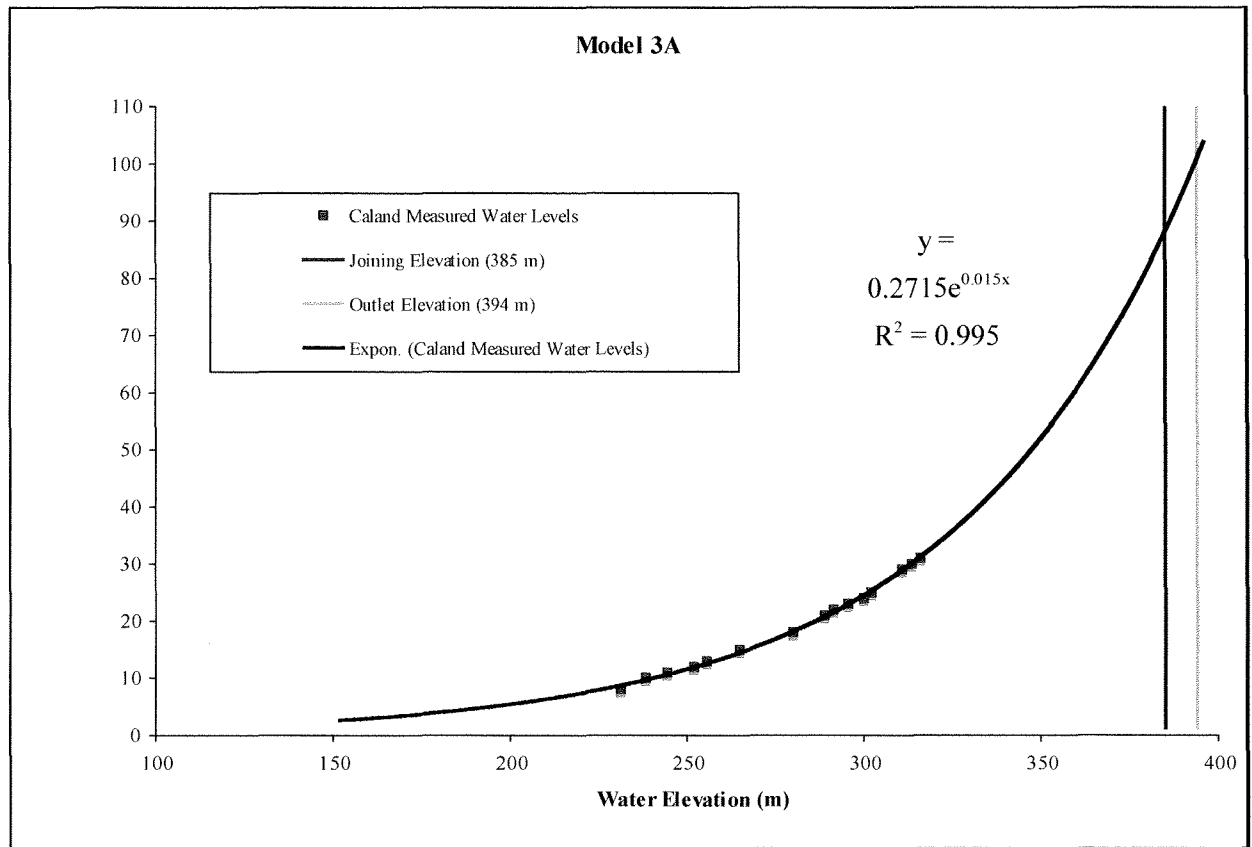
Model 2B - Hogarth Pit Lake/Middle Arm											
Year	Annual Precipitation	Runoff Pit	Runoff Land	Pit Evaporation	Gwi - Gwo	Change in Storage	Accu. Volume	Measured Water Elevation	Water Elevation	Pit Lake Surface Area	Watershed Area
	mm/year	m ³ /year	m	m	m ²	m ²					
1979	714	43631	2084474	29138		2098967	3249081	148.7	148.7	61074	7294492
1980	697	42550	2032829	33157		2042222	5291303		173.5	98793	7256773
1981	592	58436	1716953	50898		1724490	7015793		187.8	130429	7225137
1982	833	108608	2406549	62593		2452564	9468357		203.0	175222	7180344
1983	800	140143	2297136	101471		2335807	11804164		214.2	217717	7137849
1984	733	159521	2091961	90396		2161086	13965250		222.8	256917	7098649
1985	945	242658	2681869	107314		2817214	16782464		232.1	307883	7047683
1986	664	204526	1872710	166349		1910888	18693352	232.6	237.6	342376	7013190
1987	699	239252	1960327	188444		2011135	20704487		242.7	378621	6976945
1988	764	289222	2131826	225620		2195427	22899914	242.6	247.9	418127	6937439
1989	643	268972	1785084	213830	378767	2218992	25118907	247.8	252.6	457997	6897569
1990	654	299689	1805360	234220	2320010	4190839	29309746	256.3	260.4	533155	6822411
1991	830	442367	2264262	272656	-1776710	657263	29967009	257.5	261.5	544927	6810639
1992	872	474983	2374585	278676		2570893	32537902		265.7	590936	6764630
1993	711	419999	1923145	302204		2040939	34578841	267.9	268.8	627421	6728145
1994	765	479883	2058412	320863		2217432	36796273		271.9	667023	6688543
1995	795	530284	2126957	341116		2316124	39112397		275.0	708350	6647216
1996	1010	715575	2686007	362250		3039332	42151729	281.6	278.8	762525	6593041
1997	578	440587	1523784	389955		1574415	43726145		280.7	790564	6565002
1998	676	534026	1773863	404295		1903595	45629740		282.9	824446	6531120
1999	813	670604	2124965	412622		2373948	48003688	289.5	285.4	866669	6488897
2000	775	671755	2011818	443215	-325867	1914491	49918179	291.4	287.4	900697	6454869
2001	941	847556	2429613	460617	1207698	4024250	53942429	295.0	291.4	972160	6383406
2002	732	711427	1868551	497163	1516054	3598869	57541297	298.1	294.6	1036000	6319566
2003	842	872623	2129188	529811	172406	2644406	60185704	300.2	296.9	1082870	6272696
2004	868	940148	2178382	553780	625289	3190039	63375743		299.5	1139369	6216197
2005	905	1031129	2250263	582674	625289	3324008	66699751		302.1	1198195	6157371
2006	740	886185	1821597	612757	625289	2720314	69420065		304.2	1246304	6109262
2007	740	921767	1807364	637360	625289	2717060	72137126	306.9	306.1	1294327	6061239
2008	740	957284	1793157	661919	625289	2713812	74850937	309.3	308.0	1342265	6013301
2009	740	992739	1778975	686434	625289	2710569	77561507	311.2	309.8	1390119	5965447
2010	740	1028132	1764818	710907	625289	2707332	80268839	312.8	311.5	1437890	5917676
2011	740	1063464	1750685	735337	625289	2704101	82972940	313.7	313.2	1485580	5869986
2012	740	1098735	1736577	759726	625289	2700875	85673816		314.8	1533190	5822376
2013	740	1133947	1722492	784073	625289	2697655	88371471		316.4	1580719	5774847
2014	740	1169100	1708431	808380	625289	2694440	91065911		317.9	1628171	5727395
2015	740	1204195	1694393	832646	625289	2691231	93757142		319.4	1675544	5680022
2016	740	1239232	1680378	856873	625289	2688026	96445168		320.8	1722840	5632726
2017	740	1274213	1666386	881060	625289	2684827	99129995		322.2	1770060	5585506
2018	740	1309136	1652416	905209	625289	2681633	101811628		323.6	1817204	5538362
2019	740	1344004	1638469	929318	625289	2678444	104490073		324.9	1864274	5491292
2020	740	1378817	1624544	953390	625289	2675261	107165333		326.2	1911269	5444297
2021	740	1413574	1610641	977423	625289	2672082	109837415		327.4	1958190	5397376
2022	740	1448277	1596760	1001418	625289	2668908	112506323		328.7	2005038	5350528
2023	740	1482926	1582900	1025377	625289	2665739	115172063		329.9	2051814	5303752
2024	740	1517522	1569062	1049298	625289	2662575	117834638		331.0	2098518	5257048
2025	740	1552064	1555245	1073182	625289	2659416	120494054		332.1	2145150	5210416
2026	740	1586553	1541449	1097030	625289	2656262	123150317		333.3	2191712	5163854
2027	740	1620990	1527675	1120841	625289	2653113	125803429		334.3	2238203	5117363
2028	740	1655375	1513921	1144617	625289	2649968	128453397		335.4	2284624	5070942
2029	740	1689708	1500188	1168357	625289	2646828	131100225		336.4	2330975	5024591
2030	740	1723989	1486475	1192061	625289	2643693	133743918		337.4	2377257	4978309
2031	740	1758220	1472783	1215729	625289	2640562	136384481		338.4	2423471	4932095
2032	740	1792399	1459111	1239363	625289	2637437	139021917		339.4	2469616	4885950
2033	740	1826528	1445459	1262962	625289	2634315	141656233		340.4	2515693	4839873
2034	740	1860607	1431828	1286526	625289	2631199	144287431		341.3	2561703	4793863
2035	740	1894636	1418216	1310055	625289	2628086	146915518		342.2	2607646	4747920
2036	740	1928615	1404625	1333550	625289	2624979	149540497		343.1	2653522	4702044
2037	740	1962545	1391053	1357011	625289	2621876	152162372		344.0	2699331	4656235
2038	740	1996425	1377501	1380438	625289	2618777	154781150		344.9	2745074	4610492
2039	740	2030257	1363968	1403831	625289	2615683	157396833		345.7	2790572	4564814
2040	740	2064040	1350455	1427190	625289	2612594	160009427		346.5	2836363	4519203
2041	740	2097774	1336961	1450516	625289	2609508	162618935		347.4	2881910	4473656
2042	740	2131461	1323486	1473809	625289	2606428	165225363		348.2	2927932	4428174
2043	740	2165099	1310031	1497068	625289	2603351	167828714		349.0	2972809	4382757
2044	740	2198690	1296595	1520295	625289	2600279	170428993		349.7	3018162	4337404
2045	740	2232323	1283178	1543488	625289	2597212	173026205		350.5	3063451	4292115
2046	740	2265728	1269779	1566649	625289	2594148	175620353		351.3	3108676	4246890
2047	740	2299177	1256400	1589777	625289	2591089	178211443		352.0	3153838	4201728
2048	740	2332578	1243039	1612873	625289	2588035	180799477		352.7	3198936	4156630
2049	740	2365933	1229697	1635936	625289	2584984	183384461		353.5	3243972	4111594
2050	740	2399241	1216374	1658967	625289	2581938	185966399		354.2	3288944	4066622
2051	740	2432503	1203069	1681966	625289	2578896	188545295		354.9	3333855	4021711
2052	740	2465719	1189783	1704933	625289	2575858	191121153		355.6	3378703	3976863
2053	740	2498889	1176515	1727869	625289	2572825	193693978		356.2	3423489	3932077
2054	740	2532012	1163266	1750772	625289	2569795	196263773		356.9	3468213	3887353

2055	740	2565090	1150035	1773644	625289	2566770	198830543	357.6	3512876	3842690
2056	740	2598123	1136821	1796485	625289	2563749	201394292	358.2	3557477	3798089
2057	740	2631110	1123627	1819294	625289	2560732	203955025	358.9	3602017	3753549
2058	740	2664052	1110450	1842072	625289	2557720	206512744	359.5	3646497	3709069
2059	740	2696949	1097291	1864818	625289	2554711	209067455	360.1	3690915	3664651
2060	740	2729801	1084150	1887534	625289	2551707	211619162	360.7	3735274	3620292
2061	740	2762608	1071027	1910219	625289	2548706	214167868	361.3	3779571	3575995
2062	740	2795371	1057922	1932873	625289	2545710	216713578	361.9	3823809	3531757
2063	740	2828089	1044835	1955496	625289	2542718	219256295	362.5	3867987	3487579
2064	740	2860763	1031765	1978089	625289	2539729	221796025	363.1	3912105	3443461
2065	740	2893393	1018713	2000651	625289	2536745	224332770	363.7	3956164	3399402
2066	740	2925979	1005679	2023182	625289	2533765	226866535	364.3	4000163	3355403
2067	740	2958521	992662	2045684	625289	2530789	229397324	364.8	4044104	3311462
2068	740	2991019	979663	2068155	625289	2527817	231925141	365.4	4087985	3267581
2069	740	3023474	966681	2090595	625289	2524849	234449990	365.9	4131807	3223759
2070	740	3055885	953717	2113006	625289	2521885	236971875	366.5	4175571	3179995
2071	740	3088252	940770	2135387	2026390	3920025	240891900	367.3	4243584	27716869
2072	740	3138554	8199759	2170169	2026390	11194534	252086434	369.6	4437717	27522736
2073	740	3282136	8142326	2269449	2026390	11181403	263267837	371.8	4631492	27328961
2074	740	3425452	8085000	2368545	2026390	11168296	274436133	373.9	4824915	27135538
2075	740	3568507	8027778	2467461	2026390	11155213	285591346	376.0	5017991	26942462
2076	740	3711306	7970658	2566201	2026390	11142153	296733499	377.9	5210727	26749726
2077	740	3853853	7913639	2664766	2026390	11129117	307862616	379.8	5403127	26557326
2078	740	3996153	7856719	2763159	2026390	11116103	318978719	381.6	5595196	26365257
2079	740	4138207	7799898	2861383	2026390	11103111	330081830	383.3	5786940	26173513
2080	740	4280020	7743172	2959441	2026390	11090142	341171971	385.0	5978361	25982092
2081	740	4421596	7686542	3057334	2026390	11077194	352249165	386.6	6169464	25790989
2082	740	4562935	7630006	3155064	2026390	11064268	363313433	388.2	6360253	25600200
2083	740	4704043	7573563	3252633	2026390	11051363	374364796	389.7	6550731	25409722
2084	740	4844920	7517212	3350044	2026390	11038479	385403274	391.2	6740901	25219552
2085	740	4985570	7460952	3447297	2026390	11025616	396428890	392.6	6930767	25029686
2086	740	5125995	7404782	3544394	2026390	11012773	407441663	394.0	7120332	24840121
2087	740	5266197	7348702	3641338	2026390	10999951	418441614	395.3	7309598	24650855

Caland Groundwater Calculations			
Function	m ³ /car	m ³ /day	gpm
MAX	-1182958	-3241	-495
MIN	5552848	15213	2324
AVERAGE	2106246	5771	881

Model 2B Caland Pit Lake and Fairweather Lake/East and Southeast Arms

Year	Annual Precipitation mm ³ /car	Runoff Pit m ³ /car	Runoff Land m ³ /car	Pit Evaporation m ³ /car	Gwi-Gwo m ³ /car	Change in Storage m ³ /car	Accu. Volume m ³ /car	Measured Water Elevation	Water Elevation m	Pit Lake Surface Area m ²	Watershed Area m ²
1982	833	63735	5581882	36732	1401100	7009986	6598563		151.7	76541	16758382
1983	800	159335	5322095	115368	1401100	6767162	13365726		187.3	199219	16635704
1984	733	229208	4842296	129885	1401100	6342719	19708445		207.0	312826	16522097
1985	945	421629	6191582	186463	1401100	7827849	27536293		223.8	446405	16388518
1986	664	344226	4335685	279972		4399940	31936233	231.3	231.3	518178	16316745
1987	699	362103	4560857	285205		4637754	36573987		238.2	591424	16243499
1988	764	451778	4963248	352429		5062597	41636584	238.3	244.7	668765	16166158
1989	643	430203	4159740	342006	1832437	6080373	47716957	244.4	251.6	758358	16076565
1990	654	496229	4207858	387824	4134976	8451238	56168195	252.1	259.8	877533	15957390
1991	830	728102	5296034	448770	-1182958	4392408	60560603	255.7	263.7	937255	15897668
1992	872	816954	5542852	479312		5880494	66441097		268.3	1015058	15819865
1993	711	721437	4497495	519100		4699832	71140929	264.9	271.8	1175594	15759329
1994	765	822669	4821416	550059		5094027	76234955		275.3	1039675	15695248
1995	795	906042	4991089	582830		5314301	81549256		278.7	1204941	15629982
1996	1010	1217231	6315763	616207		6916788	88466044	280.1	282.8	1287634	15547289
1997	578	743995	3593289	658496		3678788	92144832		284.8	1330645	15504278
1998	676	898850	4189256	680492		4407615	96552447		287.2	1381339	15453584
1999	813	1123581	5027978	706417		5445142	101997589	288.9	290.0	1442771	15392152
2000	775	1118292	4772183	737833	-436292	4716350	106713939	291.4	292.3	1494968	15339955
2001	941	1406765	5773959	764527	2176092	8592289	115306228	295.6	296.2	1587800	15247123
2002	732	1161952	4463138	812001	4244185	9057274	124363502	299.9	300.0	1682723	15152200
2003	842	1417357	5105079	860544	-960738	4701154	129064656	302.0	301.9	1730889	15104034
2004	868	1502757	5245329	885176	1401100	7264010	136328667		304.6	1803921	15031002
2005	905	1632549	5441223	922525	1401100	7552346	143881013		307.4	1878163	14956760
2006	740	1389089	4424808	960492	1401100	6254505	150135518		309.5	1938417	14896506
2007	740	1433653	4406982	991306	1401100	6250429	156385948	310.9	311.6	1997578	14837345
2008	740	1477409	4389480	1021562	1401100	6246428	162632376	313.6	313.5	2055701	14779222
2009	740	1520396	4372285	1051285	1401100	6242496	168874872	316.1	315.4	2112832	14722091
2010	740	1562651	4355383	1080502	1401100	6238632	175113504	317.9	317.3	2169019	14665904
2011	740	1604207	4338761	1109236	1401100	6234832	181348336	318.9	319.0	2224303	14610620
2012	740	1645095	4322406	1137509	1401100	6231092	187579428		320.7	2278723	14562600
2013	740	1685343	4306306	1165339	1401100	6227411	193806839		322.4	2332314	14502609
2014	740	1724979	4290452	1192745	1401100	6223786	200030625		324.0	2385111	144219776
2015	740	1764028	4273499	1219746	1401100	8518881	208549506		326.1	2456194	14348693
2016	740	1816601	4252469	1256098	1401100	8514073	217063580		328.1	2525935	142708952
2017	740	1868182	4231837	1291763	1401100	8509356	225572935		330.1	2594401	142010486
2018	740	1918819	4211582	1326777	1401100	8504725	234077660		331.9	2661653	141343234
2019	740	1968559	4191686	1361170	1401100	8500176	242577836		333.7	2727750	140717137
2020	740	2017444	4172132	1394971	1401100	8495705	251073541		335.5	2792742	140182145
2021	740	2065512	4152905	1428208	1401100	8491309	259564850		337.2	2856680	140748207
2022	740	2112801	4133990	1460906	1401100	8486984	268051835		338.8	2919609	140365278
2023	740	2159343	4115373	1493088	1401100	8482728	276534562		340.4	2981570	140263317
2024	740	2205169	4097042	1524775	1401100	8478537	285013099		341.9	3042603	140162284
2025	740	2250309	4078986	1555987	1401100	8474408	293487508		343.4	3102745	140102142
2026	740	2294790	4061194	1586744	1401100	8470340	301957848		344.8	3162029	140042858
2027	740	2338637	4043655	1617062	1401100	8466330	310424179		346.2	3220489	140034398
2028	740	2381874	4026360	1646958	1401100	8462376	318886555		347.5	3278155	140026732
2029	740	2424523	4009301	1676448	1401100	8458476	327345031		348.9	3335054	140019833
2030	740	2466606	3992468	1705546	1401100	8454627	335799658		350.2	3391213	140013674
2031	740	2508141	3975853	1734266	1401100	8450828	344250486		351.4	3446658	140008229
2032	740	2549149	3959450	1762621	1401100	8447078	352697564		352.6	3501413	140003474
2033	740	2589645	3943252	1790623	1401100	8443375	361140939		353.8	3555500	140009387
2034	740	2629648	3927251	1818283	1401100	8439716	369580655		355.0	3608941	140005946
2035	740	2669173	3911441	1845612	1401100	8436101	378016756		356.1	3661755	140003132
2036	740	2708234	3895816	1872622	1401100	8432529	386449285		357.3	3713962	140000925
2037	740	2746847	3880371	1899320	1401100	8428998	394878283		358.3	3765581	140009306
2038	740	2785024	3865100	1925718	1401100	8425506	403303789		359.4	3816628	1400078259
2039	740	2822778	3849999	1951823	1401100	8422053	411725843		360.5	3867120	1400073767
2040	740	2860122	3835061	1977645	1401100	8418638	420144481		361.5	3917072	1400067815
2041	740	2897067	3820283	2003191	1401100	8415259	428559740		362.5	3966501	1400063886
2042	740	2933624	3805660	2028468	1401100	8411916	436971656		363.5	4015419	1400059468
2043	740	2969804	3791188	2053485	1401100	8408607	445380263		364.4	4063842	14000541045
2044	740	3005617	3776863	2078249	1401100	8405332	453785595		365.4	4111781	14000493106
2045	740	3041073	3762680	2102765	1401100	8402089	462187685		366.3	4159250	14000445637
2046	740	3076181	3748637	2127040	1401100	8398878	470586563		367.2	4206260	14000398627
2047	740	3110950	3734730	2151081	1401100	8395699	478982262		368.1	4252823	14000352064
2048	740	3145388	3720955	2174894	1401100	8392549	487374811		369.0	4298950	14000305937
2049	740	3179504	3707308	2198483	1401100	8389429	495764240		369.8	4344652	14000260235
2050	740	3213305	3693788	2221855	1401100	8386338	504150578		370.7	4389938	14000214949
2051	740	3246798	3680390	2245015	1401100	8383275	512533853		371.5	4434819	14000170068
2052	740	3279992	3667113	2267967	1401100	8380239	520914092		372.3	4479304	14000125583
2053	740	3312894	3653952	2290716	1401100	8377230	529291322		373.1	4523240	14000081485
2054	740	3345508	3640906	2313268	1401100	8374247	537665569		373.9	4567122	14000037765
2055	740	3377843	3627972	2335626	1401100	8371290	546036859		374.7	4610471	14000094116
2056	740	3409905	3615148	2357795	1401100	8368358	554405217		375.5	4653459	14000051428
2057	740	3441698	3602430	2379779	1401100	8365450	562770667		376.2	4696093	14000008794
2058	740	3473230	3589818	2401582	1401100	8362566	571133233		377.0	4738380	1400006507
2059	740	3504506	3577307	2423208	1401100	8359706	579492939		377.7	4780328	14000021459
2060	740	3535531	3564897	2444660	1401100	8356869	587849808		378.4	4821944	140000782943
2061	740	3566310	3552586	2465942	1401100	8354054	596203862		379.2	4863234	14000034653
2062	740	3596848	3540371	2487058	1401100	8351261	604555123		379.9	4904206	14000090681
2063	740	3627151	3528250	2508011	1401100	8348490	612903612		380.5	4944865	14000046022
2064	740	3657222	3516221	2528804	1401100	8345739	621249352		381.2	4985217	140000019670
2065	740	3687067	3504283	2549440	1401100	8343010	629592362		381.9	5025269	140000579618
2066	740	3716689	3492434	2569923	1401100	8340301	637932663		382.6	5065026	140000139861
2067	740	3746093	3480672	2590254	1401100	8337612	646270275		383.2	5104494	14000069393
2068	740	3775284	3468996	2610438	1401100	8334942	654605217				



Model 3A - Caland Pit Lake/East Arm					
Year	Water Elevation (m)	Year	Water Elevation (m)	Year	Water Elevation (m)
1979	86.9	2027	346.4	2075	391.9
1980	133.1	2028	347.7	2076	392.6
1981	160.2	2029	349.0	2077	393.3
1982	179.3	2030	350.3	2078	393.9
1983	194.2	2031	351.6	2079	394.6
1984	206.4	2032	352.9		
1985	216.6	2033	354.1		
1986	225.5	2034	355.3		
1987	233.4	2035	356.5		
1988	240.4	2036	357.6		
1989	246.8	2037	358.8		
1990	252.6	2038	359.9		
1991	257.9	2039	361.0		
1992	262.9	2040	362.1		
1993	267.5	2041	363.1		
1994	271.8	2042	364.2		
1995	275.8	2043	365.2		
1996	279.6	2044	366.2		
1997	283.2	2045	367.2		
1998	286.6	2046	368.2		
1999	289.9	2047	369.2		
2000	293.0	2048	370.2		
2001	296.0	2049	371.1		
2002	298.8	2050	372.0		
2003	301.5	2051	373.0		
2004	304.1	2052	373.9		
2005	306.6	2053	374.8		
2006	309.1	2054	375.6		
2007	311.4	2055	376.5		
2008	313.7	2056	377.4		
2009	315.9	2057	378.2		
2010	318.0	2058	379.1		
2011	320.0	2059	379.9		
2012	322.0	2060	380.7		
2013	323.9	2061	381.5		
2014	325.8	2062	382.3		
2015	327.6	2063	383.1		
2016	329.4	2064	383.9		
2017	331.2	2065	384.6		
2018	332.8	2066	385.4		
2019	334.5	2067	386.2		
2020	336.1	2068	386.9		
2021	337.7	2069	387.6		
2022	339.2	2070	388.4		
2023	340.7	2071	389.1		
2024	342.2	2072	389.8		
2025	343.6	2073	390.5		
2026	345.0	2074	391.2		

Model 3B - Hogarth Pit Lake/Middle Arm							
Year	Water Elevation (m)	Year	Water Elevation (m)	Year	Water Elevation (m)	Year	Water Elevation (m)
1979	136.1	2027	330.7	2075	364.9	2123	385.0
1980	170.8	2028	331.7	2076	365.4	2124	385.3
1981	191.1	2029	332.7	2077	365.9	2125	385.7
1982	205.4	2030	333.7	2078	366.4	2126	386.0
1983	216.6	2031	334.6	2079	366.9	2127	386.3
1984	225.7	2032	335.6	2080	367.4	2128	386.7
1985	233.4	2033	336.5	2081	367.9	2129	387.0
1986	240.1	2034	337.4	2082	368.4	2130	387.3
1987	246.0	2035	338.3	2083	368.8	2131	387.7
1988	251.3	2036	339.2	2084	369.3	2132	388.0
1989	256.0	2037	340.0	2085	369.8	2133	388.3
1990	260.4	2038	340.9	2086	370.2	2134	388.6
1991	264.4	2039	341.7	2087	370.7	2135	388.9
1992	268.1	2040	342.5	2088	371.2	2136	389.3
1993	271.5	2041	343.3	2089	371.6	2137	389.6
1994	274.8	2042	344.1	2090	372.1	2138	389.9
1995	277.8	2043	344.9	2091	372.5	2139	390.2
1996	280.7	2044	345.6	2092	372.9	2140	390.5
1997	283.4	2045	346.4	2093	373.4	2141	390.8
1998	285.9	2046	347.1	2094	373.8	2142	391.1
1999	288.4	2047	347.8	2095	374.2	2143	391.4
2000	290.7	2048	348.6	2096	374.7	2144	391.7
2001	292.9	2049	349.3	2097	375.1	2145	392.0
2002	295.0	2050	350.0	2098	375.5	2146	392.3
2003	297.1	2051	350.7	2099	375.9	2147	392.6
2004	299.0	2052	351.3	2100	376.3	2148	392.9
2005	300.9	2053	352.0	2101	376.7	2149	393.2
2006	302.7	2054	352.7	2102	377.1	2150	393.5
2007	304.5	2055	353.3	2103	377.5	2151	393.8
2008	306.2	2056	354.0	2104	377.9	2152	394.1
2009	307.8	2057	354.6	2105	378.3		
2010	309.4	2058	355.2	2106	378.7		
2011	311.0	2059	355.9	2107	379.1		
2012	312.5	2060	356.5	2108	379.5		
2013	313.9	2061	357.1	2109	379.9		
2014	315.3	2062	357.7	2110	380.3		
2015	316.7	2063	358.3	2111	380.7		
2016	318.0	2064	358.9	2112	381.0		
2017	319.3	2065	359.4	2113	381.4		
2018	320.6	2066	360.0	2114	381.8		
2019	321.8	2067	360.6	2115	382.1		
2020	323.0	2068	361.1	2116	382.5		
2021	324.2	2069	361.7	2117	382.9		
2022	325.3	2070	362.2	2118	383.2		
2023	326.5	2071	362.8	2119	383.6		
2024	327.6	2072	363.3	2120	383.9		
2025	328.6	2073	363.8	2121	384.3		
2026	329.7	2074	364.4	2122	384.6		

APPENDIX V
Sensitivity Analysis: Water Balance & Rebound Model Results

Sensitivity Analysis - Summary of Evaporation Results			
Model 2B Evaporation Rate = 511.4 mm/year			
Evaporation Rate Variations		(mm/year)	
plus 5%	536.97	minus 5%	485.83
plus 10%	562.54	minus 10%	460.26
plus 20%	613.68	minus 20%	409.12
plus 30%	664.82	minus 30%	357.98
plus 40%	715.96	minus 40%	306.84
Rebound Rates		Join	Outflow
Model2b Rebound Rate		2070	2087
minus 40%	2065	2078	9
minus 30%	2066	2080	7
minus 20%	2067	2082	5
minus 10%	2069	2085	2
minus 5%	2070	2086	1
plus 5%	2071	2088	-1
plus 10%	2072	2089	-2
plus 20%	2073	2091	-4
plus 30%	2075	2094	-7
plus 40%	2077	2097	-10

Sensitivity Analysis - Summary of Precipitation Results			
Model 2B Precipitation Rate 739.6 mm/year			
Precipitation Rate Variations		(mm/year)	
plus 5%	776.58	minus 5%	702.62
plus 10%	813.56	minus 10%	665.64
plus 20%	887.52	minus 20%	591.68
plus 30%	961.48	minus 30%	517.72
plus 40%	1035.44		
Rebound Rates		Join	Outflow
Model2b Rebound Rate		2070	2087
minus 30%	2099	2186	99
minus 20%	2087	2109	22
minus 10%	2078	2096	9
minus 5%	2074	2091	4
plus 5%	2067	2083	-4
plus 10%	2064	2079	-8
plus 20%	2059	2072	-15
plus 30%	2055	2067	-20
plus 40%	2052	2063	-24

Sensitivity Analysis - Summary of Net Groundwater Influx Results			
	Caland (m³/year)	Hogarth (m³/year)	
Model 2B Net Groundwater Influx Rates	1401100	625289	
Net Groundwater Influx Rate Variations			
minus 90%	140110	62529	
minus 70%	420330	187587	
minus 50%	700550	312645	
minus 30%	980770	437703	
minus 20%	1120880	500232	
minus 10%	1260990	562760	
minus 5%	1331045	594025	
plus 5%	2662091	1188050	
plus 10%	2381871	1062992	
plus 20%	2101651	937934	
plus 30%	1821430	812876	
plus 50%	1681320	750347	
plus 70%	1541210	687818	
Rebound Rates	Join	Outflow	Difference Relative to Model 2B
Model2b Rebound Rate	2070	2087	
minus 90%	2082	2103	16
minus 70%	2079	2099	12
minus 50%	2075	2095	8
minus 30%	2074	2092	5
minus 20%	2072	2090	3
minus 10%	2071	2088	1
minus 5%	2071	2088	1
plus 5%	2070	2086	-1
plus 10%	2069	2085	-2
plus 20%	2068	2084	-3
plus 30%	2067	2082	-5
plus 50%	2066	2081	-6
plus 70%	2063	2077	-10

Sensitivity Analysis - Summary of Runoff Results			
Model 2B Rentention Factor = 40%			
Rebound Rates	Join	Outflow	Difference Relative to Model 2B
Model2b Rebound Rate	2070	2087	
20%	2095	2131	44
30%	2084	2103	16
35%	2077	2094	7
45%	2065	2080	-7
50%	2060	2075	-12
60%	2053	2066	-21

APPENDIX VI
Rebound Model – Pit Geometry Modeled Using Linear Interpolation

Pit Geometry Model

Hogarth & South Roberts

Caland & Fairweather Lake

Elevation (masl)	Surface Area (m ²)	Volume (m ³)	Elevation (masl)	Accu. Vol. (m ³)	Elevation (masl)	Elevation (masl)	Surface Area (m ²)	Volume (m ³)	Elevation (masl)	Accu. Vol. (m ³)	Elevation (masl)
107	11148		107		107	91	7989		91		91
108	13483	12316	108	12316	108	92	8784	8387	92	8387	92
109	15251	14367	109	26683	109	93	9578	9181	93	17567	93
110	17019	16135	110	42818	110	94	10371	9975	94	27542	94
111	18787	17903	111	60721	111	95	11165	10768	95	38310	95
112	20555	19671	112	80392	112	96	11959	11562	96	49872	96
113	22322	21439	113	101830	113	97	12753	12356	97	62229	97
114	24090	23206	114	125037	114	98	13547	13150	98	75379	98
115	25858	24974	115	150011	115	99	14341	13944	99	89323	99
116	27626	26742	116	176753	116	100	15135	14738	100	104061	100
117	29394	28510	117	205262	117	101	15929	15532	101	119593	101
118	31161	30278	118	235540	118	102	16723	16326	102	135919	102
119	32929	32045	119	267585	119	103	17517	17120	103	153039	103
120	34697	33813	120	301398	120	104	18311	17914	104	170952	104
121	36465	35581	121	336979	121	105	19105	18708	105	189660	105
122	38233	37349	122	374328	122	106	19899	19502	106	209162	106
123	40000	39117	123	413444	123	107	20438	20168	107	229330	107
124	41768	40884	124	454329	124	108	23781	22110	108	251440	108
125	43536	42652	125	496981	125	109	26311	25046	109	276486	109
126	45304	44420	126	541401	126	110	28841	27576	110	304062	110
127	47072	46188	127	587588	127	111	31371	30106	111	334168	111
128	48839	47956	128	635544	128	112	33901	32636	112	366804	112
129	50607	49723	129	685267	129	113	36430	35166	113	401969	113
130	52375	51491	130	736758	130	114	38960	37695	114	439664	114
131	54143	53259	131	790017	131	115	41490	40225	115	479890	115
132	55911	55027	132	845044	132	116	44020	42755	116	522644	116
133	57678	56795	133	901838	133	117	46550	45285	117	567929	117
134	59446	58562	134	960401	134	118	49079	47815	118	615744	118
135	61214	60330	135	1020731	135	119	51609	50344	119	666088	119
136	62982	62098	136	1082829	136	120	54139	52874	120	718962	120
137	65030	64006	137	1146834	137	121	56669	55404	121	774366	121
138	66746	65888	138	1212722	138	122	59199	57934	122	832300	122
139	68788	67767	139	1280489	139	123	61728	60464	123	892763	123
140	70830	69809	140	1350298	140	124	64258	62993	124	955756	124
141	72872	71851	141	1422149	141	125	66788	65523	125	1021280	125
142	74914	73893	142	1496042	142	126	69318	68053	126	1089332	126
143	76956	75935	143	1571978	143	127	71848	70583	127	1159915	127
144	78998	77977	144	1649955	144	128	74377	73113	128	1233028	128
145	81041	80019	145	1729974	145	129	76907	75642	129	1308670	129
146	83083	82062	146	1812036	146	130	79437	78172	130	1386842	130
147	85125	84104	147	1896140	147	131	81967	80702	131	1467544	131
148	87167	86146	148	1982285	148	132	84497	83232	132	1550776	132
149	89209	88188	149	2070473	149	133	87026	85762	133	1636537	133
150	91251	90230	150	2160703	150	134	89556	88291	134	1724828	134
151	93293	92272	151	2252975	151	135	92086	90821	135	1815650	135

152	95335	94314	152	2347289	152	136	94616	93351	136	1909000	136
153	97377	96356	153	2443646	153	137	97545	96080	137	2005081	137
154	99419	98398	154	2542044	154	138	101636	99590	138	2104671	138
155	101462	100440	155	2642484	155	139	106512	104074	139	2208745	139
156	103504	102483	156	2744967	156	140	111389	108951	140	2317696	140
157	105546	104525	157	2849492	157	141	116266	113827	141	2431523	141
158	107588	106567	158	2956058	158	142	121142	118704	142	2550227	142
159	109630	108609	159	3064667	159	143	126019	123581	143	2673808	143
160	111672	110651	160	3175318	160	144	130895	128457	144	2802265	144
161	113714	112693	161	3288011	161	145	135772	133334	145	2935599	145
162	115756	114735	162	3402746	162	146	140649	138210	146	3073809	146
163	117798	116777	163	3519524	163	147	145525	143087	147	3216896	147
164	119840	118819	164	3638343	164	148	150402	147964	148	3364859	148
165	121883	120861	165	3759204	165	149	155278	152840	149	3517699	149
166	123925	122904	166	3882108	166	150	160155	157717	150	3675416	150
167	125967	124946	167	4007054	167	151	165032	162593	151	3838009	151
168	127273	126620	168	4133673	168	152	169908	167470	152	4005479	152
169	130929	129101	169	4262774	169	153	174785	172347	153	4177826	153
170	133611	132270	170	4395044	170	154	179661	177223	154	4355049	154
171	136293	134952	171	4529996	171	155	184538	182100	155	4537149	155
172	138975	137634	172	4667631	172	156	189415	186976	156	4724125	156
173	141658	140317	173	4807947	173	157	194291	191853	157	4915978	157
174	144340	142999	174	4950946	174	158	199168	196730	158	5112707	158
175	147022	145681	175	5096627	175	159	204044	201606	159	5314313	159
176	149704	148363	176	5244990	176	160	208921	206483	160	5520796	160
177	152386	151045	177	5396035	177	161	213798	211359	161	5732155	161
178	155069	153728	178	5549763	178	162	218674	216236	162	5948391	162
179	157751	156410	179	5706172	179	163	223551	221113	163	6169504	163
180	160433	159092	180	5865264	180	164	228427	225989	164	6395493	164
181	163115	161774	181	6027038	181	165	233304	230866	165	6626359	165
182	165797	164456	182	6191495	182	166	238181	235742	166	6862101	166
183	168480	167139	183	6358633	183	167	243057	240619	167	7102720	167
184	171162	169821	184	6528454	184	168	246185	244621	168	7347341	168
185	173844	172503	185	6700957	185	169	255730	250958	169	7598298	169
186	176526	175185	186	6876142	186	170	262746	259238	170	7857537	170
187	179208	177867	187	7054009	187	171	269762	266254	171	8123790	171
188	181891	180550	188	7234559	188	172	276778	273270	172	8397060	172
189	184573	183232	189	7417790	189	173	283793	280286	173	8677346	173
190	187255	185914	190	7603704	190	174	290809	287301	174	8964647	174
191	189937	188596	191	7792300	191	175	297825	294317	175	9258964	175
192	192619	191278	192	7983579	192	176	304841	301333	176	9560297	176
193	195302	193961	193	8177539	193	177	311857	308349	177	9868646	177
194	197984	196643	194	8374182	194	178	318872	315365	178	10184010	178
195	200666	199325	195	8573507	195	179	325888	322380	179	10506390	179
196	203348	202007	196	8775514	196	180	332904	329396	180	10835787	180
197	206030	204689	197	8980203	197	181	339920	336412	181	11172198	181
198	209386	207708	198	9187911	198	182	346936	343428	182	11515626	182
199	206333	207860	199	9395771	199	183	353951	350444	183	11866070	183
200	203285	204809	200	9600580	200	184	360967	357459	184	12223529	184
201	205704	204495	201	9805075	201	185	367983	364475	185	12588004	185
202	208124	206914	202	10011989	202	186	374999	371491	186	12959495	186
203	210545	209335	203	10221323	203	187	382015	378507	187	13338002	187
204	212966	211755	204	10433079	204	188	389030	385523	188	13723524	188
205	215387	214176	205	10647255	205	189	396046	392538	189	14116062	189
206	217807	216597	206	10863852	206	190	403058	399552	190	14515614	190
207	220228	219018	207	11082869	207	191	409562	406310	191	14921924	191
208	222649	221438	208	11304308	208	192	416072	412817	192	15334741	192
209	225069	223859	209	11528167	209	193	422581	419326	193	15754068	193
210	227493	226281	210	11754447	210	194	429090	425836	194	16179903	194
211	230459	228976	211	11983423	211	195	435600	432345	195	16612248	195
212	233429	231944	212	12215368	212	196	442109	438854	196	17051102	196
213	236400	234915	213	12450282	213	197	448618	445363	197	17496466	197
214	239370	237885	214	12688167	214	198	455127	451873	198	17948338	198
215	242340	240855	215	12929022	215	199	461637	458382	199	18406720	199
216	245310	243825	216	13172847	216	200	468151	464894	200	18871614	200
217	248280	246795	217	13419642	217	201	474677	471414	201	19343028	201
218	251251	249766	218	13669408	218	202	481209	477943	202	19820971	202
219	254221	252736	219	13922143	219	203	487741	484475	203	20305446	203
220	257195	255708	220	14177851	220	204	494273	491007	204	20796453	204
221	264104	260649	221	14438500	221	205	500805	497539	205	21293991	205
222	271012	267558	222	14706059	222	206	507336	504070	206	21798062	206
223	277921	274467	223	14980525	223	207	513868	510602	207	22308664	207

224	284829	281375	224	15261901	224	208	520400	517134	208	22825798	208
225	291738	288284	225	15550184	225	209	526932	523666	209	23349464	209
226	298646	295192	226	15845376	226	210	533470	530201	210	23879666	210
227	305555	302100	227	16147476	227	211	539644	536557	211	24416223	211
228	312463	309009	228	16456485	228	212	545813	542728	212	24958951	212
229	319371	315917	229	16772402	229	213	551981	548897	213	25507848	213
230	326279	322825	230	17095227	230	214	558149	555065	214	26062913	214
231	332018	329148	231	17424375	231	215	564318	561233	215	26624147	215
232	337766	334892	232	17759267	232	216	570486	567402	216	27191548	216
233	343515	340641	233	18099908	233	217	576654	573570	217	27765118	217
234	349263	346389	234	18446297	234	218	582822	579738	218	28344856	218
235	355012	352138	235	18798435	235	219	588991	585907	219	28930763	219
236	360761	357886	236	19156321	236	220	595153	592072	220	29522835	220
237	366509	363635	237	19519956	237	221	605634	600394	221	30123229	221
238	372258	369384	238	19889339	238	222	616114	610874	222	30734103	222
239	378006	375132	239	20264471	239	223	626594	621354	223	31355457	223
240	383755	380881	240	20645352	240	224	637074	631834	224	31987291	224
241	389711	386733	241	21032085	241	225	647554	642314	225	32629604	225
242	395656	392684	242	21424769	242	226	658034	652794	226	33282398	226
243	401602	398629	243	21823398	243	227	668514	663274	227	33945672	227
244	407547	404574	244	22227972	244	228	678994	673754	228	34619426	228
245	413492	410520	245	22638492	245	229	689474	684234	229	35303659	229
246	419438	416465	246	23054957	246	230	699952	694713	230	35998372	230
247	425383	422410	247	23477367	247	231	710039	704995	231	36703368	231
248	431328	428356	248	23905723	248	232	720176	715107	232	37418475	232
249	437273	434301	249	24340023	249	233	730313	725244	233	38143719	233
250	443218	440246	250	24780269	250	234	740450	735381	234	38879100	234
251	450529	446873	251	25227143	251	235	750587	745518	235	39624618	235
252	457841	454185	252	25681327	252	236	760724	755655	236	40380273	236
253	465153	461497	253	26142824	253	237	770861	765792	237	41146065	237
254	472465	468809	254	26611633	254	238	780998	775929	238	41921994	238
255	479777	476121	255	27087754	255	239	791135	786066	239	42708060	239
256	487089	483433	256	27571186	256	240	801325	796230	240	43504290	240
257	494401	490745	257	28061931	257	241	813820	807572	241	44311862	241
258	501713	498057	258	28559988	258	242	826317	820069	242	45131931	242
259	509024	505369	259	29065356	259	243	838814	832565	243	45964496	243
260	516338	512681	260	29578037	260	244	851310	845062	244	46809558	244
261	524132	520235	261	30098272	261	245	863807	857559	245	47667116	245
262	531927	528029	262	30626301	262	246	876304	870055	246	48537172	246
263	539722	535824	263	31162125	263	247	888800	882552	247	49419724	247
264	547517	543619	264	31705744	264	248	901297	895049	248	50314773	248
265	555312	551414	265	32257158	265	249	913794	907546	249	51222318	249
266	563107	559209	266	32816367	266	250	926292	920043	250	52142361	250
267	570902	567004	267	33383372	267	251	940036	933164	251	53075525	251
268	578697	574799	268	33958171	268	252	953779	946908	252	54022433	252
269	586492	582594	269	34540765	269	253	967523	960651	253	54983084	253
270	594288	590390	270	35131154	270	254	981266	974394	254	55957478	254
271	602256	600772	271	35731926	271	255	995009	988137	255	56945615	255
272	620224	613740	272	36345666	272	256	1008752	1001881	256	57947496	256
273	633192	626708	273	36972375	273	257	1022495	1015624	257	58963120	257
274	646160	639676	274	37612051	274	258	1036239	1029367	258	59992487	258
275	659128	652644	275	38264695	275	259	1049982	1043110	259	61035597	259
276	672096	665612	276	38930306	276	260	1063724	1056853	260	62092450	260
277	685064	678580	277	39608886	277	261	1078552	1071138	261	63163588	261
278	698032	691548	278	40300434	278	262	1093378	1085965	262	64249553	262
279	711000	704516	279	41004950	279	263	1108204	1100791	263	65350344	263
280	723967	717483	280	41722433	280	264	1123031	1115618	264	66465962	264
281	740815	732391	281	42454824	281	265	1137857	1130444	265	67596406	265
282	757663	749239	282	43204063	282	266	1152684	1145271	266	68741676	266
283	774511	766087	283	43970150	283	267	1167510	1160097	267	69901773	267
284	791359	782935	284	44753085	284	268	1182337	1174923	268	71076697	268
285	808207	799783	285	45552868	285	269	1197163	1189750	269	72266447	269
286	825054	816630	286	46369498	286	270	1211989	1204576	270	73471023	270
287	841902	833478	287	47202977	287	271	1232596	1222292	271	74693315	271
288	858750	850326	288	48053303	288	272	1253204	1242900	272	75936215	272
289	875598	867174	289	48920477	289	273	1273813	1263509	273	77199724	273
290	892445	884021	290	49804498	290	274	1294421	1284117	274	78483841	274
291	918541	905493	291	50709991	291	275	1315029	1304725	275	79788566	275
292	944638	931590	292	51641581	292	276	1335638	1325334	276	81113899	276
293	970735	957686	293	52599267	293	277	1356246	1345942	277	82459841	277
294	996831	983783	294	53583050	294	278	1376854	1366550	278	83826391	278
295	1022928	1009880	295	54592930	295	279	1397463	1387159	279	85213550	279

296	1049025	1035977	296	55628907	296	280	1418072	1407767	280	86621317	280
297	1075122	1062073	297	56690980	297	281	1437555	1427814	281	88049131	281
298	1101218	1088170	298	57779150	298	282	1457040	1447297	282	89496428	282
299	1127315	1114267	299	58893417	299	283	1476524	1466782	283	90963210	283
300	1153413	1140364	300	60033781	300	284	1496008	1486266	284	92449476	284
301	1180929	1167171	301	61200951	301	285	1515493	1505751	285	93955227	285
302	1208445	1194687	302	62395638	302	286	1534977	1525235	286	95480462	286
303	1235960	1222202	303	63617841	303	287	1554462	1544720	287	97025182	287
304	1263476	1249718	304	64867559	304	288	1573946	1564204	288	98589386	288
305	1290992	1277234	305	66144793	305	289	1593431	1583688	289	100173074	289
306	1318507	1304750	306	67449542	306	290	1612916	1603173	290	101776247	290
307	1346023	1332265	307	68781807	307	291	1660877	1636897	291	103413144	291
308	1373539	1359781	308	70141588	308	292	1708839	1684858	292	105098002	292
309	1401054	1387297	309	71528885	309	293	1756801	1732820	293	106830822	293
310	1428569	1414812	310	72943697	310	294	1804763	1780782	294	108611604	294
311	1451442	1440006	311	74383703	311	295	1852725	1828744	295	110440347	295
312	1474314	1462878	312	75846581	312	296	1900687	1876706	296	112317053	296
313	1497186	1485750	313	77332331	313	297	1948648	1924667	297	114241720	297
314	1520058	1508622	314	78840953	314	298	1996610	1972629	298	116214350	298
315	1542929	1531494	315	80372446	315	299	2044572	2020591	299	118234941	299
316	1565801	1554365	316	81926812	316	300	2092535	2068553	300	120303494	300
317	1588673	1577237	317	83504049	317	301	2125975	2109255	301	122412749	301
318	1611545	1600109	318	85104158	318	302	2159417	2142696	302	124555445	302
319	1634417	1622981	319	86727138	319	303	2192858	2176137	303	126731583	303
320	1657287	1645852	320	88372990	320	304	2226299	2209578	304	128941161	304
321	1680114	1668700	321	90041691	321	305	2259740	2243020	305	131184181	305
322	1702942	1691528	322	91733218	322	306	2293181	2276461	306	133460641	306
323	1725770	1714356	323	93447575	323	307	2326622	2309902	307	135770543	307
324	1748598	1737184	324	95184759	324	308	2360064	2343343	308	138113886	308
325	1771427	1760013	325	96944772	325	309	2393505	2376784	309	140490670	309
326	1794255	1782841	326	98727612	326	310	2426946	2410226	310	142900896	310
327	1817083	1805669	327	100533281	327	311	2466199	2446573	311	145347469	311
328	1839911	1828497	328	102361779	328	312	2505451	2485825	312	147833294	312
329	1862740	1851326	329	104213104	329	313	2544704	2525078	313	150358371	313
330	1885570	1874155	330	106087259	330	314	2583956	2564330	314	152922701	314
331	1909489	1897529	331	107984788	331	315	2623209	2603582	315	155526284	315
332	1933408	1921448	332	109906237	332	316	2662461	2642835	316	158169119	316
333	1957326	1945367	333	111851604	333	317	2701713	2682087	317	160851206	317
334	1981245	1969285	334	113820889	334	318	2740966	2721340	318	163572546	318
335	2005163	1993204	335	115814093	335	319	2780218	2760592	319	166333138	319
336	2029082	2017122	336	117831215	336	320	2819470	2799844	320	169132982	320
337	2053000	2041041	337	119872256	337	321	2860787	2840128	321	171973110	321
338	2076918	2064959	338	121937215	338	322	2902102	2881444	322	174854555	322
339	2100837	2088878	339	124026093	339	323	2943417	2922759	323	177777314	323
340	2124754	2112795	340	126138888	340	324	2984732	2964074	324	180741388	324
341	2148671	2136736	341	128274237	341	325	3026047	3005390	325	183746778	325
342	2172588	2160653	342	130430777	342	326	3067362	3046705	326	186793482	326
343	2196505	2184570	343	132608509	343	327	3108677	3088020	327	189881502	327
344	2220422	2208487	344	134807431	344	328	3149993	3129335	328	193010837	328
345	2244339	2232404	345	137027545	345	329	3191308	3170650	329	196181487	329
346	2268256	2256469	346	139268850	346	330	3232622	3211965	330	199393452	330
347	2292173	2280482	347	141513347	347	331	3273937	3253280	331	202654477	331
348	2316090	2304299	348	143815035	348	332	3315252	3294595	332	205915502	332
349	2340007	2328216	349	146116722	349	333	3356567	3335910	333	209176527	333
350	2363924	2352133	350	148418409	350	334	3397882	3377225	334	212437552	334
351	2387841	2376049	351	150720096	351	335	3439197	3418540	335	215698577	335
352	2411758	2400000	352	153021783	352	336	3480512	3459855	336	218959602	336
353	2435675	2423917	353	155323470	353	337	3521827	3501170	337	222220627	337
354	2459592	2447834	354	157625157	354	338	3563142	3542485	338	225481652	338
355	2483509	2471776	355	160026844	355	339	3604457	3583800	339	228742677	339
356	2507426	2495763	356	162428531	356	340	3645772	3625115	340	232003702	340
357	2531343	2519800	357	164830218	357	341	3687087	3666430	341	235264727	341
358	2555260	2543717	358	167231905	358	342	3728402	3707745	342	238525752	342
359	2579177	2567534	359	169633592	359	343	3769717	3749060	343	241786777	343
360	2603094	2591700	360	172035279	360	344	3811032	3790375	344	245047802	344
361	2627011	2615467	361	174436966	361	345	3852347	3831690	345	248308827	345
362	2650928	2639233	362	176838653	362	346	3893662	3873005	346	251569852	346
363	2674845	2663000	363	179240340	363	347	3934977	3914320	347	254830877	347
364	2698762	2686766	364	181642027	364	348	3976292	3955635	348	258091902	348
365	2722679	2710535	365	184043714	365	349	4017607	3996950	349	261352927	349
366	2746596	2734391	366	186445401	366	350	4058922	4038265	350	264613952	350
367	2770513	2758247	367	188847088	367	351	4100237	4079580	351	267874977	351

368	2739059	2728152	368	194166422	368	352	4721976	4696841	352	286014302	352
369	2760874	2749967	369	196916389	369	353	4772245	4747111	353	290761412	353
370	2782689	2771781	370	199688170	370	354	4822515	4797380	354	295558792	354
371	2805176	2793932	371	202482103	371	355	4872784	4847649	355	300406442	355
372	2827663	2816420	372	205298523	372	356	4923053	4897919	356	305304360	356
373	2850150	2838907	373	208137430	373	357	4973323	4948188	357	310252548	357
374	2872637	2861394	374	210998824	374	358	5023592	4998457	358	315251006	358
375	2895124	2883881	375	213882705	375	359	5073861	5048727	359	320299732	359
376	2917611	2906368	376	216789072	376	360	5124131	5098996	360	325398728	360
377	2940098	2928855	377	219717927	377	361	5168231	5146181	361	330544910	361
378	2962585	2951342	378	222669269	378	362	5212332	5190282	362	335735191	362
379	2985072	2973829	379	225643098	379	363	5256433	5234383	363	340969574	363
380	3007558	2996315	380	228639413	380	364	5300534	5278484	364	346248058	364
381	3932370	3469964	381	232109377	381	365	5344635	5322584	365	351570642	365
382	4857181	4394776	382	236504153	382	366	5388736	5366685	366	356937327	366
383	5781993	5319587	383	241823740	383	367	5432837	5410786	367	362348114	367
384	6706804	6244399	384	248068139	384	368	5476938	5454887	368	367803001	368
385	7631616	7169210	385	255237349	385	369	5521039	5498988	369	373301989	369
386	8556427	8094021	386	263331370	386	370	5565141	5543090	370	378845079	370
387	9481238	9018833	387	272350203	387	371	5698059	5631600	371	384476679	371
388	10406050	9943644	388	282293847	388	372	5830979	5764519	372	390241198	372
389	11330861	10868456	389	293162303	389	373	5963899	5897439	373	396138638	373
390	12255672	11793267	390	304955569	390	374	6096819	6030359	374	402168997	374
391	12539173	12397423	391	317352992	391	375	6229739	6163279	375	408332276	375
392	12822675	12680924	392	330033916	392	376	6362659	6296199	376	414628475	376
393	13106177	12964426	393	342998342	393	377	6495579	6429119	377	421057594	377
394	13389678	13247927	394	356246270	394	378	6628499	6562039	378	427619633	378
395	13673180	13531429	395	369777699	395	379	6761419	6694959	379	434314591	379
396	13956682	13814931	396	383592630	396	380	6894340	6827879	380	441142471	380
397	14240183	14098432	397	397691062	397	381	7430473	7162406	381	448304877	381
398	14523685	14381934	398	412072996	398	382	7966606	7698539	382	456003416	382
399	14807186	14665436	399	426738431	399	383	8502739	8234673	383	464238089	383
400	15090689	14948937	400	441687369	400	384	9038872	8770806	384	473008895	384
						385	9575006	9306939	385	482315834	385
						386	10111139	9843072	386	492158906	386
						387	10647272	10379206	387	502538112	387
						388	11183405	10915339	388	513453450	388
						389	11719539	11451472	389	524904923	389
						390	12255672	11987605	390	536892528	390
						391	12538931	12397302	391	549289830	391
						392	12822432	12680682	392	561970511	392
						393	13105933	12964183	393	574934694	393
						394	13389434	13247684	394	588182377	394
						395	13672935	13531185	395	601713562	395
						396	13956436	13814686	396	615528247	396
						397	14239937	14098187	397	629626434	397
						398	14523438	14381688	398	644008121	398
						399	14806939	14665189	399	658673310	399
						400	15090689	14948814	400	673622124	400

Rebound Model Results

Hogarth												
Year	Annual Precipitation	Runoff Pit	Runoff Land	Pit Evaporation	Gw i - Gw o	Change in Storage	Accu. Volume	Year	Measured Water Elevation	Water Elevation	Pit Lake Surface Area	Watershed Area
	mm/year	m ³ /year		m	m	m ²	m ²					
1979	714	62272	2077018	41587	198925	2296627	1982285	1979	148.7	148.7	87167	7268399
1980	697	60729	2025557	47323	198925	2237889	4220174	1980		168.0	127273	7228293
1981	592	75282	1710214	69097	198925	1915325	6135499			181.0	163115	7192451
1982	833	135826	2395662	88555	198925	2641857	8777356			196.0	203348	7152218
1983	800	162638	2288138	110398	198925	2539303	11316659			208.0	222649	7132917
1984	733	163135	2090515	120876	198925	2331699	13648358			217.0	248280	7107286
1985	945	234501	2685132	134791	198925	2983767	16632125			228.0	312463	7043103
1986	664	207569	1871493	169636	198925	2108351	18740476		232.6	234.0	349263	7006303
1987	699	244065	1958402	189615	198925	2211777	20952253			240.0	383755	6971811
1988	764	293144	2130257	208341	198925	2413985	23366238		242.6	246.0	419438	6936128
1989	643	269815	1784746	227713	198925	2025774	25392012		247.8	251.0	450529	6905037
1990	654	294802	1807315	244592	198925	2056450	27448462		256.3	255.0	479777	6875789
1991	830	398078	2281978	260471	198925	2618510	30066972		257.5	260.0	516338	6839228
1992	872	450063	2384553	280320	198925	2753222	32820193			266.0	563107	6792459
1993	711	400220	1931056	305711	198925	2224491	35044684		267.9	269.0	586492	6769074
1994	765	448579	2070934	318406	198925	2400031	374444715			273.0	633192	6722374
1995	795	503388	2137715	343760	198925	2496268	39940983			277.0	685064	6670502
1996	1010	692051	2695417	371921	198925	3214472	43155454		281.6	281.0	740815	6614751
1997	578	428043	1528801	402189	198925	1753581	44909035			284.0	791359	6564207
1998	676	534563	1773649	429629	198925	2077508	46986543			286.0	825054	6530512
1999	813	671099	2124767	447922	198925	2546869	49533412		289.5	289.0	875598	6479968
2000	775	678676	2009049	475362	198925	2411288	51944701		291.4	292.0	944638	6410928
2001	941	888904	2413073	512844	198925	2988059	54932759		295.0	295.0	1022928	6332638
2002	732	748579	1853690	555348	198925	2245846	57178605		298.1	297.0	1075122	6280444
2003	842	905575	2116007	583684	198925	2636824	59815429		300.2	299.0	1127315	6228251
2004	868	978735	2162947	612019	198925	2728588	62544016			302.0	1208445	6147121
2005	905	1093642	2225258	656065	198925	2861761	65405777			304.0	1263476	6092090
2006	740	934972	1803259	685941	198925	2251215	67656992			306.0	1318507	6037059
2007	740	975695	1786969	715818	198925	2245772	69902764		306.9	307.0	1346023	6009543
2008	740	996057	1778825	730756	198925	2243051	72145815		309.3	309.0	1401054	5954512
2009	740	1036780	1762535	760632	198925	2237608	74383423		311.2	310.0	1428569	5926997
2010	740	1057141	1754391	775570	198925	2234887	76618310		312.8	312.0	1474314	5881252
2011	740	1090992	1740851	800405	198925	2230363	78848673		313.7	314.0	1520058	5835508
2012	740	1124843	1727310	825239	198925	2225839	81074512			315.0	1542929	5812637
2013	740	1141768	1720540	837656	198925	2223577	83298089			316.0	1565801	5789765
2014	740	1158693	1713770	850073	198925	2221315	85519404			318.0	1611545	5744021
2015	740	1192543	1700230	874908	198925	2216791	87736194			319.0	1634417	5721149
2016	740	1209468	1693460	887325	198925	2214529	89950723			320.0	1657287	5698279
2017	740	1226392	1686691	899741	198925	2212267	92162990			322.0	1702942	5652624
2018	740	1260177	1673177	924527	198925	2207752	94370741			323.0	1725770	5629796
2019	740	1277070	1666420	936921	198925	2205494	96576235			324.0	1748598	5606968
2020	740	1293963	1659662	949314	198925	2203236	98779471			326.0	1794255	5561311
2021	740	1327749	1646148	974101	198925	2198721	100978192			327.0	1817083	5538483
2022	740	1344642	1639391	986494	198925	2196463	103174655			328.0	1839911	5515655
2023	740	1361534	1632634	998888	198925	2194205	105368860			329.0	1862740	5492826
2024	740	1378427	1625877	1011281	198925	2191948	107560808			330.0	1885570	5469996
2025	740	1395321	1619119	1023676	198925	2189690	109750498			331.0	1909489	5446077
2026	740	1413022	1612039	1036662	198925	2187324	111937822			333.0	1957326	5398240
2027	740	1448421	1597879	1062632	198925	2182593	114120415			334.0	1981245	5374321
2028	740	1466121	1590799	1075618	198925	2180227	116300642			335.0	2005163	5350403
2029	740	1483821	1583719	1088603	198925	2177862	118478504			336.0	2029082	5326484
2030	740	1501520	1576639	1101588	198925	2175496	120654001			337.0	2053000	5302566
2031	740	1519220	1569560	1114574	198925	2173131	122827131			338.0	2076918	5278648
2032	740	1536920	1562480	1127559	198925	2170765	124997897			339.0	2100837	5254729
2033	740	1554619	1555400	1140544	198925	2168400	127166296			340.0	2124754	5230812
2034	740	1572318	1548320	1153529	198925	2166034	129332331			341.0	2145944	5209622

2035	740	1587999	1542048	1165033	198925	2163939	131496269	342.0	2167136	5188430
2036	740	1603680	1535775	1176538	198925	2161843	133658112	343.0	2188327	5167239
2037	740	1619362	1529503	1188043	198925	2159747	135817859	344.0	2209518	5146048
2038	740	1635043	1523230	1199547	198925	2157651	137975510	345.0	2230710	5124856
2039	740	1650725	1516958	1211052	198925	2155555	140131066	346.0	2251901	5103665
2040	740	1666407	1510685	1222557	198925	2153460	142284525	347.0	2273092	5082474
2041	740	1682088	1504412	1234062	198925	2151364	144435889	348.0	2294283	5061283
2042	740	1697770	1498140	1245566	198925	2149268	146585157	349.0	2315475	5040091
2043	740	1713451	1491867	1257071	198925	2147172	148732329	350.0	2336667	5018899
2044	740	1729134	1485594	1268577	198925	2145076	150877405	351.0	2359453	4996113
2045	740	1745996	1478849	1280947	198925	2142823	153020228	351.0	2359453	4996113
2046	740	1745996	1478849	1280947	198925	2142823	155163050	352.0	2382241	4973325
2047	740	1762858	1472104	1293319	198925	2140569	157303619	353.0	2405028	4950538
2048	740	1779721	1465359	1305690	198925	2138315	159441935	354.0	2427816	4927750
2049	740	1796584	1458614	1318061	198925	2136062	161577996	355.0	2450603	4904963
2050	740	1813446	1451869	1330432	198925	2133808	163711804	356.0	2473391	4882175
2051	740	1830309	1445124	1342804	198925	2131554	165843358	357.0	2496178	4859388
2052	740	1847172	1438379	1355175	198925	2129301	167972659	358.0	2518966	4836600
2053	740	1864035	1431634	1367546	198925	2127047	170099706	358.0	2518966	4836600
2054	740	1864035	1431634	1367546	198925	2127047	172226752	359.0	2541753	4813813
2055	740	1880897	1424889	1379918	198925	2124793	174351546	360.0	2564542	4791024
2056	740	1897761	1418143	1392290	198925	2122539	176474085	361.0	2586356	4769210
2057	740	1913904	1411686	1404133	198925	2120382	178594467	362.0	2608171	29352282
2058	740	1930047	1405229	1415976	198925	2118225	180714850	363.0	2630000	29120494
2059	740	1946190	1398772	1427819	198925	2116068	182835233	364.0	2651829	28888706
2060	740	1962333	1392290	1440712	198925	2113911	184955616	365.0	2673658	28656918
2061	740	1978475	1385763	1451506	198925	2111754	187076000	366.0	2695487	28425130
2062	740	1994618	1379194	1462299	198925	2109597	189196383	367.0	2717316	28193342
2063	740	2010761	1372725	1473093	198925	2107440	191316767	368.0	2739145	27961554
2064	740	2026904	1366256	1483886	198925	2105283	193437150	369.0	2760974	27729766
2065	740	2043047	1359787	1494680	198925	2103126	195557534	370.0	2782803	27497978
2066	740	2059190	1353318	1505473	198925	2100969	197677917	371.0	2804632	27266190
2067	740	2075333	1346849	1516267	198925	2098812	199798301	372.0	2826461	27034402
2068	740	2091476	1340380	1527060	198925	2096655	201918684	373.0	2848290	26802614
2069	740	2107619	1333911	1537854	198925	2094498	204039068	374.0	2870119	26570826
2070	740	2123762	1327442	1548647	198925	2092341	206159451	375.0	2891948	26339038
2071	740	2139905	1320973	1559441	198925	2090184	208279835	376.0	2913777	26107250
2072	740	2156048	1314504	1570234	198925	2088027	210400218	377.0	2935606	25875462
2073	740	2172191	1308035	1581028	198925	2085870	212520602	378.0	2957435	25643674
2074	740	2188334	1301566	1591821	198925	2083713	214640985	379.0	2979264	25411886
2075	740	2204477	1295097	1602615	198925	2081556	216761369	380.0	3001093	25180098
2076	740	2220620	1288628	1613408	198925	2079399	218881752	381.0	3022922	24948310
2077	740	2236763	1282159	1624202	198925	2077242	221002136	382.0	3044751	24716522

Caland

Year	Annual Precipitation	Runoff Pt	Runoff Land	Pt Evaporation	Gwi - Gw o	Change in Storage	Accu. Volume	Year	Measured Water Elevation	Water Elevation	Pit Lake Surface Area	Watershed Area
	mm/year	m ³ /year		m	m	m ²	m ²					
1979	714											
1980	697											
1981	592											
1982	833											
1983	800											
1984	733											
1985	945											
1986	664	471679	4284704	338759	198925	4616549	36703368		231.3	231.3	710039	16124884
1987	699	496175	4507228	385480	198925	4816848	41520215			237.0	770861	16064062
1988	764	588847	4908421	418500	198925	5277692	46797908	238.3		243.0	838814	15996109
1989	643	539591	4115984	455392	198925	4399108	51197016	244.4		248.0	901297	15933626
1990	654	589761	4170445	489314	198925	4469817	55666833	252.1		253.0	967523	15867400
1991	830	802768	5266167	525268	198925	5742592	61409425	255.7		259.0	1049982	15784941
1992	872	915212	5503549	570035	198925	6047651	67457076			264.0	1123031	15711892
1993	711	798178	4466799	609693	198925	4854208	72311284	264.9		269.0	1197163	15637760
1994	765	915652	4784223	649940	198925	5248860	77560144			273.0	1273813	15561110
1995	795	1012681	4948433	691553	198925	5468486	83028630			277.0	1356246	15478677
1996	1010	1370080	6254624	736306	198925	7087323	90115953	280.1		282.0	1457040	15377883
1997	578	841878	3554136	791027	198925	3803912	93919865			284.0	1496008	15338915
1998	676	1010554	4144575	812183	198925	4541870	98461735			287.0	1554462	15280461
1999	813	1264399	4971651	843917	198925	5591058	104052793	288.9		291.0	1660877	15174046
2000	775	1287346	4704561	901690	198925	5289142	109341935	291.4		294.0	1804763	15030160
2001	941	1698282	5657352	979806	198925	6574753	115916688	295.6		297.0	1948648	14886275
2002	732	1426021	4357510	1057921	198925	4924535	120841223	299.9		300.0	2092535	14742388
2003	842	1762542	4967005	1136037	198925	5792435	126633658	302.0		302.0	2159417	14675506
2004	868	1874806	5096510	1172347	198925	5997893	132631552			305.0	2259740	14575183
2005	905	2045065	5276216	1226813	198925	6293393	138924945			308.0	2360064	14474859
2006	740	1746447	4284558	1281279	198925	4948652	143873597			310.0	2426946	14407977
2007	740	1795940	4264761	1317589	198925	4942037	148815634	310.9		312.0	2505451	14329472
2008	740	1854034	4241524	1360210	198925	4934273	153749907	313.6		314.0	2583956	14250967
2009	740	1912128	4218286	1402830	198925	4926509	158676416	316.1		316.0	2662461	14172462
2010	740	1970221	4195049	1445450	198925	4918745	163595161	317.9		318.0	2740966	14093957
2011	740	2028315	4171811	1488070	198925	4910981	168506141	318.9		319.0	2780218	14054705
2012	740	2057361	4160193	1509380	198925	4907099	173413240			321.0	2860787	13974136
2013	740	2116982	4136344	1553121	198925	4899130	178312370			323.0	2943417	13891506
2014	740	2178128	4111886	1597981	198925	4890958	183203329			324.0	2984732	21620155
2015	740	2208702	6399566	1620411	198925	7186782	190390110			327.0	3108677	21496210
2016	740	2300421	6362878	1687701	198925	7174523	197564634			329.0	3191308	21413579
2017	740	2361568	6338419	1732561	198925	7166351	204730985			331.0	3289430	21315457
2018	740	2434178	6309375	1785831	198925	7156647	211887632			333.0	3403048	21201839
2019	740	2518256	6275744	1847515	198925	7145410	219033042			335.0	3516667	21088220
2020	740	2602334	6242113	1909199	198925	7134173	226167215			337.0	3630286	20974601
2021	740	2686412	6208482	1970882	198925	7122936	233290151			339.0	3743905	20860982
2022	740	2770489	6174851	2032566	198925	7111699	240401851			341.0	3882787	20722100
2023	740	2873263	6133742	2107965	198925	7097964	247499815			343.0	4046932	20557955
2024	740	2994729	6085155	2197079	198925	7081730	254581545			344.0	4129004	20475883
2025	740	3055463	6060861	2241636	198925	7073613	261655158			346.0	4293148	20311739
2026	740	3176930	6012275	2330750	198925	7057379	268712537			348.0	4457293	20147594
2027	740	3298397	5963688	2419864	198925	7041145	275753682			349.0	4539365	20065522
2028	740	3359130	5939394	2464421	198925	7033028	282786710			351.0	4671707	19933180
2029	740	3457063	5900221	2536270	198925	7019940	289806650			352.0	4721976	19882911
2030	740	3494262	5885342	2563561	198925	7014968	296821618			354.0	4822515	19782372
2031	740	3568661	5855582	2618143	198925	7005025	303826643			355.0	4872784	19732103
2032	740	3605860	5840702	2645434	198925	7000053	310826696			357.0	4973323	19631564
2033	740	3680259	5810943	2700017	198925	6990110	317816806			358.0	5023592	19581295
2034	740	3717458	5796063	2727308	198925	6985138	324801945			359.0	5073861	19531026

2035	740	3754657	5781184	2754599	198925	6980167	331782111	361.0	5168231	19436656
2036	740	3824491	5753250	2805833	198925	6970833	338752945	362.0	5212332	19392555
2037	740	3857126	5740196	2829775	198925	6986472	345719417	363.0	5256433	19348454
2038	740	3889760	5727142	2853718	198925	6962110	352681527	365.0	5344635	19260252
2039	740	3955030	5701035	2901602	198925	6953387	359634914	366.0	5388736	19216151
2040	740	3987665	5687981	2925545	198925	6949026	366583940	367.0	5432837	19172050
2041	740	4020299	5674927	2949487	198925	6944664	373528604	369.0	5521039	19083848
2042	740	4085569	5648819	2997372	198925	6935941	380464545	370.0	5565141	19039746
2043	740	4118204	5635765	3021315	198925	6931579	387396124	371.0	5698059	18968628
2044	740	4216564	5596421	3093476	198925	6918433	394314557	372.0	5830979	18773908
2045	740	4314925	5557077	3165639	198925	6905288	401219845	373.0	5963899	18640988
2046	740	4413285	5517732	3237801	198925	6892142	408111987	374.0	6096819	18508068
2047	740	4511646	5478388	3309963	198925	6878996	414990983	376.0	6362659	18242228
2048	740	4708368	5399699	3454288	198925	6852705	421843687	377.0	6495579	18109308
2049	740	4806728	5360355	3526450	198925	6839559	428683246	378.0	6628499	17976388
2050	740	4905089	5321011	3598612	198925	6826413	435509659	379.0	6761419	17843468
2051	740	5003450	5281667	3670774	198925	6813267	442322927	380.0	6894340	17710547
2052	740	5101811	5242322	3742937	198925	6800121	449123048	381.0	7430473	17174414
2053	740	5498550	5083627	4034004	198925	6747098	455870146	381.0	7430473	17174414
2054	740	5498550	5083627	4034004	198925	6747098	462617243	382.0	7966606	16638281
2055	740	5895288	4924931	4325070	198925	6694074	469311318	383.0	8502739	16102148
2056	740	6292027	4766236	4616137	198925	6641051	475952368	384.0	9038872	15566015
2057	740	6688766	4607540	4907204	198925	6588027	482540395	385.0	9575006	15029881
2058	740	7085504	4448845	5198271	198925	6535003	0	385.0	9575006	15029881
2059	740	7085504	4448845	5198271	198925	6535003	0	385.0	9575006	15029881
2060	740	7085504	4448845	5198271	198925	6535003	0	385.0	9575006	15029881
2061	740	7085504	4448845	5198271	198925	6535003	0	385.0	9575006	15029881
2062	740	7085504	4448845	5198271	198925	6535003	0	385.0	9575006	15029881
2063	740	7085504	4448845	5198271	198925	6535003	0	385.0	9575006	15029881
2064	740	7085504	4448845	5198271	198925	6535003	0	385.0	9575006	15029881
2065	740	7085504	4448845	5198271	198925	6535003	0	385.0	9575006	15029881
2066	740	7085504	4448845	5198271	198925	6535003	0	385.0	9575006	15029881
2067	740	7085504	4448845	5198271	198925	6535003	0	385.0	9575006	15029881
2068	740	7085504	4448845	5198271	198925	6535003	0	385.0	9575006	15029881
2069	740	7085504	4448845	5198271	198925	6535003	0	385.0	9575006	15029881
2070	740	7085504	4448845	5198271	198925	6535003	0	385.0	9575006	15029881
2071	740	7085504	4448845	5198271	198925	6535003	0	385.0	9575006	15029881
2072	740	7085504	4448845	5198271	198925	6535003	0	385.0	9575006	15029881
2073	740	7085504	4448845	5198271	198925	6535003	0	385.0	9575006	15029881
2074	740	7085504	4448845	5198271	198925	6535003	0	385.0	9575006	15029881
2075	740	7085504	4448845	5198271	198925	6535003	0	385.0	9575006	15029881
2076	740	7085504	4448845	5198271	198925	6535003	0	385.0	9575006	15029881
2077	740	7085504	4448845	5198271	198925	6535003	0	385.0	9575006	15029881

APPENDIX VII
Example DYRESM Input Files

```
<#5>
! DYRESM configuration file: Hogarth
1991145          # Simulation start day
158             # Simulation length (unit=days)
.FALSE.         # Run CAEDYM (.TRUE. or .FALSE.)
1              # Output Interval (in days, or -9999 for every time step)
0.82           # Light extinction coefficient (m-1)
0.5            # Min layer thickness (m)
250            # Max layer thickness (m)
10800          # Time Step (s)
3              # Number of Output Selections
SALINITY TEMPTURE DENSITY # List of Output Selections
.FALSE.        # Activate destrat system (.TRUE. or .FALSE.)
.FALSE.        # Activate non-neutral atmospheric stability (.TRUE. or .FALSE.)
```

<#3>

Comment line: Hogarth Morphometry (3Hv2)

```

+48 # latitude
390.0 # height above MSL
3 # number of inflows
SURF 74.7 85.0 0.016 Inflow1 # entry height, 1/2-angle, slope, drag coeff, name
100.0 74.7 10.0 0.016 Grdwat # entry height, 1/2-angle, slope, drag coeff, name
SURF 74.7 10.0 0.016 FROMCAL # entry height, 1/2-angle, slope, drag coeff, name
107.0 # zero-ht elevation (i.e., bottom elev.)
397.0 # crest elevation [m]
1 # number of outlets
394.0 # outlet heights
25 # number of stg survey points after header line

```

Elev[m] SurfArea_[m^2]

```

107 11148
137 65030
168 127273
198 209025
200 203285
210 227493
220 257195
230 326279
240 383765
250 443218
260 516338
270 594288
280 723967
290 892445
300 1153413
310 1428569
320 1657287
330 1885570
340 2124754
350 2336667
360 2564542
370 2782689
380 3007558
390 12255672
400 15090689

```

Initial profile: Spring 1991145 – Adjusted for Scenario 3

184 # number of initial profile points

Height (m)	T (Cel)	S (pss)
121.5	4.75	1.1465
122.1	4.75	1.2661
122.9	4.75	1.5673
123.3	4.75	1.7433
123.9	4.71	2.0966
125.7	4.7	2.1108
126.3	4.7	2.1117
127.4	4.7	2.1126
127.5	4.7	2.1108
128.2	4.7	2.1055
129.1	4.69	2.1115
130.1	4.69	2.1124
130.8	4.69	2.1080
131.6	4.69	2.1116
132.7	4.69	2.1125
133.7	4.69	2.1153
135.0	4.69	2.1126
136.2	4.69	2.1127
137.2	4.69	2.1127
137.8	4.69	2.1109
138.7	4.69	2.1092
139.8	4.69	2.1119
140.6	4.69	2.1111
141.3	4.68	2.1126
142.6	4.68	2.1090
144.0	4.69	2.1130
145.0	4.68	2.1154
145.8	4.69	2.1077
146.8	4.69	2.1095
147.3	4.68	2.1128
148.7	4.69	2.1114
149.5	4.68	2.1147
150.3	4.68	2.1120
151.3	4.69	2.1124
152.3	4.69	2.1124
153.2	4.69	2.1133
154.2	4.69	2.1134
155.2	4.69	2.1134
156.0	4.69	2.1090
157.0	4.69	2.1153
157.9	4.69	2.1117
159.0	4.69	2.1127
159.7	4.69	2.1118
160.5	4.69	2.1136
161.4	4.69	2.1101
162.4	4.69	2.1128
163.1	4.69	2.1092
163.9	4.69	2.1084
164.7	4.69	2.1120
165.9	4.69	2.1102
166.9	4.69	2.1103
167.6	4.69	2.1094
168.6	4.69	2.1103
169.6	4.68	2.1137
170.6	4.69	2.1194
171.5	4.69	2.1168
172.3	4.68	2.1129
173.3	4.69	2.1132
174.1	4.68	2.1094
174.9	4.69	2.1097
175.8	4.68	2.1085
176.4	4.69	2.1025
177.5	4.69	2.1206

178.3	4.69	2.1089
179.1	4.69	2.1081
180.1	4.69	2.1072
180.9	4.69	2.1054
181.9	4.69	2.1181
182.8	4.69	2.1127
183.6	4.69	2.1100
184.4	4.69	2.1128
185.1	4.68	2.1134
185.9	4.69	2.1110
186.0	4.68	2.1053
186.8	4.68	2.1054
187.7	4.68	2.1099
188.5	4.68	2.1180
188.5	4.68	2.1144
189.3	4.69	2.1112
190.2	4.69	2.1112
191.1	4.69	2.1112
192.0	4.68	2.1137
192.7	4.68	2.1191
193.5	4.68	2.1173
194.5	4.69	2.1105
195.2	4.68	2.1039
195.9	4.68	2.1075
196.6	4.68	2.1066
197.2	4.68	2.1148
198.1	4.68	2.1130
198.6	4.68	2.1139
199.0	4.68	2.1076
199.8	4.68	2.1095
200.6	4.68	2.1032
201.4	4.69	2.1170
202.2	4.68	2.1033
203.0	4.68	2.0988
203.7	4.68	2.1087
204.3	4.68	2.1123
205.1	4.68	2.1106
205.9	4.68	2.1142
206.7	4.68	2.1179
207.6	4.68	2.1098
208.2	4.68	2.1116
209.0	4.68	2.1098
209.7	4.68	2.1081
210.3	4.68	2.1099
211.0	4.68	2.1099
211.8	4.68	2.1099
212.6	4.68	2.1082
213.5	4.68	2.1046
214.3	4.68	2.1100
215.1	4.68	2.1110
216.0	4.68	2.1101
216.8	4.68	2.1101
217.7	4.68	2.1102
219.1	4.68	2.1084
220.1	4.68	2.1139
220.9	4.68	2.1157
221.7	4.68	2.1103
222.6	4.67	2.1074
224.1	4.67	2.1128
225.4	4.67	2.1093
226.2	4.68	2.1123
227.7	4.67	2.1112
228.6	4.67	2.1049
229.5	4.67	2.1157
231.0	4.67	2.1113
231.8	4.67	2.1167

233.2	4.67	2.1042
234.1	4.67	2.1069
235.3	4.67	2.1070
235.4	4.67	2.1151
236.5	4.67	2.1079
237.7	4.67	2.1098
238.6	4.67	2.1125
239.6	4.67	2.1089
240.7	4.67	2.1081
241.8	4.67	2.1081
243.1	4.67	2.1073
244.4	4.67	2.1118
245.3	4.66	2.1098
246.4	4.66	2.1098
247.3	4.66	2.1089
248.6	4.66	2.1081
249.6	4.67	2.1093
250.5	4.67	2.1085
251.5	4.67	2.1094
252.7	4.68	2.1079
253.8	4.68	2.1044
254.7	4.68	2.1053
255.4	4.68	2.1017
256.2	4.69	2.1057
257.1	4.7	2.0979
257.8	4.71	2.0946
258.7	4.72	2.0967
259.6	4.72	2.1004
260.6	4.75	2.0932
261.8	4.76	2.0980
262.9	4.77	2.0930
264.3	4.8	2.1011
265.4	4.82	2.0936
266.5	4.85	2.0838
266.5	4.84	2.0880
267.7	4.88	2.0838
268.8	4.93	2.0871
269.8	4.94	2.0848
270.8	5	2.0803
271.2	5	2.0830
272.2	5	2.0804
273.2	4.85	2.0840
274.4	4.63	2.0775
275.6	4.21	2.0994
276.9	3.3	2.0803
278.2	2.44	2.1190
279.5	2.29	2.1151
280.9	2.03	2.1280
282.0	1.78	2.1442
283.2	1.5	2.1636
284.4	1.44	2.1726
285.2	1.41	2.1687
286.2	1.32	2.1827
287.2	0.3	2.2239
288.0	0.01	0.3547

<#3>

Weather File: Hogarth

86400

met data input time step (seconds)

CLOUD_COVER

longwave radiation type (NETT_LW, INCIDENT_LW, CLOUD_COVER)

FIXED_HT 290.3 # sensor type (FLOATING, FIXED_HT), height in metres (above water surface, above lake bottom)

JulDay SW [W/m2] Cloud-Cover [%] AIR TEMP [C] VAP PRESS [mb] Wind Speed [m/s] Rain [m]

1991145	349.06	0.41	16.90	12.78	1.32	0
1991146	306.40	0.16	16.30	11.76	0.88	0
1991147	321.47	0.32	18.80	13.78	0.54	0
1991148	315.19	0.28	20.10	14.04	1.18	0
1991149	289.65	0.17	21.80	15.61	1.36	0
1991150	122.59	0.57	21.90	15.43	3.22	0
1991151	169.03	0.94	12.10	11.38	2.95	0.003
1991152	167.67	0.57	8.00	7.21	2.30	0
1991153	355.76	0.53	8.70	9.19	2.21	0.0018
1991154	169.03	0.92	16.60	13.98	3.61	0.0062
1991155	126.39	0.55	9.40	7.33	1.94	0
1991156	284.03	0.45	9.30	6.92	1.24	0
1991157	327.12	0.66	13.40	8.04	2.41	0
1991158	327.12	0.66	17.50	13.05	4.14	0.0084
1991159	165.90	0.15	6.30	4.99	3.18	0
1991160	342.86	0.55	14.80	10.36	1.63	0
1991161	94.02	0.85	15.60	12.42	1.84	0.01
1991162	321.32	0.87	10.30	10.58	2.69	0.0002
1991163	335.31	0.23	13.80	11.78	3.48	0
1991164	178.83	0.24	12.80	8.75	2.77	0.001
1991165	206.15	0.45	11.70	9.14	2.59	0
1991166	178.85	0.85	11.90	12.83	0.78	0.023
1991167	107.43	0.46	8.80	7.81	3.76	0.0004
1991168	258.31	0.10	10.80	8.53	1.59	0
1991169	307.72	0.44	17.10	12.69	0.88	0
1991170	263.56	0.32	20.10	13.82	2.08	0
1991171	358.55	0.63	17.50	12.97	2.88	0.0126
1991172	83.43	0.95	21.20	21.42	2.13	0.0002
1991173	194.05	0.75	18.20	16.22	3.39	0.0394
1991174	80.20	0.65	10.50	9.57	3.29	0.0018
1991175	198.98	0.41	9.30	8.17	1.15	0
1991176	339.90	0.79	14.20	13.55	2.70	0.008
1991177	252.65	0.81	21.20	22.81	1.55	0.0274
1991178	101.85	0.51	17.60	13.51	2.21	0
1991179	186.64	0.35	15.10	11.32	2.51	0.0012
1991180	343.02	0.55	12.70	9.31	2.00	0
1991181	356.64	0.53	13.80	10.85	1.00	0
1991182	273.41	0.85	15.40	14.32	1.24	0.006
1991183	167.89	0.26	13.20	10.44	1.67	0
1991184	150.60	0.66	15.50	12.26	2.41	0
1991185	202.23	0.87	20.00	18.90	1.92	0.0018
1991186	259.48	0.94	21.30	21.94	2.96	0.0034
1991187	208.60	0.54	19.40	13.28	5.46	0
1991188	294.76	0.13	19.30	13.47	4.51	0
1991189	132.09	0.75	16.20	13.02	0.68	0
1991190	157.35	0.40	17.00	14.63	1.12	0.0004
1991191	126.33	0.74	14.20	13.01	1.59	0
1991192	279.02	0.99	15.10	11.23	2.81	0.002
1991193	242.66	1.00	12.70	12.85	3.47	0.0036
1991194	350.15	0.92	14.80	14.61	1.53	0.0016
1991195	341.93	0.44	14.90	13.37	1.37	0
1991196	316.11	0.56	18.50	16.76	1.23	0
1991197	259.26	0.93	19.30	19.53	0.76	0
1991198	275.45	0.98	22.80	25.06	2.26	0.001
1991199	233.47	0.65	25.10	23.08	1.38	0
1991200	138.58	0.63	21.30	17.10	1.97	0.0004
1991201	149.58	0.65	17.20	14.75	1.46	0.0026
1991202	314.12	0.58	16.60	13.50	2.26	0
1991203	253.83	0.33	18.90	15.46	1.41	0
1991204	318.90	0.74	20.30	19.60	2.65	0.003

1991205	234.76	0.74	22.70	19.28	3.29	0
1991206	117.95	0.30	17.20	12.66	1.89	0
1991207	327.97	0.55	16.90	12.83	1.63	0
1991208	285.36	0.83	17.80	15.70	0.91	0
1991209	172.53	0.59	18.10	15.50	1.15	0
1991210	305.43	0.52	19.60	15.60	1.00	0
1991211	297.95	0.74	18.70	14.51	2.33	0
1991212	341.93	0.40	15.10	12.05	2.81	0.0014
1991213	170.03	0.63	14.00	13.85	1.54	0.0104
1991214	125.59	0.85	14.60	13.97	1.82	0.0044
1991215	72.49	0.94	17.60	15.69	1.98	0
1991216	192.26	0.67	16.80	15.21	1.05	0.0008
1991217	128.33	0.77	17.70	16.38	0.79	0.0004
1991218	215.95	0.50	17.10	14.53	1.71	0
1991219	280.59	0.86	17.70	17.40	1.27	0.0034
1991220	289.85	0.68	18.10	15.59	2.29	0.0034
1991221	195.36	0.70	15.00	14.51	1.49	0.0004
1991222	80.19	0.75	12.60	9.84	3.11	0.0006
1991223	67.89	0.44	13.30	10.18	1.49	0
1991224	277.95	0.34	14.5	11	2	0
1991225	193.68	0.71	19.4	18	2	0.0002
1991226	134.24	1.00	17.2	17	1	0
1991227	216.97	0.52	19.7	17	1	0
1991228	201.04	0.69	19.2	12	3	0.0002
1991229	237.42	0.32	13	10	2	0
1991230	283.00	0.10	13.6	10	1	0
1991231	278.00	0.26	16.9	13	3	0
1991232	185.63	0.74	14	11	4	0.0088
1991233	209.65	0.13	11.3	9	1	0
1991234	217.99	0.90	9.1	10	2	0.011
1991235	65.23	0.42	13.1	12	2	0
1991236	231.03	0.61	11.6	10	2	0
1991237	270.31	0.81	16.7	15	3	0.0014
1991238	52.80	0.63	6.6	7	3	0
1991239	146.79	0.38	6	7	2	0.0004
1991240	211.22	0.62	9.6	8	2	0
1991241	176.76	0.55	11.6	9	2	0
1991242	104.94	0.18	14.4	12	2	0
1991243	226.05	0.79	19.7	18	1	0.0058
1991244	81.88	1.00	13.2	14	3	0.0052
1991245	219.97	1.00	10	11	3	0.0088
1991246	195.72	1.00	16.3	18	3	0.0176
1991247	44.92	0.69	13.1	12	4	0.0006
1991248	48.02	0.72	7.8	7	5	0.0002
1991249	63.01	0.65	4.6	6	2	0
1991250	228.19	0.46	7.4	7	3	0
1991251	147.81	0.38	7.7	6	3	0
1991252	149.46	0.81	9.6	9	1	0
1991253	45.57	0.98	13	12	1	0.0006
1991254	212.09	0.92	8.6	9	1	0.0008
1991255	151.66	0.54	9.1	10	3	0.0028
1991256	114.26	0.49	4.2	6	2	0
1991257	183.87	0.80	3.8	6	1	0
1991258	60.52	0.29	4.4	6	1	0
1991259	33.00	0.51	5.5	6	2	0.0002
1991260	79.20	1.00	9.2	11	2	0.0212
1991261	73.53	0.96	7.7	9	1	0
1991262	101.75	0.77	6.7	8	1	0
1991263	182.63	0.58	9.8	10	1	0
1991264	154.36	0.95	8.6	11	2	0.0236
1991265	33.43	0.73	13.7	13	3	0.0012
1991266	80.59	0.31	11.7	11	2	0
1991267	49.79	0.64	13.9	12	1	0
1991268	70.06	0.99	13.2	12	4	0.0016
1991269	145.44	1.00	12.1	13	4	0.0016
1991270	142.89	1.00	9.5	11	2	0.0008

1991271	76.74	1.00	9	10	1	0.0004
1991272	55.13	0.93	12.2	13	1	0.006
1991273	34.03	0.31	8.2	9	2	0
1991274	68.47	0.42	6.9	8	0	0
1991275	111.44	0.77	6.2	9	1	0.0184
1991276	20.24	0.85	3.5	6	3	0.0002
1991277	55.59	0.77	2.4	6	2	0.002
1991278	35.78	0.80	2.5	5	5	0.0004
1991279	120.21	0.79	0.1	5	2	0.0004
1991280	28.59	0.96	7.3	9	2	0.0094
1991281	104.46	0.64	3	4	3	0
1991282	112.77	0.23	-0.4	4	1	0
1991283	119.09	0.83	3.9	6	4	0.0041
1991284	27.09	1.00	4.6	7	2	0.0006
1991285	61.39	1.00	1.9	5	3	0
1991286	119.58	1.00	1.2	6	1	0.0064
1991287	20.44	1.00	2.1	6	2	0.0012
1991288	60.79	0.97	2.8	5	3	0
1991289	56.76	0.77	1	5	1	0
1991290	62.30	0.21	2.8	6	1	0
1991291	104.94	0.18	5.7	7	2	0
1991292	110.98	0.11	10	8	1	0
1991293	52.97	0.52	8.4	7	1	0
1991294	43.22	0.66	8.7	8	1	0
1991295	13.43	0.55	8.5	8	2	0
1991296	52.47	0.94	4.3	6	1	0
1991297	51.40	0.38	2.6	6	1	0
1991298	23.34	0.14	2.3	6	0	0
1991299	86.31	0.79	1	5	2	0
1991300	41.09	0.44	1	6	2	0
1991301	22.58	1.00	6.3	7	3	0
1991302	33.00	0.50	1	3	2	0

Inflows:3H					
3		#number of inflow streams			
Inflow1		# inflow 1			
Grdwat		# inflow 2			
FROMCAL		# inflow 3			
YrDayNum	InfNum	VOLUME	TEMPTURE	SALINITY	
1991145 1	13416	16.90	1.3467		
1991145 2	1713	3	0.4321		
1991145 3	22821	16.5	0.3514		
1991146 1	13416	16.30	1.3467		
1991146 2	1713	3	0.4321		
1991146 3	22821	18.9	0.3516		
1991147 1	13416	18.80	1.3467		
1991147 2	1713	3	0.4321		
1991147 3	22821	21.0	0.3518		
1991148 1	13416	20.10	1.3467		
1991148 2	1713	3	0.4321		
1991148 3	22821	23.1	0.3521		
1991149 1	13416	21.80	1.3467		
1991149 2	1713	3	0.4321		
1991149 3	22821	24.5	0.3526		
1991150 1	13416	21.90	1.3467		
1991150 2	1713	3	0.4321		
1991150 3	22821	24.0	0.3535		
1991151 1	13416	12.10	1.3467		
1991151 2	1713	3	0.4321		
1991151 3	22821	21.9	0.3542		
1991152 1	17426	8.00	1.3467		
1991152 2	1713	3	0.4321		
1991152 3	22821	19.0	0.3529		
1991153 1	17426	8.70	1.3467		
1991153 2	1713	3	0.4321		
1991153 3	22821	18.9	0.3532		
1991154 1	17426	16.60	1.3467		
1991154 2	1713	3	0.4321		
1991154 3	22821	19.2	0.3530		
1991155 1	17426	9.40	1.3467		
1991155 2	1713	3	0.4321		
1991155 3	22821	18.8	0.3529		
1991156 1	17426	9.30	1.3467		
1991156 2	1713	3	0.4321		
1991156 3	22821	17.9	0.3547		
1991157 1	17426	13.40	1.3467		
1991157 2	1713	3	0.4321		
1991157 3	22821	18.7	0.3550		
1991158 1	17426	17.50	1.3467		
1991158 2	1713	3	0.4321		
1991158 3	22821	18.5	0.3548		
1991159 1	17426	6.30	1.3467		
1991159 2	1713	3	0.4321		
1991159 3	22821	18.4	0.3548		
1991160 1	17426	14.80	1.3467		
1991160 2	1713	3	0.4321		
1991160 3	22821	18.6	0.3574		
1991161 1	17426	15.60	1.3467		
1991161 2	1713	3	0.4321		
1991161 3	22821	19.0	0.3564		
1991162 1	17426	10.30	1.3467		
1991162 2	1713	3	0.4321		
1991162 3	22821	19.0	0.3556		
1991163 1	17426	13.80	1.3467		
1991163 2	1713	3	0.4321		
1991163 3	22821	18.3	0.3571		
1991164 1	17426	12.80	1.3467		
1991164 2	1713	3	0.4321		
1991164 3	22821	18.3	0.3573		

1991165 1	17426	11.70	1.3467
1991165 2	1713	3	0.4321
1991165 3	22821	18.2	0.3574
1991166 1	17426	11.90	1.3467
1991166 2	1713	3	0.4321
1991166 3	22821	18.5	0.3561
1991167 1	17426	8.80	1.3467
1991167 2	1713	3	0.4321
1991167 3	22821	17.9	0.3561
1991168 1	17426	10.80	1.3467
1991168 2	1713	3	0.4321
1991168 3	22821	17.6	0.3563
1991169 1	17426	17.10	1.3467
1991169 2	1713	3	0.4321
1991169 3	22821	19.1	0.3564
1991170 1	17426	20.10	1.3467
1991170 2	1713	3	0.4321
1991170 3	22821	20.7	0.3566
1991171 1	17426	17.50	1.3467
1991171 2	1713	3	0.4321
1991171 3	22821	21.9	0.3556
1991172 1	17426	21.20	1.3467
1991172 2	1713	3	0.4321
1991172 3	22821	22.3	0.3545
1991173 1	17426	18.20	1.3467
1991173 2	1713	3	0.4321
1991173 3	22821	22.0	0.3495
1991174 1	17426	10.50	1.3467
1991174 2	1713	3	0.4321
1991174 3	22821	19.1	0.3535
1991175 1	17426	9.30	1.3467
1991175 2	1713	3	0.4321
1991175 3	22821	18.7	0.3536
1991176 1	17426	14.20	1.3467
1991176 2	1713	3	0.4321
1991176 3	22821	19.6	0.3533
1991177 1	17426	21.20	1.3467
1991177 2	1713	3	0.4321
1991177 3	22821	21.5	0.3487
1991178 1	17426	17.60	1.3467
1991178 2	1713	3	0.4321
1991178 3	22821	21.6	0.3454
1991179 1	17426	15.10	1.3467
1991179 2	1713	3	0.4321
1991179 3	22821	20.3	0.3460
1991180 1	17426	12.70	1.3467
1991180 2	1713	3	0.4321
1991180 3	22821	20.3	0.3519
1991181 1	17426	13.80	1.3467
1991181 2	1713	3	0.4321
1991181 3	22821	21.7	0.3524
1991182 1	10386	15.40	1.3467
1991182 2	1713	3	0.4321
1991182 3	22821	23.0	0.3520
1991183 1	10386	13.20	1.3467
1991183 2	1713	3	0.4321
1991183 3	22821	22.5	0.3518
1991184 1	10386	15.50	1.3467
1991184 2	1713	3	0.4321
1991184 3	22821	21.0	0.3525
1991185 1	10386	20.00	1.3467
1991185 2	1713	3	0.4321
1991185 3	22821	21.3	0.3520
1991186 1	10386	21.30	1.3467
1991186 2	1713	3	0.4321
1991186 3	22821	22.9	0.3516

1991187 1	10386	19.40	1.3467
1991187 2	1713	3	0.4321
1991187 3	22821	21.5	0.3521
1991188 1	10386	19.30	1.3467
1991188 2	1713	3	0.4321
1991188 3	22821	21.4	0.3525
1991189 1	10386	16.20	1.3467
1991189 2	1713	3	0.4321
1991189 3	22821	21.5	0.3527
1991190 1	10386	17.00	1.3467
1991190 2	1713	3	0.4321
1991190 3	22821	21.5	0.3527
1991191 1	10386	14.20	1.3467
1991191 2	1713	3	0.4321
1991191 3	22821	21.4	0.3528
1991192 1	10386	15.10	1.3467
1991192 2	1713	3	0.4321
1991192 3	22821	21.5	0.3530
1991193 1	10386	12.70	1.3467
1991193 2	1713	3	0.4321
1991193 3	22821	21.5	0.3530
1991194 1	10386	14.80	1.3467
1991194 2	1713	3	0.4321
1991194 3	22821	21.9	0.3531
1991195 1	10386	14.90	1.3467
1991195 2	1713	3	0.4321
1991195 3	22821	23.1	0.3532
1991196 1	10386	18.50	1.3467
1991196 2	1713	3	0.4321
1991196 3	22821	24.4	0.3536
1991197 1	10386	19.30	1.3467
1991197 2	1713	3	0.4321
1991197 3	22821	25.9	0.3540
1991198 1	10386	22.80	1.3467
1991198 2	1713	3	0.4321
1991198 3	22821	27.4	0.3542
1991199 1	10386	25.10	1.3467
1991199 2	1713	3	0.4321
1991199 3	22821	28.4	0.3547
1991200 1	10386	21.30	1.3467
1991200 2	1713	3	0.4321
1991200 3	22821	27.7	0.3555
1991201 1	10386	17.20	1.3467
1991201 2	1713	3	0.4321
1991201 3	22821	26.0	0.3559
1991202 1	10386	16.60	1.3467
1991202 2	1713	3	0.4321
1991202 3	22821	24.9	0.3541
1991203 1	10386	18.90	1.3467
1991203 2	1713	3	0.4321
1991203 3	22821	24.9	0.3542
1991204 1	10386	20.30	1.3467
1991204 2	1713	3	0.4321
1991204 3	22821	25.7	0.3542
1991205 1	10386	22.70	1.3467
1991205 2	1713	3	0.4321
1991205 3	22821	25.6	0.3546
1991206 1	10386	17.20	1.3467
1991206 2	1713	3	0.4321
1991206 3	22821	24.9	0.3546
1991207 1	10386	16.90	1.3467
1991207 2	1713	3	0.4321
1991207 3	22821	24.9	0.3549
1991208 1	10386	17.80	1.3467
1991208 2	1713	3	0.4321
1991208 3	22821	26.1	0.3551

1991209 1	10386	18.10	1.3467
1991209 2	1713	3	0.4321
1991209 3	22821	26.2	0.3556
1991210 1	10386	19.60	1.3467
1991210 2	1713	3	0.4321
1991210 3	22821	26.6	0.3554
1991211 1	10386	18.70	1.3467
1991211 2	1713	3	0.4321
1991211 3	22821	26.9	0.3562
1991212 1	10386	15.10	1.3467
1991212 2	1713	3	0.4321
1991212 3	22821	26.4	0.3559
1991213 1	10375	14.00	1.3467
1991213 2	1713	3	0.4321
1991213 3	22821	25.8	0.3557
1991214 1	10375	14.60	1.3467
1991214 2	1713	3	0.4321
1991214 3	22821	25.4	0.3554
1991215 1	10375	17.60	1.3467
1991215 2	1713	3	0.4321
1991215 3	22821	24.9	0.3554
1991216 1	10375	16.80	1.3467
1991216 2	1713	3	0.4321
1991216 3	22821	24.7	0.3556
1991217 1	10375	17.70	1.3467
1991217 2	1713	3	0.4321
1991217 3	22821	24.7	0.3556
1991218 1	10375	17.10	1.3467
1991218 2	1713	3	0.4321
1991218 3	22821	24.9	0.3558
1991219 1	10375	17.70	1.3467
1991219 2	1713	3	0.4321
1991219 3	22821	25.6	0.3557
1991220 1	10375	18.10	1.3467
1991220 2	1713	3	0.4321
1991220 3	22821	25.9	0.3555
1991221 1	10375	15.00	1.3467
1991221 2	1713	3	0.4321
1991221 3	22821	25.4	0.3559
1991222 1	10375	12.60	1.3467
1991222 2	1713	3	0.4321
1991222 3	22821	24.5	0.3561
1991223 1	10375	13.30	1.3467
1991223 2	1713	3	0.4321
1991223 3	22821	23.5	0.3564
1991224 1	10375	14.5	1.3467
1991224 2	1713	3	0.4321
1991224 3	22821	23.1	0.3566
1991225 1	10375	19.4	1.3467
1991225 2	1713	3	0.4321
1991225 3	22821	23.2	0.3568
1991226 1	10375	17.2	1.3467
1991226 2	1713	3	0.4321
1991226 3	22821	23.6	0.3569
1991227 1	10375	19.7	1.3467
1991227 2	1713	3	0.4321
1991227 3	22821	24.0	0.3570
1991228 1	10375	19.2	1.3467
1991228 2	1713	3	0.4321
1991228 3	22821	23.6	0.3572
1991229 1	10375	13	1.3467
1991229 2	1713	3	0.4321
1991229 3	22821	23.4	0.3575
1991230 1	10375	13.6	1.3467
1991230 2	1713	3	0.4321
1991230 3	22821	23.9	0.3578

1991231	1	10375	16.9	1.3467
1991231	2	1713	3	0.4321
1991231	3	22821	23.5	0.3580
1991232	1	10375	14	1.3467
1991232	2	1713	3	0.4321
1991232	3	22821	23.1	0.3580
1991233	1	10375	11.3	1.3467
1991233	2	1713	3	0.4321
1991233	3	22821	22.6	0.3580
1991234	1	10375	9.1	1.3467
1991234	2	1713	3	0.4321
1991234	3	22821	22.4	0.3578
1991235	1	10375	13.1	1.3467
1991235	2	1713	3	0.4321
1991235	3	22821	21.9	0.3576
1991236	1	10375	11.6	1.3467
1991236	2	1713	3	0.4321
1991236	3	22821	21.5	0.3578
1991237	1	10375	16.7	1.3467
1991237	2	1713	3	0.4321
1991237	3	22821	21.6	0.3579
1991238	1	10375	6.6	1.3467
1991238	2	1713	3	0.4321
1991238	3	22821	21.0	0.3582
1991239	1	10375	6	1.3467
1991239	2	1713	3	0.4321
1991239	3	22821	19.9	0.3585
1991240	1	10375	9.6	1.3467
1991240	2	1713	3	0.4321
1991240	3	22821	19.5	0.3587
1991241	1	10375	11.6	1.3467
1991241	2	1713	3	0.4321
1991241	3	22821	19.3	0.3589
1991242	1	10375	14.4	1.3467
1991242	2	1713	3	0.4321
1991242	3	22821	19.0	0.3591
1991243	1	10375	19.7	1.3467
1991243	2	1713	3	0.4321
1991243	3	22821	19.2	0.3590
1991244	1	10042	13.2	1.3467
1991244	2	1713	3	0.4321
1991244	3	22821	19.4	0.3586
1991245	1	10042	10	1.3467
1991245	2	1713	3	0.4321
1991245	3	22821	19.1	0.3583
1991246	1	10042	16.3	1.3467
1991246	2	1713	3	0.4321
1991246	3	22821	19.3	0.3574
1991247	1	10042	13.1	1.3467
1991247	2	1713	3	0.4321
1991247	3	22821	19.0	0.3568
1991248	1	10042	7.8	1.3467
1991248	2	1713	3	0.4321
1991248	3	22821	17.2	0.3632
1991249	1	10042	4.6	1.3467
1991249	2	1713	3	0.4321
1991249	3	22821	16.4	0.3634
1991250	1	10042	7.4	1.3467
1991250	2	1713	3	0.4321
1991250	3	22821	16.0	0.3635
1991251	1	10042	7.7	1.3467
1991251	2	1713	3	0.4321
1991251	3	22821	15.7	0.3637
1991252	1	10042	9.6	1.3467
1991252	2	1713	3	0.4321
1991252	3	22821	15.6	0.3639

1991253 1	10042	13	1.3467
1991253 2	1713	3	0.4321
1991253 3	22821	15.5	0.3639
1991254 1	10042	8.6	1.3467
1991254 2	1713	3	0.4321
1991254 3	22821	15.6	0.3639
1991255 1	10042	9.1	1.3467
1991255 2	1713	3	0.4321
1991255 3	22821	15.7	0.3639
1991256 1	10042	4.2	1.3467
1991256 2	1713	3	0.4321
1991256 3	22821	15.3	0.3639
1991257 1	10042	3.8	1.3467
1991257 2	1713	3	0.4321
1991257 3	22821	15.1	0.3640
1991258 1	10042	4.4	1.3467
1991258 2	1713	3	0.4321
1991258 3	22821	14.9	0.3641
1991259 1	10042	5.5	1.3467
1991259 2	1713	3	0.4321
1991259 3	22821	14.4	0.3641
1991260 1	10042	9.2	1.3467
1991260 2	1713	3	0.4321
1991260 3	22821	14.0	0.3636
1991261 1	10042	7.7	1.3467
1991261 2	1713	3	0.4321
1991261 3	22821	13.9	0.3630
1991262 1	10042	6.7	1.3467
1991262 2	1713	3	0.4321
1991262 3	22821	13.7	0.3630
1991263 1	10042	9.8	1.3467
1991263 2	1713	3	0.4321
1991263 3	22821	13.8	0.3631
1991264 1	10042	8.6	1.3467
1991264 2	1713	3	0.4321
1991264 3	22821	14.2	0.3617
1991265 1	10042	13.7	1.3467
1991265 2	1713	3	0.4321
1991265 3	22821	13.8	0.3617
1991266 1	10042	11.7	1.3467
1991266 2	1713	3	0.4321
1991266 3	22821	13.7	0.3617
1991267 1	10042	13.9	1.3467
1991267 2	1713	3	0.4321
1991267 3	22821	13.5	0.3617
1991268 1	10042	13.2	1.3467
1991268 2	1713	3	0.4321
1991268 3	22821	13.5	0.3617
1991269 1	10042	12.1	1.3467
1991269 2	1713	3	0.4321
1991269 3	22821	13.6	0.3616
1991270 1	10042	9.5	1.3467
1991270 2	1713	3	0.4321
1991270 3	22821	13.2	0.3693
1991271 1	10042	9	1.3467
1991271 2	1713	3	0.4321
1991271 3	22821	13.2	0.3693
1991272 1	10042	12.2	1.3467
1991272 2	1713	3	0.4321
1991272 3	22821	13.2	0.3691
1991273 1	10042	8.2	1.3467
1991273 2	1713	3	0.4321
1991273 3	22821	13.0	0.3690
1991274 1	7256	6.9	1.3467
1991274 2	1713	3	0.4321

1991274	3	22821	12.7	0.3690
1991275	1	7256	6.2	1.3467
1991275	2	1713	3	0.4321
1991275	3	22821	12.6	0.3685
1991276	1	7256	3.5	1.3467
1991276	2	1713	3	0.4321
1991276	3	22821	12.3	0.3681
1991277	1	7256	2.4	1.3467
1991277	2	1713	3	0.4321
1991277	3	22821	11.8	0.3682
1991278	1	7256	2.5	1.3467
1991278	2	1713	3	0.4321
1991278	3	22821	11.2	0.3682
1991279	1	7256	0.1	1.3467
1991279	2	1713	3	0.4321
1991279	3	22821	10.4	0.3782
1991280	1	7256	7.3	1.3467
1991280	2	1713	3	0.4321
1991280	3	22821	10.0	0.3777
1991281	1	7256	3	1.3467
1991281	2	1713	3	0.4321
1991281	3	22821	9.9	0.3778
1991282	1	7256	-0.4	1.3467
1991282	2	1713	3	0.4321
1991282	3	22821	9.6	0.3779
1991283	1	7256	3.9	1.3467
1991283	2	1713	3	0.4321
1991283	3	22821	9.4	0.3779
1991284	1	7256	4.6	1.3467
1991284	2	1713	3	0.4321
1991284	3	22821	9.2	0.3778
1991285	1	7256	1.9	1.3467
1991285	2	1713	3	0.4321
1991285	3	22821	9.0	0.3779
1991286	1	7256	1.2	1.3467
1991286	2	1713	3	0.4321
1991286	3	22821	8.8	0.3778
1991287	1	7256	2.1	1.3467
1991287	2	1713	3	0.4321
1991287	3	22821	8.6	0.3776
1991288	1	7256	2.8	1.3467
1991288	2	1713	3	0.4321
1991288	3	22821	8.4	0.3776
1991289	1	7256	1	1.3467
1991289	2	1713	3	0.4321
1991289	3	22821	8.1	0.3777
1991290	1	7256	2.8	1.3467
1991290	2	1713	3	0.4321
1991290	3	22821	7.9	0.3777
1991291	1	7256	5.7	1.3467
1991291	2	1713	3	0.4321
1991291	3	22821	7.8	0.3777
1991292	1	7256	10	1.3467
1991292	2	1713	3	0.4321
1991292	3	22821	8.1	0.3777
1991293	1	7256	8.4	1.3467
1991293	2	1713	3	0.4321
1991293	3	22821	7.8	0.3778
1991294	1	7256	8.7	1.3467
1991294	2	1713	3	0.4321
1991294	3	22821	7.8	0.3777
1991295	1	7256	8.5	1.3467
1991295	2	1713	3	0.4321
1991295	3	22821	7.6	0.3777
1991296	1	7256	4.3	1.3467
1991296	2	1713	3	0.4321

1991296	3	22821	7.5	0.3777
1991297	1	7256	2.6	1.3467
1991297	2	1713	3	0.4321
1991297	3	22821	7.3	0.3777
1991298	1	7256	2.3	1.3467
1991298	2	1713	3	0.4321
1991298	3	22821	7.1	0.3777
1991299	1	7256	1	1.3467
1991299	2	1713	3	0.4321
1991299	3	22821	6.9	0.3777
1991300	1	7256	1	1.3467
1991300	2	1713	3	0.4321
1991300	3	22821	6.7	0.3777
1991301	1	7256	6.3	1.3467
1991301	2	1713	3	0.4321
1991301	3	22821	6.6	0.3778
1991302	1	7256	-4.3	1.3467
1991302	2	1713	3	0.4321
1991302	3	22821	6.3	0.3778
1991303	1	7256	-3.8	1.3467
1991303	2	1713	3	0.4321
1991303	3	22821	5.9	0.3778
1991304	1	7256	3.8	1.3467
1991304	2	1713	3	0.4321
1991304	3	22821	5.4	0.4044

Comment line: Hogarth Outflow Scenario 3 [m³/day]

1 # number of withdrawal outlets

Date TOWEST

1991145 91355
1991146 91355
1991147 91355
1991148 91355
1991149 91355
1991150 91355
1991151 91355
1991152 91355
1991153 91355
1991154 91355
1991155 91355
1991156 91355
1991157 91355
1991158 91355
1991159 91355
1991160 91355
1991161 91355
1991162 91355
1991163 91355
1991164 91355
1991165 91355
1991166 91355
1991167 91355
1991168 91355
1991169 91355
1991170 91355
1991171 91355
1991172 91355
1991173 91355
1991174 91355
1991175 91355
1991176 91355
1991177 91355
1991178 91355
1991179 91355
1991180 91355
1991181 91355
1991182 91355
1991183 91355
1991184 91355
1991185 91355
1991186 91355
1991187 91355
1991188 91355
1991189 91355
1991190 91355
1991191 91355
1991192 91355
1991193 91355
1991194 91355
1991195 91355
1991196 91355
1991197 91355
1991198 91355
1991199 91355
1991200 91355
1991201 91355
1991202 91355
1991203 91355
1991204 91355
1991205 91355
1991206 91355
1991207 91355

1991208 91355
1991209 91355
1991210 91355
1991211 91355
1991212 91355
1991213 91355
1991214 91355
1991215 91355
1991216 91355
1991217 91355
1991218 91355
1991219 91355
1991220 91355
1991221 91355
1991222 91355
1991223 91355
1991224 91355
1991225 91355
1991226 91355
1991227 91355
1991228 91355
1991229 91355
1991230 91355
1991231 91355
1991232 91355
1991233 91355
1991234 91355
1991235 91355
1991236 91355
1991237 91355
1991238 91355
1991239 91355
1991240 91355
1991241 91355
1991242 91355
1991243 91355
1991244 91355
1991245 91355
1991246 91355
1991247 91355
1991248 91355
1991249 91355
1991250 91355
1991251 91355
1991252 91355
1991253 91355
1991254 91355
1991255 91355
1991256 91355
1991257 91355
1991258 91355
1991259 91355
1991260 91355
1991261 91355
1991262 91355
1991263 91355
1991264 91355
1991265 91355
1991266 91355
1991267 91355
1991268 91355
1991269 91355
1991270 91355
1991271 91355
1991272 91355
1991273 91355

1991274 91355
1991275 91355
1991276 91355
1991277 91355
1991278 91355
1991279 91355
1991280 91355
1991281 91355
1991282 91355
1991283 91355
1991284 91355
1991285 91355
1991286 91355
1991287 91355
1991288 91355
1991289 91355
1991290 91355
1991291 91355
1991292 91355
1991293 91355
1991294 91355
1991295 91355
1991296 91355
1991297 91355
1991298 91355
1991299 91355
1991300 91355
1991301 91355
1991302 91355

<#7>

Dyresm Parameters File for DYCD V4.0.0

1.3E-3 # bulk aerodynamic mmt. transport coeff. (priv. comm. [Imberger, 1998])
0.08 # mean albedo of water
0.96 # emissivity of a water surface (Imberger & Patterson [1981,p316])
3.00 # critical wind speed [m s⁻¹]
43200 # time of day for output (secs from midnight) (54000 s = 15:00 HR)
0.012 # bubbler entrainment coefficient (priv. comm. [Alexander,2000])
0.083 # buoyant plume entrainment coefficient [Fischer et al. 1979]
0.06 # shear production efficiency (eta_K)
0.20 # potential energy mixing efficiency (eta_P)
0.4 # wind stirring efficiency (eta_S)
1.0E+7 # effective surf. area coeff. (priv. com. [Yeates,2002])
1.4E-5 # BBL detrainment diffusivity (priv. com. [Yeates,2002])
200 # vertical mix coeff. (priv. com. [Yeates,2002])

APPENDIX VIII
Glossary of Terms

Mixolimnion: The circulating upper stratum.

Monimolimnion: The deeper stratum of water that is perennially or periodically isolated.

Chemolimnion: The interfacing stratum of steep salinity (density) gradient between the mixolimnion and the monimolimnion.

Epilimnion: An upper stratum of less dense more or less uniformly warm, circulating, and fairly turbulent water

Hypolimnion: The lower stratum of more dense, cooler, and relatively quiescent water lying below the epilimnion.

Metalimnion: The transitional stratum of marked thermal change between the epilimnion and the hypolimnion.